# OPTIMUM PREY CAPTURE TECHNIQUES IN FISH

JOHAN L. VAN LEEUWEN

# OPTIMUM PREY CAPTURE TECHNIQUES IN FISH

Proefschrift
ter verkrijging van de graad van
doctor in de landbouwwetenschappen,
op gezag van de rector magnificus,
dr. C.C. Oosterlee,
hoogleraar in de veeteeltwetenschap,
in het openbaar te verdedigen
op woensdag 29 juni 1983
des namiddags te vier uur in de aula
van de Landbouwhogeschool te Wageningen.

ISN = 186 131 - 03

# Inhoud/Contents

# STELLINGEN

### 1.

Maximization of the initial prey distance by an exact adjustment of mouth expansion is useless for a fish, contrary to an adjustment that maximizes the velocity of the prey while it enters the mouth.

This thesis.

### 2.

Jaw protrusion is the most efficient way, achieved in fish, to increase the relative prey velocity towards the fish's mouth.

This thesis.

### 3.

The opercular and branchiostegal valves are important control devices to optimize the flow rate through the mouth aperture during suction feeding in fish.

This thesis.

### 4.

Conclusions to unfunctional morphology by Lauder and Liem (1981) are caused by a lack of physical insight. There is no evidence for an unfunctional construction in *Luciocephalus pulcher*.

This thesis contra Lauder, G. V. & Liem, K. F. (1981). Prey capture by *Luciocephalus pulcher*: implications for models of jaw protrusion in teleost fishes. *Env. Biol. Fish.* 6, 257–268.

### 5.

Functional morphology can support phylogenetic studies in fish, as argued by Liem and Greenwood (1981). In their examples, however, the authors merely add movement- and EMG-patterns to the list of morphological features already used by taxonomists. They do not show the relations between form and function.

Contra Liem, K. F. & Greenwood, P. H. (1981). A functional approach to the phylogeny of pharyngognath teleosts. *Amer. Zool.* 21, 83–101.

## 6.

The available data strongly suggest that the importance of tendon elasticity to reduce the energetic cost of terrestrial locomotion decreases with a smaller size of the animal.

Biewener, A. A., Alexander, R. McN. & Heglund, N. C. (1981). Elastic storage in the hopping kangaroo rats (*Dipodomis spectabilis*). *J. Zool.*, Lond., 195, 369–383.

Heglund, N. C., Fedak, M. A., Taylor, C. R. & Cavagna, G. A. (1982). Energetics and mechanics of terrestrial locomotion. IV. Total mechanical energy changes as a function of speed and body size in birds and mammals. *J. exp. Biol.* 97, 57–66.

## 7.

Voor het interpreteren van ethologische gegevens is kennis van de functionele morfologie van belang.

## 8.

Bij het toetsen van de rijvaardigheid van automobilisten dient het vermogen tot stereoscopisch zien in de beoordeling te worden betrokken.

## 9.

Het betoog van PvdA-leider Den Uyl tegen de door hem aangeduide 'one issue partijen' wijst alleen maar op het belang van het bestaan van bedoelde groeperingen. Het is in dit verband interessant om na te gaan wanneer, na de anti-kernenergie gedachte, ook de gedachte van de economische nulgroei zal postvatten in de PvdA.

Contra Drs. J. den Uyl, Volkskrant 14 mei 1983, pag. 13.

## 10.

Met de toenemende werkeloosheid moeten velen steeds harder gaan werken om betaald werk te kunnen blijven uitvoeren.

## 11.

In het kader van de bezuinigingen en gelet op de toenemende papierwinkel ten behoeve van planning en coördinatie van het universitair onderwijs en onderzoek verdient het aanbeveling om alle wetenschappelijke medewerkers te benoemen tot wetenschappelijk ambtenaar.

## 12.

Bij de beoordeling van een proefschrift dient de aan het werk bestede tijdsduur in de beschouwing te worden betrokken. Een politiek waarbij de beschikbare (betaalde) tijdsduur wordt verkort en de eisen onveranderd blijven is onmenselijk en verwerpelijk.

# Voorwoord

Dit proefschrift werd bewerkt bij de sectie Functionele morfologie van de vakgroep Experimentele diermorfologie en celbiologie van de Landbouwhogeschool te Wageningen. Dit onderzoek werd mogelijk gemaakt door mijn aanstelling bij BION/ZWO (14.90.18) voor een periode van (effectief) drie jaar. Het onderzoek werd gestart op 1 december 1979, aanvankelijk voor halve dagen als student assistent, na mijn afstuderen op 23 januari 1980 op "full time" basis. Een aantal personen wil ik bedanken die een belangrijke rol hebben gespeeld in mijn opleiding tot bioloog en/of het tot stand komen van dit proefschrift.

Mijn promotor Jan Osse dank ik voor zijn stimulerende onderwijs in de dierkunde, zijn vele goede ideeën en adviezen, het op zich nemen van organisatorische taken, waardoor het onderzoek kon starten en voortgang vinden, en het kritisch doornemen en bespreken van de manuscripten, waardoor deze veel aan duidelijkheid wonnen.

Mijn vriend en begeleider Mees Muller heeft mij in belangrijke mate ingevoerd in de regeltechniek, hydrodynamica en kennis van vissen. Met plezier denk ik terug aan onze talloze discussies, die zeer veel hebben bijgedragen tot dit proefschrift.

Arie Terlouw dank ik voor zijn deskundige technische assistentie. Met genoegen herinner ik me onze vele, altijd in prima sfeer verlopen experimenten.

Jan Verhagen dank ik voor zijn deskundige hydrodynamische adviezen.

Neill Alexander en Alan Jayes hebben mij begeleid gedurende mijn doctoraalstage in Leeds, die tesamen met de vele geschriften van Neill van veel betekenis was voor mijn wetenschappelijke vorming. Thank you very much!

Johan van der Veer en Ton de Lange dank ik voor hun adviezen op fotogrammetrisch gebied, en de constructeurs van de TFDL voor het vervaardigen van de nodige hulpmiddelen. Gert van Eck verrichtte wonderen bij het opstarten van onze onmisbare MINC-11 computer.

De bijdragen die Jan Kremers, Ineke Oomen, Maarten Drost en Ben Cattel als doctoraal student aan dit werk hebben geleverd stel ik zeer op prijs.

De vriendschap en belangstelling van de collega's van de sectie Functionele morfologie, Rie Akster en Nand Sibbing, en van de mensen van de secties Histologie en Celbiologie heb ik altijd bijzonder gewaardeerd.

Wim Valen dank ik voor zijn goede tekenwerk en fotografische hulp en Sietse Leenstra, Piet van Kleef en Sytse van de Berg voor de verzorging van de proefdieren en de technische hulp. Chris Secombes, Nicolas Cohen en Seamus Ward dank ik voor hun adviezen wat betreft het Engels. Annet Kroon dank ik voor het kritisch doorlezen en corrigeren van de manuscripten.

Tenslotte wil ik al diegenen bedanken die nog niet genoemd zijn maar toch hebben bijgedragen tot dit proefschrift.

# Inleiding

In dit proefschrift wordt getracht om via het hanteren van fysische principes (deductieve methode) te komen tot een verklaring van een aantal aspecten van de bouw en werking van het voedselopname-mechanisme van vissen. Het gepresenteerde werk sluit in sterke mate aan op het proefschrift van Muller (1983), waarin een uitgebreide inleiding, inclusief literatuuroverzicht, te vinden is omtrent het prooiopname-mechanisme van vissen. Tevens wordt daarin de gevolgde methodologie aan de orde gesteld. Ik zal dan ook relatief kort zijn over deze aspecten en de nadruk leggen op de resultaten van het onderzoek.

*Het proces van prooiopname*
Van de meer dan 20,000 recente soorten vissen zuigt ruim de helft de prooi aan door een expansie en kompressie van de buccale en operculaire holtes (tesamen aangeduid als mondholte in het vervolg van deze inleiding). Niet alleen de prooi met het omringende water wordt verplaatst, maar de vis zuigt zichzelf hierbij ook vooruit. Bij veel vissoorten wordt de zuigbeweging aangevuld met zwemmen en een vooruitschuiven (protrusie) van de kaken. Vissen hebben de mogelijkheid om meer water door de mondopening op te nemen dan de mondholte maximaal kan bevatten, doordat op een zeker ogenblik in het zuigproces de operculaire en branchiostegaal kleppen (hieronder kortweg aangeduid als "kleppen") geopend worden. Het vooraan opgenomen water stroomt daarna weg via de kieuwspleten. De zuigbeweging wordt meestal binnen 50 tot 100 msec uitgevoerd, waarbij versnellingen van het water of delen van de vis van 10 maal de zwaartekrachtversnelling of zelfs hoger optreden. Het voedselopname-proces is dus hoogst instationair en de watersnelheid kan niet uit de druk worden afgeleid (zie ook Muller et al., 1982). Als gevolg van de bekexpansie kunnen onderdrukken tot 0.4 tot 0.6 atmosfeer (40 tot 60 kPa) worden gegenereerd. Een bestudering van het proces van prooiopname is nuttig, niet alleen omdat hiermee inzicht wordt verworven omtrent bouwprincipes van vissen, maar ook omdat habitat-preferenties, ethologie en voedselzoekstrategieën van vissen beter kunnen worden begrepen.

*Modelvorming*
Het prooiopname-mechanisme van vissen is door vele auteurs bestudeerd (zie voor overzichten Osse, 1969 en Muller, 1983). Veelal betreffen dit morfologische studies, soms in combinatie met experimentele waarnemingen (zie bijvoorbeeld Osse, 1969). Deze soms gedetailleerde werken geven een indruk van de bouw en verrichtingen van een gering aantal soorten, maar resulteerden nog niet in een generale beschrijving van het zuigproces, omdat de deductieve methode niet

7

of nauwelijks is toegepast of de modelvorming van de stromingsverschijnselen foutief is (zie Muller, 1983, voor een gedetailleerde bespreking van deze materie).

Recent hebben Muller et al. (1982) en Muller & Osse (in press) een hydrodynamisch model van de zuigende voedselopname van vissen gepresenteerd, dat een belangrijke stap vormt in de richting van een meer generale beschouwing van dit proces.

De dichtheid van water ligt in dezelfde orde van grootte als die van de prooi. Dit maakt het mogelijk om de prooi met de waterstroom mee naar binnen te zuigen. De door de vis opgewekte waterstroom bepaalt dan ook in sterke mate of de prooi al dan niet gevangen wordt. Door het bestuderen van de hydrodynamica van het zuigproces kunnen morfologische en kinematische kriteria worden opgesteld waaraan de vis zou moeten voldoen als deze de waterstroom zodanig manipuleert dat de prooivangkans wordt geoptimaliseerd. Via deze weg blijkt het mogelijk om een uitspraak te doen over de mate van aangepastheid van structuren aan bepaalde functies. Tevens kan de samenhang tussen de bouw van verschillende structuren binnen het expansie-apparaat aangetoond worden en kunnen wijzigingen in het prooiopname-proces als aanpassing aan verschillende uitwendige omstandigheden logisch worden verklaard. Een aantal voorbeelden zullen hieronder worden vermeld.

Muller et al. (1982) hebben de waterstroom voor de bek van de vis gemodelleerd als een combinatie van een circulair wervelfilament en een parallelstroom. De wervelsingulariteiten (hier is de snelheid oneindig) liggen op de lippen van de vis en de wervelsterkte wordt bepaald door de volume vergroting of verkleining van de mondholte door expansie of compressie en door de voortbeweging van de vis. Een snellere voortbeweging reduceert de bijdrage van de wervel aan de waterstroom door de mondopening. De voorwaartse beweging van de vis wordt evenals een eventuele protrusie van de kaken verdisconteerd in de sterkte van de parallelstroom. De mondholte wordt in bovenbedoeld model voorgesteld als een rotatie-symmetrisch profiel. Bij het simuleren van bekbewegingen van de vis wordt vrijwel altijd uitgegaan van een aan de voorzijde afgeknotte kegel. Een belangrijk aspect van de modelvorming was het onderscheiden van een aardvast en een bewegend assenstelsel. In het aardvaste assenstelsel (gefixeerd t.o.v. het aquarium) dienen krachten, drukken en impulsen berekend te worden. Het bewegende assenstelsel (gefixeerd t.o.v. de bek van de vis) wordt gebruikt voor de bestudering van de prooivangkans.

*Experimentele toetsing van modeluitspraken*

Het model is op diverse wijzen door Muller & Osse (in press) getoetst. Van een achttal vissoorten zijn snelle films gemaakt van de voedselopname (tot 400 beelden/sec). Vanaf deze films konden de bewegingen van de vis en de prooi worden opgemeten. Daarnaast is door het aanbrengen van polystyreen bolletjes van 0.5 of 1 mm doorsnede de stroming rond de vis en de prooi gevisualiseerd. Deze bolletjes zijn klein ten opzichte van de diameter van de bek en hebben vrijwel dezelfde dichtheid als water, waardoor ze de waterstroom zeer goed volgen. Voor het meten van watersnelheden in de bek zijn zogenaamde "hot-film

8

anemometers" gebruikt, met een grote bandbreedte zodat snel wisselende water-snelheden goed geregistreerd kunnen worden. Voor het meten van drukken in de mondholte zijn metingen verricht met een aantal verschillende typen transducers.

Behalve de "hot-film anemometry" heb ik al deze technieken ten nutte gemaakt voor mijn onderzoek. Een aantal technieken heb ik verder verfijnd.

In hoofdstuk 1 wordt onder meer een stereoscopische filmtechniek behandeld waarmee het mogelijk is om vorm- en positie-veranderingen van de predator en van de prooi in de ruimte te registreren. Een stereoscopische opname van de opstelling in een vroeg stadium van ontwikkeling is gegeven in Fig. 1. Tevens kan via de polystyreen bollen de in de tijd varierende waterstroom in de ruimte worden bestudeerd. De nauwkeurigheid van de gebruikte methode wordt beperkt door het kleine oppervlak van de beelden van een 16 mm film. Een grotere nauwkeurigheid werd bereikt m.b.v. multi-flash fotografie, waarvan een voorbeeld staat afgedrukt op pag. 11. Andere voorbeelden zijn te vinden in hoofdstuk 1. Door een afnemende intensiteit van de opeenvolgende flitsen is de bewegingsrichting van de objecten aangegeven. Met behulp van deze technieken werd aangetoond dat de forel na klepopening ongeveer vijf maal zoveel water door de mond opneemt als voor klepopening. Tevens werd een goede indicatie verkregen over de initiële vorm van het opgezogen volume water. In
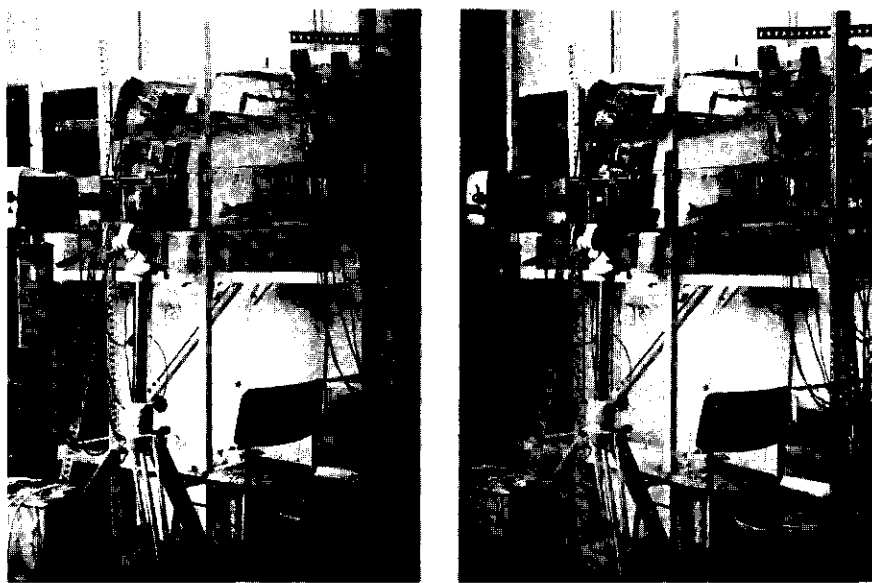


Fig. 1. De stereoscopische filmopstelling in een vroeg stadium van ontwikkeling. Een belichtingstijd van 1/4000 tot 1/2000 seconde is nodig om bewegingsonscherpte te vermijden. De batterij filmlampen maakt het mogelijk om toch met een diafragma van 8 of 11 te werken. Verder zijn te zien de high-speed camera en het stereo-voorzetstuk. Dit stereopaar kan bekeken worden met een pocket-stereoscoop, waardoor een ruimtelijk beeld ontstaat. Die is m.b.v. twee lenzen met een brandpuntsafstand van ± 120 mm gemakkelijk te vervaardigen.

9

hoofdstuk 1 wordt ook beschreven hoe door het aanbrengen van draden bij de operculaire spleten variaties in de bewegingsrichting van het water op deze plaats kunnen worden afgeleid. In hoofdstuk 3 worden voor- en nadelen van een aantal technieken voor het meten van de drukken in de vissebek behandeld. Met behulp van Fourier analyse zijn de dynamische responsies van een aantal drukopnemers en de frequentie-inhoud van een aantal drukregistraties bepaald.

## De balans tussen zuigen en zwemmen

De vis kan op een aantal manieren de prooi naar zijn mond toe doen bewegen. Het naar de prooi toe zwemmen is een effectieve methode als de prooi nog relatief ver weg is. Dicht bij de mondopening dreigt de prooi echter met het hem omringende water vooruit geduwd te worden. Dit laatste kan worden voorkomen door de expansie van de mondholte van de vis, waardoor water aangezogen wordt. Als deze expansie snel genoeg verloopt zal het water in de mondopening van de vis naar achteren bewegen, terwijl tegelijkertijd bij gesloten kleppen het water achterin de mondholte naar voren toe geduwd wordt; dit alles in een aardvast assenstelsel. Ergens in de mondholte zal dan het water stilstaan. De positie van dit stilstandspunt, is een functie van de tijd en kan als de kleppen gesloten zijn exact berekend worden. Bij geopende kleppen kan tot nu toe slechts een benadering gegeven worden van deze positie (zie hoofdstuk 1). De benodigde expansie-snelheid om het stilstandspunt halverwege in de mondholte te houden met gesloten kleppen, de kritische expansie-snelheid, neemt toe met de zwemsnelheid en de straal van de mondopening. Het wordt dus voor de vis steeds moeilijker om met het wijder openen van de mond deze expansie-snelheid nog te halen en het stilstandspunt zou uit de mondopening verdwijnen (met als direkt gevolg stuwing van de prooi), als niet de kleppen zouden openen. Klepopening heeft tot gevolg dat:
1) water door de operculaire spleten kan uitstromen.
2) het stilstandspunt in de mondholte gehouden wordt, of mogelijk zelfs de mondholte aan de achterzijde verlaat.
3) het debiet door de mondopening gemaximaliseerd kan worden.

De regenboogforel (*Salmo gairdneri*, zie Fig. 2) is in de eerste fase van het proces, waarbij de kleppen gesloten zijn, zeer goed in staat om het stilstandspunt achterin de mondholte te houden (zie hoofdstuk 1, Fig. 18). Ditzelfde is gevonden voor een zestal andere vissoorten (nog niet gepubliceerd werk van Oomen, Van Leeuwen, Muller en Kremers). Daarna zou het punt echter zeer snel naar de mondopening bewegen (binnen 10 msec) als de kleppen continu gesloten zouden blijven. Voor het creëren van een efficiënte waterstroom is het van groot belang dat de kleppen snel geopend kunnen worden. Een te vroeg openen heeft een caudale instroming door de operculaire spleten tot gevolg en dientengevolge een gevaar van beschadiging van de fragiele kieuwfilamenten. Een te late opening veroorzaakt stuwing van de prooi, juist op het moment van prooiopname. De forel heeft een relatief langzaam klepopeningsmechanisme (ongeveer 10 msec, afhankelijk van de grootte van de vis), waardoor het begin van klepopening noodzakelijk voor het "ideale tijdstip" van klepopenen ligt. De verwachte,
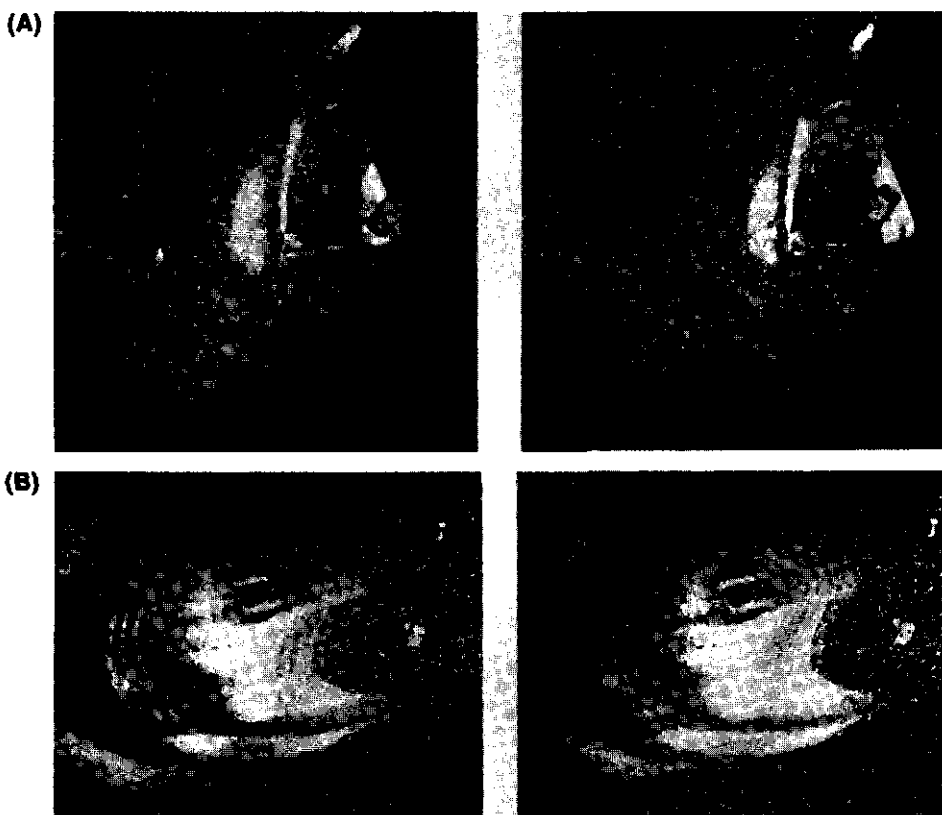
10

Fig. 2. A. Stereopaar van een "mishap" van een regenboogforel. De vis richtte op de moer waarmee de voedselbrok werd neergelaten. Let op de vrijwel rotatie-symmetrische bek en de van elkaar af staande kieuwbogen, waarlangs het water naar achteren kan wegstromen.
B. Stereopaar van de stroming voor de bek van een regenboogforel tijdens de voedselopname, verkregen d.m.v. "multi-flash" fotografie.

zeer geringe caudale instroming is inderdaad experimenteel aangetoond met behulp van de bovengenoemde draden (hoofdstuk 1).

De ontwikkeling van een veel sneller klepopeningsmechanisme binnen de Paracanthopterygii en de Acanthopterygii kan worden beschouwd als een essentiële stap in het creëren van een meer effectieve waterstroom door de mond.

De korte mondbuis van uitgestorven Palaeoniscoidea als *Pteronisculus* heeft naar alle waarschijnlijkheid een vroeg openingstijdstip van de kleppen noodzakelijk gemaakt. De zeer korte branchiostegaal stralen bij deze vis kunnen ook geen gesloten kleppen bij een grote operculumabductie hebben toegestaan. Dit staat in schril contrast met de lange mondbuis en lange aciniforme branchiostegaal stralen in de Paracanthopterygii (bijvoorbeeld de kabeljauw) en de Acanthopterygii (bijvoorbeeld de baars), die het voedselopname-proces minder afhankelijk hebben gemaakt van zwemmen.

11

Speciale aandacht verdient de protrusie van de kaken. Hierdoor wordt de mondholte verlengd en derhalve de kritische expansie-snelheid verlaagd. Protrusie treedt bijvoorbeeld in extreme mate op bij *Luciocephalus pulcher*, een vis die bij oppervlakkige beschouwing veel op de snoek (*Esox lucius*) lijkt. De snoek heeft echter geen protrusie en *Luciocephalus* protrudeert de kaken over ongeveer 30 procent van de (rust)koplengte. Door de als gevolg van protrusie verlengde kop kan de vis het stilstandspunt langer achterin de bek houden dan de snoek, waardoor bijgevolg de kleppen later moeten openen. De hiervoor benodigde lange branchiostegaalstralen zijn inderdaad bij *Luciocephalus* aanwezig. Ik wil hier benadrukken dat de uitleg van Lauder & Liem (1981) van het prooiopname-proces van *Luciocephalus* foutief is omdat ze onder andere het effect van stuwing over het hoofd hebben gezien (zie hoofdstuk 1).

*Optimalisatie van de vangkans van de prooi*

In hoofdstuk 2 worden de effecten van zuigen, voortwaartse beweging van de vis en protrusie van de kaken op de snelheid van de prooi in het bewegende assenstelsel eerst afzonderlijk en later ook gezamenlijk gekwantificeerd. Het blijkt dat de effecten van zuigen en zwemmen sterk afhangen van de afstand van de prooi tot de mondopening. Op een grote afstand heeft het geen effect voor de vis om te zuigen (afgezien van de bijdrage aan de eigen snelheid). Als de prooi zich dicht bij de mondopening bevindt zou stuwing van de prooi op kunnen treden; het relatieve zwemeffect (hoofdstuk 2) nadert hier tot nul. Zuigen heeft nu juist wel een sterk effect. Protrusie heeft een tweeledig effect op de prooi-snelheid in het bewegende assenstelsel. In de eerste plaats is er het translatie-effect op de prooisnelheid. Dit is onafhankelijk van de prooiafstand, hetgeen een groot voordeel inhoudt t.o.v. zuigen en zwemmen. Bovendien vereist het protruderen van de kaken slechts weinig energie, in tegenstelling tot activiteiten als zuigen en zwemmen waar relatief grote massa's moeten worden versneld. Zoals boven vermeld wordt door protrusie de mondholte verlengd, waardoor de watersnelheid in de mondopening t.g.v. zuigen wordt vergroot. De invloed van dit effect van de protrusie op de prooisnelheid blijkt bij de koraalduivel (*Pterois russelli*) en de bot (*Platichthys flesus*) een ondergeschikte rol te spelen.

De op de bodem levende zeeduivel (*Lophius piscatorius*) beschikt over een uiterst effectief prooiopname-mechanisme. Deze vis (Fig. 3) zet zich af van het substraat waardoor het geleverde vermogen (bij een stevige ondergrond) vrijwel geheel aan de eigen voortbeweging ten goede komt. Ook is deze predator in staat tot een geweldige bekexpansie. Bovendien kan de zeeduivel de kaken over een aanzienlijke afstand protruderen. Alle mogelijke manieren om de snelheid van de prooi ten opzichte van de mondopening zo hoog mogelijk te maken zijn dus benut (zie formule 8 uit hoofdstuk 2).

De richting en de snelheid van een eventuele vluchtreactie van de prooi is moeilijk voorspelbaar, zowel voor ons als waarschijnlijk ook voor de vis. Prooi-en die snel kunnen vluchten, zoals vissen, wekken een snellere zuigbeweging op van de snoekbaars (*Stizostedion lucioperca*) dan wormen (zie Elshoud-Olden-have, 1979). Ook voor andere vissen is een dergelijke respons waargenomen.
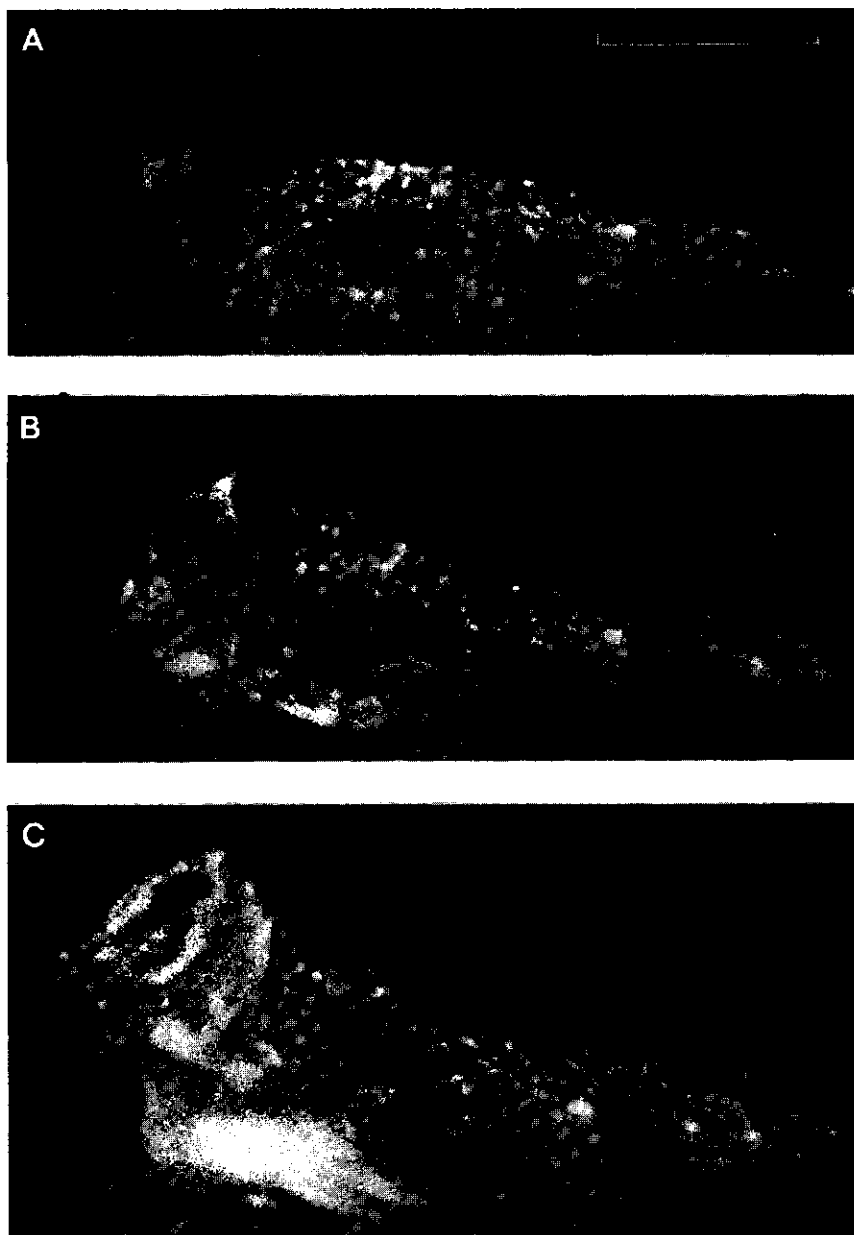
12

Fig. 3. De zeeduivel (*Lophius piscatorius*, standaardlengte 215 mm) is een uitstekend gecamoufleerde bodemvis (zie A), die m.b.v. het zogenaamde "ilicium" prooien naar zich toe lokt. Als de prooi dicht genoeg genaderd is wordt deze razendsnel opgeslokt. (B) en (C) zijn respectievelijk 30.7 msec en 61.4 msec na (A) opgenomen. Let op de enorme levatie van de schedel en de protrusie van de kaken. De maatverdeling in (A) duidt een afstand aan van 50 mm.

Vrijwel altijd orienteert een vis zich zodanig dat de prooi zich op de lengte-as van de kop bevindt.

Men kan zich afvragen van welke afstand een vis z'n prooi zou moeten aanzuigen, zodat deze op een gedefinieerd tijdstip door de mondopening naar binnen stroomt. Dit tijdstip kan zijn het moment waarop de mondopening maximaal is (als de prooi groot is), of eerder, als de vis de snelheid van de prooi zo groot mogelijk wil maken (zie hoofdstuk 2). Indien het gewenste tijdstip van prooiopname bekend is kan door een terugberekening de initiële prooiafstand worden bepaald. Uit modelsimulaties blijkt dat een maximalisatie van de initiële prooiafstand door een precies afstemmen van de expansie van het rostrale deel van de mondholte op de abductie van de opercula weinig nut heeft voor de vis. De dimensies van de kop bepalen namelijk in sterke mate het aandeel van het zuigen in de initiële afstand. Zwemmen en protrusie van de kaken zijn veel effectievere middelen voor het vergroten van de initiële afstand. Het is voor de vis veel gunstiger om met zijn zuigapparaat de uiteindelijke prooisnelheid te maximaliseren, dat is de snelheid van de prooi als deze de mondopening passeert. Om dit te bereiken dient de vis de kieuwdeksels met de maximale snelheid te abduceren als de prooi naar binnen spoelt.

Een verhoging van de zwemsnelheid vergroot het gevaar dat de prooi voortgestuwd wordt in het aardvaste assenstelsel (zie boven). Stagnatie-effecten kunnen (deels) worden vermeden door de maximale mondopening te verkleinen bij een vergroting van de zwemsnelheid. Hiermee wordt echter tevens de maximale prooigrootte verkleind. Opening van de kleppen maakt het mogelijk dat ook bij een hoge zwemsnelheid grote prooien kunnen worden gevangen.

Zowel de gemiddelde als de uiteindelijke prooisnelheid kunnen worden vergroot door de prooi voor het tijdstip van de maximale mondopening naar binnen te laten spoelen. Dit is met name van belang als de prooi dicht benaderd kan worden, zoals bij voedselopname vanaf een substraat. Als ook de kieuwdeksels relatief vroeg abduceren wordt dit effect nog versterkt. Het samengaan van een tijdstip van prooiopname voor het tijdstip van maximale mondopening, met een vroeg moment van operculumabductie vinden we bijvoorbeeld bij de koraalduivel. Een beschouwing van de kinematica van de kop levert op dat voor deze wijze van prooivangst een relatief kort hyoid voordelig is. Met korte hyoiden kan echter relatief weinig water worden opgezogen. Aangezien het bezit van een protrusie-apparaat het mogelijk maakt de hoeveelheid opgezogen water te reduceren, vormen relatief korte hyoiden hiermee een goede combinatie.

*Simulaties van drukfluctuaties in de mondholte*

De mechanische belasting tijdens de zuigende voedselopname is veel hoger dan die tijdens de meeste andere activiteiten. Het kunnen voorspellen van de drukfluctuaties in de mondholte tijdens de voedselopname is daarom van belang voor een interpretatie van de bouw van de vissekop. M.b.v. het hydrodynamische model van Muller et al. (1982) zijn drukfluctuaties in de mondholte van de moddersnoek (*Amia calva*), de snoek (*Esox lucius*), de regenboog forel (*Salmo gairdneri*) en de kabeljauw (*Gadus morhua*) gesimuleerd (zie hoofdstuk 3). Hier-

14

toe worden de bewegingen van de mondopening en de operculumabductie op-gemeten vanaf de film en ingevoerd in het model, benevens een aantal andere parameters. De versnellingen van de bewegingen kunnen niet nauwkeurig vanaf de film worden bepaald. De gegenereerde druk is juist erg gevoelig voor variatie van deze versnellingen. Hierdoor kunnen in eerste instantie grote verschillen optreden tussen de gemeten en de gesimuleerde druk. Door geringe veranderin-gen van de modelparameters, binnen de foutengrenzen van de bewegingsregis-tratie, kan echter een zeer goede overeenstemming tussen modeluitkomst en drukregistratie worden verkregen. Dit betekent dat de modelbeschouwing een goede benadering is van het feitelijk optredende zuigproces.

In hoofdstuk 2 wordt beargumenteerd hoe een vis zijn mond zou moeten ex-panderen om de prooivangkans zo groot mogelijk te maken en tegelijkertijd de gegenereerde onderdruk zo veel mogelijk te reduceren.

### *Perspectieven*

De voorspellingen in dit proefschrift van de bewegingen die een vis zou moeten maken om de kans van prooivangst te optimaliseren leveren belangrijke infor-matie voor gedragsstudies van vissen. Een vergelijking van de reactietijd en de vluchtsnelheid van diverse prooien met de snelheid die door de predator aan de prooi gegeven kan worden, kan laten zien welke range van prooien gevangen kan worden. Dit gegeven kan bij oecologische studies of oecologische ingrepen een belangrijke voorspellende waarde hebben.

Vanaf het embryonale stadium dienen door predatoire vissen gedurende elke fase van de groei prooien gevangen te worden. Ook de meeste later niet predatoi-re vissen leven aanvankelijk van levend zoöplankton. De in dit proefschrift aan-gegeven lijn van onderzoek maakt het mogelijk om te voorspellen hoe de groei zou moeten verlopen als het prooiopname-apparaat steeds zo goed mogelijk zou zijn aangepast aan zijn functie. Uit recente studies blijkt dat boven bepaalde afmetingen van de vis een verdere groei onmogelijk is omdat de kans van prooi-vangst te veel is afgenomen (Kremers & Van Leeuwen, in prep.).

Een zeer kritische fase in het leven van de vis is, vanwege de hoge mortaliteit, het larvale stadium. Gedetailleerde kennis van het prooiopname-mechanisme in deze fase maakt een gerichte manipulatie van milieuomstandigheden mogelijk ter verbetering van de levenskansen.

### *Referenties*
Elshoud-Oldenhave, M.J.W. (1979). Prey capture in the pike-perch, *Stizostedion lucioperca* (Teleos-tei, Percidae): A structural and functional analysis. *Zoomorphologie* 93: 1-32.
Kremers, J.J.M. & Leeuwen, J.L. van (in prep.). The influence of growth on the prey capture mecha-nism of the pike (*Esox lucius*).
Lauder, G.V. & Liem, K.F. (1981). Prey capture by *Luciocephalus pulcher:* implications for models of jaw protrusion in teleost fishes. *Env. Biol. Fish.* 6, 257-268.
Leeuwen, J.L. van (in prep.). A quantitative study of flow in prey capture by rainbow trout, with general consideration of the actinopterygian system.
Leeuwen, J. L. van & Muller, M. (in press). Optimum sucking techniques for predatory fish. *Trans. Zool. Soc. Lond.*
Leeuwen, J.L. van & Muller, M. (in prep.). The recording and interpretation of pressures in prey sucking fish.

Muller, M. (1983). *Hydrodynamics of suction feeding in fish*. Proefschrift, Landbouwhogeschool Wageningen.

Muller, M. & Osse, J.W.M. (in press). Hydrodynamics of suction feeding in fish. *Trans. Zool. Soc. Lond.*

Muller, M., Osse, J.W.M. & Verhagen, J.H.G. (1982). A quantitative hydrodynamical model of suction feeding in fish. *J. theor. Biol.* 95: 49-79.

Osse, J.W.M. (1969). Functional morphology of the head of the perch (*Perca fluviatilis* L.): an electromyographic study. *Neth. J. Zool.* 19 (3): 289-392.

# General summary

In this thesis hydrodynamic principles are used to quantify relations between form and function in the prey capture mechanism of actinopterygian fish. This work is closely related to the papers on the hydrodynamics of fish feeding by Muller et al. (1982) and Muller & Osse (in press). The effectiveness of different head forms and movements for prey uptake (in various habitats) is investigated by model simulations and verified by flow visualization and pressure measurements.

Chapter 1 presents a technique to visualize the flow in 3-D around the mouth of the fish, sucking its prey. An expanding and compressing cylindrical or conical model of the fish's mouth cavity is used to quantify the relation between head movements and swimming. The opercular and branchiostegal valves are shown to function as control devices to obtain an optimal flow rate through the mouth aperture. The theoretical predictions were verified experimentally for the rainbow trout (*Salmo gairdneri*). Likewise, data from the literature appeared to agree with these hypotheses.

Chapter 2 quantifies the contributions of the forward movement of the fish, the expansion of the mouth cavity and a possible protrusion of the jaws to the velocity of the prey. Optimum sucking techniques (i.e. techniques maximizing the chance of prey capture) in relation to swimming speed and habitat properties are derived by model simulations. Maximization of the initial prey distance by an exact adjustment of mouth expansion is rather useless for a fish. Much more is gained if the fish abducts its opercula at the maximal rate when the prey enters the mouth.

Chapter 3 discusses recording techniques for pressures in prey-sucking fish. The dynamic properties of different measurement systems are investigated by Fourier analysis. Also, the frequency content of records of the fluctuating pressure inside the fish's mouth during feeding is shown. Prey capture events of different fish species are simulated using the hydrodynamical model of Muller et al. (1982). Measured and simulated pressure curves are compared and the effects of the use of different boundary conditions in the model are discussed. The literature on pressure measurements in prey-sucking fish is reviewed.

*References*

Muller, M. & Osse, J.W.M. (in press). Hydrodynamics of suction feeding in fish. *Trans. Zool. Soc. Lond.*

Muller, M., Osse, J.W.M. & Verhagen, J.H.G. (1982). A quantitative hydrodynamical model of suction feeding in fish. *J. theor. Biol.* 95:49-79.

HOOFDSTUK 1/CHAPTER 1

# A quantitative study of flow in prey capture by rainbow trout, with general consideration of the actinopterygian feeding mechanism.

# A quantitative study of flow in prey capture by rainbow trout, with general consideration of the actinopterygian feeding mechanism.

JOHAN L. VAN LEEUWEN

(Department of Experimental Animal Morphology and Cell Biology,
Agricultural University, Marijkeweg 40,
6709 PG Wageningen, The Netherlands).

## Summary

Prey suction events of the rainbow trout (*Salmo gairdneri*, Richardson) were filmed stereoscopically (175 to 400 frames/sec). Polystyrene spheres (density 1033 kg/m$^3$) were put in the water surrounding the prey, as a means for flow visualization. Individual spheres could be recognized in successive frames, and particle path lines were obtained in 3-D. Additionally, multi-flash photography was used for flow visualization.

The water in front of the trout, containing the prey, appeared almost stationary in an earth-bound frame during feeding (except very close to the mouth), although separate pushing and sucking effects could be distinguished. Hence, the impulse added to this water by the swimming and suction movements of the predator was small. At distances greater than about 15% of the head length ahead of the fish's mouth aperture, the flow towards the mouth (enclosed by the dividing streamline) was close to a uniform stream of varying strength and cross-sectional area. The total volume of water entering the mouth during feeding was about 5.5 times the volume taken up till the actual moment of opercular and branchiostegal valve opening. Thus outflow through the opercular slits is highly important in the suction process. The maximal distance from which water was taken into the mouth was slightly more than the fish's head length.

With a cylinder and cone model it was shown that the mouth of the forward moving fish must expand at least at a threshold rate to prevent pushing of the prey in front of its mouth before the moment of caudal valve opening. The optimal moment of valve opening, such that the volume flow through the mouth aperture is maximized, was calculated from the fish's head length, swimming velocity, mouth radius, mouth expansion rate, opercular abduction and opercular abduction rate. After valve opening the fish must at least reach a threshold translational velocity, to prevent an inflow through the opercular slits. A minor initial inflow through the opercular slits of the rainbow trout was detected. Good agreement was found between theory and experiment. Many morphological and kinematic features of the feeding system of "higher teleosts" serve to generate a unidirectional flow inside the mouth.

Possible feeding strategies of actinopterygian fish in relation to their head construction and swimming velocity were discussed in the light of the above results. Previous papers on feeding mechanisms in fish could be properly explained with the current approach.

21

# Contents

# 1. Introduction

Feeding by suction, accomplished by a rapid expansion and contraction of the buccal and opercular cavities (together denoted as the mouth cavity), generally supported by swimming movements, is the dominant mode of prey capture

in teleost fish (see Osse and Muller, 1980). The mechanical events during prey capture have been amply dicussed (e.g. Alexander, 1967; Anker, 1974 and Osse, 1969). Little attention has been paid to the interaction between the suction and swimming apparatus during prey capture. Nyberg (1971), Osse and Muller (1980), Muller et al. (1982) and Muller and Osse (in press) recognized the importance of pushing induced by swimming. They also found that swimming contributes to directing the flow towards the mouth. This last aspect was also put forward by Weihs (1980). Recently, Muller and Osse (in press) were able to deduce the flow in front of the mouth from the velocity of the water in the mouth aperture and the predator's velocity.

The present paper aims to quantify the relation between the fish's swimming velocity and the expansion rate of the mouth. The approach to this problem was a combination of an experimental flow analysis and the use and elaboration of the hydrodynamical model of Muller et al. (1982) and Muller and Osse (in press). Suction as used in the present paper denotes the contribution to the flow due to mouth expansion.

An analysis of the flow induced by a prey sucking fish shows the amount of energy and momentum put into the water, the force exerted on the prey during its capture, the size and shape of the sucked volume of water and permits one to estimate the chance of prey capture. Furthermore, it checks the validity of hydrodynamical models of prey suction in fish as constructed by Alexander (1967), Weihs (1980) and Muller et al. (1982).

Flow visualization techniques have been used to study the flight of birds and insects (ref. e.g. Kokshaysky, 1979; Spedding, Oxford S.E.B. conference 1980 and Ellington, 1978) and the swimming of fish (see e.g. Hertel, 1966 and McCutchen, 1977). Muller and Osse (1978 and in press) visualized the flow in front of and behind the mouth of a sucking fish. With their method, however, it is hard to trace particle path lines in 3-dimensional space.

The present paper describes a technique for visualizing the flow induced by sucking fish, using high-speed stereoscopic filming and multi-flash stereoscopic photography. Compared to the method of Muller and Osse it provides the coordinates of particle path lines in 3 dimensions and a direct stereoscopic view of the field of flow. Some important conclusions about the feeding mechanism of the rainbow trout (*Salmo gairdneri*, Richardson), such as the relation between the mouth aperture and the maximal flow rate into the mouth and the adjustment of swimming and suction during feeding, are drawn from an analysis of the flow pattern in front of its mouth.

The rainbow trout, a protacanthopterygian, was chosen as the main experimental animal because of relatively primitive features in its feeding mechanism (e.g. short spatiform branchiostegal rays and the absence of a protrusion mechanism of the upper jaws). The study of its feeding mechanism, founded upon a thorough model approach, allows extrapolations to extinct groups as well as to more advanced teleosts.

Using the model, constraints were formulated for the mouth expansion rate and the time of the opening of the opercular and branchiostegal valves as func-

tions of the fish's swimming velocity. They showed good agreement with experimental data and were particularly useful in a general consideration of the actinopterygian feeding mechanism.

## 2. Materials and methods

### 2.1. EXPERIMENTAL SET UP

One specimen each of *Pterois russelli* (lionfish, s.l. 13.8 cm) and *Salmo gairdneri* (rainbow trout, s.l. 34.3 cm) were used in the analysed experiments. (Feeding acts of other specimens of *Salmo gairdneri* were filmed and used for a qualitative comparison with the above specimen.) The lionfish was kept in a tank of 80x40x40 cm at 25 °C. It was fed with live or freshly killed fish. The trout was fed with live fish (*Barbus conchonius*) or chopped cow heart and kept at 15°C in a 190x60 cm tank, with water 20 cm deep. The size of the aquarium allowed swimming velocities of more than 2 m/sec. The nitrite content of the water was checked weekly, and always found to be less than 0.05 mg/l. The oxygen content was always above 80% of the saturation.

To visualize the flow unexpanded polystyrene spheres (density 1,033 kg/m³) were put in the water surrounding the prey, as was done by Muller and Osse (1978). For the lionfish, spheres of 0.5 mm diameter were used; for the trout a mixture of 0.5 mm and 1 mm spheres. With the lionfish the density of the water was adjusted to match that of the spheres by slightly varying the salinity. This could not be done for the trout. Hence, a difference of 0.034 kg/m³ between the density of the spheres and the water had to be accepted. The sinking speed of the 0.5 mm and 1 mm spheres in quiet water was 4.4 mm/sec and 10.2 mm/sec respectively. The prey was always sucked into the mouth within 50 msec. During this time the displacement due to gravity is 44% of the diameter for 0.5 mm spheres and 51% for 1 mm spheres.

Feeding events of both fishes were filmed at 175 to 400 frames/sec, using a Teledyne DBM 54 16 mm high-speed camera with an Angénieux 10x12A zoom lens. Filming was done with KODAK double-X negative films (25 DIN / 250 ASA). Films were taken with continuous light (power input of 12 kW, effectively, however, almost 24 kW due to focussing) and an exposure time of $4000^{-1}$ sec in most cases. Warming of the aquaria by the filming lights was reduced by filtering out the red part of the spectrum and cooling of the water in the aquaria. The temperature increase never exceeded 1°C.

The animals were trained to feed under the high light intensities before films were taken. Training lasted about 2 weeks or longer when needed. The prey was often jerked from the water with a nylon thread to elicit forceful and rapid feeding acts. As the trout leaped out of the water to the food during training as it does in the wild, the filmed sequences are presumably close to normal feeding behaviour. For both *Pterois* and *Salmo* more than 20 feeding acts were filmed. All films of *Pterois* were taken by Mr. M. Muller and will be discussed

24

elsewhere in detail (ref. Muller and Osse, in press).

To reveal the direction of the flow near the opercular slits black cotton threads (approximate length 1 cm) were sewn to the specimen of *Salmo gairdneri* near the right slit, at the positions indicated in Fig. 10. During sewing the animal was anesthetized in a solution of MS 222 (80 mg/l). It recovered within half an hour. Next day 14 feeding acts were filmed. No abnormal behaviour was observed.

Apart from the cine filming, photographs were taken during several feeding attempts using a NIKON camera with a 55 mm macro lens. Lightning was by three Braun 410 VC electronic flash units in the variopower mode. Flash duration ranged from 0.1 to 0.4 msec. An electronic device was built to obtain three sequential flashes (for one exposure) at intervals in the range from 0.5 to 7.5 msec, with a preset accuracy of 0.1 msec. Flashes were recorded with a photodiode and the sequence displayed on a storage oscilloscope screen. So the intervals could be measured. Sequential flashing was used to obtain particle path- and streamlines around the fish's head, with accuracy up to 6 times that of cine filming.

### 2.2. THE ACQUISITION OF A THREE DIMENSIONAL PICTURE

Initially films were taken with a mirror placed at 45° to the horizontal plane ventrally from the fish. This was done in all films of *Pterois*. Both a lateral (or
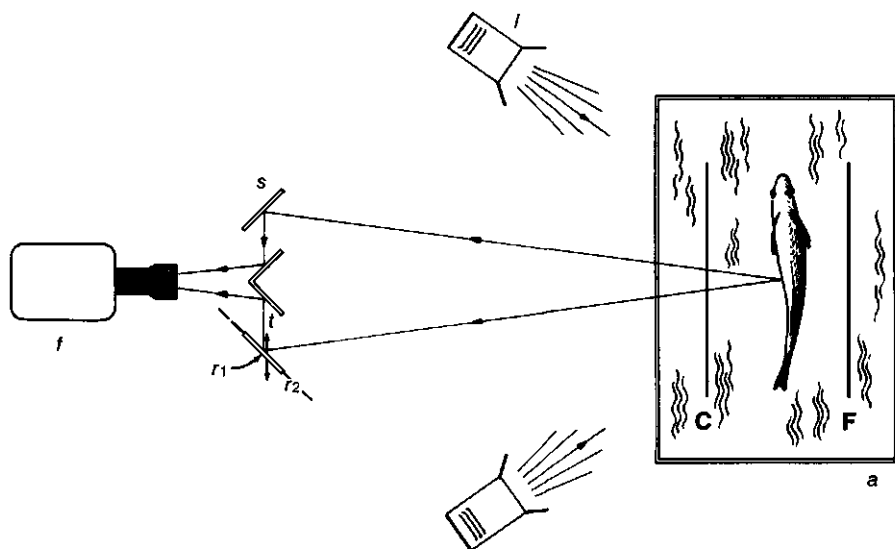


Fig. 1. A diagrammatic representation of the experimental set up seen from above. Abbreviations: *a*, aquarium with fish; **C**, control plane of calibration frame; *f*, film camera; **F**, fiducial plane of reference frame; *l*, filming lights; $r_1$, $r_2$ axes of possible rotations of the outer mirrors; *s*, stereo adaptor with surface mirrors; *t*, direction of possible translation of the outer mirrors. Further explanations are given in the text.

frontal) and a ventral view of the fish were so obtained. However, it was almost impossible to obtain the three dimensional coordinates of the polystyrene spheres as it was hard to recognize individual spheres on both views. Therefore the mean velocity between successive frames of the film could be estimated only roughly.

In later experiments, all those with *Salmo*, a stereoscopic method was used (see Fig. 1). A set of mirrors was positioned in front of the objective of the camera to record a stereoscopic pair of pictures on each frame. Two aluminized front-surface mirrors (flatness < 1 nm, quartz coated, 50x80 mm each) were positioned directly in front of the objective at a distance of about 3 cm, at 45° to the plane of the objective. At both sides slightly larger mirrors (75x100 mm each) were positioned, almost parallel to the nearest medial one, but slightly toed in so as to get two stereoscopic views of the same scene on each film frame. The distance between these mirrors could be varied. To obtain an optimal accuracy this distance was as big as could be without making the views so different that the mind could not fuse them into a three dimensional impression. An almost lateral view of the fish thus obtained was sometimes combined with a ventral view. The film could be watched in stereo by using the mirror set up as a stereoviewer. The position of individual spheres or selected points on the fish could be seen in space and their coordinates could be calculated accurately (see paragraph 2.4.) if stationary reference markers were put in the aquarium. Two parallel black bars, set 295 mm apart in a rigid frame, were used. Each bar bore white dots (diam. = 0.85 mm), with known Cartesian coordinates. The bars were set in a plane about parallel to the plane of the objective.

Account was taken of all rotations made by the fish during suction when measurements of moving head parts of the fish were made. A ventral view of the fish is needed to measure suspensorial and opercular abduction. Lens aberations were measured but appeared to introduce no significant errors. The stereo adapter used for cine filming was also applied in the multi-flash photography experiments.

### 2.3. THE ACQUISITION OF PARTICLE PATH- AND STREAMLINES; EARTH-BOUND AND MOVING FRAME

The curves described by the fluid particles in time are called path lines. Streamlines are everywhere tangential to the instantaneous velocity in the fluid. Path lines can be obtained by printing subsequent frames of a high-speed movie over each other and connecting the successive images of the individual spheres by solid lines. Path lines are directly obtained (in an earth-bound frame) when multi-flash photography is applied.

The recognition of particular spheres in successive frames is a prerequisite for this method. With the stereoscopic technique a clear three-dimensional view is obtained, and it is usually easy to follow chosen spheres. The path lines can be seen as dotted lines in three dimensional space, by printing successive frame over each other. The flow direction can be made unambiquous by using different

26

exposure times when printing the successive frames over each other. So the dotted line appears heaviest at, for example, the early end.

The flow can be described in different ways. One can consider the flow relative to an earth-bound frame. The frame of reference (e.g. the aquarium) is kept stationary. Thus fiducial bars are kept in the same position when successive frames of the film are printed over each other. Or one can analyse the flow relative to a particular part of the moving fish, keeping that part in a fixed position when the photographs are printed or analysed (See also Muller et al., 1982 and Muller and Osse, in press). In the present paper, the centroid of the mouth aperture, $M$, (the point halfway along the line between the most rostral points on the snout and the symphysis of the lower jaws, see Fig. 3A) was the datum for the moving, "fish-bound" frame. The earth-bound frame must be used to calculate forces and impulses. For prey capture the flow with respect to the moving frame is most useful.

When velocities change relatively little between two successive frames, path lines approximate streamlines. However, suction feeding in fish is a highly unsteady process. In the mouth aperture of a sucking trout the absolute value of the velocity might increase about 0.5 m/sec per msec in the fish-bound frame, an acceleration of $50g$ (Osse and Muller, 1980).

Thus during the worst period, the first 15 msec of the suction process, the streamline pattern might change dramatically in and near the mouth aperture in 2.5 msec, the smallest time interval between two successive frames, and path lines are far from being streamlines. At other times path- and streamlines will be less dissimilar.

Although accelerations of the fish are generally less than those of the water entering the mouth in the fish-bound frame they can approach values of $10g$ at some stages of the suction process. Thus an increase of about 0.25 m/sec in fish velocity might occur between successive frames, using a film speed of 400 fr/sec.

The accuracy of calculations of fluctuations in the velocity (and thus of the streamlines) increases when a higher filming rate is used. However, the distance travelled by the particles from frame to frame decreases with a higher frame rate, thus increasing the error in the calculation of the mean velocity between successive frames. In the appendix (7.1.) it is shown that for the present velocity range a filming rate of about 200 fr/sec gives most reliable velocity data.

The path lines of the polystyrene spheres will generally deviate from the fluid path lines due to the density difference between spheres and fluid. In 0.1 sec the sinking distance due to gravity is about equal to the sphere diameter for both the 0.5 mm and 1 mm spheres (see paragraph 2.1.). When the path lines are curved the spheres will deviate from the fluid path lines (centrifugal effect). This is unimportant when the centripetal acceleration of the fluid is no bigger than the gravitational acceleration, a condition fulfilled, except close to the edges of the mouth, where higher accelerations were observed (up to $10g$).

Particles entrained in a shearing flow will suffer lift forces in the direction of the velocity gradient (Merzkirch, 1974), and again particle path lines will

27

differ from fluid path lines. In the case of a sucking fish the largest velocity is likely to occur at the centre of the field of flow. Hence the polystyrene spheres will tend to deviate to the centre. This effect, however, will be negligible when the dimensions of the particles are small relative to the dimensions of the fine structure of the field of flow to be studied (Merzkirch, 1974). During more than 50% of the suction event the mouth diameter is an order of magnitude larger than the largest sphere diameter. During this phase passes more than 90% of the total volume to be drawn into the mouth (see Fig. 12). Only at the start and end of the suction event, when the mouth aperture is smaller, might quite large deviations of the spheres from the fluid streamlines be present.

At any solid wall fluid is stationary, and large velocity gradients will be found in the boundary. Large accelerations round the fish's lips will likewise cause large gradients. Spheres of 0.5 mm are too large for a study of the flow in this area (Merzkirch, 1974), but will nevertheless follow the streamlines much better than most food particles.

## 2.4. CALCULATION OF POSITION- AND VELOCITY VECTORS IN 3-D

Displacements, and hence the velocities of the polystyrene spheres can be calculated using reference markers mentioned earlier. (Care must be taken that
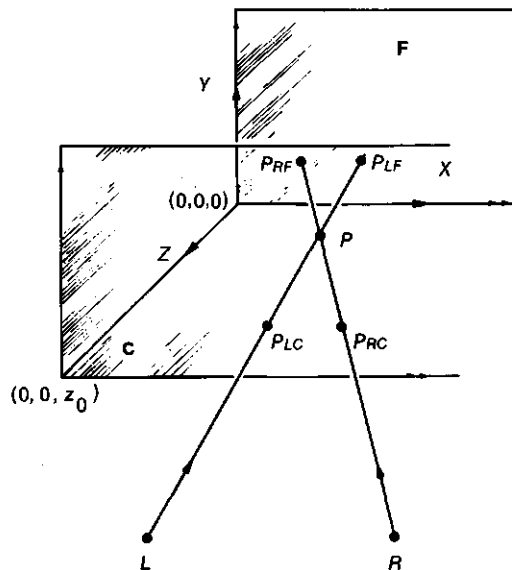


Fig. 2. Frame of reference for the calculation of the coordinates of points in 3-D. Lines $P_{LF} P_{LC}$ and $P_{RF} P_{RC}$ are seen as one point in the left ($L$) and right ($R$) pictures of a stereograph. Abbreviations: C, control plane; F, fiducial plane; P, point in space; $P_{LC}$ and $P_{LF}$, left projections of $P$ on planes C and F; $P_{RC}$ and $P_{RF}$, right projections of $P$ on C and F; $X,Y,Z$, axes of reference frame; $z_0$, distance between planes C and F.

these markers fall within the depth of focus). A simple method of calculation was used. A list of symbols used is given in Table 1. A more advanced method, applied to X-ray photogrammetry, can be found in Selvik (1974), where statistical methods and a special calibration procedure are used to improve the accuracy of the method.

Suppose that a set of reference points is put in a plane $F$ (the fiducial plane) and another set in plane $C$ (the control plane), parallel to $F$ (see Fig. 2). Let the distance between the planes be $z_0$. A Cartesian coordinate system is defined with the $Y$- and $X$-axis in $F$ and the $Z$-axis perpendicular to $F$. The coordinates of a point $P$ are denoted as $(x_P, y_P, z_P)$.

The two pictures of a stereoscopic pair are denoted with $L$ (left) and $R$ (right). The projections of $P$ on $F$ and $C$ in $L$ are denoted as $P_{LF}$ $(x_{LF}, y_{LF}, z_{LF})$ and $P_{LC}$ $(x_{LC}, y_{LC}, z_{LC})$. Similarly for $R$. The coordinates of the projections of $P$ on $F$ and $C$ for $L$ and $R$ can be measured from a stereoscopic pair of pictures. $P$ lies on the intersection of the lines $P_{LF} P_{LC}$ and $P_{RF} P_{RC}$.
The equation of $P_{LF}P_{LC}$ is:

$$
\begin{pmatrix} x_L \\ y_L \\ z_L \end{pmatrix} = \begin{pmatrix} x_{LF} \\ y_{LF} \\ z_{LF} \end{pmatrix} + \frac{z_L}{z_0} \begin{pmatrix} x_{LC} - x_{LF} \\ y_{LC} - y_{LF} \\ z_{LC} - z_{LF} \end{pmatrix} \tag{1}
$$

Table 1: Symbols and notation
All physical quantities are expressed in SI units.

| | |
|---|---|
| $a$ | Parameter describing relation between $U_f$ and $u'_1$ as a result of suction. |
| $A$ | Cross-sectional area of expanding and compressing profile. |
| $b$ | Parameter describing relation between $U_f$ and $u'_1$ as a result of suction and swimming |
| $B$ | Range of oscillating velocity (see 7.2.) |
| $C$ | Control plane |
| $c, d$ | Constants used in correction for perspective distortion |
| $f$ | Frequency of oscillating velocity (see appendix 7.1.) |
| $F$ | Fiducial plane |
| $g$ | Gravitational acceleration |
| $h(x',t)$ | Profile radius |
| $h; h_1, h_2$ | Radius of cylinder; radius at $x' = l$ and $x' = 0$ |
| $\dot{h}; \dot{h}_1, \dot{h}_2$ | Expansion rate of cylinder; anterior and posterior expansion rates of cone |
| $\dot{h}_t, \dot{h}_{1,t}$ | Threshold expansion rates for cylinder and cone model |
| $\dot{h}_c, \dot{h}_{1,c}$ | Critical expansion rates for cylinder and cone |
| $h_{1\,effective}$ | Effective radius of the mouth aperture |
| $i$ | Frame number of film |
| $l$ | Length of cylinder, cone and fish's head |

29

| | |
|---|---|
| $L$ | Left picture of stereograph |
| $M$ | Centroid of mouth aperture |
| $P$ | Point in space |
| $P_{LF}, P_{LC}$ | Projections of $P$ on $\mathbf{F}$ and $\mathbf{C}$ in $L$ |
| $P_{RF}, P_{LC}$ | Idem for $R$ |
| $P_{ebf}$ | Point where the water is at rest in the earth-bound frame |
| $P_{mf}$ | Idem for moving frame $X', Y', Z'$ |
| $P_{1ebf}, P_{2ebf}$ | Points of zero flow in cone with open valves in earth-bound frame during mouth closure phase. |
| $P_{1mf}, P_{2mf}$ | Idem for moving frame $X', Y', Z'$ |
| $\mathbf{q}; q$ | Velocity vector in earth-bound frame; idem for speed (scalar) |
| $\mathbf{q}', q'$ | Idem in moving frame |
| $q'_{prey}$ | Speed of the prey in the moving frame |
| $\mathbf{q_m}, \mathbf{q_o}$ | Mean velocity and oscillating velocity as defined in 7.1. |
| $\mathbf{Q}; Q$ | Velocity of the origin of the moving frame, $M$, in the experimental approach; idem for speed |
| $R$ | Right picture of a stereograph |
| $r_{asymptote}$ | Radius of asymptote of dividing streamline |
| $\mathbf{s}$ | Distance along contour |
| $S$ | Scale factor explained in appendix 7.2. |
| $t; t_i$ | Time; Moment at which frame $i$ was taken |
| $t_{h2max}$ | Moment of maximal opercular abduction |
| $t_{prey}$ | Moment of prey passage through mouth aperture |
| $u_i, v_i, w_i$ | Velocity components of $\mathbf{q}$ in $X$-, $Y$- and $Z$-directions at frame $i$ |
| $U_i, V_i, W_i$ | Idem for $\mathbf{Q}$ |
| $u', r', t'$ | Velocity components in cylindrical coordinates in moving frame |
| $U_f$ | Velocity of cylinder, cone or fish in model approach |
| $U_t$ | Threshold translational velocity |
| $u'_1$ | Velocity at $x' = l$, relative to moving frame |
| $u'_2$ | Idem for $x' = 0$ |
| $u'_v(x',t)$ | Velocity of water in moving frame before valve opening |
| $w_l$ | Half of the width of the mouth aperture |
| $x'_{rc}, x'_{ro}$ | Positions of $P_{ebf}$ before and after valve opening |
| $x, y, z$ | Cartesian coordinates in earth-bound frame |
| $X, Y, Z$ | Axes of earth-bound frame |
| $x', y', z'$ | Cartesian coordinates in moving frame |
| $X', Y', Z'$ | Axes of moving frame |
| $x_{AP}, y_{AP}$ | Actual projected coordinates of $P$ on distorted plane |
| $y_{DP}$ | Explained in 7.2. |
| $x_{\perp P}$ | Coordinate of $P$ along $X_\perp$-axis |
| $X_\perp$ | Axis defined in 7.2. |
| $z_o$ | Distance between planes $\mathbf{F}$ and $\mathbf{C}$ |
| $\delta\mathbf{q_m}, \delta\mathbf{q_o}$ | Error in $\mathbf{q_m}$ and $\mathbf{q_o}$ |
| $\delta t, \delta x$ | Errors in determination of time and position |
| $\tau_a, \tau_i$ | Actual and ideal moments of valve opening |

30

and for $P_{RF} P_{RC}$:

$$\begin{pmatrix} x_R \\ y_R \\ z_R \end{pmatrix} = \begin{pmatrix} x_{RF} \\ y_{RF} \\ z_{RF} \end{pmatrix} + \frac{z_R}{z_0} \begin{pmatrix} x_{RC} - x_{RF} \\ y_{RC} - y_{RF} \\ z_{RC} - z_{RF} \end{pmatrix} \qquad (2)$$

At the intersection of the two lines $z_L = z_R = z_P$, hence:

$$\frac{z_P}{z_0} = \frac{x_{RF} - x_{LF}}{(x_{LF} - x_{LC}) - (x_{RF} - x_{RC})} = \frac{y_{RF} - y_{LF}}{(y_{LF} - y_{LC}) - (y_{RF} - y_{RC})} \qquad (3)$$

The mirror set up is positioned almost parallel to the $X$-axis. Hence the $X$-parallax will be much larger than the $Y$-parallax. Thus the expression in $x$ for $z_P$ should be used in calculating $P$. The coordinates of $P$ are found by substituting $z_P$ for $z_L$ in equation (1). The optical axes of the left and right views are not perpendicular to planes **F** and **C**. Hence, these planes will be subject to perspective distortions, leading to errors in the measurements of the projections of $P$ on both planes up to 5%. Because this would cause serious errors in the calculations of the $z$-coordinates, the measurements from the film were corrected for perspective distortions before the above calculations were carried out (the correction is explained in appendix 7.2.).

The positions of $P$ can be calculated for a particular sequence of frames (each representing a stereoscopic pair). The distance travelled by $P$ between successive frames can be calculated by using three-dimensional Pythagoras. The components in the $X$, $Y$ and $Z$-directions $u_i$, $v_i$ and $w_i$ of the velocity **q** (a vector) of $P$ for a particular frame $i$ were calculated with the following formulas:

$$u_i = \frac{x_{i+1} - x_{i-1}}{t_{i+1} - t_{i-1}}$$

$$v_i = \frac{y_{i+1} - y_{i-1}}{t_{i+1} - t_{i-1}} \qquad (4)$$

$$w_i = \frac{z_{i+1} - z_{i-1}}{t_{i+1} - t_{i-1}}$$

where $(x_{i-1}, y_{i-1}, z_{i-1})$ are the coordinates of $P$ at the foregoing frame $i$-1, and $t_{i-1}$ the time at which frame $i$-1 was taken. Similarly for the next frame $i + 1$. The speed $q$ (a scalar quantity) of $P$ is given by:

$$q = \sqrt{u^2_i + v^2_i + w^2_i} \qquad (5)$$

The velocity of $P$ can also be calculated relative to a particular (moving) point $M$, with velocity $\mathbf{Q} = \mathbf{U_i} + \mathbf{V_i} + \mathbf{W_i}$. The "relative velocity components" are given by:

$$(u_i - U_i), (v_i - V_i), (w_i - W_i). \qquad (6)$$

The directions of the above components are defined by the reference frame. However, the relative velocity will be more informative when resolved into com-
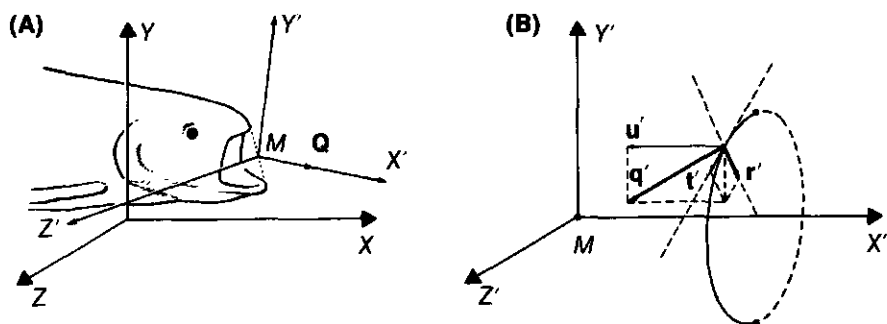
31

Fig. 3. A. Drawing showing the earth-bound frame, with $X$-, $Y$- and $Z$-axes and the moving frame with $X'$-, $Y'$- and $Z'$-axes. In this figure the centroid of the mouth aperture, $M$, is chosen as the origin of the moving frame. In paragraph 3.2. the mouth aperture is taken at $x' = l$. The $X'$-axis is chosen along $Q$, the velocity of the fish in the earth-bound frame.
B. The velocity $q'$ in the moving frame $X', Y', Z'$ can be calculated in cylindrical coordinates with components $u'$, $r'$ and $t'$, in the $X'$-, radial and tangential direction respectively. $M$ represents the origin of the moving frame.

ponents whose directions follow the orientation of the fish (see Fig. 3), with perpendicular axes $X'$, $Y'$, $Z'$. The $X'$-axis was chosen in the direction of movement of the fish, thus along $Q$ and the $Z'$-axis parallel to the $ZX$-plane. The centroid of the mouth aperture $M$ was chosen as the origin of the moving frame. For practical reasons, however, in paragraph 3.2. $M$ will be laid along the $X'$-axis at $x' = l$, where $l$ is the fish's head length. This last frame equals the moving coordinate system chosen by Muller et al. (1982) when they are concerned with the flow inside the mouth. For this transformation, which involves both rotation and translation for each frame of the film to be analysed, standard formulas were used (See Spiegel (1968), p. 49). Cylindrical coordinates (Spiegel, 1974; ps. 137, 138 and 143) proved to be useful for the expression of the velocity in the moving frame, as the sign of the radial component shows directly whether the flow is contracting or diverging. The coordinate systems and velocity components are illustrated in Fig. 3.

The above calculation can be carried out for each of a chosen set of polystyrene spheres throughout the suction act of the fish. The results obtained have a maximal error of about 1 to 1.5 mm in the calculated positions of the spheres. This was determined with a calibration object bearing a set of points whose coordinates were known to the nearest 0.05 mm. The same calculations can be performed for the multi-flash experiments. The complete capture event cannot then be traced, but the accuracy of measurements increased to about 0.3 mm. The maximal error in the velocity calculations from the cine films was about 0.15 m/sec.

All calculations were carried out by means of FORTRAN-programs run on a MINC-11-computer (Digital) and the DEC-10 system of the Agricultural university.

32

Fig. 4. A composition of three successive frames of a 200 fr/sec film of a feeding *Pterois russelli*. Thus this picture represents a time interval of 10 msec (at 21% to 32% of the phase that a mouth aperture is present). The white dots represent polystyrene spheres. The mouth aperture was kept at a fixed position during successive printing. Thus the flow is visualized in the fish-bound frame. The estimated dividing streamline is shown by dashed curves. Upper part: lateral aspect; lower part: ventral aspect, obtained via a mirror. A 10 mm scale is present at the left side of the picture.

## 3. Results

### 3.1. EXPERIMENTAL OBSERVATIONS

*3.1.1. Pterois*

Both ventral and lateral views at a certain stage of a feeding event of *Pterois russelli* are shown in Fig. 4. Three successive frames of a 200 fr/sec film were printed over each other. The mouth aperture of the fish was kept at a fixed position, hence the path lines shown are relative to the sucking fish. Only when a particular sphere was unequivocally followed from exposure to exposure was a path line constructed. A striking feature of Fig. 4 is the directedness of the flow. The flow is discussed in more detail in Muller and Osse (in press).

33

### 3.1.2. *Salmo: observations from cine film and multi-flash photography*

Fig. 5 shows a stereograph of a feeding *Salmo gairdneri*. The frame was taken just before prey capture and peak mouth gape.

Fig. 6 shows three stages in the course of the same feeding event. The flow was visualized relative to an earth-bound frame. Two successive frames were printed over each other for each stage. These pictures show that whereas the fish was in motion the water in front of its mouth was almost at rest, as is apparent from the positions of the spheres and prey. This observation suggests that the flow is highly directed relative to the fish.

The flow relative to the centroid of the fish's mouth is shown in Fig. 7, a stereograph of another feeding act of *Salmo gairdneri*. As expected from Fig. 6 the flow contracted only slightly towards the mouth. The estimated height of the dividing streamline far from the mouth was about the same as the height of the fish, as predicted by Muller et al. (1982). (The dividing streamline is the instantaneous boundary that envelops the water that tends to flow into the mouth).

Fig. 8 shows the results of a movement analysis of the feeding event of Figs. 5 and 6. The plots of mouth opening and opercular abduction show a delay
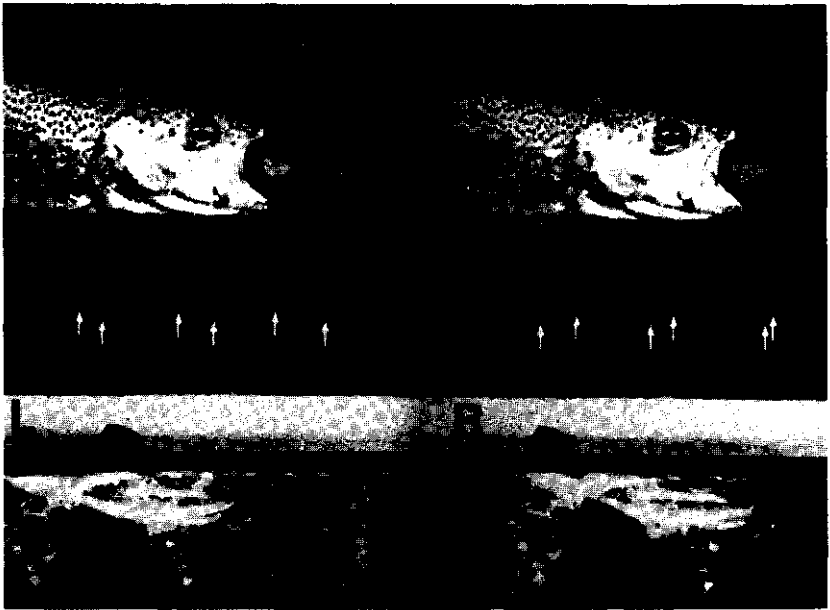


Fig. 5. A stereoscopic pair of pictures of a feeding *Salmo gairdneri*, printed from a frame of a high-speed movie (about 175 fr/sec). An image with depth can be obtained when these pictures are seen through a simple pocket stereoscope (or directly by a trained person). The points denoted with arrows are part of a reference frame used for calculation of coordinates (distance between subsequent points is 5 cm, see paragraph 2.4.). Other white dots represent polystyrene spheres, used for flow visualization. This picture shows a moment just before the maximal mouth opening and prey capture. *L* and *R* denote left and right pictures of stereograph.

34

between rostral and caudal expansion. The branchiostegal and opercular valves (caudal valves) opened relatively early, before the maximal mouth opening had been reached and before the operculars had reached half of their maximal abduction. This is not so in several other fish species (see Muller and Osse, in press). The prey entered the mouth at the moment it was opened widest, as was noted also by Muller and Osse (in press). The mouth closed faster than it opened. Perhaps this increases the chance of prey capture. The plot of the distance between the prey and the centroid of the mouth aperture (this point is depicted in Fig. 3) as a function of time did not deviate much from a straight line, nor did the displacement curve of the centroid of the mouth aperture whose slope was opposite and about equal in magnitude. These two curves show that the speed of the predator was fairly constant and that most of the time the prey was almost at rest in an earth-bound frame. Careful analysis, however, showed that the prey was initially slightly pushed forward, about 2 mm, by the fish. Then for a period it was stationary, so that no significant impulse was given to it. This situation altered when the prey was 20 mm away from the mouth aperture (about 25% of the fish's head length). From this moment on the prey moved towards the mouth in an earth-bound frame, but at a much lower speed than that of the predator (see also Fig. 6, A and B and chapter 2).

To investigate the flow at other places the movements of three polystyrene spheres were analysed. Their positions at the start of the suction process are shown in Fig. 13. They were all slightly pushed away by the predator (in an earth-bound frame) when they came close to the mouth. This is shown by the upward curving of the graphs of the distances between the spheres and the centroid of the mouth aperture given in Fig. 8. This slope is also influenced by the velocity of the predator. A check on this, combined with the actual positions of the spheres in an earth-bound frame as functions of time revealed, however, that changes in the velocity of the fish were of minor importance in this respect.

Sphere 1, originally situated between the fish and the prey, was drawn into the mouth preceding prey capture. Sphere 2 was originally situated above the prey, near the boundary of the volume of water eventually sucked in. Before it entered the mouth it was also pushed away, demonstrating that during this phase the speed in the moving frame increased towards the $X'$-axis (depicted in Fig. 3). The same phenomenon was observed by Nyberg (1971) for the large mouth bass (*Micropterus salmoides*). The third sphere was not sucked into the mouth, but pushed away just before and after the mouth closed.

Flow patterns were also examined using multi-flash stereoscopic photography with decreasing intensity in successive flashes. Over one hundred fifty stereographs were taken, each comprising 3 exposures in 5 msec, of the same number of feeding acts of *Salmo gairdneri*. The stage of the feeeding act at which each photograph was made could be identified easily with the information from the high-speed film A series of stereographs at stages throughout the feeding act (obtained from different feeding events) is shown in Fig. 9.

The experiment with threads revealed a minor inflow through the caudal parts of the opercular slits just after caudal valve opening, followed by a significant
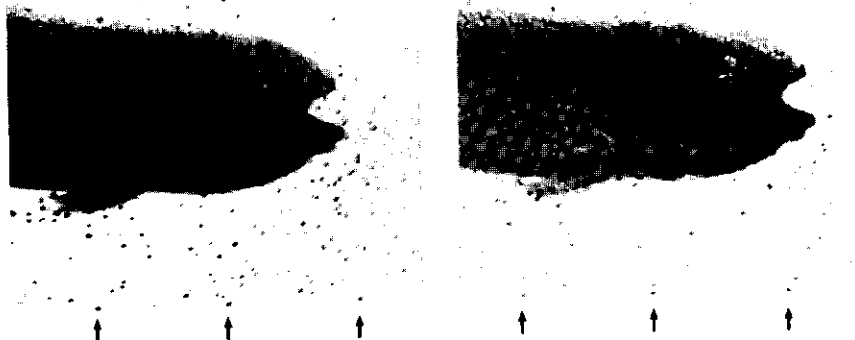
35

**(A)**
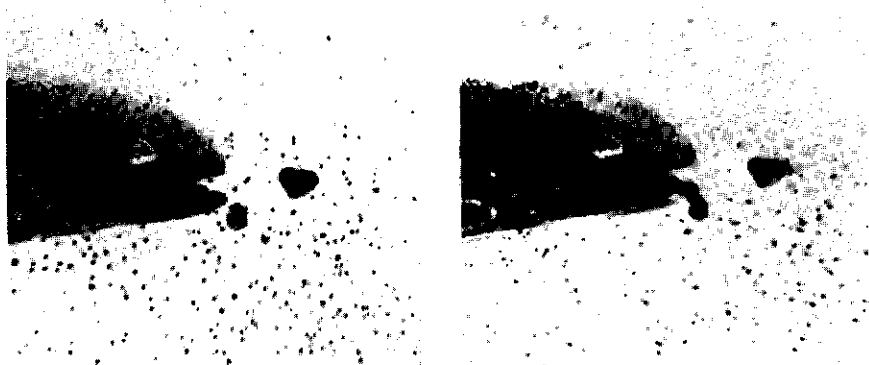


**(B)**
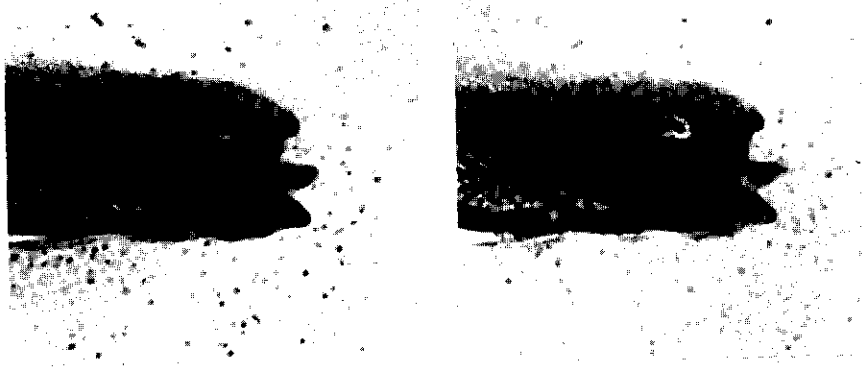


**(C)**



Fig. 6. Flow visualization in an earth-bound frame of some stages of the same feeding event of *Salmo gairdneri* as presented in Fig. 5. Two successive frames, each representing a stereograph,

36

**PLAATSINGSKENMERK** (stack number) NNO8200,946/8201946

**BOEK** (monograph)
auteur (author): Leeuwen, J.-l.
titel (title): Prey capture met technique en fish.

**TIJDSCHRIFT** (periodical)
titel (title):

FOTOKOPIE: JA / NEEN
PHOTOCOPY: YES / NO

deel (vol.nr):                     afl.nr (issue nr):                     jaar (yr):                     pag. (page):

**AANGEVRAAGD DOOR** (requested by):
naam: J- Verlingten
adres: Gravelstaa weg 13

datum:                                              evt. instituut:

Dit formulier is ALLEEN bestemd om werken uit de magazijnen ter inzage aan te vragen.
(This form is meant only to request items from our closed stacks within this library.)

CB 43a

outflow (see Fig. 10). Just before mouth closure a second minor inflow was detected. Fig. 9 and 10 are further explained in section 3.2.

### 3.1.3. Salmo: velocity- and volume calculations

Mouth expansion causes water to flow rearward in front of and inside the mouth in an earth-bound frame. This mass of water has rearward momentum. Mouth expansion adds also forward momentum to the fish and an additional mass of water posteriorly inside the mouth (see Muller and Osse, in press and 3.2.1.). The latter effect cannot be easily demonstrated by an increase in the velocity of the centroid of the mouth aperture, because it is superimposed on presumably larger effects due to swimming. The fish's forward velocity was about 1.3 m/sec (about 3 body lengths/sec). The slight oscillations (about 40 Hz) in the curve of the speed of the centroid of the mouth aperture, given in Fig. 11, cannot result from snout motions caused by swimming, because at a speed of 3 body lengths/sec the swimming undulations occur at about 5 Hz. The 40 Hz oscillations may be due to mouth opening and closure movements of the jaws or errors in the velocity calculation.



Fig. 7. Visualization of the flow induced by *Salmo gairdneri*, relative to the fish. Two successive stereographs of a high-speed movie (200 fr/sec) were printed over each other, representing the phase that the mouth had reached about 90% of its maximal aperture. The centroid of the mouth aperture was kept at a fixed position. Note the directedness of the flow.
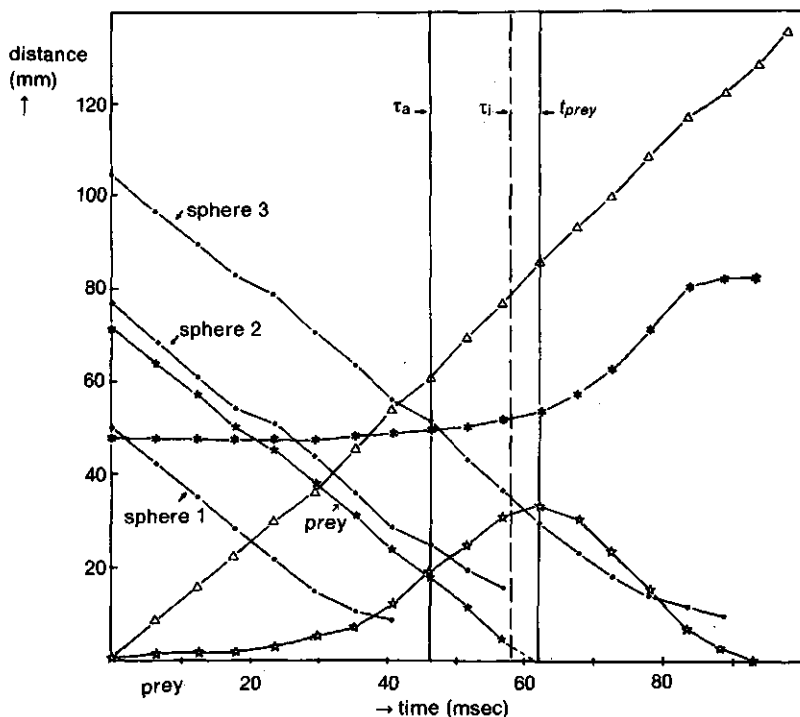
37

Fig. 8. Plots of a movement analysis of the prey capture event of Figs. 5 and 6 of *Salmo gairdneri*. Symbols used: ☆–☆ The height of the mouth aperture; *–* Distance between the caudal edges of the left and right opercula (the opercular abduction); △–△ The distance travelled by the centroid of the mouth aperture (depicted in Fig. 3); ★–★ The distance between the centroid of the mouth aperture and the prey (a piece of cow heart). The distances between 3 polystyrene spheres and the centroid of the mouth aperture are denoted near their respective graphs. The initial positions of the prey and polystyrene spheres are depicted in Fig. 13. The vertical line denoted with $\tau_a$ represents the moment of the actual start of the opening of the opercular and branchiostegal valves. The dashed line depicted with $\tau_i$ denotes the ideal moment of valve opening discussed in paragraphs 3.2.2. and 3.2.3. The vertical line denoted with $t_{prey}$ stands for the moment that the prey passed the mouth aperture. Further explanations are given in the text.

Fig. 9. A series of stereographs of *Salmo gairdneri* obtained by multi-flash photography (3 flashes were used). Polystyrene spheres were used for flow visualization. A decreasing light output was used from the first flash to the third one, so that structures are printed darker with increasing time. Obviously, the flow is visualized relative to the earth-bound frame. Events are described relative to this frame. Stereographs (A) to (D) represent different stages in the activity of the feeding mechanism, however, obtained from different feeding acts. Time intervals between successive flashes were 2.5 msec. The speed of the fish (m/sec) is denoted near each stereograph. The pictures do not show all details given in the description as there were not enough polystyrene spheres at all places of the field of flow in one picture. Missing details were obtained from other feeding acts.
A. Phase just after the moment of mouth opening. Water was sucked towards the mouth aperture and pushed by the fish's lips and other head parts. A circulation around the fish's expanding mouth was started. An anterior 'vortex' was formed due to suction and a posterior one due to forward motion of the fish (see paragraph 3.2.1.). The posterior vortex is partly replaced by the fish's body and therefore difficult to recognize. Only the dorsal aspects of the vortices can be seen in the illustration.
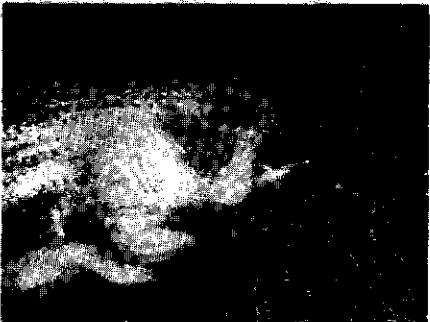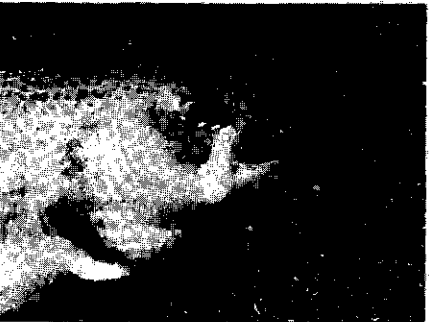
38
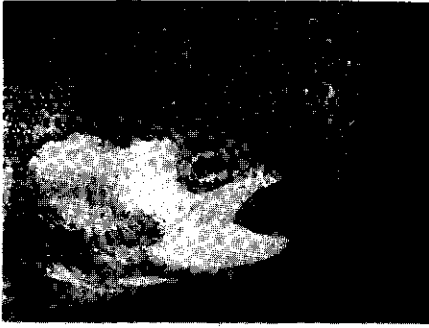
**(A)** 1.65 m/s

**(B)** 1.36 m/s

**(C)** 1.76 m/s

**(D)** 1.45 m/s

Fig. 9.

B. Flow at the moment of the opening of the caudal valves. The circulation of water continued to be present. Water was sucked towards the mouth. The prey started to be moved in the direction of the mouth aperture. The speed of the predator, however, was very much higher. Water was pushed by the forward moving the lips, neurocranium and mouth bottom. Seemingly, quite some water is sucked into the mouth from above the neurocranium, from underneath the mouth bottom and from the cheeks. However, the considerable forward motion of the fish prevents most of this water to enter the mouth. In fact, the flow is highly directed relative to the fish's mouth (see Fig. 7 and 21). This stresses the importance to make a distinction between earth-bound and moving frame.

C. Phase after the maximal mouth opening. Water continued to flow towards the mouth aperture due to the continuing caudal expansion. Note the pushing effects of the fish's head. Two 'vortices' were present around the fish's head (see 3.2.4.). In the moving frame the flow inside the mouth was unidirectional (in a caudal direction). Water outside the mouth flowed towards the caudal parts of the opercular slits, however, a net caudal outflow still exists. The prey was already captured.

D. Phase just before mouth closure. Water was very slightly pushed forward in the mouth aperture. From other multi-flash pictures and the thread experiment (Fig. 10) it appeared that a clear outflow through the rostro-ventral parts of the opercular slits during this phase exists, whereas a slight inflow through the caudal parts of the slits is present. Presumably only one 'vortex' around the fish's head is left at this phase. Unfortunately the complete field of flow has not yet been visualized. However, the results obtained until now corroborate with the single-vortex hypothesis (see paragraph 3.2.4.). Note the direction of the polystyrene spheres near the fish's lips and compare those with the direction of the streamlines of Fig. 19D.


Before valve opening the speed of the predator, $Q$, in the earth-bound frame was generally higher than the speed of the prey in the moving frame, $q'_{prey}$ (passive prey, cow heart, was used so the prey would not swim, see Fig. 11). After valve opening the reverse was true. Thus the prey was pushed slightly before the opening of the valves, and actively sucked towards the mouth by the predator (in an earth-bound frame), once the valves had opened. The observed pushing effect in $q'_{prey}$ falls within the maximal error of velocity calculation. It was, however, also observed in the position data for a series of feeding events. A calculation of the (rearward) velocity in the mouth aperture, using

Fig. 10. Series of selected pictures of a stereoscopic high-speed film (215 fr/sec) of *Salmo gairdneri* feeding. Each picture shows a lateral and a ventral aspect of the fish's head. Pictures (A), (D), (E) and (H) are given as stereographs. Pictures (B), (C), (F) and (G) represent only the right pictures of the stereographs. The time from the start of mouth expansion onwards is given in msec near each picture. Black threads were sewn to the flap of the gill cover ($\rightarrow$ position 1, see C, initially crossing the thread at position 2), a position just anterior to the pectoral fin ($\rightarrow\rightarrow$ position 2, see C, one thread lies dorsally from the pectoral fin and another ventrally) and at a position near the rostro-ventral part of the opercular slit ($\rightarrow\rightarrow\rightarrow$ position 3, see ventral aspect of Fig. C, with two free ends). The movements of the free ends of the threads depict the flow direction in the moving frame if compared to their fixed ends on the fish. The initial, rostrally directed, movements of the threads at positions 1 and 2, depict the initial caudal inflow before the instant $\tau_i$(A to D). Before the instant $\tau_a$ these threads already moved towards the opercular cavity (A to C). Thus a minor leak current was already present before actual valve opening. After the initial inflow a clear outflow occurred demonstrated by thread 2 being swept caudally (D to F). During this caudal outflow the mouth reaches its maximal aperture, and the prey is generally captured At the end of the mouth closure phase a minor secondary caudal inflow is indicated by the movement of thread 2 in a rostral direction (G to H). The threads at position 3 were not noteworthy drawn into the direction of the slits, so, an inflow at this position was absent. The prey is not clearly visable. The nut was used to drop the prey. The prey was captured quite early (at 43 msec).
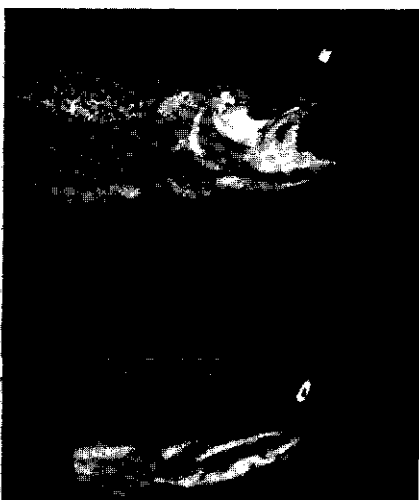
**(E)**

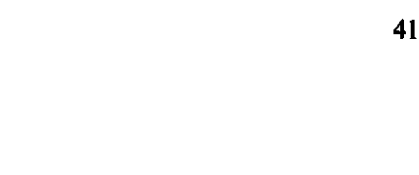55.8 msec
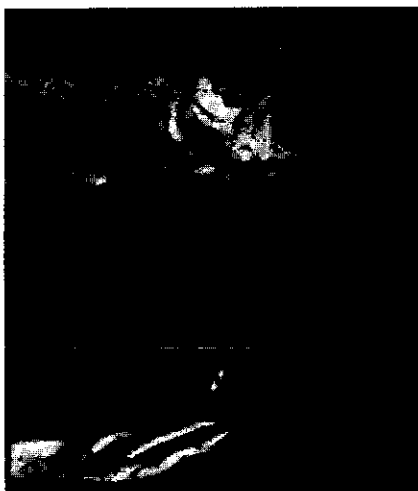
**(F)**

65.1 msec

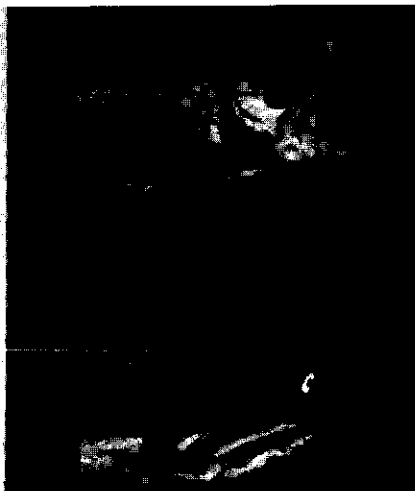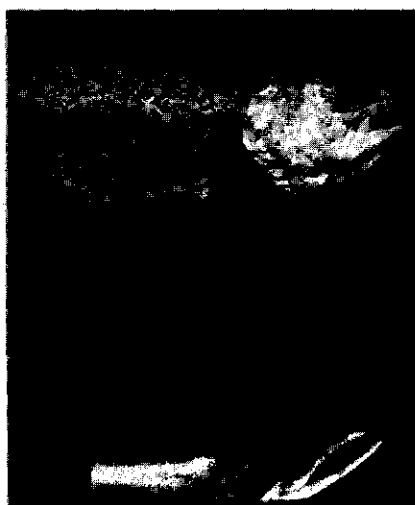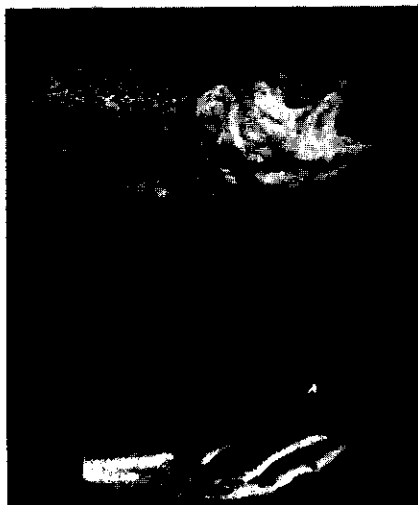**(G)**
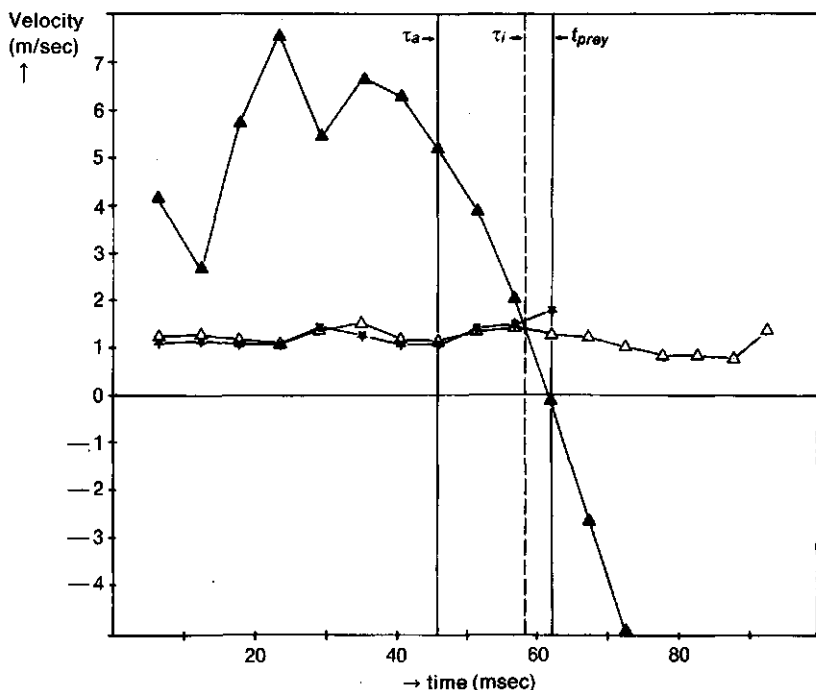
79.1 msec

**(H)**

88.4 msec

42

Fig. 11. Graphs of velocity calculations of the feeding event of *Salmo gairdneri* of figs. 5, 6 and 8. Symbols: $\triangle$–$\triangle$, the speed of the centroid of the mouth aperture in an earth-bound frame, $Q$; $\bigstar$–$\bigstar$, the speed of the prey in the fish-bound frame, $q'_{prey}$; $\blacktriangle$–$\blacktriangle$, the threshold swimming speed needed for the fish to prevent a caudal inflow in case of open valves, $U_t$ (calculation via formula (14), paragraph 3.2.2.). $q'_{prey}$ is about equal to $Q$, indicating that the prey is almost at rest in the earth-bound frame. The actual and ideal moments of caudal valve opening ($\tau_a$ and $\tau_i$) and the moment of prey capture are denoted as in Fig. 8. $\tau_i$ falls at the moment where the curves $U_t$ and $Q$ intersect (at 58 msec). In the model approach (paragraph 3.2) it is assumed that the fish moves with velocity $U_f$ along the $X$-axis. Pushing occurs in the earth-bound frame when $q'_{prey}$ is less than $Q$. Finally, the prey is clearly sucked towards the mouth.

the multi-flash flow visualization technique, revealed a maximal magnitude of only 25% of the fish's forward velocity. Except just before mouth closure, a pushing effect occurred only at the edges of the flow entering the mouth. It was caused by the forward moving lips.

As the movements of the prey and spheres in front of the mouth were small compared to the movements of the predator, the volume drawn into the mouth by the fish was calculated by assuming that all the water had zero velocity in an earth-bound frame. In other words, in the moving frame there existed a uniform flow into the mouth of the fish, so the volume of water sucked into the mouth in a time interval $\Delta t = t_{i+1} - t_i$ equals the area of the mouth aperture times the distance travelled by the mouth during the interval. The area of the mouth aperture was taken equal to $\pi h_1 w_1$, where $h_1$ is half its height and $w_1$ half its width, to account for the elliptical shape of the mouth. For the prey

43

capture event presented above $w_1$ could not be measured on all relevant frames. Therefore the relation between $h_1$ and $w_1$ was determined from a frontally filmed suction event. The flow rate through the mouth aperture was obtained by numerical differentiation as carried out for the velocities (formula (4)). The above calculation underestimates the volume taken in by a maximal value of 25%.

The graph of the intake of water (Fig. 12, calculated for the feeding event of Figs. 5,6,8 and 11) shows that the flow rate was highest when the mouth was maximally opened and the branchiostegal and opercular valves had been opened (compare Fig. 8 and 12). Spheres were seen to flow out of the opercular slits during this instant (moving frame). This caudal outflow supports the flow through the mouth aperture. A striking feature of Fig. 12 is the highly variable flow rate. Fig. 13 depicts the fish at the start of the mouth opening and the water that will be ingested during the suction event. This picture was made with the assumption of a uniform stream into the mouth. The greatest distance from
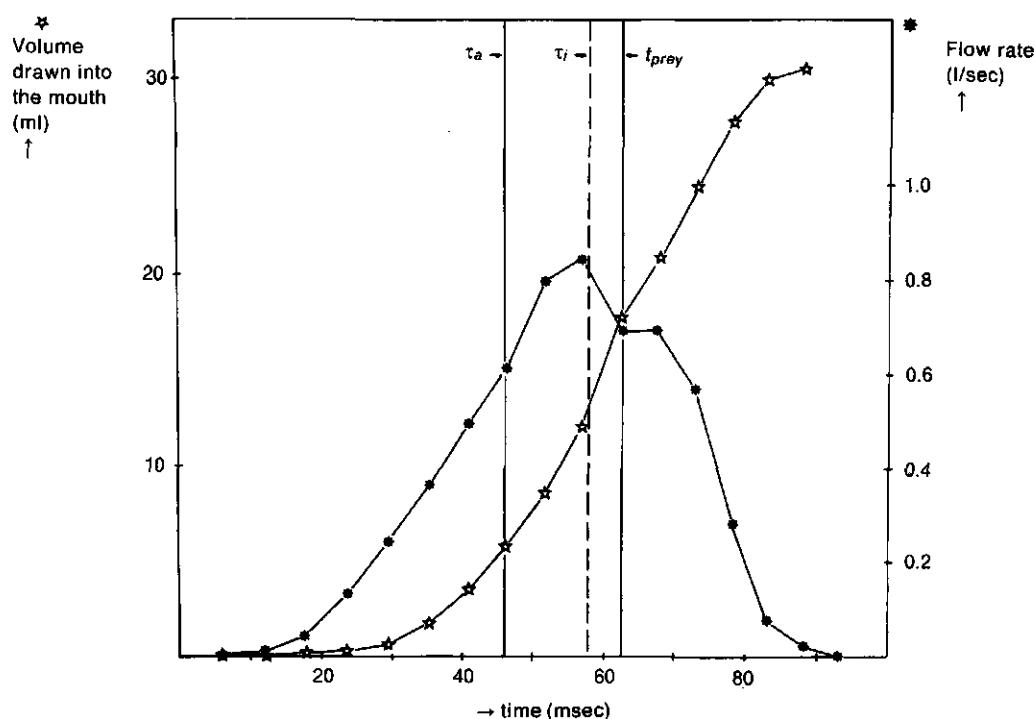


Fig. 12. Graphs of the volume drawn into the mouth by *Salmo gairdneri* and the occurring flow rate through the mouth aperture. Calculations were done for the feeding event of Figs. 5, 6, 8 and 11. So Figs. 8, 11 and 12 can be directly compared to each other. Symbols: ☆–☆, the volume sucked into the mouth; ★–★, the flow rate through the mouth aperture. The flow rate is highly variable and reaches its peak value when the mouth aperture has almost reached its maximal amplitude. The actual and ideal moments of caudal valve opening ($\tau_a$ and $\tau_i$) and the moment of prey capture are denoted as in Fig. 8. Further explanations are given in the text.

44

which water was sucked in (indicated in Fig. 13) was about 1.3 times the fish's head length. This distance equals the translation of the fish during the period that the mouth is open.

The maximally ingested volume was about 5.5 times the volume ingested at the moment of the opening of the opercular and branchiostegal valves. Using a cone approximation to calculate the volume of the mouth cavity (see Muller et al., 1982) it was estimated that at the peak volume change of the mouth (at about 67 msec) maximally 30% of the ingested volume of water had already flowed out through the opercular slits. Peak volume change was calculated as the difference between the maximal volume of the mouth cavity (with valves open!) and the volume at the start of the expansion. The prey was at the centre of the mass of the volume of water to be sucked in. This position may be optimal for its capture. Films of fifteen feeding events were studied carefully. Changes were found in the contributions of the expansion of the mouth and the forward motion of the fish. The events described above, however, were recognized in each feeding attempt, though in some cases the position of the prey deviated significantly from the centre of mass of the volume to be drawn into the mouth.

### 3.2. A QUANTIFICATION OF THE RELATION BETWEEN SUCTION AND SWIMMING

Muller et al. (1982) have developed a hydrodynamical model of suction feeding. Many biological applications of the model are worked out by Muller and Osse (in press). The model is here used to derive quantitative conditions for relating the fish's forward velocity and its mouth expansion. Many of the simplifying approximations that are needed to be made, like the neglecting of viscous forces, rotational symmetry of the expanding mouth and the neglecting of influences of the prey on the flow, are extensively treated by Muller and Osse and are not repeated here. Two points, however, need further discussion, the pushing
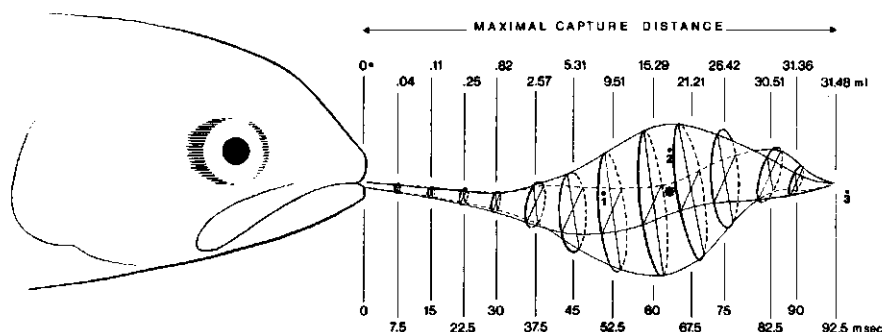


Fig. 13. A reconstruction of *Salmo gairdneri* at the start of the feeding event of Figs. 5, 6, 8, 11 and 12 and the volume of water that will be ingested during the suction act. The black dots denoted with 1,2 and 3 depict the initial positions of polystyrene spheres 1,2 and 3 (see paragraph 3.1.2.). The initial position of the prey is depicted with an asterisk. The ingested volume (ml) at time intervals of 7.5 msec is denoted in the illustration.

effects by the fish's body and head parts, and the physical impossibility of instantaneous opening of the opercular and branchiostegal valves. Several aspects of how a fish should optimize its flow rate into the mouth will be dealt with. Symbols are explained in Table 1.

### 3.2.1. *Suction with closed valves; the avoidance of pushing effects*

To investigate the conditions under which pushing occurs, imagine that the fish's head is a cylinder that moves along the $X$-axis with velocity $U_f$ and at the same time expands radially. Let the length of the cylinder be $l$ and its radius $h$. Let its rear end be closed. The origin of the frame moving with the cylinder was chosen to lie at the centre of its rear end, so that its anterior opening is at $x' = l$.

Around the cylinder circulation will be present. This circulation was calculated by Muller et al. (1982).

Fig. 14 shows streamline patterns induced by the cylinder at various combinations of expansion and translation. The expanding cylinder will not only suck water through its frontal opening, but will also tend to suck itself forward. In general, the flow patterns of Fig. 14 require an external force on the cylinder, directed forward or aft along the $X$-axis. In the fish, this force could be supplied by the swimming apparatus. No attempt has been made to distinguish between the relative contributions to forward motion by the expansion and swimming apparatus. Fig. 14A shows the streamlines around the cylinder when it expands in a fixed position. Such a situation is physically impossible in a free moving fish (if it is not swimming backward). Around the cylinder only one vortex is present.

A more complicated situation arises in the earth-bound frame when a certain amount of forward translation is added. Then, posteriorly a vortex is present due to translation and anteriorly a vortex occurs due to expansion (Fig. 14B). The anterior vortex was visualized during feeding in rainbow trout (see Fig. 9A,B). The posterior vortex is partly replaced by the fish's body and is therefore not as clear as in the cylinder. Note that the mentioned vortices deviate from free circular vortices, as they are more or less "bound" to the profile wall, and also because the circulation ($\oint \mathbf{q} \cdot d\mathbf{s}$) is not constant for different closed contours. In fact a vorticity distribution is present along the profile wall. The term vortex was used due to a lack of a better alternative.

Fig. 14C shows the streamlines in the moving frame when the cylinder moves forward, but does not expand. Now water is pushed forward in front of the cylinder. Behind the cylinder a wake is present, which in the case of the fish is replaced by the fish's body. Figs. 14D to 14F show flow patterns in the *moving frame* with varying contributions of expansion and translation. In Fig. 14E the flow into the cylinder is uniform; the suction and translation effects compensate for each other in front of the cylinder. In an earth-bound frame the water in front of the mouth is at rest. This situation has been characterized as suction with parameter $b = 0$ by Muller and Osse (in press). Fig. 14D shows a situation where pushing in an earth-bound frame occurs. Here the dividing streamline
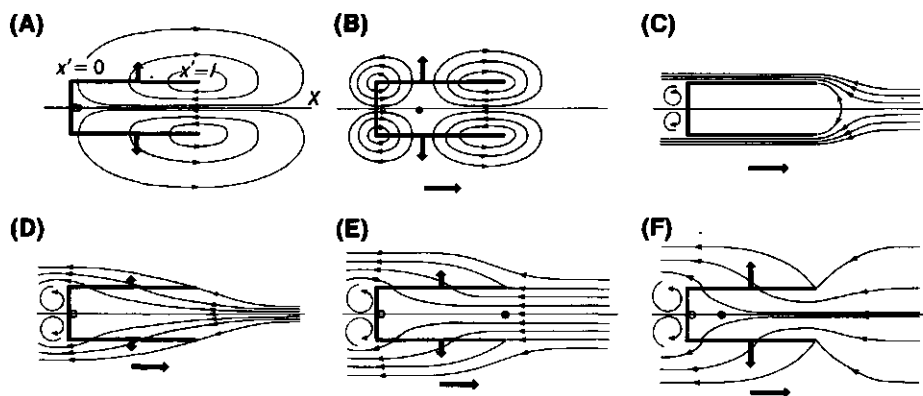
46

Fig. 14. Flow around a cylinder with several combinations of expansion and forward motion. Note that the entire profile and flow pattern is rotationally symmetrical; only a section through the central axis is given. The posterior end of the cylinder is closed, to simulate the closed opercular and branchiostegal valves. The anterior end of the cylinder is open and can be compared to the mouth aperture. Symbols: ○, $P_{mf}$ the point where the water is at rest in the moving frame; ●, $P_{ebf}$ the point where the fluid is at rest in the earth-bound frame. In (A) the streamlines are given in the earth-bound as well as in the moving frame as the cylinder stands still. In (B) the flow is given in the earth-bound frame. Suction dominates. In (C) to (F) the flow is depicted in the moving frame. External forces required to make situations (A) to (E) possible are omitted in the illustrations. Without an external force in the X-direction (in case of the fish to be delivered by the swimming apparatus) only situation (F) is possible (and (B) if the posterior and anterior vortex are of equal magnitude and the cylinder has no mass). Heavy arrows depict magnitude and direction of expansion rate and swimming velocity. Further explanations are given in the text.

diverges towards the aperture of the cylinder ($b > 0$). In Fig. 14F the reverse is true: water is actively moved towards the aperture in an earth-bound frame ($b < 0$). The dividing streamline contracts towards the aperture.*

Two important points can be distinguished along the $X'$-axis. In one point, $P_{mf}$, the fluid is at rest relative to the cylinder. Due to the closed posterior end of the cylinder it lies at $x' = 0$. At the other point the fluid is at rest in the earth-bound frame. In this point, $P_{ebf}$, pushing effects due to forward motion and suction effects due to expansion eliminate each other. Behind $P_{ebf}$ the fluid is pushed forward in an earth-bound frame, whereas in front of $P_{ebf}$ the water is sucked backwards. When the cylinder is at rest both $P_{mf}$ and $P_{ebf}$ lie at $x' = 0$.

Generally, however, the position of $P_{ebf}$ is a function of time, depending on the relative contributions of translation and expansion. $P_{ebf}$ lies in between the two vortices, opposite in sign, present when the cylinder moves forward.

The momentum of the water must be considered in the earth-bound frame. In the moving frame all the water inside the profile flows rearward. This does not mean that all this water has rearward momentum. Behind $P_{ebf}$ it has forward

---

*
A simple addition of the effects of expansion and translation close to the cylinder wall is impossible. The particular effects in this region are not important in this discussion and therefore not treated here.

47

momentum and in front of $P_{ebf}$ it has rearward momentum.

For pushing to be avoided in the mouth aperture the velocity of the water at this position $u'_1$ (relative to the cylinder or fish) should be equal to or less than $-U_f$. Thus with a given $U_f$ the fish should at least reach a certain threshold expansion rate, $h_t$, such that $P_{ebf}$ lies at the mouth aperture. Muller et al. (1982) derived for the velocity of the water in a rotationally symmetrical expanding or compressing profile with closed valves, $u'_v$ (velocity relative to the moving frame):

$$u'_v(x',t) = - \frac{1}{A} \int_0^{x'} \frac{\partial A}{\partial t} \, dx' \tag{7}$$

where $A$ is the cross-sectional area of the profile. The integral represents the rate of change of the volume of the profile. When the point of zero flow $P_{ebf}$ lies at the mouth aperture $U_f$ equals $-u'_1$. Using (7) we obtain for this threshold condition the following relation:

$$U_f = \frac{2}{h_1^2} \int_0^l h \frac{\partial h}{\partial t} \, dx' \tag{8}$$

where $h_1$ is the radius at $x' = l$. From (8) the threshold expansion rate for the cylinder can be derived:

$$h_t = \frac{h U_f}{2l} \tag{9}$$

The expansion rate of the mouth cavity and the fish's translational velocity are thus not at all independent if pushing is to be avoided. The threshold relative expansion rate $h_t/h$ is constant if $U_f$ is constant. At the same time there is a mechanical limit to how wide a fish can expand its mouth cavity. Towards this value $h$ will again decrease. Therefore a critical value of $h$ will exist, above which the expansion rate of the mouth cavity cannot reach the threshold value, and considerable pushing would occur if the opercular and branchiostegal valves are kept closed.

The cylinder model can be generalized to a cone model, for which the anterior and posterior expansion can be varied separately. This permits the area of the mouth aperture to be less dependent of head volume. Let the anterior radius be $h_1$ and the posterior radius be $h_2$. From formula (8) it follows that:

$$h_{1,t} = \frac{3h_1^2 U_f}{l(2h_1 + h_2)} - \frac{(2h_2 + h_1)}{(2h_1 + h_2)} \cdot h_2 \tag{10}$$

where $h_{1,t}$ is the new threshold expansion rate, for the anterior opening ('the fish's mouth aperture'). The flexibility is increased by the addition of an independent parameter. The caudal expansion can significantly reduce the required ante-

48

rior mouth expansion rate, especially when $h_2 >> h_1$. Note again the importance of the mouth radius in this formula.

For the trout its actual mouth expansion rate $\dot{h}_1$ (measured in a vertical direction), actual opercular expansion rate $\dot{h}_2$ and the threshold expansion rate (calculated both for the cylinder and cone model and using the experimentally obtained $h_1$, $h_2$, $\dot{h}_1$ and $\dot{h}_2$) were plotted in Fig. 15. The actual mouth expansion rate is well above the threshold expansion rate, so that pushing at the mouth aperture is unlikely to occur during the phase that the valves are closed. At a certain instant (at $t = 62$ msec for the cylinder model) pushing would have occurred if the valves were still closed. In fact the actual moment of the opening of the valves fell earlier than required for the avoidance of a pushing effect in the mouth aperture. This important aspect is further discussed in paragraph 3.2.3. Anyhow, the predator avoids pushing of prey and water at the crucial moment of capture. Note that for the cone model a secondary phase is present (from about 70 to 86 msec) where $\dot{h}_{1,t} < \dot{h}_1$. During this phase pushing could have been avoided if the valves were closed.

Pushing in front of the mouth aperture is unlikely to occur when the valves are open. However, mouth expansion with open valves might cause another problem: inflow through the opercular slits.

### 3.2.2. *Suction with open valves; the avoidance of an inflow through the opercular slits*

Inflow of water through the opercular slits, after valve opening, might be partly avoided by rearward inertia of water sucked in before valve opening, as has been hypothesised for the perch (*Perca fluviatilis*) by Osse (1969). For several reasons this effect is probably for the trout of minor importance. First, not all the water inside the mouth has rearward momentum at the time of valve opening. Posteriorly to $P_{ebf}$ the water has forward momentum. This effect is particularly important for a fast swimming fish like the trout (see 3.2.1.).

Second, mouth expansion in the trout continues after valve opening and the mass of water sucked before valve opening is only about $1/(5.5)$ of the total volume of the water drawn into the mouth (see 3.1.3.). Thus the time that advantage can be taken of an inertia effect is limited and the flow pattern after valve opening will rapidly resemble the flow pattern with a continuous open valve.

Third, the flow visualization experiments revealed a minor initial inflow through the opercular slits and two vortices around the fish's head after valve opening, which is consistent with my expectations. This will be explained below.

Let us consider the case for the cylinder model for which inertia is of prime importance for a caudal outflow. Imagine that first the situation of Fig. 14A is attained. Then the caudal valve opens instantaneously and radial expansion is stopped (or greatly reduced) at the same time. A flow pattern as shown in Fig. 16A would result, very differently from the flow in *Salmo* (see Fig. 9C). Note, that forward motion of the profile is absent and that an enormous deceleration of mouth expansion would be necessary. These features are absent in the rainbow trout and other free swimming fish. As mouth expansion should
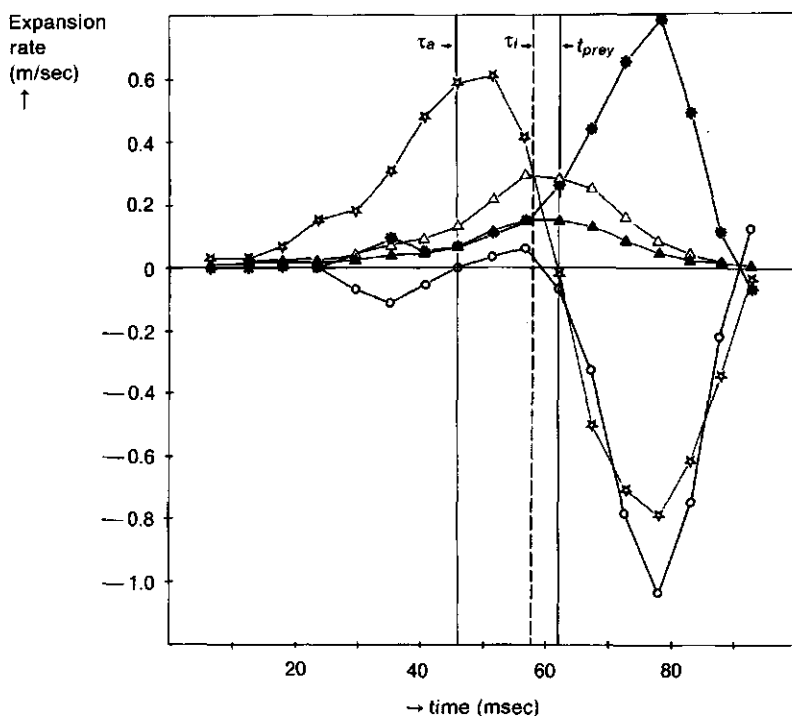
49

Fig. 15. Comparison between actual and threshold expansion rates. Calculations are carried out for the feeding event of Figs. 5, 6, 8, 11, 12,and 13. All these figures can be compared to each other. Symbols: ☆ –☆ actual mouth expansion rate, $h_1$ (measured in a vertical direction); ★–★ actual opercular expansion rate, $h_2$ (measured in a transverse direction); ▲–▲ threshold expansion rate for the cylinder model, $h_t$; ○–○ threshold expansion rate for the cone model, $h_{1,t}$; △–△ critical expansion rate for the cylinder model, $h_c$, discussed in paragraph 3.2.3. The actual and ideal moments of caudal valve opening ($\tau_a$ and $\tau_i$) and the moment of prey capture, $t_{prey}$, are denoted as in Fig. 8. $\tau_i$ falls at the moment where the curves of $h_1$ and $h_c$ intersect. From about 71 to 86 msec it seems to be favourable for the fish to have its valves again closed (only for the cone model). This phase corresponds to the secondary caudal inflow phase discussed in paragraph 3.2.4. (see Figs. 10 and 19).

dominate forward motion at the moment of valve opening for rearward inertia to be important, the effect might only be important in relatively stationary fish.

The forward velocity of the trout is probably most important for the outflow of water through the opercular slits although it diminishes the rearward momentum of the water sucked in before valve opening. To appreciate this consider again the cylinder, but now opened at both ends and at rest. When the cylinder expands radially water will be sucked in from both ends (see Fig. 16B). Halfway inside the cylinder the velocity in the X-direction is zero. Thus here a stagnation point is present at the X-axis. Now consider a cylinder that is not expanding but moving along the X-axis. In this case a uniform flow will be present relative to the cylinder (see Fig. 16C).

50

Now consider the combination of translation with expansion. As for the posteriorly closed cylinder there is one point where the water is at rest relative to the expanding profile and another where the water is at rest relative to the earthbound frame. These points are again denoted as $P_{mf}$ and $P_{ebf}$ respectively. The combination of translation with expansion may lead to one of the three following possibilities (description given relative to the cylinder):

1. $P_{mf}$ lies still in the cylinder, but is displaced to a position between the rear end and the middle of the cylinder (Fig. 16D). There still is an inflow at the rear end, corresponding to a caudal inflow into the gill cavity. Note that $P_{mf}$ cannot come to lie anteriorly of $x' = 0.5l$ if the cylinder is moving forward.

2. $P_{mf}$ lies at the rear end of the cylinder when the translational velocity reaches a certain threshold value $U_t$ (see Fig. 16E). The same of course holds when the expansion has a critical value at a particular forward velocity. There is no net in- or outflow at the rear end of the cylinder. Behind the cylinder a trailing vortex will be present, again, where in case of the fish the fish's body is present. $U_t$ will be a function of the volume increase of the cylinder and its cross-sectional area (to be calculated below).

3. $P_{mf}$ has vanished and an outflow at the rear end of the cylinder occurs if the velocity of the cylinder is larger than $U_t$. A diverging flow is present directly behind the cylinder (Fig. 16F). A diverging flow behind the opercular slits of *Pterois russelli* has indeed been visualized by Muller et al. (1982).
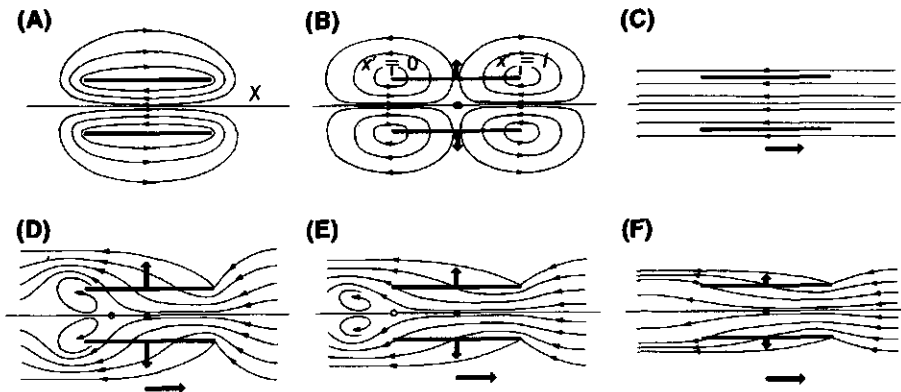


Fig. 16. Flow around a cylinder, open at both ends, with several combinations of expansion and forward motion. The entire profile and flow are rotationally symmetrical; only a section through the central axis is given. Streamlines are given in the moving frame. In (A) and (B) the cylinder stands still, so earth-bound and moving frame overlap. Symbols: ○, $P_{mf}$ point where water is at rest in the moving frame; ●, $P_{ebf}$ point where water is at rest in an earth-bound frame. External forces required to make all situations possible are left out. In the calculations mean velocities over the cross-sectional area are used. The position where the mean velocity of the water is zero (for both frames) may slightly differ from the position where the velocity is zero along the $X$- or $X'$-axis. Heavy arrows depict magnitude and direction of expansion rate and swimming velocity. Further explanations are given in the text.

Similar to the posteriorly closed cylinder, an external force along the $X$-axis is needed to make all situations possible. In case of the fish this force could again be supplied by the swimming apparatus. The flow towards the frontal opening is contracting in all three cases of translation and expansion; an expanding cylinder, open at both ends will never push water forward (except near the cylinder wall when this has a certain thickness). Water will always be moved towards its frontal opening in an earth-bound frame, a flow pattern actually observed for the trout after the moment of valve opening (see Figs. 7 and 9C). *Thus active suction is important after valve opening.* In paragraph 3.2.1. it was explained that pushing would have occured when the valves would have been closed after their actual moment of opening. *Therefore, the resistance of the gill arches and gill filaments must be low after valve opening.*

This last conclusion is supported by observations from high-speed films, and photographs taken during prey capture, where the arches were seen to be separated and the gill filaments of individual arches adducted. These features were also demonstrated for *Pterois russelli* by Muller et al. (1982), for *Perca fluviatilis* by Osse (1969) and for several other species, including the rainbow trout, by Muller and Osse (in press). Fig. 17 shows an example of this situation, from which it is also clear that most of the water may be "shunted" between the hyoid arch and the first gill arch.

Inflow of water through the opercular slits should be avoided by the fish to optimize the flow rate through the mouth aperture and to avoid damage of the gills (see also Muller and Osse, in press). Thus the fish's translational velocity should at least reach the threshold velocity for a given expansion rate during the phase that the valves are opened. Thus the prerequisite for valve opening with garanteed outflow is:

$$U_f > U_t \tag{11}$$

where $U_f$ is the fish's velocity along the long-axis of its mouth. When $U_f < U_t$ the point where the fluid is at rest relative to the moving fish can only be laid at the rear end of the mouth when the valves are closed. Hence knowledge of $U_t$ is required to determine the optimal moment of valve opening, so that the flow rate through the mouth aperture is maximized.

Suppose that the velocity in the $X$-direction of the cylinder, open at both ends, equals zero. Then the mean velocity through its frontal opening will be half the velocity of the closed situation under similar conditions:

$$u'_1 = -\frac{l}{h} \cdot \dot{h} \tag{12}$$

The mean velocity at the posterior end, $u'_2$, will be:

$$u'_2 = -u'_1 \tag{13}$$

and hence:

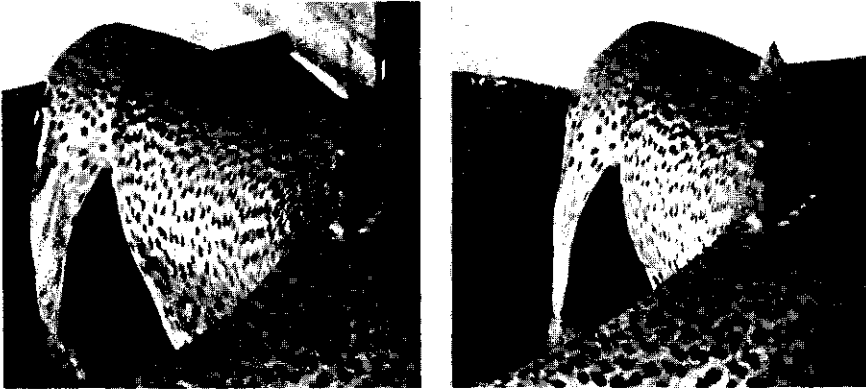$$U_t = \frac{l}{h} \cdot \dot{h} \tag{14}$$

52

Fig. 17. Stereograph of *Salmo gairdneri* after the opening of the opercular and branchiostegal valves. The gill filaments of each arch are adducted. A large opening is present between the hyoid arch and the first gill arch (the "hyoid shunt"). Also the gill arches are separated after the valve opening, apart from filament adduction. This feature, however, is more clearly shown in Muller and Osse (in press). Part of the filament endings are bent by the flow.

The limit of $U_t$ for $t$ approximates 0 is infinity when both $h$ and $\dot{h}$ approach zero, and zero when $h(t) > 0$. At the first stage of the suction act both $h$ and $\dot{h}$ are increasing, however, both with variable rates. As a result the ratio between the two can be subject to strong fluctuations during this period. Hence the streamlines in case of an open valve in this stage would change very rapidly their direction. This phenomenon might explain the early activity of the M. adductor operculi during feeding, recorded for instance for the perch (*Perca fluviatilis*, Osse, 1969), the ruff (*Gymnocephalus cernuus*, Elshoud-Oldenhave and Osse, 1976) and others. The initial adductor activity was also made feasible by an analysis of the pressure regime near the valves by Muller and Osse (in press).

Using the cylinder model of the mouth, $U_t$ was calculated (see Fig. 11) for the above described feeding event of the trout (cf. 3.1.2.). For $h$ half the height of the mouth was taken and for $l$ the head length. As expected at first instance $U_t$ fluctuates quite strongly (0-15 msec), but is, however, already very soon higher than $U_f$. Then (15-40 msec) $U_t$ is in the order of 6.5 m/sec, very much higher than $U_f$. As expected the valves were closed during this phase. Thereafter $U_t$ drops fast and equals $U_f$ at about 58 msec, the expected ideal moment of valve opening $\tau_i$. The decline of $U_t$ was caused by a decreasing mouth expansion rate and a still increasing mouth radius. The moment the valves actually started to open, $\tau_a$, fell about 12 msec earlier than $\tau_i$, but during the fast decline of $U_t$. Note that $\tau_a$ was determined in a high-speed movie when only the faintest indication of an open opercular slit is seen. Hence, at $\tau_a$ the opening is still virtually zero and the interval $\tau_i$-$\tau_a$ is effectively smaller than Fig. 11 suggests. Nevertheless a slight inflow through the opercular slits was expected to occur between $\tau_a$ and $\tau_i$. This was indeed detected experimentally (see Fig. 10). The observed difference between $\tau_i$ and $\tau_a$ will be discussed further in paragraph 3.2.3.

53

The above calculation was done with a cylinder model (formula 14). A similar procedure seems possible for an expanding cone. However, calculation of the position of $P_{mf}$ of an expanding cone without translation cannot be carried out easily, as unsteady effects due to the differing amount of expansion along the $X'$-axis play a role. $P_{mf}$ might even vanish. Anyhow, the cylinder model is very useful as with it a right order of magnitude of $U_t$ can easily be obtained.

The fish could use an unsteady effect due to a cone like movement of its mouth to avoid an inflow through the gill slits. For a fast swimming fish like the trout this effect seems to be of negligible value (note the good resemblance between cylinder model and feeding mechanism of the trout). For suction feeding at relatively low swimming speeds it might be more important (see also paragraphs 3.2.4. and 4.5.).

### 3.2.3. Maximization of the flow rate into the mouth and the choice of the moment of valve opening

Generally, there may be one point, $P_{ebf}$, in an expanding and translating cylinder or mouth cavity where the fluid is at rest in an earth-bound frame. The position of $P_{ebf}$ (which varies with time) was expressed relative to the moving frame. When the valves are closed its $X'$-coordinate will be denoted as $x'_{rc}$ and when they are open as $x'_{ro}$.

As mentioned, with closed valves water is pushed forward in the earth-bound frame posteriorly to $P_{ebf}$, whereas anteriorly to $P_{ebf}$ water is sucked backwards. To maximize the flow rate through the mouth aperture the fish should keep $P_{ebf}$ as caudally as possible during the suction act. When (theoretically) $x'_{rc} < x'_{ro}$ it will be best for the fish to have its valves closed. However, when $x'_{rc} > x'_{ro}$ it will be optimal for the fish to have its valves open.

In calculating $x'_{rc}$ and $x'_{ro}$, $P_{ebf}$ was assumed to be positioned at the cross-sectional area over which the mean velocity of the water equals zero.

In case of open valves and no rearward or forward overall inertial effect due to a previous situation with closed valves, it can be derived for the cylinder that:

$$x'_{ro} = 0.5 \ l \tag{15}$$

For the cone $x'_{ro}$ depends on $h_1$, $h_2$, $\dot{h}_1$, $\dot{h}_2$ and previous events (unsteady effect) and cannot easily be derived.

When the valves are closed pushing and suction effects will eliminate each other in $x'_{rc}$, so that:

$$U_f(t) + u'_v(x'_{rc},t) = 0 \tag{16}$$

where $u'_v(x'_{rc}, t)$ is the velocity in the $X'$-direction in the moving frame at $x'_{rc}$. We obtain for the cylinder (from (7) and (16)):

$$x'_{rc} = \frac{hU_f}{2\dot{h}} \tag{17}$$

54

And for the cone model (also from (7) and (16)):

$$x'_{rc} = \frac{3h_1{}^2 U_f}{(2h_1 + h_2) h_1 + (2h_2 + h_1) h_2} \tag{18}$$

As expected, when the fish expands its mouth with the threshold expansion rate we obtain: $x'_{rc} = l$. For the cylinder model the ideal time of the opening of the valves is determined by:

$$x'_{rc} = x'_{ro} = 0.5\, l \text{ and } \frac{dx'_{rc}}{dt} > 0 \tag{19}$$

When $x'_{rc}$ is greater than $0.5\, l$ it would be advantageous to open the valves, because a caudal outflow would be garanteed and through this the volume flow through the mouth aperture enhanced.

$x'_{rc}$ was calculated for the suction act of *Salmo gairdneri* discussed in paragraph 3.1.2. for both the cylinder and the cone model, using formula (17) and (18), and plotted in Fig. 18. When suction starts the fish pushes water so $x'_{rc}$ will be large. $x'_{rc}$ drops rapidly to about 10% of $l$ for the cylinder model and even less for the cone model. Closed valves are undoubtedly advantageous during this phase. From about 40 msec onwards $x'_{rc}$ increases rapidly for both models. At about 58 msec $x'_{rc} = 0.5l$ for both models. Thus for the cylinder model $\tau_i$ is 58 msec. For the cone this moment would not differ much from this value due to the rapid increase of $x'_{rc}$. Thus the error made in the determination of $\tau_i$ due to the uncertainty about the position of $P_{ebf}$ after valve opening is very small.

The actual moment of the start of valve opening $\tau_a$ fell about 12 msec earlier than $\tau_i$. This will be partly due to the physical impossibility of an instantaneous complete opening of the valves (an infinite force would be required). As mentioned the valves are still virtually closed at the instant $\tau_a$. If the fish would postpone valve opening to the ideal instant pushing would occur at the critical moment of actual prey capture. Furthermore, the cone- and cylinder models overestimate the volume sucked (>100% for the trout). Hence, actually, $P_{ebf}$ is positioned more anteriorly and $\tau_i$ falls earlier than the calculations suggest.

Summarizing, if $\tau_a > \tau_i$ a reduced flow rate through the mouth aperture would result, if $\tau_a < \tau_i$ a slight inflow through the opercular slits would occur (see 3.2.2. and Fig. 16D). The initial inflow between $\tau_a$ and $\tau_i$ should be regarded as an investment for an enlargement of the flow rate through the mouth when the mouth aperture has reached about its maximal value and the prey actually flows into the mouth (see also Muller and Osse, in press, for a discussion of this point).

Even before the instant $\tau_a$ a thread, sewed to the posterior flap (without a bony support) of the gill cover, was seen to move rostrally in the *moving frame*. Also a thread sewed directly rostrally from the pectoral fin was observed to move slightly towards the opercular cavity (Fig. 10). This flow can be regarded as a leak current, discussed by Muller and Osse (in press). It continued for about 10 msec after the instant $\tau_a$. The inflow could not be clearly demonstrated by
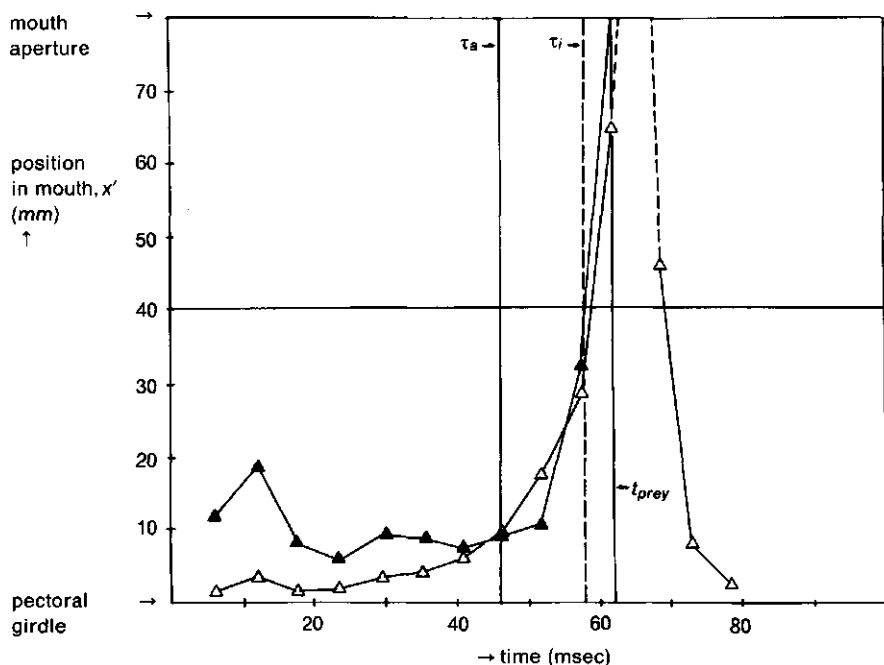
55

Fig. 18. Graphs of the position where the mean velocity over the cross-sectional area is zero in the mouth of *Salmo gairdneri*, in an earth-bound frame. Calculations were done for the prey capture event of Figs. 5, 6, 8, 11, 12, 13 and 15. All these figures can be compared to each other. Water is pushed forward caudally of $x'_{rc}$, whereas anteriorly of $x'_{rc}$ suction dominates. Symbols: ▲ – ▲, $x'_{rc}$ calculated for the cylinder model; △–△, $x'_{rc}$ calculated for the cone model. The horizontal line at $x' = 40$ mm $= 0.5 l$ denotes the position of $x'_{ro}$, with the assumption of the cylinder model and no overall inertia effect of water sucked in before valve opening. Ideally the caudal valves should open when the curves of $x'_{rc}$ and $x'_{ro}$ intersect. At the start of mouth expansion $x'_{rc}$ will be very large (position outside the mouth). This is not incorporated in this figure. $\tau_a$, $\tau_i$ and $t_{prey}$ are denoted as in Fig. 8. Further explanations are given in the text.

spheres, as no cases were found where spheres were close enough to the slits. A similar minor inflow, just before the moment of the maximal opercular abduction, was found during respiration in the rainbow trout by Dr. C.M. Ballintijn (personal communication). Lauder (1980) mentions that particles suspended near the opercular slits of *Lepomis* were carried into the gill cavity as the valves first opened. The author made no distinction between the earth-bound and the moving frame. In this case, however, it seems clear that the flow was considered relative to the moving frame. So, the expected initial net caudal inflow presumably also occurs in *Lepomis*. Lauder failed to explain this feature as the author tried to derive the flow direction from the pressure regime in an essentially unsteady process (see Muller et al., 1982).

The initial caudal inflow is reduced if the length of the time interval $\tau_i$–$\tau_a$ is minimized by the fish. To obtain this a rapid opening of the valves is required as then $\tau_a$ could be delayed and hence $\tau_i$–$\tau_a$ reduced. Another possibility to

56

reduce $\tau_i - \tau_a$ is a decrease of the effective head length of the fish directly after $\tau_a$, due to the opening of the rostro-ventral extensions of the branchiostegal valves. In the trout the valves started to open at about $0.1l$. Opening proceeded rapidly in both a dorso-caudal and a ventro-rostral direction. Within 10 msec the rostral boundary of the opercular slits had reached $0.3l$. This reduction of the effective head length reduces $\tau_i$ and thereby the interval $\tau_i - \tau_a$. However, it decreases the suction capacity of the mouth after valve opening.*

For the cone model with closed valves $P_{ebf}$ again enters the mouth cavity just before its rostral closure (Fig. 18). So eventually closed valves would again be favourable for the fish. However, this is impossible due to the large abduction of the opercula and the short branchiostegal rays. When $x'_{rc}$ is less than about $0.5l$ a *secondary inflow* would again be expected (from about 70 msec onwards). This was actually shown to be the case by the experiment with the threads sewed near the opercular slit (see Fig. 10). It was demonstrated for all 14 feeding acts recorded in this experiment thus supporting the theoretical expectations.

From (17) and (19) we obtain for the cylinder model a critical expansion rate $\dot{h}_c$ for the mouth cavity with closed valves:

$$\dot{h}_c = \frac{h}{l} \cdot U_f = 2\dot{h}_t \tag{20}$$

To obtain of a maximal flow rate through the mouth aperture the opercular- and branchiostegal valves should be open when $\dot{h}_1 < \dot{h}_c$. $\dot{h}_c$ was calculated for the trout and plotted in Fig. 15. By definition, $\tau_i$ falls at the moment of the intersection of the curves of $\dot{h}_1$ and $\dot{h}_c$ (at 58 msec). Note that $\dot{h}_c$ is also the maximal expansion rate whereby a caudal inflow does not occur in case of open valves (with a given forward velocity).

With (18) and (19) we obtain an estimate for the cone model:

$$\dot{h}_{1,c} = \frac{6{h_1}^2 U_f}{l(2h_1 + h_2)} - \frac{(2h_2 + h_1)}{(2h_1 + h_2)} \dot{h}_2 \tag{21}$$

showing that $\tau_i$ might be significantly delayed for increasing $h_2$ and $\dot{h}_2$. From (20) and (21) it is clear that $\tau_i$ tends to decrease with an increasing swimming velocity, whereas the reverse is true for an increasing head length.

### 3.2.4. *The mouth closure phase*

So far little attention has been paid to the mouth closure phase. For comparison a cylinder model can be put forward. A compressing cylinder with both ends open pushes water in both an anterior and a posterior direction (earth-bound frame). After having reached its maximal mouth diameter the mouth

---

* The reader might question the necessity of a detailed discussion of minor inflow effects through the opercular slits in *Salmo gairdneri*. However, these effects probably were major problems during the evolution of a suction mechanism from a filter system (see also paragraph 4.4.).

cavity of the trout deviates significantly from a cylinder as the caudal parts of the mouth cavity are still expanding when the mouth aperture decreases.

The main events, however, can be explained by a comparison with a cone, compressing at its anterior end while expanding posteriorly. Let us first consider the flow if the cone does not translate (see Fig. 19A). Three 'vortices' might be distinguished around the cone. In this case two points of zero flow are present in the cone denoted with $P_{1ebf}$ and $P_{2ebf}$. Water flows out the anterior end of the cone, whereas water is sucked in posteriorly. Halfway inside the cone water is moved posteriorly. At one point along the $X'$-axis the expansion rate of the cone is zero. This point separates $P_{1ebf}$ and $P_{2ebf}$. The middle 'vortex'
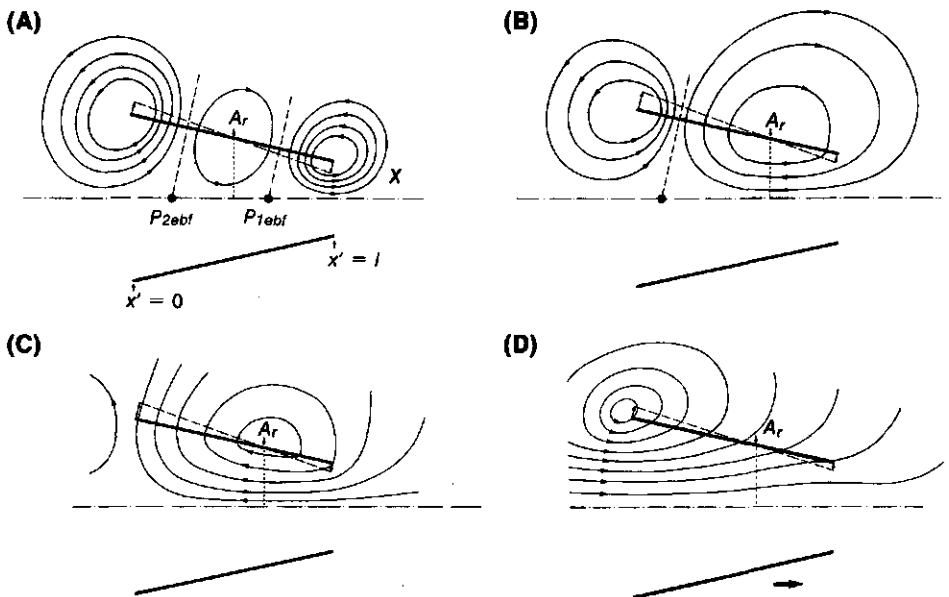


Fig. 19. Schematized streamline patterns in a cone, expanding at its posterior end and contracting at the opposite end. The cone is open at both ends. Arrows at both ends denote the direction of movement of the wall. Note that the entire flow is rotationally symmetrical, only a section is given in each case. $P_{1ebf}$ and $P_{2ebf}$ are denoted with black dots. Pictures (A) to (D) represent streamline patterns in the earth-bound frame. In (A) to (C) the profile is at rest, in (D) the cone translates forward (denoted with a heavy arrow).
A. Situation with 3 distinguishable regions. In the middle a region of rotation is present. At both ends vortex-like regions occur. The fluid is at rest at two positions along the X-axis.
B. Situation where two such regions are present; only $P_{2ebf}$ is left in the cone. Two 'vortices' were indeed visualized for the rainbow trout (Fig. 9C).
C. Theoretical situation with only one 'vortex' and a caudally directed flow inside the entire cone. Both $P_{1ebf}$ and $P_{2ebf}$ are absent.
D. Situation with only one 'vortex'. The cone moves forward. Rostrally, the forward velocity of the wall is much larger than the compression rate. Hence the streamlines are directed outwards in this area and a triple-vortex effect cannot occur. Compare this illustration with Fig. 9D, the actual situation in the rainbow trout. $A_r$ denotes the cross-sectional area where the expansion rate is zero.

deviates stronly from a true vortex, and may be better denoted as a region of rotation (see also 3.2.1.).

The positions of $P_{1ebf}$ and $P_{2ebf}$ depend on $h_1$, $h_2$, $\dot{h}_1$, $\dot{h}_2$, $l$ and previous events (unsteady flow effect). One or both of these points may even vanish. When $P_{2ebf}$ is absent a caudal outflow exists. When $P_{1ebf}$ is absent an anterior inflow occurs (depicted in Fig. 19B). When both points are absent the flow can be directed either posteriorly inside the entire cone (Fig. 19C) or directed anteriorly. If the cone translates fast enough along its long axis all situations described above can be forced to give a posteriorly unidirectional flow in the moving frame.

Once a vortex (or a region of rotation) has been created it cannot be easily destroyed as it represents a certain amount of energy, a fact to be considered in the analysis of the sucking fish. Two vortices are present around a forward moving, expanding cylinder closed at its posterior end (paragraph 3.2.1.). The posterior vortex is a result of forward motion. The total circulation of the posterior vortex compared to that of the anterior one can be a measure for the relative importance of forward motion and suction. The same holds for a totally expanding cone and also for the fish (with its entire mouth expanding and its valves closed, see Fig. 9A). Part of the streamlines of the posterior vortex will go through the fish's body in the earth-bound frame. After valve opening the two vortices remained associated with the trout's head. So, the posterior vortex was *not* left behind as a free vortex. If this occurred a single vortex around the fish's head could develop and hence a unidirectional flow, even in the earth-bound frame. This effect could be important for feeding at low swimming speeds. In this case the posterior vortex would already be of a small magnitude before the opening of the valves.

A double vortex during the mouth closure phase was demonstrated for the rainbow trout by multi-flash photography (Fig. 9C). The caudal vortex was not strong enough to cause a net inflow through the opercular slits during this phase. Water was still sucked towards the mouth (in an earth-bound frame, cf Fig. 9C).

Just before mouth closure water was slightly pushed at the mouth aperture, together with a net caudal inflow through the opercular slits (see Figs. 9D and 10). Such a situation can be understood when a third vortex is added. In the mouth aperture water will be accelerated in a forward direction and the circulation of the anterior region will be diminished. Its centre may be moved caudally. Anteriorly, a new vortex is formed with an opposite direction to the previous anterior one. This situation in the earth-bound frame resembles that of Fig. 19A (note that a forward velocity of the profile is not taken into account in this illustration). I propose to call the addition of a third 'vortex' the *triple-vortex effect*. However, when the forward velocity of the fish is relatively high compared to the rostral compression rate there cannot exist streamlines going through the mouth wall and directed inwards (earth-bound frame). Hence an anterior addition of a third vortex is impossible in this case.

A triple-vortex effect will generally be absent in the rainbow trout due to its fast swimming. It was indeed not found by flow visualization experiments

59

during feeding in the open water. On the contrary, the observations pointed to only one vortex (with opposite flow direction compared to Fig. 19C), although the field of flow is not yet visualized in its entirety (Fig. 9D). This flow pattern would result if the posterior vortex of Fig. 19B would enlarge and the anterior one diminish and eventually vanish. I propose to call this transition the *single-vortex effect*. The resulting flow is illustrated in Fig. 19D for a forward moving cone.

A diagram of the flow relative to the fish's head is given in Fig. 20. There is one point of zero flow, $P_{2mf}$, present inside the mouth; a net caudal inflow occurs. To protect the gills, it would be favourable for the fish if it could keep $P_{2mf}$ caudally from the gill filaments.

The single-vortex effect may also be reached via the triple-vortex effect through a diminution of the middle region of rotation, followed by a unification of the anterior and posterior vortices. Further experimental data are needed.
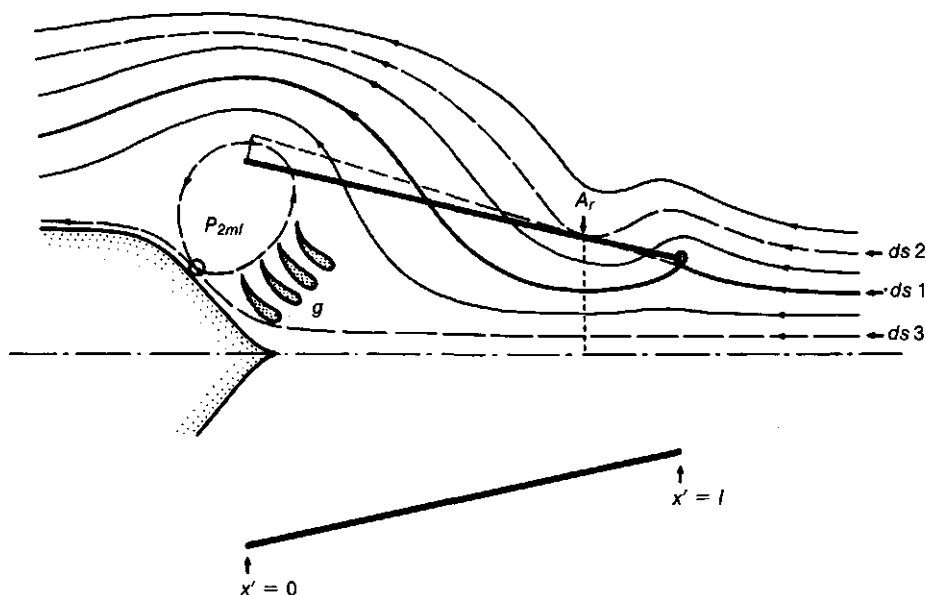


Fig. 20. Schematized situation of streamline pattern around a fish's mouth in the moving frame. In the earth-bound frame the flow would resemble the situation of Fig. 19A, however, with forward movement of the profile. A similar flow pattern arises from a situation with only one 'vortex' (cf. Fig. 19D). At the anterior end a pushing effect is present and a diverging flow towards the mouth results. At the posterior end a caudal inflow occurs. Both effects were detected experimentally just before the actual moment of mouth closure (see Figs. 9D and 10). At $P_{2mf}$ the fluid is at rest in the moving frame. Abbreviations:

$A_r$: cross-sectional area where expansion rate of profile wall is zero; $ds1$: dividing streamline that envelops the water that tends to flow through the mouth aperture; $ds2$: streamline enclosing all streamlines that go through the the mouth; $ds3$: streamline enclosing all streamlines that do not pass the profile wall; $g$: gill filaments.

### 3.2.5. *Streamlines in the moving frame throughout the feeding act*

This paragraph summarizes the variable streamline pattern relative to the trout during one complete feeding act.

Muller et al. (1982) relate quantitatively the mouth radius to the radius of the dividing streamline for $x'$ approaches infinity (formula 32). In their formula a parameter $a$, is used describing the ratio between the velocity of the water in the mouth aperture in the earth-bound frame and $-U_f$. The authors argue that their formula is only valid for $a > 1$. However, it is probable that the formula also holds for $0 < a < 1$ as the same third power root is present in both the formula for $r_{asymptote}$ and $h_{1\,effective}$ (formulas 29 and 30 in Muller et al., 1982). These roots cancel in their formula 32 where $r_{asymptote}$ is devided by $h_{1\,effective}$. Rearranged formula 32 of Muller et al. becomes:

$$r_{asymptote} = h_{1\,effective} \sqrt{\frac{u'_1}{-U_f}} \tag{22}$$

where $r_{asymptote}$ is the radius of the dividing streamline at $x' \to \infty$ and $u'_1$ the mean velocity of the water in the mouth aperture in the moving frame. $h_{1\,effective}$ is the effective mouth aperture (see Muller et al., 1982).

Fig. 21 shows the results obtained for the rainbow trout. Muller and Osse (in press) relate the type of flow to the ratio between the velocity of the water in the mouth aperture in an earth-bound frame and the fish's forward velocity. This ratio, denoted as $b$ by Muller and Osse, will be given for the stages of the trout described below.

Fig. 21A shows the flow in the initial overall pushing phase. The speed of the water relative to the fish just in front of the mouth was already larger than the velocity at a large distance. The flux through each cross sectional area of the dividing streamline is constant. Hence, the diameter of the dividing streamline increases with the distance from the mouth (parameter $b < 0$; see for comparison Fig. 9A, giving the flow in the earth-bound frame). The prey was still about one head length away from the mouth.

Thereafter suction of the predator almost exactly eliminated the effect of its own motion on the prey, resulting in a stationary prey (omitting the prey's own movements). Again the flow contracted towards the mouth ($b < 0$). The opercular and branchiostegal valves started to open (Fig. 21B).

In Fig. 21C the maximal mouth diameter is reached and the prey sucked into the mouth ($b < 0$). A considerable caudal outflow occurs. The chance of escape seems to be minimized by this flow pattern (see also Fig. 13). In Fig. 21D the mouth is halfway its closing phase. Water in the mouth aperture is almost at rest in the earth-bound frame ($b = 0$). Mouth closure is nearly completed in Fig. 21E ($b > 0$).
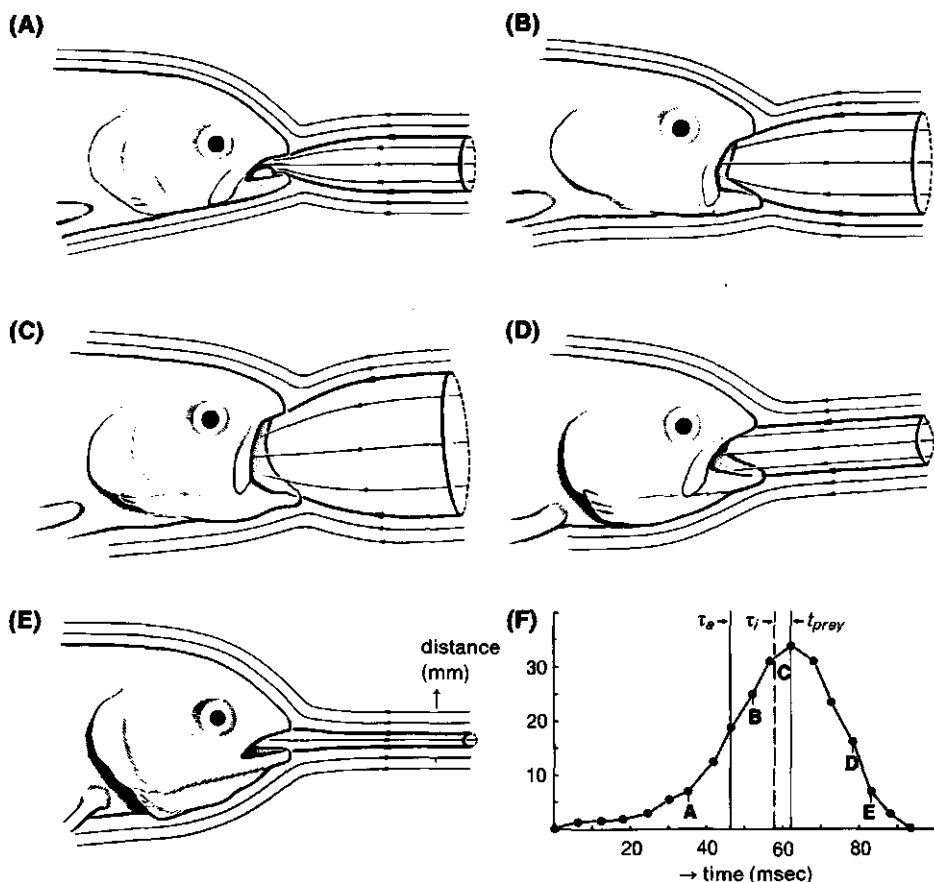
Fig. 21. Diagrams of streamline patterns in a fish-bound frame at various moments of a feeding act of *Salmo gairdneri*, as deduced from movements of polystyrene spheres and model approach. The bolt lines represent the dividing streamline. The form of the fish's head is taken from a film. This figure should be compared to the events in the earth-bound frame, shown in Fig. 9. A. Phase just after the start of mouth opening, corresponds approximately to Fig. 9A; B. Situation at the moment of actual valve opening, corresponds to Fig. 9B; C. Situation at peak mouth gape. Caudal valves are open; D. Flow pattern during mouth closure. Note depression of mouth bottom from A to D; E. Flow just before final mouth closure; F. Graph of the height of the mouth aperture, with the timing of moments A to E. Further explanations are given in the text.

## 4. Discussion

### 4.1. HYDRODYNAMIC MODELS OF THE FLOW DURING SUCTION FEEDING

The present approach, using stereoscopic flow visualization techniques, has resulted in a complete picture of the flow throughout the feeding act. These techniques do not interfere with the fish's movements (as most flow velocity

62

transducers). Therefore they were used to test the predictions from hydrodynamic models of fish suction.

Several models have been put forward to describe the flow in front of the mouth of a sucking fish. Alexander (1967) modelled the mouth cavity as a tube. Close to the tube aperture ("the mouth aperture") he assumed a uniform flow to be present. At larger distances the tube aperture was regarded as a sink. Alexander calculated a maximal distance from which food can be sucked into the mouth. The obtained value of one quarter of the fish's mouth length was an underestimate as a caudal outflow through the opercular slits and the forward motion of the predator were not taken into account. This first model has several disadvantages. The mouth aperture cannot be defined exactly and the velocity approaches infinity at this position. Therefore, Alexander had to assume a uniform flow at the mouth aperture. Also, the water is sucked into the mouth from all directions, so that much energy would be wasted by the fish in sucking prey-free water. It is also in contrast with the general observation that a fish aims at his prey and then proceeds to capture it.

Osse (1969) showed that the perch (*Perca fluviatilis*) is able to capture preys from an initial distance of half the length of the head. To his opinion jaw protrusion contributes to direct the flow towards the prey. Besides, Osse hypothesized that suction might be important after valve opening. However, at that time solid experimental evidence was still lacking.

Nyberg (1971) observed that the sink model of Alexander does not hold for the largemouth bass (*Micropterus salmoides*). The flow generated by the bass appeared to be more directed.

Weihs (1980) added a uniform flow to the sink model of Alexander to take account of the forward motion of the fish. He obtained a more directed flow than Alexander. Weihs assumed a constant rate of intake of water into the mouth, thus neglecting the unsteady nature of the feeding process. For the maximal intake of water he took the maximal mouth volume change (not defined by Weihs) as a measure. At least for the rainbow trout these two assumptions are proven to be incorrect (the present paper). Osse (1969) had already hypothesized that a caudal outflow after valve opening might be important in the perch. The disadvantage of the infinite velocity at the mouth aperture still exists in the model of Weihs. Weihs did not pay attention to stagnation effects due to swimming.

The necessity to distinguish between the earth-bound and the fish-bound frame was for the first time recognized by Muller and Osse (1978) and Osse and Muller (1980), who modelled the field of flow in front of the mouth aperture as the combination of a circular vortex and a uniform flow. The mathematical implications of this model are worked out in Muller et al. (1982). The singular points (in these points the vorticity does not equal 0 and the velocity is infinite) are positioned at the lips of the fish. So a circular mouth aperture can be defined. The rate of intake is coupled with the actual volume change of the mouth cavity (modelled as an expanding cone) and is a time dependent variable. Thus the unsteady nature of the process is taken into account. At a certain moment a

caudal valve ("the opercular and branchiostegal valves") opens and water can flow out of the cone. Thus the model permits a larger volume of water to be sucked in than the peak volume change of the mouth cavity during feeding might suggest. In my experiments (see fig. 12) the importance of this effect was shown. The field of flow can be varied by changing the relative contributions of the vortex and the uniform flow. The share of the uniform flow is due to the forward movement of the mouth aperture in an earth-bound frame, accomplished by a variable combination of the suction itself, a possible protrusion of the jaws and additional swimming. During most of the time the shape of the flow in front of the mouth generated by a sucking trout resembles the shape predicted by the model, except close to the fish's lips. The model does not incorporate quantitative expressions for stagnation effects due to the translation of the fish although they were recognized by the authors. Discussions about this subject can be found in Muller and Osse (in press), in the present paper and chapter 2.

Flow patterns cannot be derived from the pressure regime as the process is essentially unsteady (Muller et al., 1982). Approaches in this direction (see e.g. Lauder, 1980) were therefore left out in this discussion.


### 4.2. THE FEEDING MECHANISM OF THE TROUT: A COMBINATION OF SUCTION AND SWIMMING

Important elements in the type of feeding used by *Salmo gairdneri* in the open water are:
1. Initial approach with a closed mouth to reduce the pressure drag in swimming and to reduce the start volume of the mouth cavity.
2. Only close to the mouth the prey is significantly accelerated towards the mouth in the earth-bound frame (see 3.1.). Thus, the impulse added to the prey by the combination of suction and swimming is small. This feature makes early detection of the predator by a live prey more difficult and therefore enhances the chance of prey capture (see also Muller and Osse, in press).
3. The fish's hydrodynamical constraints are changed almost instantly by caudal valve opening. A caudal outflow through the opercular slits enhances significantly the flow rate into the mouth after the early moment of caudal valve opening (see 3.1.3.). This outflow is mainly due to the forward velocity of the fish (see 3.2.2.).
4. Mouth expansion continues to add to the flow towards the mouth after valve opening (see 3.1.2. and 3.2.2.).
5. Gill resistance is low after caudal valve opening and water is "shunted" along the hyoids (see 3.2.2.).

To investigate whether these elements are also found in other salmonids, the paper on *Salvelinus fontinalis* by Lauder and Liem (1980) was analysed. As the relative timing of the mouth opening and the opening of the caudal valves are not described, nor details on swimming speed the comparison is based on mea-

surements made from their Fig. 1, consisting of a series of frames from a high-speed film.

The head length of their fish was about 45 mm and its velocity during prey capture about 0.3 m/sec. Initially, the prey was very slightly pushed forward; about 1 mm in 10 msec (frame 1 to 3, earth-bound frame). Thereafter, the prey was sucked towards the mouth; about 3 mm in 10 msec (frame 6 to 8), representing a mean velocity of 0.3 m/sec in an earth-bound frame. Thus, in this interval the mean speed of the prey in an earth-bound frame was about equal to the speed of the predator.

The caudal valves were presumably already open when the prey passed the mouth aperture (concluded from the dark stripe at the rear end of the operculum). The maximal mouth aperture divided by the fish's head length was about 0.17. Its relative hyoid depression at the time of the maximal mouth opening (measured from the ventral side of the eye sphere to the most rostro-ventral point of the hyoid) was 0.7. For the feeding act of the rainbow trout analysed in the present paper (Fig. 8) these last two values are: 0.44 and 0.46. Unfortunately, opercular abduction could not be measured from the pictures given by Lauder and Liem.

Comparing the two feeding events we can conclude (event SG: *Salmo gairdneri*; event SF: *Salvelinus fontinalis*):
1. The predator's speed is very much lower in SF than in SG (also, when scaling is done to correct for the difference in body length).
2. The relative maximal mouth aperture is kept smaller in SF, whereas the buccal expansion is increased. From considerations of continuity it follows that the relative speed in the mouth aperture will increase and hence:
3. In SF the prey has a higher mean speed towards the mouth in an earth-bound frame. The speed in the moving frame, however, has decreased.

The above comparison indicates that salmonids adjust their head movements to their swimming speed to optimize the velocity in the moving frame and hence the chance of prey capture. The different EMG-patterns found in the head muscles of *Salvelinus* in mid-water and bottom feeding (Lauder and Liem, 1980) support this view. A similar strategy is used by other fish (see 4.3.).

Muller and Osse (in press) have characterized the feeding type of the trout as *low-τ-suction with swimming*, being especially suitable in relatively open water, where swimming is not limited by an abundance of obstacles. During searching for food and feeding by the trout far more energy will be spent by swimming than by head expansion. Therefore, the energetics of swimming needs to be known if one is concerned with optimal foraging strategies in salmonids.

### 4.3. A COMPARISON WITH OTHER FISH

*Esox*

In a preliminary study Mr. Jan Kremers and I have applied the model to the pike (*Esox lucius*), also a fast swimming protacanthopterygian fish. The cylinder model was insuffient to predict the time of the opening of the caudal valves.

The cone model, however, gave accurate predictions. With a decreasing maximal swimming speed (ranging from 2 to 0.5 m/sec) the mouth expansion rate tended to be more rapid and the valves opened slightly earlier, but at a larger mouth aperture and buccal expansion. Thus more water was sucked into the mouth before valve opening. Also, the maximal speed of the prey in an earth-bound frame tended to be larger at a lower swimming speed. In all cases stagnation in front of the mouth aperture was avoided. All prey capture events were carried out within the constraints (cone model) formulated in paragraph 3.2. In terms of the feeding types distinguished by Muller and Osse (in press) a shift from low-$\tau$-suction towards high-$\tau$-suction (with less swimming) can be achieved by the pike. The data of the chain pickerel (*Esox niger*) presented by Rand and Lauder (1981) are in accordance with our findings for the pike. Unfortunately, the data were not suitable for an analysis as given in paragraph 3.2. as the data of individual feeding acts were lumped and the moment of valve opening was not given.

The enlarged flexibility of the cone model as compared to the cylinder can only be taken full advantage of when the structure of the branchiostegal apparatus allows the valves to be kept closed at a broad range of abduction states of the suspensoria and the opercular. (So that the second term of formula (21) can be used to decrease the critical expansion rate of the mouth aperture). The short, spathiform branchiostegal rays (McAllister, 1968) of the trout allow only a relatively small abduction of the opercular before the valves open. Therefore, the effectiveness of the trout's feeding mechanism will be significantly less (resulting in a small capture region and a low mean flow rate through the mouth aperture) at a relatively low swimming speed than at a relatively high swimming speed.

The pike also has rather short, spathiform branchiostegal rays. However, they are relatively longer than in the trout, suggesting that the pike has more flexibility in its feeding mechanism than the trout has. These differences are in accordance with the characteristic habitats of both species. The same holds for the bowfin (*Amia calva*), which was observed to feed at a broad range of swimming speeds. Osse (1976) already indicated that the valves are important in the suction mechanism of the bowfin.

*Pteronisculus*

Schaeffer and Rosen (1961) gave reconstructions of the head of the extinct palaeoniscoid fish *Pteronisculus* in an unexpanded and an expanded state (see their Figs. 1A and 2A). The effective head length of this fish is short due to the notched mouth and the short opercular region. With a given forward velocity and mouth radius (and a scaled head length) *Pteronisculus* would require a critical expansion rate of 1.9 times that of *Salmo gairdneri* to prevent stagnation (calculation with formula (20)).

After valve opening the threshold swimming speed required for *Pteronisculus* to prevent inflow through the opercular slits was estimated to be about half of the speed required for *Salmo gairdneri* (after scaling and with a given mouth

radius and mouth expansion rate, formula 14). The use of an inertial effect to obtain an outflow through the opercular slits must have been even less important than in *Salmo*.

This suggests that the valves opened much earlier in *Pteronisculus* than in *Salmo*, as it is probable that *Pteronisculus* (with its complete dermal skeleton) was only for a short time able to expand its mouth faster than the high critical rate. *Pteronisculus* had even shorter branchiostegal rays than the trout (also spathiform), which indeed would have allowed only a very small abduction before the moment of valve opening. The flow through the mouth aperture probably was largely dependent on the swimming speed. Unfortunately, no studies have been made, to my knowledge, of the possible swimming capacity of palaeoniscoids. However, it is likely that the swimming apparatus was further developed than the suction apparatus, due to its early appearance in the chordates. Suction feeding at low swimming speeds (e.g. bottom feeding and feeding from crevices) was probably very ineffective. This suggests that *Pteronisculus* (and other palaeoniscoids with a similar morphology) captured their prey mainly in the open water, or their prey consisted of sluggish bottom organisms.

A directed flow towards the mouth could probably have been established by *Pteronisculus*, in spite of its notched mouth, due to the presumably relatively large importance of swimming in its feeding mechanism.

### Gymnocephalus

The paracanthopterygians and acanthopterygians have developed long, curved, highly rotatable aciniform branchiostegal rays (McAllister, 1968). This allows feeding with the advantages of the cone model, i.e. effective feeding at a broad range of swimming speeds. How this is used is demonstrated by the feeding mechanism of the ruffe (*Gymnocephalus cernuus*), an acanthopterygian, studied by Elshoud-Oldenhave and Osse (1976). The authors distinguished relatively stationary bottom feeding (type A) and mid-water feeding (type B), where large swimming velocities can be expected. In A mouth expansion is faster, although the critical relative expansion rate $h_c/h$ is lower. The maximal mouth opening is kept relatively small in A (see Elshoud-Oldenhave and Osse, Fig. 14.1). From the continuity equation it follows that larger speeds of the water in front of the mouth will be generated in A than in B. Additionally, protrusion of the upper jaws (a means to increase the speed of the prey in the moving frame, as has been argued by Nyberg, 1971) starts earlier in type A. The valves open at the maximal opercular abduction in A. Hence, a caudal inflow is prevented. The valves open later, but at a smaller abduction of the opercula, in type B, due to the slower expansion rate. Now, a caudal inflow will be avoided by the high forward body velocity. (So, the instant $\tau_a$ is not coupled to a fixed volume of the mouth). Thus, bottom feeding is shortened and intensified relative to mid-water feeding and larger velocities of the water in front of the mouth (in an earth-bound frame) are generated. In mid-water feeding a large relative speed of the prey is obtained by the velocity of the predator itself.

67

*Luciocephalus*

A last example is the feeding mechanism of *Luciocephalus pulcher* studied by Lauder and Liem (1981). *Luciocephalus* is an acanthopterygian fish with a body, closely resembling the pike. It also suddenly darts at the prey and reaches a high velocity at the moment of prey capture (about 1.5 m/sec was recorded by Lauder and Liem). Very differently from the trout and the pike, *Luciocephalus* protrudes its premaxillae, very early in the suction phase, to the enormous value of about 30% of its head length. The caudal valves with long aciniform rays open when the mouth is about maximally opened. From the observation that the prey is relatively stationary in an earth-bound frame Lauder and Liem have misinterpreted the fish's feeding mechanism, because a sound physical insight in the flow was lacking. On page 261 they conclude:

"*Luciocephalus* uses suction only to a negligible degree and relies almost exclusively on body velocity to overtake and surround the prey with the buccal cavity". On page 266 they write about the protrusion mechanism: "In *Luciocephalus*, however, the prey remains nearly stationary throughout the feeding sequence (Fig. 1,4; compare the relative positions of predator and prey against the background) despite the enormous jaw protrusion. Thus protrusion is not an obligatory correlate of suction feeding. In this case, the behavior of the predator (initial mouth opening followed by a rapid forward lunge) limits the potential increase in the 'suction efficiency' obtainable by protrusion".

However, from previous work and the present paper it is clear that:
1. Protrusion contributes to the directedness of the flow in the fish-bound frame (Nyberg, 1971 and Muller and Osse, in press, Fig. 21). A fast swimming predator like *Luciocephalus*, however, already creates a directed flow by its forward velocity (Muller et al., 1982; Muller and Osse, in press and the present paper, Fig. 21). So protrusion seems to be of no advantage for *Luciocephalus* in this respect. Besides, protrusion may decrease the effectiveness of the biting mechanism.
2. However, the early achieved protrusion lengthens the mouth and hence increases the effect of a given expansion rate. Therefore the point where the fluid is at rest in an earth-bound frame can be kept more caudally when the caudal valves are still closed (see 3.2.3.). Hence due to protrusion the effect of the suction apparatus has increased relative to that of the swimming apparatus. After protrusion has been established the flow is less directed than it would be without protrusion.
3. The additional head lengthening will result in a decrease of the critical mouth expansion rate (see paragraph 3.2.3.) and therefore in an increase in the ideal time of the opening of the valves. This requires long branchiostegal rays that allow the valves to be closed with a relatively large abduction of the opercula. These are indeed present. This is an example of the interdependence of separate morphological features within the sucking system.
4. Muller and Osse (in press) distinguished an extreme feeding type for fishes with protrusion that do not use extensive swimming (*low-τ-suction with protrusion*). They argued that protrusion enlarges the velocities relative to the mouth aperture. Hence, the feeding act can be shortened and the total impulse added to the fish's

body and the water containing the prey can be kept small. The valves open relatively early. *Luciocephalus*, when feeding in the open water, applies another extreme feeding type, having an opposite aim in comparison to low-$\tau$-suction with protrusion. It enlarges the impulse enormously through a combination of head lengthening (larger volume sucked), a relatively late opening of the caudal valves and extensive swimming. This impulse is mainly put into the fish's body, as the prey was found to be relatively stationary in the earth-bound frame. I propose to call the open water feeding type of *Luciocephalus high-$\tau$-suction with protrusion and swimming*. All morphological features, distinguished so far, necessary for low-$\tau$-suction with protrusion are present in *Luciocephalus*. Therefore, it may also be able to suck efficiently close to solid substrates.

5. Compared to the pike *Luciocephalus* has increased the suction capacity. Biting, however, is less effient due to the protrusable upper jaws. Therefore *Luciocephalus* seems to be specialized in sucking relatively small preys in one gulp, from a large initial distance.

6. The kinematic behaviour of *Luciocephalus* is perfectly adjusted to its morphology and hydrodynamical constraints and conclusions as to *un*functional morphology made by Lauder and Liem are unjustified.

## 4.4. Optimizations for a unidirectional flow; the key role of the valves

The key role of the gill cover in the feeding mechanism of the bony fishes is apparent from the above examples. The valves allow the fish to change almost instantaneously its hydrodynamical conditions during feeding. In the first instance they close the mouth cavity at its posterior end to avoid a caudal inflow and to maximize the flow rate through the mouth aperture. Later, they form no obstacle when the flow rate can be enhanced through a caudal outflow. Furthermore the gill covers lengthen the mouth (see e.g. 4.3. for the advantages of a longer mouth).

A biphasic inflow through the opercular slits occurs during feeding in the rainbow trout (at least in the range of observed swimming speeds, 0.5 to 2 m/sec, see Fig. 10). Now, it will be discussed that several morphological and kinematic features, developed in the actinopterygian feeding mechanism, serve to generate a caudally directed flow inside the whole mouth during the entire feeding act.

The initial inflow through the opercular slits might be reduced by a faster opening mechanism. Then a delay of $\tau_a$ would be possible and hence a reduction of $\tau_i$-$\tau_a$ would occur (see 3.2.3.). Second the valves may open in a rostral direction, thereby diminishing the effective head length and hence $\tau_a$. Again a reduction of $\tau_i$-$\tau_a$ would be the result. However, the effect of mouth expansion on the flow towards the mouth is also diminished in this case. This last effect may not be too harmful for the fast swimming trout which indeed opens the opercular slits relatively far rostrally. A fish feeding at low swimming speeds, like the lionfish (*Pterois russelli*), an acanthopterygian, may benefit more from a fast opening mechanism. The isthmus of the branchiostegal membranes in *Pterois* lies far backward (especially at the moment of valve opening) as is apparent from high-

69

speed films made by Muller et al. (1982). The lionfish, however, possesses relatively long curved aciniform branchiostegal rays allowing a significant opercular slit to be formed within only 2.5 msec (Muller et al. 1982, Fig. 9B), a second advantage of this type of branchiostegals (see also 4.3.).

Films made by Lauder and Liem (1981) show that the isthmus in *Luciocephalus* lies also far caudally and that the valves open rapidly (at frame 6 the valves are still firmly closed whereas at frame 8 they are widely open, film of 200 fr/sec; cf Fig. 2 of Lauder and Liem, 1982, unfortunately the important frame 7 is not shown by the authors). This aspect again supports the view that suction is relatively important in *Luciocephalus* compared to other fast swimming fish.

I suggest that a faster opening mechanism of the valves allows a longer effective mouth length after valve opening and hence a more caudal isthmus. In this way the contribution of mouth expansion relative to swimming is increased. More research, however, is needed to be certain about this point.

Pushing in the mouth aperture combined with a (secondary) net caudal inflow through the opercular slits may occur if the caudal parts of the mouth are still expanding, while the rostral parts are compressing (see paragraph 3.2.4.). A reduction or even a complete avoidance of a secondary inflow can be achieved by:

1. A high swimming velocity. The effect of swimming will be small just before mouth closure, when only a minor mouth aperture is present. At that time, however, escape of the prey is unlikely to occur.

2. A relative delay of $\tau_a$. When $\tau_a$ is increased the time available between $\tau_a$ and $t_{h2max}$ (the moment of the maximal opercular abduction) is decreased. Hence, a secondary caudal inflow becomes more unlikely. This relative delay is e.g. found in the pike, if feeding at a low swimming speed. The lionfish (see Muller et al., 1982 and Muller and and Osse, in press) opens the valves before $t_{h2max}$, however, at a relatively larger opercular abduction than in the rainbow trout. A secondary inflow was indeed not found by flow visualization by Muller and Osse. In the bottom feeding type of the ruffe (see 4.3.) $\tau_a$ is even postponed till the instant $t_{h2max}$. This was also found in the cod (*Gadus morhua*), a paracanthopterygian, with long aciniform branchiostegals, when feeding at a low swimming speed (see Muller and Osse, in press, Fig. 5). Muller and Osse also found that the cone like movement of the mouth could cause a biphasic caudal inflow if the valves would open earlier (see their Fig. 18).

3. An earlier achieved maximal opercular abduction. This may lead to a mouth cavity compressing over its entire length, with an open mouth and open caudal valves. This obviously prevents a caudal inflow. This possibility seems to be only useful when the mouth aperture is already quite small, so that a blowing out of the prey is avoided. From Muller and Osse (in press, Fig. 11) it appears that this effect is present in e.g. *Amia calva, Gadus morhua, Stizostedion lucioperca* and *Pterois russelli* (in all cases with the expected small mouth aperture).

4. A reduction of $h_2$ after valve opening. If $h_2$ is less than a particular critical value (with the other parameters constant, see paragraph 3.2.3.) inflow is avoided.

70

5. Use of unsteady effects. An increased overall caudally directed impulse before valve opening may delay a possible triple- or single-vortex effect and prevent a net secondary caudal inflow (but *not* the initial inflow). As argued in 3.2.2. this may only be important at a very low forward body velocity. Other unsteady effects, due to the cone like movement may also play a role. Note that points 1 to 5 are intimately related to each other.

6. A reduced rostral extension of the opercular slits (see paragraph 3.2.4.). These extensions are very prominent in the palaeoniscoid *Pteronisculus*, whereas they are small in the highly advanced lionfish.

The development of a gill cover, allowing a large opercular abduction with closed valves and a rapid valve opening, in the actinopterygian feeding mechanism has made prey capture less dependent on swimming. Therefore, the number of options to obtain a prey has increased, also within a single species.

A single gill cover for all gill arches of one side was probably first developed within the acanthodians as pointed out by Miles (1971). If this is true, then the basis for the suction feeding mechanism of the teleostomes can probably be found in this group. This suggestion from a functional point of view corroborates the conclusion of Miles (1973) that the acanthodians are probably more closely related to the osteichthyans than to the chondrichthyans.

Schaeffer and Rosen (1961) distinguished adaptive levels in the actinopterygian feeding mechanism, mainly based on the biting function of the jaws. Osse (1976) and Osse and Muller (1980) stressed that suction is at least as important as biting, and that therefore the evolution of the gill cover should be incorporated in a study of the actinopterygian feeding mechanism. The present results support this view.


## 5. Conclusions

1. The analysis of the feeding system of *Salmo gairdneri* showed that:

a. initially the prey was slightly pushed forward in the earth-bound frame.

b. later the prey was sucked backward, toward the mouth, in the earth-bound frame. This suction continued even after the opercular and branchiostegal valves had opened.

c. about 90% of the total volume drawn into the mouth was originally present in a sphere, centered on the prey, with a slightly larger radius than that of the maximal mouth aperture (see Fig. 13).

d. the flow rate into the mouth is highly variable, but maximal at the instant of prey capture.

2. Constraints on an optimized feeding mechanism can be deduced from a cylinder and a cone model of the fish's mouth (based on the model approach by Muller et al., 1982 and Muller and Osse, in press). The constraints relate morphological and kinematic parameters, such as head length, mouth radius, mouth expansion rate and swimming speed. Good agreement was found between model predictions and experimental data.

71

3. To avoid pushing effects, the fish should at least reach a threshold expansion rate of its mouth aperture when the opercular and branchiostegal valves are closed. This rate depends on the fish's swimming speed, its mouth radius, its mouth length and an expansion rate in the opercular region. The rainbow trout exceeds this rate or opens the caudal valves.

4. After the valves have opened a threshold translational velocity should be reached by the fish to avoid inflow through the opercular slits. This velocity depends on the fish's head length, mouth radius and mouth expansion rate and a possible unsteady effect. This last effect was shown to be small in the rainbow trout.

5. The opercular and branchiostegal valves from an important control device for the acquisition of an optimal flow rate through the mouth aperture, by the possibility of changing almost instantly the fish's hydrodynamical constraints. They should be open when the mouth expansion rate is less than a certain critical value (see paragraph 3.2.3.).

6. Head expansion and thereby suction are continued after valve opening in the rainbow trout. Head expansion contributes also after valve opening to prey capture by increasing the flow rate through the mouth aperture. Generally, this flow is enhanced by a caudal outflow through the opercular slits at the actual moment of prey capture.

7. A minor biphasic caudal inflow through the opercular slits of *Salmo gairdneri*, expected on theoretical grounds, was indeed detected experimentally. Many kinematic and morphological features of actinopterygian fishes can be explained as adaptations to obtain (or approach) a posteriorly directed flow inside the whole mouth throughout the feeding act.

8. The quantitative picture of the flow in suction feeding developed in the present paper allows a better understanding of the feeding mechanism of actinopterygian fish in general as explained for *Pteronisculus†, Amia, Esox, Salvelinus, Gadus, Pterois, Luciocephalus* and *Gymnocephalus*.

9. The prey capture mechanism of palaeoniscoids like *Pteronisculus* was probably largely dependent on swimming. The evolution of the prey capture mechanism shows various adaptations (e.g. an increased effective head length and a larger possible abduction of the gill cover without opening of the caudal valves) leading to an increased independence of the feeding process from swimming. However, if the situation allows it swimming is continued to be taken advantage of, as a way to increase the flow rate through the mouth aperture.

10. The stereoscopic flow visualization technique described in the present paper is an important tool in the study of the prey capture mechanism of actinopterygian fish, as with it the predator, prey and surrounding water can be followed through time in 3-dimensional space. With it information is gained about the volume flow of water into the mouth, the shape of the volume drawn into the mouth, the velocity of the predator and prey, particle path lines, the momentum given to the water and the prey by the fish, the occurrence of stagnation effects, the relation between suction and swimming and the role of the opercular and branchiostegal valves during suction feeding.

72

## 6. References

Alexander, R.McN. (1967). The function and mechanisms of the protrusible upper jaws of some acanthopterygian fish. *J. Zool. Lond.* **151**, 43-64.

Anker, G.Ch. (1974). Morphology and kinetics of the head of the stickleback, *Gasterosteus aculeatus*. *Trans. Zool. Soc. Lond.* **32**, 311-416.

Ellington, C.P. (1978). The aerodynamics of normal hovering flight. In: *Comparative Physiology - Water, Ions and Fluid Mechanics* (ed. K. Schmidt-Nielsen, L. Bolis and S.H.P. Maddrell), pp. 327-345. Cambridge University Press.

Elshoud-Oldenhave, M.J.W. & Osse, J.W.M. (1976). Functional morphology of the feeding system of the ruff-*Gymnocephalus cernua* (L. 1758)-(Teleostei, Percidae). *J. Morph.* **150**, 399-422.

Hertel, H. (1966). *Structure, Form and Movement*. New York. Reinhold.

Kokshaysky, N.V. (1979). Tracing the wake of a flying bird. *Nature* **279**, 146-148.

Lauder, G.V. (1980). The suction feeding mechanism in sunfishes (*Lepomis*): an experimental analysis. *J. exp. Biol.* **88**, 49-72.

Lauder, G.V. & Liem, K.F. (1980). The feeding mechanism and cephalic myology of *Salvelinus fontinalis*: form, function and evolutionary significance. In: *Charrs Salmonid Fishes of the Genus Salvelinus* (ed. E.K. Balon), pp. 365-390. Dr. W. Junk Publishers, The Hague.

Lauder, G.V. & Liem, K.F. (1981). Prey capture by *Luciocephalus pulcher*: implications for models of jaw protrusion in teleost fishes. *Env. Biol. Fish.* **6**, 257-268.

Leeuwen, J.L. van & Muller, M. (in prep.). The recording and interpretation of pressures in prey sucking fish.

McAllister, D.E. (1968). Evolution of branchiostegals and classification of telestome fishes. *Bull. Nat. Mus. Can.* **221**, i-xiv: 1-239.

McCutchen, C.W. (1977). Froude propulsive efficiency of a small fish, measured by wake visualization. In: *Scale effects in animal locomotion* (ed. T.J. Pedley), pp. 339-363. London, New York and San Fransisco. Academic Press.

Merzkirch, W. (1974). *Flow Visualization*. New York and London. Academic Press.

Miles, R.S. (1971). In: *Palaeozoic fishes* (J.A. Moy-Thomas), 2nd ed. London. Chapman & Hall.

Miles, R.S. (1973). Relationships of acanthodians. In: *Interrelationships of fishes* (ed. P.H. Greenwood, R.S. Miles & C. Patterson), pp. 63-104. London. Academic Press.

Muller, M. & Osse, J.W.M. (1978). Structural adaptations to suction feeding in fish. In: *Proceedings of the ZODIAC symposium on adaptation*, pp. 57-60. Wageningen. Pudoc.

Muller, M. & Osse, J.W.M. (in press). Hydrodynamics of suction feeding in fish. *Trans. Zool. Soc. Lond.*

Muller, M., Osse, J.W.M. & Verhagen, J.H.G. (1982). A quantitative hydrodynamical model of

suction feeding in fish. *J. theor. Biol.* **95**, 49-79.

Nyberg, D.W. (1971). Prey capture in the largemouth bass. *Am. Midl. Nat.* **86**, 128-144.

Osse, J.W.M. (1969). Functional morphology of the head of the perch (*Perca fluviatilis* L.): an electromyographic study. *Neth. J. Zool.* **19** (3), 289-392.

Osse, J.W.M. (1976). Mécanismes de la respiration et la prise des proies chez *Amia calva* Linnaeus. *Rev. Trav. Inst. Pêches Marit.* **40**, 701-702.

Osse, J.W.M. & Muller, M. (1980). A model of suction feeding in teleostean fishes with some implications for ventilation. In: *Environmental physiology of fishes* (ed. M.A. Ali) NATO-ASI Series A. Life Sciences. pp. 335-352. Plenum Publishing Corporation, New York.

Rand, D.M. & Lauder, G.V. (1981). Prey capture in the chain pickerel, *Esox niger*: correlations between feeding and locomotor behavior. *Can. J. Zool.* **59** (6), 1072-1078.

Schaeffer, B. & Rosen, D.E. (1961). Major adaptive levels in the evolution of the actinopterygian feeding mechanism. *Amer. Zool.* **1**, 187-204.

Selvik, G. (1974). *A roentgen stereophotogrammetric method for the study of the kinematics of the skeletal system.* Thesis. AV-centralen, Lund.

Spiegel, M.R. (1968). *Mathematical handbook of formulas and tables.* Schaum's outline series in mathematics. New York. McGraw-Hill.

Spiegel, M.R. (1974). *Theory and problems of vector analysis and an introduction to tensor analysis.* Schaum's outline series in mathematics. New York. McGraw-Hill.

Weihs, D. (1980). Hydrodynamics of suction feeding of fish in motion. *J. Fish Biol.* **16**, 425-433.

# 7. Appendix

### 7.1. Filming rate and accuracy of velocity calculations

The error made in velocity calculations by numerical means depends on the time interval used for differentiation, as shown by Muller et al (1982) for their computer model of suction feeding with the aid of the contraction formula of Banach. The same holds true for velocity calculations from position data obtained from films. Suppose that the error made in the determination of the position of a point P on each film frame is $\delta x$ and the error in the determination of the time it was taken $\delta t$. Then the error in the calculation of the mean velocity $\delta q_m$ in the time interval $\Delta t$ between two frames will be:

$$\delta q_m = \frac{2\delta x}{\Delta t} + \frac{d}{(\Delta t)^2} \cdot 2\delta t \tag{23}$$

where $d$ is the distance travelled by $P$. From (23) it is clear that $\delta q_m$ decreases hyperbolically with increasing $\Delta t$, so that a large $\Delta t$ seems to be favourable. However, fluctuations in the real velocity $q$ are better recorded with a decreasing $\Delta t$. To appreciate this consider a point with a sinusoidally fluctuating velocity $q_o$:

$$q_o = -0.5 \, B \sin 2\pi f t \tag{24}$$

where $B$ represents the velocity range and $f$ the frequency of oscillation. The maximal error $\delta q_o$ depends on $B, f$ and $\Delta t$, when no error is made in its position, and was found to be (after some algebra):

$$\delta q_o = |\, 0.5 \, B \sin \frac{3\pi}{2} \, (\frac{1}{f} \sin (-\pi f \Delta t) + 1) \,| \tag{25}$$

74

$\delta q_0$ decreases with decreasing $\Delta t$. The maximal possible error is reached for $\Delta t$ is $3f/2$. $\delta q_0$ was calculated for a range of different $B$'s and $f$'s, an example of which, together with a calculation of $\delta q_m$, is given in Fig. 22. The choice of $\Delta t$, used for numerical differentiation, depends on the frequency range needed in the analysis, and should be taken in the range where $\delta q_m$ and $\delta q_0$ are of about equal magnitude. In the present study a frequency range of 0-50 Hz, together with a $\Delta t$ of about 10 msec was found to be most suitable.

### 7.2. CORRECTION FOR PERSPECTIVE DISTORTIONS

In paragraph 2.4. it was explained how the coordinates of points in space could be calculated once the projections of these points in stereographs on planes C and F are known. A correction for perspective distortions was needed because these planes were not perpendicular to the optical axes of the stereoscopic filming set up. Planes C and F were positioned perpendicular to the horizontal plane. The optical axes were orientated parallel to the horizontal. For this particular situation the distortion of a plane is illustrated in Fig. 23. Lines parallel to the Y-axis (the vertical axis) remain parallel to each other on the film or its perpen-
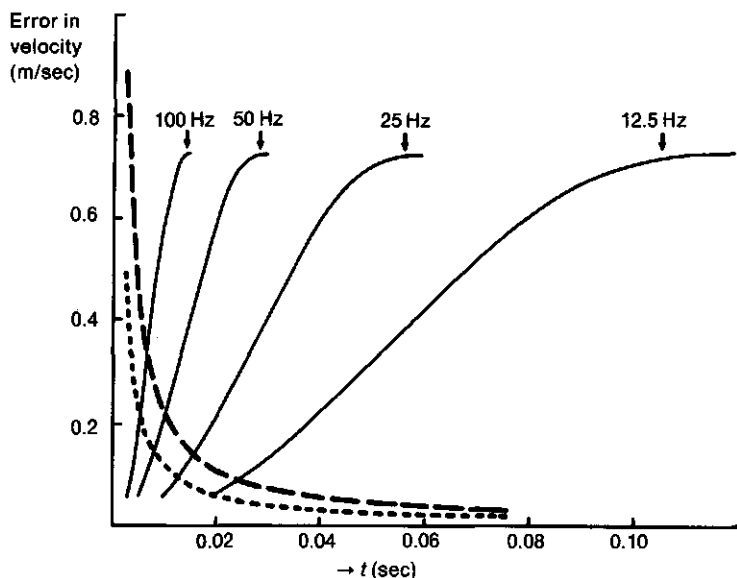


Fig. 22. Example of an analysis of the expected maximal error in the velocity obtained from position data from high-speed movies. The mean velocity was chosen to be 1.2 m/sec. The error in $q_m$ was calculated for both a $\delta x$ of 1 and 2 mm (respectively the dotted and dashed curves). For the calculation of $q_0$ it was assumed that the velocity varied sinusoidally with an amplitude of 0.6 m/sec ($B = 1.2$ m/sec). This calculation was done for $f$ equals 12.5, 25, 50, and 100 Hz (depicted near each curve). Obviously, a larger $\Delta t$ should be taken when $\delta x$ increases. The reverse is true when a higher frequency range is needed.

75

dicular projection. Along these lines the scale factor $S$ is constant. This is not true for lines originally parallel to the $X$-axis. Just one of these lines remains perpendicular to the $Y$-axis, which we shall call the $X_\perp$-axis. Along this axis $S$ varies linearly:

$$S = cx_\perp + d \qquad (26)$$

where $c$ and $d$ are constants and $x_\perp$ the coordinate along the $X_\perp$-axis.

For calculation of the actual $x$-coordinate, $x_{AP}$, of the projection of a point $P$ the following integral should be solved:

$$x_{AP} = \int_0^{x_{\perp P}} \frac{1}{S} dx_\perp \qquad (27)$$

which gives:

$$x_{AP} = \frac{1}{c} \ln (cx_{\perp P} + d) - \frac{1}{c} \ln d \qquad (28)$$

The actual $Y$-coordinate of the projection of $P$, $y_{AP}$, can be obtained by:
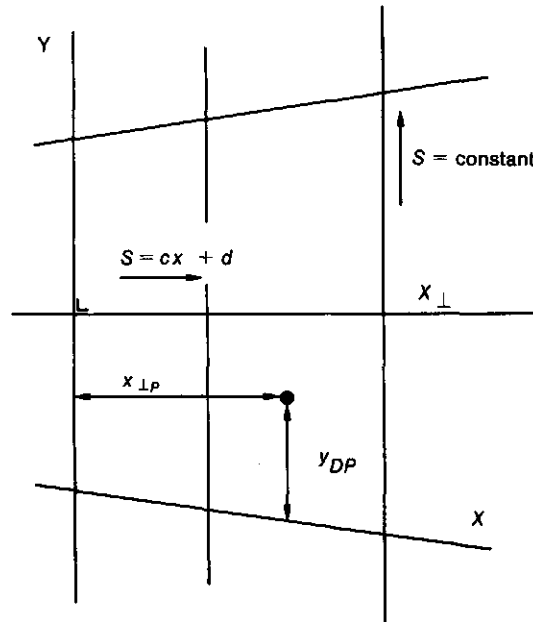
$$y_{AP} = y_{DP}/S \qquad (29)$$



Fig. 23. Diagram of a distorted plane (as explained in appendix 7.2.) illustrating the method of calculating the correction for perspective distortion. The black dot denotes the projection of $P$ on the distorted plane. Further notations are explained in the text and Table 1.

76

where $y_{DP}$ is the distance to the $X$-axis in a direction parallel to the $Y$-axis in the distorted plane. Constants $c$ and $d$ can be calculated from reference points with known coordinates on the calibration frame.

# Optimum sucking techniques for predatory fish

# Optimum sucking techniques for predatory fish

J.L. VAN LEEUWEN AND M. MULLER

Department of Experimental Animal Morphology and Cell Biology,
Agricultural University, Marijkeweg 40,
6709 PG Wageningen, The Netherlands.

## Synopsis

The hydrodynamical model of suction feeding in fish by Muller et al. (1982) and Muller & Osse (in press) was used to derive conditions for optimal prey-suction. The separate contributions of swimming, mouth expansion and a possible jaw protrusion to the velocity of the prey relative to the fish were calculated as functions of time. Account was taken of the unsteady nature of the flow. The calculations are valid if the opercular valves are closed before prey uptake. The initial prey distance is generally hardly affected by quite a large change in the fish's mouth expansion. However, the influence of mouth expansion on the velocity of the prey while it enters the mouth is very strong. These results permit to derive, together with considerations of the generated pressure, the optimal phase relationship between the expansion of the rostral end of the mouth and the abduction of the operculars. Predictions were made for the relation between the maximal mouth aperture and the swimming speed of the fish. Estimates were made of the effect of valve opening before prey capture. These theoretical predictions were tested using data from high-speed films of fish feeding. Sucking techniques are discussed for fish feeding in different habitats.

## Contents

# 1. Introduction

Prey capture mechanisms in bony fish have been frequently studied. The dominant mode of prey capture consists of a combination of suction (by a rapid expansion and compression of the buccal and opercular cavities, together denoted as the mouth cavity in this paper) and forward motion (by suction forward, protrusion and swimming). The success of a feeding event depends largely on the generated flow relative to the fish's mouth. Therefore, hydrodynamic principles may be succesfully used to study the predator-prey interaction (see e.g. Muller et al., 1982; Muller & Osse, in press and Van Leeuwen, in prep.).

The present paper attempts to derive quantitative requirements (morphologically and kinematically) for optimized prey capture techniques (i.e. such techniques that the chance of prey capture is maximized). It deals with questions like:

1) At what moment and what distance from the prey should a fish start mouth expansion?

2) How is the velocity of the prey related to the fish's mouth cavity expansion, jaw protrusion, forward velocity and distance?

3) Does the predator optimize velocity, or distance or both? Which velocity should be preferably given to the prey when it passes the mouth aperture, in order to optimize the prevention of its escape?

4) Is there an optimal combination of the expansion of the rostral end of the mouth cavity and the abduction of the operculars, to optimize the chance of prey capture (with a given effort of the predator)?

It will be shown that detailed knowledge of the escape response of the prey is not required to explain much of the behaviour of the predator during capture. Therefore the present analysis deals only with prey moving with the flow.

# 2. Definitions and symbols

$d_{prey}$           distance between prey and mouth aperture

$d_{iprey}$         distance between prey and mouth aperture at $t_{v1}$: the initial prey distance

$e_{suction}$        relative suction effect (see page 86)

82

| | |
|---|---|
| $e_{swimming}$ | relative swimming effect (see page 86) |
| $h_1$ | profile radius at 'mouth aperture' ($x' = l$) |
| $h_2$ | profile radius at 'opercular region' ($x' = 0$) |
| $h_{*max}$ | maximal value of profile radius, $* = 1$ or 2 |
| $h_{*nul}$ | minimal value of profile radius, $* = 1$ or 2 |
| $l$ | length of profile (or fish's mouth cavity), $l = l_0 + l_{prot}$ |
| $l_0$ | length of profile at $t = t_{vl}$ |
| $l_{prot}$ | distance of protrusion |
| $t$ | time |
| $t_{half*}$ | time at which $h_* = h_{*nul} + 0.1\ \Delta h_{*max}$, plus $0.5t_{r*}$ (see page 87), $* = 1$ or 2 |
| $t_{h*max}$ | time at $h_{*max}$, $* = 1$ or 2 |
| $t_{pb}$ | time at which the prey passes the mouth aperture |
| $t_{r*}$ | rise time (see page 87), $* = 1$ or 2 |
| $t_{v*}$ | delay time, $* = 1$ or 2 |
| $u$ | velocity in the $X$-direction in the earth-bound frame |
| $u'$ | idem in the $X'$-direction in the fish-bound frame |
| $u_m$ | velocity in the mouth aperture in earth-bound frame |
| $u'_m$ | idem in fish-bound frame: $u'_{mlc} + u'_{mprot} - U_{prot}$ |
| $u'_{mlc}$ | velocity in mouth aperture if protrusion were absent |
| $u'_{mprot}$ | contribution of protrusion to suction velocity in mouth aperture |
| $u_{prey}$ | velocity of the prey in earth-bound frame |
| $u'_{prey}$ | idem in fish-bound frame |
| $\bar{u}'_{prey}$ | mean speed of the prey in fish-bound frame from $t_{vl}$ till $t_{pb}$ |
| $u'_{tpb}$ | velocity of the prey at $t = t_{pb}$ in fish-bound frame |
| $U_f$ | velocity of mouth aperture: $U_{sw} + U_{prot}$ |
| $U_{prot}$ | velocity of protrusion |
| $U_{sw}$ | velocity of fish's body |
| $x$ | coordinate of long axis in earth-bound frame |
| $x'$ | idem in moving frame |
| $X,Y,Z$ | axes of earth-bound frame |
| $X',Y',Z'$ | axes of fish-bound frame |
| $\alpha_*$ | shape coefficient of profile movement, $* = 1$ or 2 |
| $\beta$ | angle between medial plane of the fish and long axis of hyoid |
| $\Delta h_{*max}$ | $h_{*max} - h_{*nul}$, $* = 1$ or 2; amplitude of movement |
| $\tau_a$ | actual moment of opening of opercular valve |

## 3. Methods

High-speed films were made of feeding *Amia calva*, (bowfin, 1 specimen), *Salmo gairdneri* (rainbow trout, 1 specimen), *Esox lucius* (pike, 3 specimens), *Gadus morhua* (cod, 1 specimen), *Stizostedion lucioperca* (pike-perch, 1 specimen), *Platichthys flesus* (flounder, 1 specimen) and *Pterois russelli* (lionfish, 1 specimen) as described by Muller & Osse (in press). The dimensions of the specimens used

83

Table 1. Fish specimen used. SL is standard length, *l* is head length, Prot. is protrusion of upper jaws. T is temperature of water, LA, WA and HA are length, width and height of aquarium.

| species | SL (mm) | *l* (mm) | Prot. (mm) | T (°C) | LA (m) | WA (m) | HA (m) |
|---|---|---|---|---|---|---|---|
| Amia calva | 365 | 92 | 0 | 17 | .9 | .5 | .4 |
| Salmo gairdneri | 343 | 80 | 0 | 15 | 1.9 | .5 | .3 |
| Esox lucius | 485 | 143 | 0 | 16 | 2.0 | .5 | .3 |
| Esox lucius | 253 | 73 | 0 | 15 | .8 | .5 | .3 |
| Esox lucius | 195 | 63 | 0 | 15 | .8 | .5 | .3 |
| Gadus morhua | 375 | 100 | 1 | 13 | .9 | .5 | .4 |
| Stizostedion lucioperca | 310 | 90 | 4.6 | 15 | .9 | .5 | .5 |
| Pterois russelli | 138 | 40 | 4.6 | 23 | .8 | .4 | .4 |
| Platichthys flesuslva | 315 | 71 | 4.7 | 15 | .6 | .4 | .2 |

and the conditions in which they were kept are given in Table 1. Visualization of the generated flow, using polystyrene spheres (0.5 and 1 mm in diameter) was carried out for *Pterois russelli* (as done by Muller & Osse, in press) and *Salmo gairdneri* (as done by Van Leeuwen, in prep.).

The experimental records were used to verify theoretical predictions, as derived from calculations of the prey velocity and initial prey distance $d_{iprey}$ ( = distance between the prey and the mouth aperture at the start of mouth expansion)

The calculations are based on the hydrodynamical model of suction feeding in fish by Muller et al. (1982). They modelled the flow towards the expanding mouth cavity as a combination of a circular vortex and a uniform flow (to take account of forward motion and a possible jaw protrusion). The singular points of the vortex are positioned at the fish's lips. Thus the radius of the mouth aperture $h_1$, corresponds to the radius of the vortex. The vortex strength is calculated from the rate of volume change of the mouth cavity. Thus account is taken of the unsteady nature of the flow. The mouth cavity was modelled as an expanding and compressing cone, of which the anterior radius can be varied independently from the posterior radius. The simplifying approximations of this model are extensively treated in Muller et al. (1982) and Muller & Osse (in press). Outlines of the model are given in Fig. 1.

The authors pointed out the necessity to make a distinction between events in the earth-bound frame (which is fixed relative to the aquarium) and events in the moving or fish-bound frame (which is fixed relative to the mouth aperture of the fish). Events in the earth-bound frame should be used to calculate forces and pressures. The flow in the fish-bound frame is very informative when the chance of prey capture is studied.

Experimental data, including pressure records (e.g. Lauder, 1980; Muller & Osse, in press and Van Leeuwen & Muller, in prep.), velocity records (Muller & Osse, in press) and flow visualization records (Muller & Osse, in press and Van Leeuwen, in prep.) could be satisfactorily explained with the model of Muller et al. (1982).
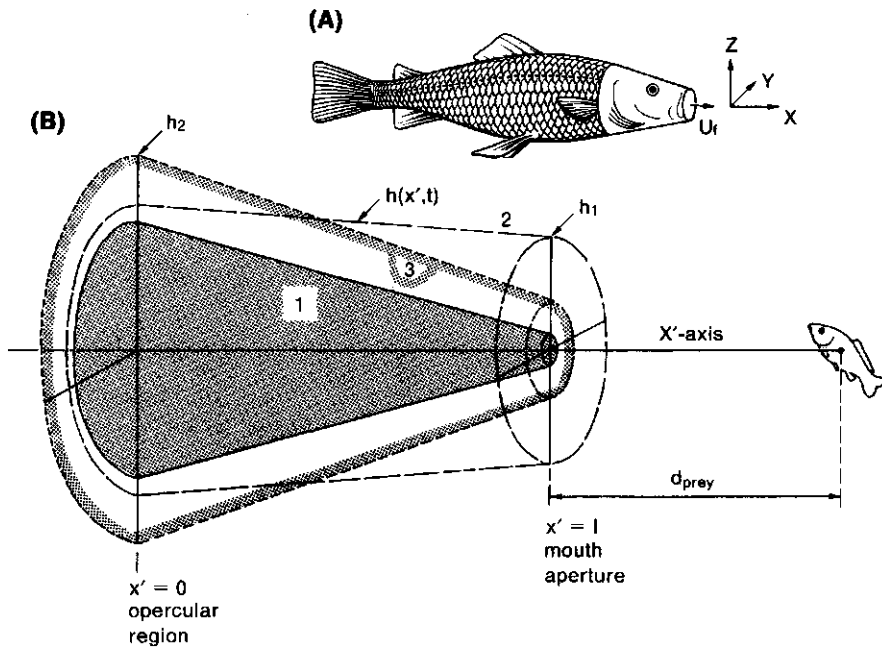
Fig. 1. Illustration of model approach as used in this paper.
A. Fish moving forward in the earth-bound frame $X,Y,Z$. The mouth aperture has velocity $U_f$ in this frame. $U_f$ is equal to the forward body velocity of the fish, $U_{sw}$, plus the velocity of protrusion of the jaws, $U_{prot}$. $U_{prot}$ is measured relative to the body of the fish. The expanding and compressing mouth cavity of the fish is schematized as a conical profile (see B).
B. Different stages of expansion and compression of conical profile. 1. Initial, and also final stage. 2. The buccal region has expanded widely; the opercular region starts to expand. 3. The buccal region contracts whereas the opercular region is still expanding. The cone is represented in the moving frame $X',Y',Z'$, so that it stands still. $X$ and $X'$-axes are taken to overlap each other. $h_1$ and $h_2$ are the radii at $x' = l$ and $x' = 0$ respectively. The prey is located at the $X'$-axis, at a distance $d_{prey}$ from the mouth.

# 4. Calculations

We assume the prey to behave as an element of the water. So the prey does not swim and its density equals that of water. Other prey reactions are paid attention to in the general discussion. Furthermore we assume that the fish aims at its prey before it starts sucking. This means that the prey is positioned at the long axis of the mouth (the $X'$-axis, taken parallel to the $X$-axis of the earth-bound frame) during the suction process. This feature was observed in the majority of the more than 200 recorded feeding events of eight different species. Muller et al. (1982) calculated the velocity of the water in the earth-bound frame along the $X$-axis (their formula 34). With this formula and the above assumptions we obtain the velocity of the prey in the earth-bound frame:

85

$$u_{prey} = \frac{u_m h_1{}^3}{\sqrt{(d^2{}_{prey} + h_1{}^2)^3}} \tag{1}$$

where $u_m$ is the velocity of the water in the mouth aperture in the earth-bound frame, and $d_{prey}$ the distance between the mouth aperture and centre of mass of the prey. The relation between velocity $u$ in the earth-bound frame and velocity $u'$ in the moving frame is:

$$u' = u - U_f \tag{2A}$$

$$u'_{prey} = u_{prey} - U_f \tag{2B}$$

$$u'_m = u_m - U_f \tag{2C}$$

Where $U_f$ is the velocity of the mouth aperture. $u'_m$ and $u'_{prey}$ are velocities in the moving frame of the water in the mouth aperture and the prey respectively. $u'_{prey}$ is chosen to have a negative value if the prey moves towards the fish's mouth. Using (2) we can rewrite (1) to obtain the velocity of the prey in the moving frame:

$$u'_{prey} = \frac{u'_m h_1{}^3}{\sqrt{(d^2{}_{prey} + h_1{}^2)^3}} + U_f \frac{(h_1{}^3 - \sqrt{(d^2{}_{prey} + h_1{}^2)^3})}{\sqrt{(d^2{}_{prey} + h_1{}^2)^3}} \tag{3}$$

(3) can be written in a simplified form:

$$u'_{prey} = u'_m\, e_{suction} + U_f\, e_{swimming} \tag{4}$$

where $e_{suction}$ is the relative suction effect and $e_{swimming}$ the relative swimming effect and:

$$e_{swimming} = e_{suction} - 1 \tag{5}$$

Furthermore we have:

$$U_f = U_{sw} + U_{prot} \tag{6}$$

where $U_{sw}$ is the forward body velocity of the fish (due to swimming and suction forward) and $U_{prot}$ the protrusion velocity. Also:

$$u'_m = u'_{mlc} + u'_{mprot} - U_{prot} \tag{7}$$

where $u'_{mlc}$ is the velocity in the mouth aperture if protrusion is absent and $u'_{mprot}$ the contribution to $u'_m$ due to the increase of $l$ as a result of protrusion. Using (5), (6) and (7) we can rewrite (4) to show the separate effects of suction, swimming and protrusion on $u'_{prey}$:

$$u'_{prey} = u'_{mlc}\, e_{suction} + u'_{mprot}\, e_{suction} + U_{sw}\, e_{swimming} - U_{prot} \tag{8}$$

The first term represents the component of the relative prey velocity due to suction of the profile if no protrusion would be present. The contribution of protrusion to the suction velocity of the prey is represented by the second term of (8). The third term gives the contribution of swimming to the relative velocity of the prey. The fourth term of (8) represents the contribution of the translation

86

velocity of protrusion to $u'_{prey}$. Note that this last effect is independent of $d_{prey}$. Protrusion causes no stagnation effect in the mouth aperture, except very close to the edges. The prey is pushed forward in the *earth-bound* frame, with velocity $U_{sw}e_{suction}$, if the fish does not suck ($u'_{mlc}$ and $u'_{mprot}$ are zero) and $-1 < e_{swimming} < 0$ (from equations 2, 5, 6 and 8). It will be shown in the results and discussion how a fish can avoid pushing effects.

Prey do have a certain size and may deviate from the $X'$-axis. A consideration of the complete field of flow (Muller & Van Leeuwen, in prep.), however, showed that this does not affect the conclusions drawn in the present paper.

Once the position of the prey at a particular moment during the suction process is known, the distance travelled by the prey is obtained by integration of (3). In a simulation we can prescribe this position at the start of mouth expansion, but then we do not know beforehand when the prey will enter the mouth. It seems reasonable to assume that in the optimal case the prey should enter the mouth when it is opened widest. Then, the size range of preys that can be caught is maximized, as may be the chance of prey capture. Muller & Osse (in press) indeed found that the moment of prey entering the mouth (at $t = t_{pb}$) correlates roughly with the moment of the maximal mouth aperture in eight different fish species. Later on we will relax this assumption (see page 105).

The initial prey capture distance can be obtained by a reverse calculation. Then $t_{pb}$ can be prescribed, which appeared most convenient. The integral to be solved (see appendix) has an implicit form, as $u'_{prey}$ depends on $d_{prey}$. Therefore, numerical integration was carried out. The time step for integration was chosen such that an accuracy of 0.03 mm of the initial distance was obtained, representing an error of less than 1 percent. The velocity in the mouth aperture due to suction ($u'_{mlc} + u'_{mprot}$) was calculated using formula (18) of Muller et al. (1982). The analytical solution for the cone is given in the appendix. $u'_m$ depends on $h_1$ and $h_2$. These variables were described by Muller et al. (1982), with functions of the following form:

$$h_*(t) = h_{*nul} + \Delta h_{*max} \left[ \frac{t - t_{v*}}{t_{h*max} - t_{v*}} \ exp \left\{ 1 - \frac{t - t_{v*}}{t_{h*max} - t_{v*}} \right\} \right]^{\alpha_*} \quad (9)$$

and: $h_*(t) = h_{*nul}$     for $(t \leqslant t_{v*})$,                        (10)

where $\Delta h_{*max} = h_{*max} - h_{*nul}$     and:
$t, t_{v*} \geqslant 0, t_{h*max} > t_{v*}, h_{*nul} > 0$
$h_{*max} > h_{*nul}$ and $\alpha_* \geqslant 2$

where $h_{*nul}$ is the minimal value of the profile radius, $h_{*max}$ the maximal value of profile radius, $(t_{v2} - t_{v1})$ the delay time between the starts of expansion of $h_1$ and $h_2$ and $\alpha_*$ the expansion coefficient of the profile. The index * from the parameters in the equations (9) and (10) may be 1 to define the movement at the mouth aperture or designate a 2 to obtain the movement in the opercular region. The rise time $t_{r*}$ of the movement curve is the time required for $h_*$ to go from $(h_{*nul} + 0.1 \ \Delta h_{*max})$ to $(h_{*nul} + 0.9 \ \Delta h_{*max})$. The moment $t_{half*}$ lies
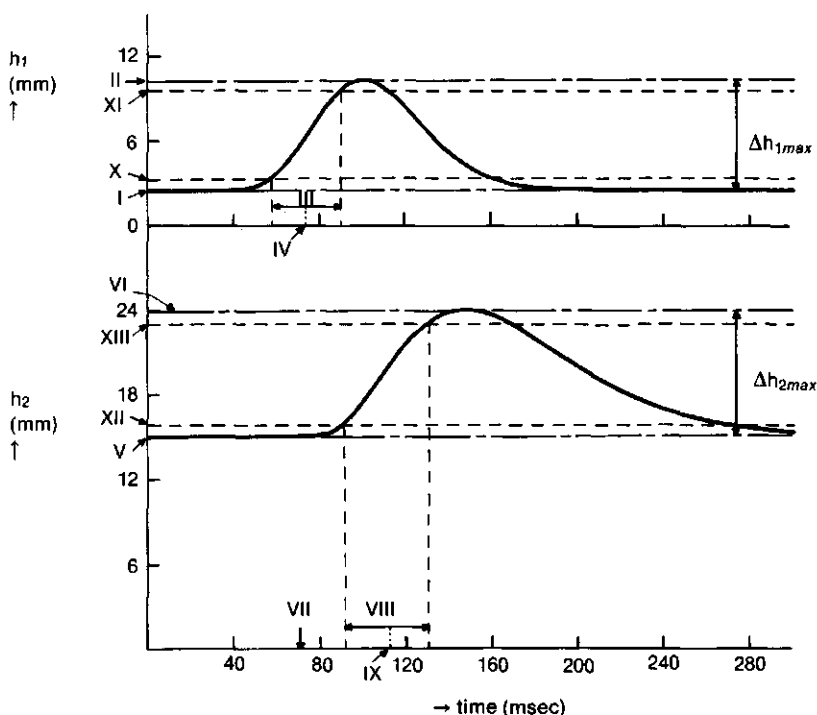
Fig. 2. Profile movements. $h_1$ *(t)* represents movement at mouth aperture $(x' = l)$. $h_2$ *(t)* is the movement in the opercular region $(x' = 0)$. All symbols are explained in the text. $h_1$ and $h_2$ represent fitted curves (see formulas 9 and 10) of a feeding attempt of a pike (*Esox lucius*, SL 253 mm). The values of the relevant parameters (see text) are: $\alpha_1 = 17.2$; I, $h_{1nul} = 2.5$ mm; II, $h_{1max} = 10.3$ mm; $t_{v1} = 0.0$ msec; $t_{h1max} = 100.0$ msec; III, $t_{r1} = 32.6$ msec; IV, $t_{half1} = 73.2$ msec; $\alpha_2 = 3.5$; V, $h_{2nul} = 15.0$ mm; VI, $h_{2max} = 24.0$ mm; VII, $t_{v2} = 72.5$ msec; $t_{h2max} = 147.5$ msec; VIII, $t_{r2} = 40.0$ msec; IX, $t_{half2} = 110.5$ msec; $l = 63$ mm, corrected for a deviation from the cone. Roman numbers are put in front of parameters shown in the illustration. Other notations: X, $h_{1nul} + 0.1$ $\Delta h_{1max}$; XI, $h_{1nul} + 0.9$ $\Delta h_{1max}$; XII, $h_{2nul} + 0.1$ $\Delta h_{2max}$; XIII, $h_{2nul} + 0.9$ $\Delta h_{2max}$. Although $t_{h1max}$ is 100 msec, $t_{r1}$ is only 32.6 msec. This is due to the relatively high value of $\alpha_1$, that was needed to obtain a good fit of the measured mouth radius.

halfway this interval (Fig. 2). The choice of $\alpha_*$ determines, with given other parameters, the shape and the rise time of the curve, as examplified by Muller & Osse (in press) in their Fig. 8. The mouth radius of the fish was measured from lateral or frontal views on the ciné films and fitted with the above function to obtain $h_1$. Similarly, $h_2$ was obtained from the simultaneously filmed ventral view of the fish (see Muller & Osse, in press).

All calculations were carried out by means of FORTRAN-programs run on a MINC-11-computer (Digital) and the DEC-10 system of the Agricultural University.

88

## 5. Results and discussion

### 5.1. EFFECTS OF SUCTION, SWIMMING AND PROTRUSION

Very often fish capture their preys by a combination of suction and swimming. It is useless for a fish to start sucking if the prey is still too far away. Also a bad strategy would be to swim too close to the prey. Now the prey will be pushed away, or cannot pass the only partly opened mouth aperture. Furthermore, the prey may become more easily aware of the predator. We will now investigate when a fish should preferably start sucking while it approaches the prey (questions 1 and 2, see page 82).

Fig. 3 shows plots of the relative suction effect and the relative swimming effect against $d_{prey}$ for various values of $h_1$ (see formulas (3), (4) and (5)). The relative suction effect is greatest close to the mouth. The relative swimming effect decreases also with the distance from the mouth. The relative suction effect increases non-linearly with the mouth radius. This can be easily observed by following this effect along the dotted vertical reference line in Fig. 3. Also, the distance from the mouth at which a particular relative suction effect is found increases proportionally to the mouth radius. (Shown by the dotted horizontal reference line in Fig. 3). Naturally, this is also true for the relative swimming effect. A larger mouth aperture does not automatically increase the distance from the mouth at which a particular magnitude of the suction velocity is found, because $u'_{mlc}$ is proportional to the mouth volume change, but inversely proportional to $h_1^2$.

During prey capture $h_1$ and $d_{prey}$ vary. Thus, the change in $e_{suction}$ for an actual feeding event intersects the contours, as illustrated in Fig. 3 for a feeding
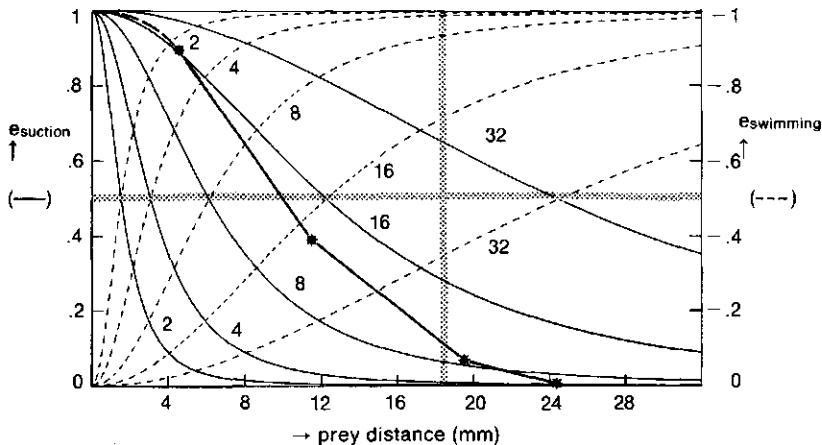


Fig. 3. Plots of relative suction effect (solid curves) and relative swimming effect (dashed curves) against prey distance. The contours show values of $h_1$ in mm. The heavy curve with asterisks denotes the actual variation of $e_{suction}$ during a feeding act of a rainbow trout (SL 343 mm). Mouth opening proceeds so that a rapid increase of $e_{suction}$ is obtained. Further explanations are given in the text.

event of a rainbow trout. The trout opens its mouth so that a rapid increase in $e_{suction}$ is obtained.

Having this knowledge, it will be interesting to see to what extent different fish use suction, swimming and protrusion to capture the prey. Figs. 4, 5 and 6 show the contributions of the different terms of formula (8) to the prey velocity, $u'_{prey}$. These curves are obtained from motion analysis of the fish's head. They are compared with the actually measured prey velocity.

Fig. 4 shows the contributions of suction and swimming to the prey velocity in the moving frame, for the prey capture event of Fig. 3 of the rainbow trout. This fish has no protrusion, although its maxillae rotate forward and thereby seal the mouth corners. Therefore the second and fourth terms of formula (8) are zero. The fish already started to expand its mouth at more than one head length away from the prey. This had little effect on $u'_{prey}$.

Remarkably, the largest negative pressures were recorded during this initial expansion (Van Leeuwen & Muller, in prep.). So, the fish seems to deliver a large effort, although this does not result directly in a contribution to $u'_{prey}$. It is important for the fish to be able to expand its mouth fast when the rapid increase of $e_{suction}$ becomes within reach (within about 30 mm from the mouth, see Fig. 3). This is impossible if the mouth aperture is still very small as then a very large force (pressure) would be required. So, initial mouth opening should be started before the possible rapid increase of $e_{suction}$. During the initial buccal expansion a slight opercular adduction was found in several fish species (see
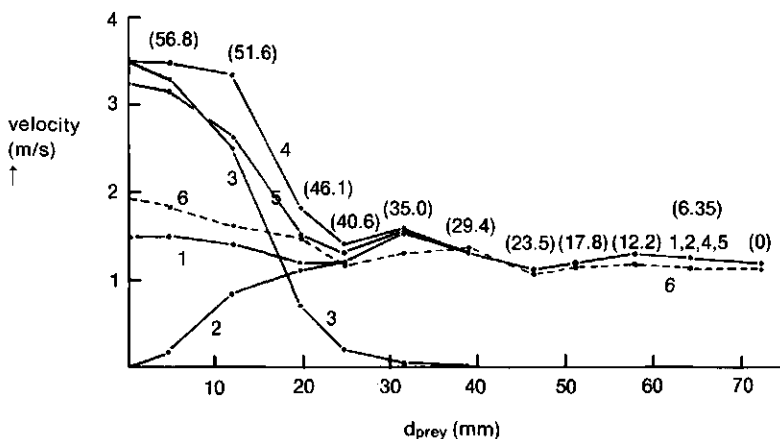


Fig. 4. Calculated contributions of suction and swimming to $u'_{prey}$ during the feeding act of the rainbow trout of Fig. 3. Protrusion of the jaws is absent in *Salmo*. The actual $d_{prey}$, as measured from the film, was used in the calculations (using formula (8)). The time in msec is given between brackets at each data point of $d_{prey}$. Notation:
1) swimming velocity. 2) minus velocity of prey due to swimming, $-U_{sw} \cdot e_{swimming}$. 3) minus velocity of prey due to suction, $-u'_{mlc} \cdot e_{suction}$. 4) $u'_{prey} =$ curve 2 + curve 3. 5) $-u'_{prey}$ with the assumption of open valves (page 91). 6) $-u'_{prey}$, measured from the film (dashed curve). The maximal errors made in calculating $U_{sw}$ and $u'_{prey}$ (directly from the film) were about 0.15 m/sec. The calculation via the cone model of $u'_{prey}$ appears to be a quite large overestimate.

90

e.g. Lauder, 1980; Muller & Osse, in press and Van Leeuwen & Muller, in prep.). This adduction will decrease the magnitude of $u'_{mlc}$, but decreases also the magnitude of the acceleration pressure and hence may increase the rate at which the mouth can be opened (see also Van Leeuwen & Muller, in prep.). Initial opercular adduction may therefore enhance the chance of prey capture. Note that the flow inside the mouth due to opercular adduction is very small, but sufficient to enlarge the initial volume of the buccal cavity. We wish to emphasize here that Lauder's explanation of this phenomenon (i.e. that the gills function as a caudal valve; Lauder, 1980) is incorrect (ref. for this point Muller & Osse, in press). Apart from these effects the early expansion may prevent stagnation effects due to swimming. The initial effort could be reduced if the fish would open its mouth initially slower and hence necessarily earlier. Too slow an expansion, however, would increase the pressure drag in swimming and is therefore not desirable.

The calculations for Fig. 4 were carried out with the assumption that the opercular and branchiostegal valves are kept closed until the maximal mouth aperture is reached (the moment of prey passage through the mouth aperture). This is not so in the rainbow trout (see Van Leeuwen, in prep.). After valve opening the effects of suction and swimming on the flow cannot be calculated exactly. The results of an estimate that $u'_{prey} = -U_{sw} + 0.5u'_{mlc}\,e_{suction}$ after valve opening are plotted in Fig. 4. It is assumed that $e_{swimming}$ has a constant value of $-1$ (similar to the translation effect of protrusion; stagnation effects are neglected) and the velocity in the mouth due to suction is only half the velocity with closed valves.

The actual prey velocity deviates quite strongly (i.e. is considerably less negative) from the calculated velocity (Fig. 4). This mainly is due to an overestimate of the volume change of the mouth with the cone model (up to 100 percent was found for *Esox lucius* by Kremers & Van Leeuwen, in prep. who measured the actual volume change). $h_2$ was measured as half the distance between the caudal edges of the opercula. The dorso-ventral expansion in this area is, however, very small, so that effectively $h_2$ will be smaller than the measured one. Likewise $h_1$ was measured as half the height of the mouth aperture, which also introduces an overestimate. Furthermore, no account was taken of the mouth corners, so that $l$ was overestimated.

If $u'_{prey}$ is greater than $-U_{sw}$, mouth expansion does not completely compensate the stagnation effects due to swimming and the prey will be pushed forward in an earth-bound frame. To avoid this the opercular and branchiostegal valves open (see Van Leeuwen, in prep. for a detailed discussion of this point). The suggestion which might rise from the calculations that valve opening would not have been needed before prey uptake in the trout (Fig. 4), should be attributed to the above mentioned overestimate.

*Platichthys* (Fig. 5) uses protrusion during prey capture. The translation effect of protrusion contributes considerably to $u'_{prey}$. The suction effect of protrusion is only small. The first term of formula (8) contributes most to $d_{iprey}$. In *Pterois* (Fig. 6) upper jaw protrusion is even more important than in *Platichthys*. Now,
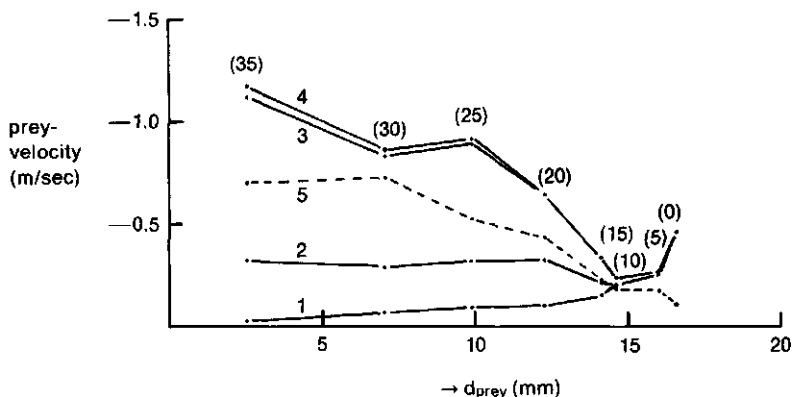
91

Fig. 5. Calculated contributions of suction, swimming and protrusion to $u'_{prey}$ in a prey capture event of the flounder (*Platichthys flesus* SL 315 mm), using formula (8). The actual position of the prey, measured from the film was used in the calculation. Notation (different from the notation of Fig. 4):
1. Contribution of forward body motion to $u'_{prey}$: $U_{sw} \cdot e_{swimming}$. 2. curve 1 plus the contribution of protrusion: $U_{sw} \cdot e_{swimming} - U_{prot}$. 3. curve 2 plus the contribution of suction, with the assumption of a constant mouth length: $u'_{mlc} \cdot e_{suction} + U_{sw} \cdot e_{swimming} - U_{prot}$. 4. curve 3 plus the suction velocity of $u'_{prey}$ due to protrusion. All terms of formula (8) are taken into account. 5. $u'_{prey}$ as measured from the film. This curve should be compared with curve 4. The time in msec is given between brackets near each datum of $d_{prey}$. The maximal error made in the calculation of curve 5 is about 0.15 m/sec. The errors made in the calculation of curves 1 and 2 are about 20%. The errors made in calculating curves 3 and 4 are difficult to give, as the exact deviation of the mouth cavity from a cone is unknown.

the translation effect of protrusion contributes most to $d_{iprey}$.

The calculations of the prey velocity in the feeding act of the flounder deviate less from the actual prey velocity than in the rainbow trout, suggesting that the cone model resembles the flounder's mouth closer than the trout's mouth. For the lionfish the actual prey velocity was approximated best.

In prey capture protrusion has two important advantages compared to forward body motion and suction. First, the relative translation effect of protrusion has a constant value of $-1$, and is independent of $d_{prey}$, whereas $e_{suction}$ and $e_{swimming}$ are not. Second, it costs less energy to accelerate the jaws than to accelerate the whole body or the water and the prey, if a particular effect on $u'_{prey}$ is to be achieved. The acceleration of the prey in the moving frame can therefore be increased and the time required for prey capture decreased. Protrusion also increases the length of the mouth cavity and hence the velocity of the water in the mouth aperture (being the result of the expansion of a longer cone, see appendix). Figs 5 and 6 show this, more costly, effect to be less important than the translation effect of protrusion. The above effects were already qualitatively described by Muller & Osse (in press) and can yet be given quantitatively.

Summarizing, it can be concluded that *Pterois* has a highly efficient feeding mechanism, due to the initial protrusion followed by a short powerful suction. In the flounder suction is relatively more important than protrusion and swimming. In the trout protrusion is absent and swimming dominates, illustrated
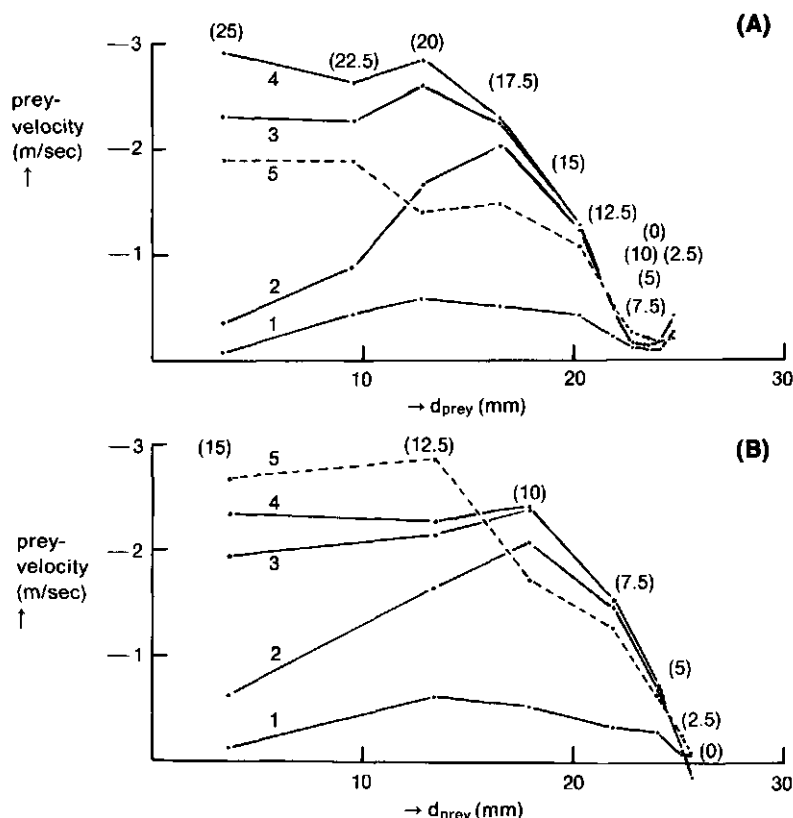
92

Fig. 6. Contributions of suction, swimming and protrusion to $u'_{prey}$ in the lionfish (*Pterois russelli*, SL 138 mm). The actual position of the prey is used in the calculations. (A) and (B) represent two different feeding acts. Notation is equal to that of Fig. 5. The errors made in the calculations are almost equal to those given in Fig. 5. Note the much larger contribution of protrusion to $u'_{prey}$ compared to that in *Platichthys*.

by the early moment of caudal valve opening. This feeding type can only be effective in relatively open water.

### 5.2. INITIAL PREY DISTANCE AND ULTIMATE PREY VELOCITY

Now we will investigate our third and fourth question (page 82). Does the fish maximize the initial prey distance, or is the prey velocity at seizure optimized, or is there a balance between possibly conflicting aims? Is there an optimal combination of mouth gape and caudal expansion to optimize prey capture?

#### 5.2.1. *Initial prey distance*
Fig. 7A shows graphs of the initial prey capture distance against $t_{v2}$, based on a feeding attempt of a pike (*Esox lucius*), of which the movement curves $h_1$ and $h_2$ are shown in Fig. 2. The mouth radius was measured from a film
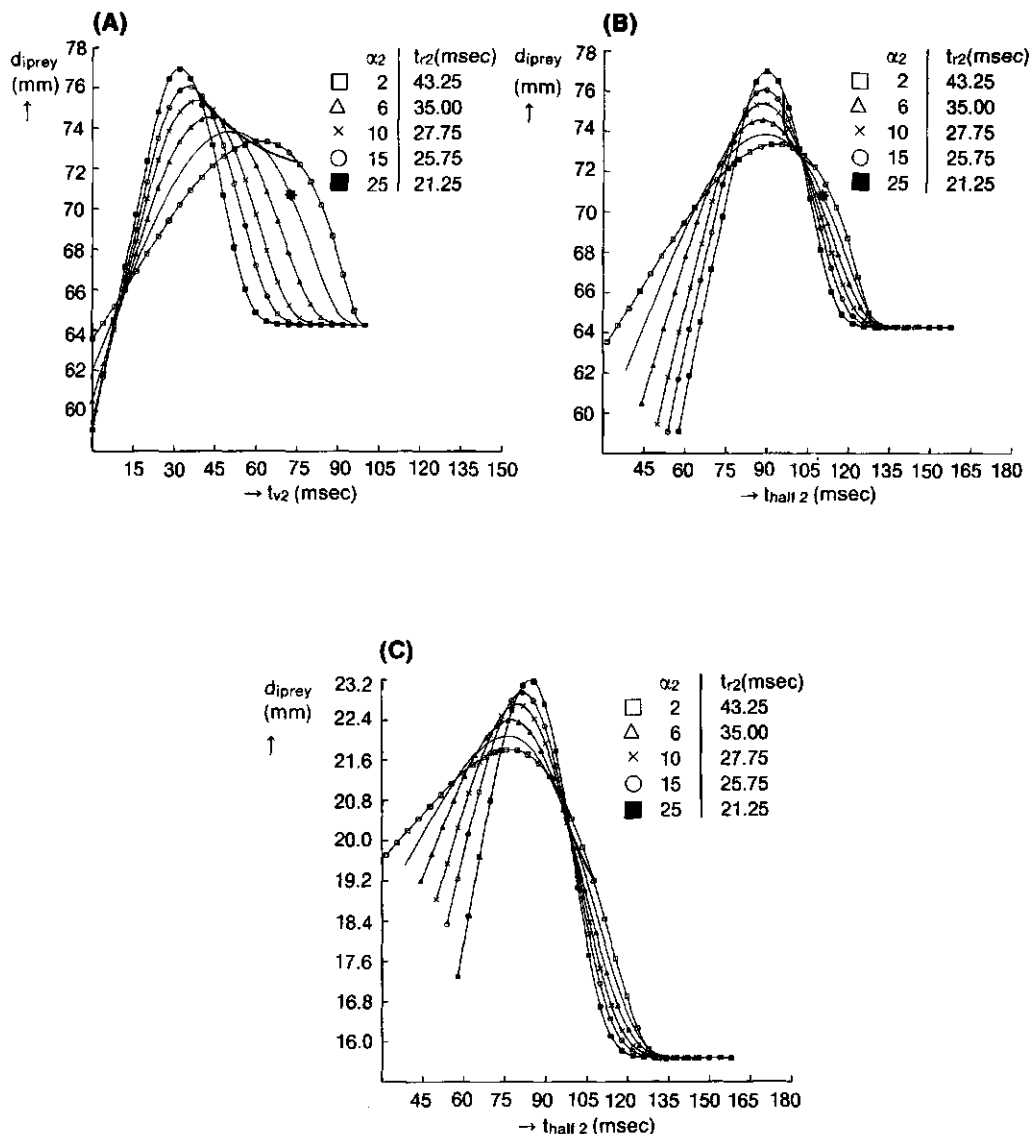
93

**(A)**

diprey (mm) ↑ 78, 76, 74, 72, 70, 68, 66, 64, 62, 60

| | α₂ | t_{r2}(msec) |
|---|---|---|
| □ | 2 | 43.25 |
| △ | 6 | 35.00 |
| × | 10 | 27.75 |
| ○ | 15 | 25.75 |
| ■ | 25 | 21.25 |

15  30  45  60  75  90  105  120  135  150
→ t_{v2} (msec)

**(B)**

diprey (mm) ↑ 78, 76, 74, 72, 70, 68, 66, 64, 62, 60

| | α₂ | t_{r2}(msec) |
|---|---|---|
| □ | 2 | 43.25 |
| △ | 6 | 35.00 |
| × | 10 | 27.75 |
| ○ | 15 | 25.75 |
| ■ | 25 | 21.25 |

45  60  75  90  105  120  135  150  165  180
→ t_{half 2} (msec)

**(C)**

diprey (mm) ↑ 23.2, 22.4, 21.6, 20.8, 20.0, 19.2, 18.4, 17.6, 16.8, 16.0

| | α₂ | t_{r2}(msec) |
|---|---|---|
| □ | 2 | 43.25 |
| △ | 6 | 35.00 |
| × | 10 | 27.75 |
| ○ | 15 | 25.75 |
| ■ | 25 | 21.25 |

45  60  75  90  105  120  135  150  165  180
→ t_{half 2} (msec)

Fig. 7. A. The initial prey capture distance against $t_{v2}$, using data of the pike (*Esox lucius*) shown in Fig. 2. The contours show values for equal $\alpha_2$ or $t_{r2}$. The contour without symbols represents the experimentally determined $\alpha_2 = 3.5$, with $t_{r2} = 40.0$ msec. Note that each point on a contour represents a simulation of a single feeding event. For each simulation it is assumed that $t_{pb} = t_{h1max}$. Note scale of initial prey distance. $U_{sw} = 0.61$ m/sec. B. As (A), but $t_{v2}$ is replaced by $t_{half2}$. $U_{sw} = 0.61$ m/sec. C. As (B), but $U_{sw} = 0.0$ m/sec.

The heavy curves crossing the contours in (A), (B) and (C) show positions of least pressure for a given initial prey distance. The asterisk in (A) and (B) denotes the actual position of the prey capture event of the pike. Further explanations are given in the text.

94

and fitted as described in the calculations (formulas (9) and (10)). The measured $h_{2nul}$ and $h_{2max}$ were used in the simulation, but the shape of the curve was varied to study its influence on the initial prey capture distance. The contours in Fig. 7A show the influence of different values of $\alpha_2$ and $t_{r2}$ on $d_{iprey}$. Note that *each point* on a contour represents a simulation of a single feeding event. The swimming speed of the fish was variable (from 0.30 m/sec to 0.78 m/sec), but its mean speed (0.61 m/sec) was used in this calculation. The prey was assumed to enter the mouth at $t = t_{h1max}$, which deviated only 10 msec from the actual situation. Protrusion is absent in the pike, so that terms 2 and 4 of formula (8) are zero. Fig. 7A shows that the maximum in the prey distance shifts to a larger $t_{v2}$ with a lower $\alpha_2$. Although the rise time shifts from a value of 43.25 msec (for $\alpha_2 = 2.0$) to a value of 21.25 msec (for $\alpha_2 = 25.0$), this has little influence on the maximum in the initial prey distance.

The value of $t_{v2}$ indicates when the opercular region starts to expand, but gives no information about the time of the peak rate of this expansion. A higher $\alpha_2$ decreases $t_{r2}$ (for the allowable range of $\alpha_2 \geqslant 2$) and increases $t_{half2}$, so effectively the expansion is delayed and shortened. Hence, $t_{v2}$ is not a good measure for studying the delay time between $h_1$ and $h_2$. The moment $t_{half2}$ closely approximates the time at which the caudal expansion rate is maximal and is therefore very useful to compare the relative timing of $h_1$ and $h_2$.

In Fig. 7B the initial prey capture distance is plotted against $t_{half2}$. Now, the maxima of all contours fall at about the same $t_{half2}$. *Thus to maximize the initial prey distance and hence the mean speed of the prey the fish should use one $t_{half2}$ (with given $U_{sw}$ and $h_1$), irrespective how it exactly expands caudally.* The actual $t_{half2}$ used by the fish was 110.5 msec, while the $t_{half2}$ for which the initial prey distance is maximal is about 90 msec. However, this difference in $t_{half2}$ affects the initial prey distance by only 4 percent.

The initial prey distance is influenced by $U_{sw}$. Fig. 7C shows similar plots as those of Fig. 7B, but now with $U_{sw} = 0$ m/sec. A slight shift of the maximum in $d_{iprey}$ towards a higher $t_{half2}$ is found with an increasing $t_{r2}$. The $t_{half2}$ at which $d_{iprey}$ is maximal would have been 76 msec for the $t_{v2}$ used actually by the pike, representing a larger deviation from the actual $t_{half2}$ than found with $U_{sw} = 0.61$. The difference in $d_{iprey}$ would have been 18 percent. Thus $d_{iprey}$ is affected more by the choice of $t_{half2}$ if $U_{sw}$ is decreased.

The simulations of $d_{iprey}$ show that the initial distance is largely influenced by $U_{sw}$. $U_{prot}$ may also have a considerable influence. At a high $U_{sw}$ $d_{iprey}$ is hardly influenced by a change in the caudal expansion. At a very low $U_{sw}$ $d_{iprey}$ is more affected, but still less than 20 percent in quite a big range of $t_{r2}$ and $t_{half2}$. *Thus maximizing the initial distance by an adjustment of the caudal expansion is rather useless for a fish.* The experimental data support this view (see below).

### 5.2.2. The ultimate prey velocity

We will now investigate a quantity more susceptable to optimization, i.e. the velocity of the prey in the mouth aperture, $u'_{tpb}$.
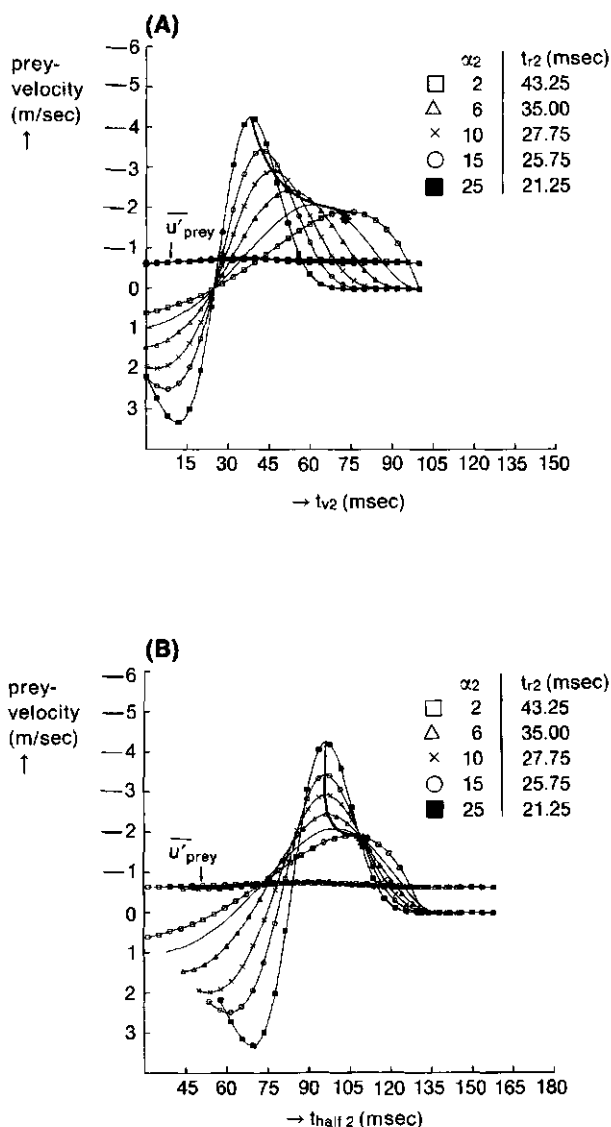
95

Fig. 8. Plot of $u'_{prey}$ and $u'_{tpb}$ against $t_{v2}$ (A) and $t_{half2}$ (B), using data of the pike as done in Fig. 7. It is assumed that $t_{pb} = t_{h1max}$. Contours connect points of equal $\alpha_2$ (and equal $t_{r2}$). Each point on a contour represents a simulation of a single feeding event. The contour without symbols denotes the actual $\alpha_2 = 3.5$ (with $t_{r2} = 40.0$ msec). Heavy curves connect prey capture events of least pressure, for each $u'_{tpb}$. $\overline{u}'_{prey}$ is only slightly affected by the choice of $\alpha_2$. This is illustrated by the bunch of curves plotted over each other. The asterisk denotes the position of the actual prey capture event of the pike. $U_{sw} = 0.61$ m/sec. For small values of $t_{v2}$ and $t_{half2}$ positive values of $u'_{tpb}$ do occur. Here the caudal region is already compressing at $t_{h1max}$. The point of intersection of all contours, describing $u'_{tpb}$ against $t_{v2}$, in (A) shows the situation of $t_{h1max} = t_{h2max}$. No expansion occurs and hence $u'_{tpb} = 0$ m/sec.

96

The chance of prey capture will increase with the rearward speed of the prey while it enters the mouth. It would be unfavourable for the fish to maximize the initial prey distance, if this seriously affects $u'_{tpb}$ (the ultimate prey velocity). A final escape could be easy for the prey if the speed given to it by the fish in the mouth aperture is close to zero. Fig. 8 shows graphs of the mean speed of the prey from $t_{v1}$ till $t_{pb}$, $\bar{u}'_{prey}$ and of $u'_{tpb}$ against $t_{v2}$ and $t_{half2}$, again for a range of $\alpha_2$ (and thus rise times of $h_2$).*

The mean velocity of the prey is little affected by the choice of $t_{half2}$, as expected from Fig. 7. The rise time of $h_2$ has also little effect on $u'_{prey}$. This is not so for the speed of the prey in the mouth aperture. The maximum increases with a shorter $t_{r2}$ (and thus a higher caudal expansion rate). The maximum of each curve falls again *at about the same* $t_{half2}$ (compare Figs. 7B and 8B). This $t_{half2}$ coincides with the time of maximal mouth opening. It is significantly larger than the $t_{half2}$ at which the maxima in the inital prey distance fall (Fig. 7B). The actual $t_{half2}$ used by the fish falls at 110.5 msec, quite close to the
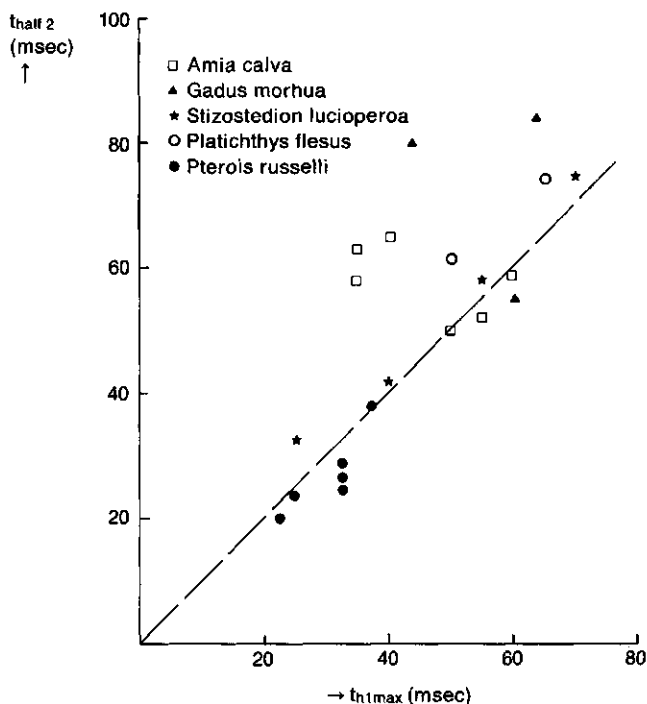


Fig. 9. The moment $t_{half2}$ against $t_{h1max}$ for prey capture events of 5 different fish species. On the dashed line the moment of the maximal opercular abduction rate equals that of peak mouth gape. $t_{half2}$ was determined as the moment at which $h_2 = h_{2nul} + 0.5\ \Delta h_{2max}$. This closely resembles the moment of peak opercular expansion rate. Further explanations are given in the text.

*The peak negative values of the velocities shown by the contours of Figs. 8, 12 and 17 are denoted as maxima in this paper. Similarly, the action of making $u'_{prey}$ more negative will be denoted as a maximization of $u'_{prey}$.

$t_{half2}$ that should be used if the speed in the mouth aperture is to be maximized (about 100 msec). The above analysis strongly suggests that *a prey sucking fish should expand caudally at the maximal rate at the moment of the maximal mouth aperture, if this moment coincides with the moment of prey capture.*

We checked this hypothesis for a range of fish species (Fig. 9). Generally, the fishes behave according to the expectations. *Pterois* however, tends to operate at a slightly lower $t_{half2}$. It also tends to capture the prey slightly before $t_{half2}$ (see Muller & Osse, in press, Fig. 17). These features will decrease the initial prey distance, but increase $\bar{u}'_{prey}$ and $u'_{tpb}$ (see also page 106). An opposite effect was observed for *Platichthys*. *Amia* and *Gadus* showed a quite variable behaviour. In *Amia* the deviation may be caused by the relatively early opening of the caudal valves. Also, at a slow forward body speed the initial prey distance and $u'_{tpb}$ may be about equally affected by the phase relationship. We found that *Amia* quite often expands its mouth aperture to the maximal width and keeps this position for some time, while expanding caudally. An example is given in Fig. 10.

### 5.3. Influence of mouth gape on initiation distance and prey velocity

The initial prey distance and ultimate prey velocity are evidently dependent on the size of the mouth aperture, as already suggested in Fig. 3. $h_1$ influences $e_{suction}$ and $e_{swimming}$ and hence $u'_{prey}$. The influence of mouth gape will now be further investigated.
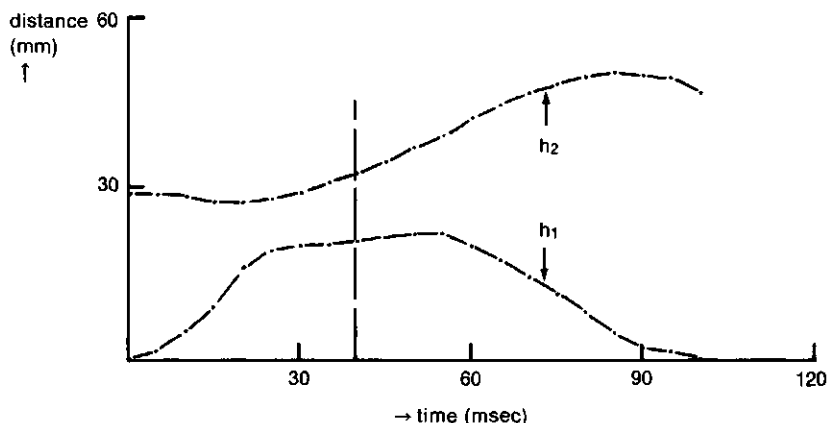


Fig. 10. Movements of mouth aperture and opercula during a feeding event of *Amia calva* (SL 365 mm). $h_1$ is measured as half the height of the mouth aperture and $h_2$ is half the distance between the caudal bony edges of the opercula. A plateau phase is present in $h_1$. Here $h_1$ is maximal at the end of the plateau phase, but it may also be maximal at the start of this phase. This largely influences the measured relative timing of $t_{half2}$ and $t_{h1max}$. Generally $t_{half2}$ is larger than $t_{h1max}$ in *Amia*, in contrast to the situation in *Pterois*. The dashed vertical line denotes the actual time of the opening of the opercular valves.
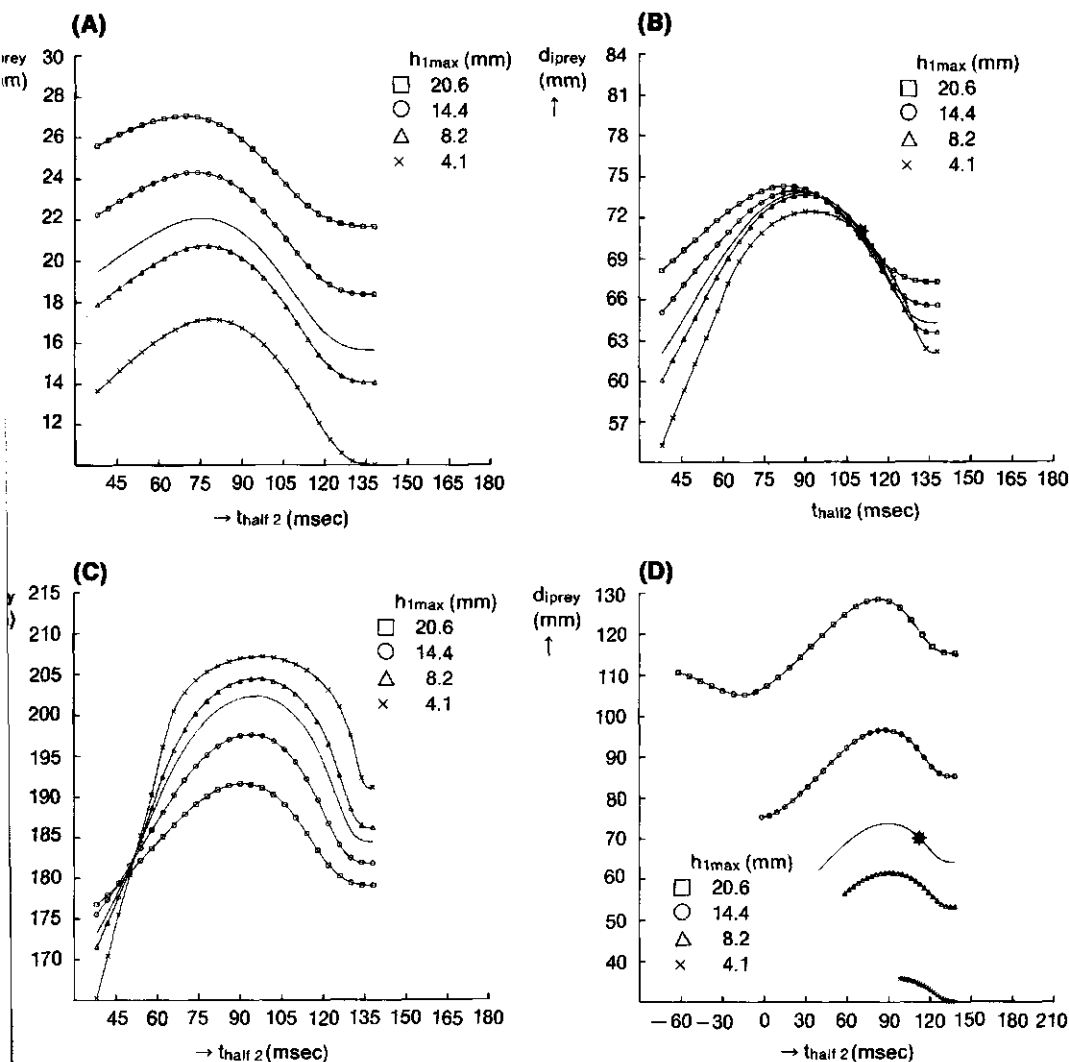
Fig. 11. Plots of $d_{iprey}$ against $t_{half2}$, using the data of the pike shown in Fig. 2. $t_{half2}$ and $h_{1max}$ are varied to study their influence on $d_{iprey}$. The prey is assumed to enter the mouth at $t_{h1max}$.

A. $U_{sw} = 0.0$ m/sec. Contours show values of $h_{1max}$. The contour without symbols shows the actual $h_{1max} = 10.3$ mm. Each point on a contour represents a single simulation of a feeding act. $t_{r1}$ was given the actual value (32.6 msec) for each simulation. Therefore, a bigger $h_{1max}$ represents also a bigger mean expansion rate. $d_{iprey}$ increases with $h_{1max}$.

B. As (A), but now $U_{sw} = 0.61$ m/sec, equal to the actual mean swimming speed. Now, $d_{iprey}$ increases with $h_{1max}$ for low values of $t_{half2}$ and high values of $t_{half2}$. At intermediate values of $t_{half2}$, about 110 msec, $d_{iprey}$ is hardly influenced by the choice of $h_{1max}$. The position of the actual feeding event is denoted with an asterisk.

C. As (A) and (B), but with $U_{sw} = 2.0$ m/sec. Now $d_{iprey}$ increases with a decreasing $h_{1max}$, except for very low values of $t_{half2}$.

99

D. $U_{sw} = 0.61$ m/sec. Contours show values of $h_{1max}$. The expansion rate of $h_1$ is equal for all contours, so that $t_{r1}$ is different for successive contours. This means that the time available for prey capture is proportional to $h_{1max}$. The moment $t_{h1max}$ is chosen to be equal for all mouth opening curves. So, $t_{v1}$ decreases with a larger $h_{1max}$. The start of the caudal expansion, $t_{v2}$, was varied from $t_{v1}$ to $t_{h1max}$. Thus the range of $t_{half2}$ for which simulations were made decreases with a smaller $h_{1max}$. The contour without symbols shows the actual $h_{1max}$. The actual feeding event of the pike is again denoted with an asterisk. The trend of an increasing $d_{iprey}$ with $h_{1max}$ was also found for other swimming velocities than 0.61 m/sec.
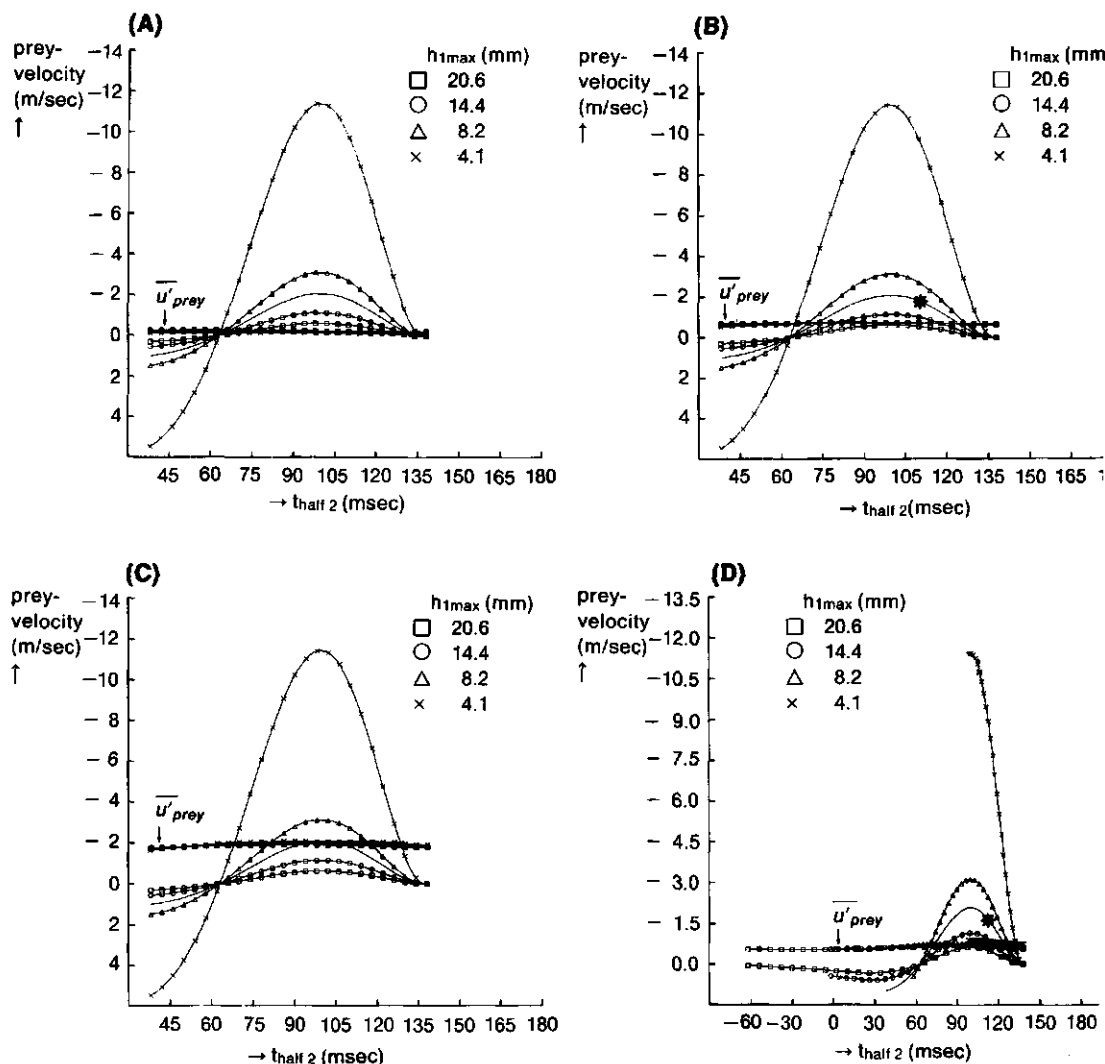


Fig. 12. Plots of $u'_{tpb}$ and $\overline{u}'_{prey}$ against $t_{half2}$, using the data of the pike as done in Fig. 11. Fig. 12A corresponds to Fig. 11A, Fig. 12B to Fig. 11B, etc. Contours in (A)–(C) show values of $h_{1max}$, with $t_{r1}$ kept equal to the actual $t_{r1}$ for each simulation. Contours in (D) show again values of $h_{1max}$, but now with the mean expansion rate kept constant. Contours without symbols denote

100

### 5.3.1. Initial prey distance

Figs. 11A-C shows plots of $d_{iprey}$ against $t_{half2}$ for three different swimming velocities and different $h_{1max}$. $h_{1max}$ and $t_{r1}$ are kept constant at each contour. Fig. 11D shows similar contours for $U_{sw} = 0.61$ m/sec, but now $h_{1max}$ and $\Delta h_{1max}/(t_{h1max} - t_{v1})$, i.e. the expansion rate of the mouth aperture, are kept constant. *A larger $h_{1max}$ increases the intial prey distance at a low swimming speed if $t_{r1}$ is kept constant, whereas the reverse is true for high swimming speeds (above 0.7 m/sec).* This effect is also illustrated in Fig. 13, see below. $d_{iprey}$ was found to increase in all cases if the expansion rate of $h_1$ is kept constant. This is not a surprise as the time available for prey capture increases too. Note that the difference in initial distance is again quite small if $t_{r1}$ is constant (19 percent for a doubling of the actual $h_{1max}$ if $U_{sw} = 0$, for a higher $U_{sw}$ this is even less). A comparison with the results of Figs. 7 and 8 suggests again that the ultimate prey velocity is a more important quantity to be optimized.

### 5.3.2. Ultimate prey velocity

The effect of a change in $h_{1max}$, with $t_{r1}$ kept constant, on $u'_{tpb}$ is shown in Fig. 12. The increase in $u'_{tpb}$ is considerable if $h_{1max}$ is kept smaller and the correct $t_{half2}$ is chosen (so that $u'_{tpb}$ is maximal). The range of $h_{1max}$ that can be used depends on the swimming speed, the generated pressure and the size of the prey. *The swimming speed limits the maximal $h_{1max}$, whereas the pressure and the size of the prey set a limit to the minimum $h_{1max}$.*

*The above results suggest that it might be advantageous for a fish, if it is feeding in the open water, to open its mouth faster and wider when it swims slower (and vice versa).*

Fig. 13 shows a plot of $\bar{u}'_{prey}$ against $U_{sw}$, using the movement curves of the pike shown in Fig. 2 and $t_{half2} = t_{h1max} = 100$ msec. It is assumed that $U_{sw}$ is constant during each simulated feeding attempt. Simulations were made for three different mouth apertures, as shown by the contours in Fig. 13. If $U_{sw}$ is zero the initial prey distance is only influenced by suction. The obtained distance in this case for the actual mouth aperture is about 32 percent of the fish's head length, slightly more than the approximate 25 percent estimated by Alexander (1967). As expected, $\bar{u}'_{prey}$ almost equals $-U_{sw}$ for high values of $U_{sw}$. At a large distance the prey will be approached with the swimming velocity (if protrusion is absent). Thus $u'_{prey} = -U_{sw}$ in this case. Close to the mouth swimming induces stagnation, which may lead to forward pushing of the prey in the earth-bound frame if stagnation is not compensated by suction. An overall

the actual $h_1$. Asterisks in (B) and (D) denote the positions of the actual feeding attempt of the pike. The bunch of curves plotted over each other in (A) to (D) show $\bar{u}'_{prey}$. The curves with clear maxima represent $u'_{tpb}$. Little is gained by maximizing $\bar{u}'_{prey}$ (or $d_{iprey}$) compared to a maximization of $u'_{tpb}$. $\bar{u}'_{prey}$ increases with $U_{sw}$ (compare (A), (B) and (C)). The fish should chose its $h_{1max}$ such, that $u'_{tpb} < \bar{u}'_{prey}$, otherwise pushing of the prey in an earth-bound frame occurs. (Note that $u'_{prey} < 0$ if the prey moves towards the mouth). A smaller $h_{1max}$ is needed with a higher swimming speed. Alternatively, the fish may open its caudal valves to avoid pushing. To capture the prey, the fish must open its mouth wide enough to let it enter the mouth. At a high swimming speed this only is possible without pushing the prey if the caudal valves open at the appropriate time.
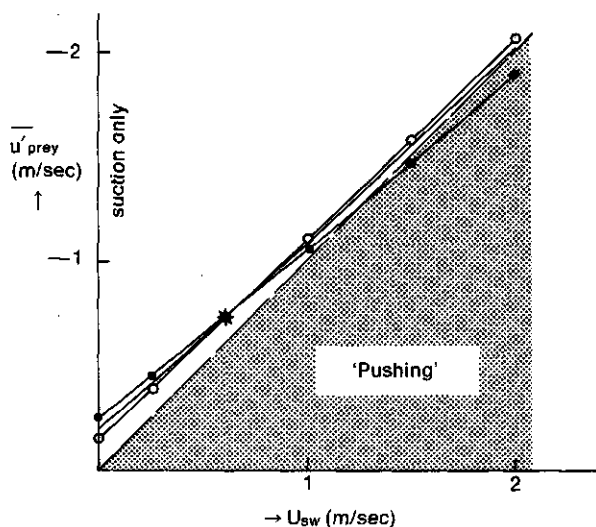
Fig. 13. Mean velocity of the prey against $U_{sw}$. $t_{half2}$ was chosen to equal $t_{h1max} = 100$ msec, and $t_{pb} = t_{h1max}$. $U_{sw}$ is assumed to be constant during each (simulated) feeding act. Contours show values of $h_{1max}$ and $t_{r1}$ kept constant. Other parameters equal those given for the pike in Fig. 2. Again, each point on a contour represents a single simulated feeding act. The actual $h_{1max}$ is 10.3 mm (contour without symbols) and the actual mean swimming velocity is 0.61 m/sec. The actual position of the feeding act of the pike is denoted by an asterisk. Black dots denote contour with $h_{1max}$ is twice the actual $h_{1max}$. Circles denote contour at which $h_{1max}$ is 0.4 times the actual $h_{1max}$. Along the dashed line $\bar{u}'_{prey} = -U_{sw}$, so that the mean speed of the prey in the earth-bound frame is zero. The shaded area denotes the range of an overall pushing effect in the earth-bound frame. Further explanations are given in the text.

stagnation effect occurs when $\bar{u}'_{prey}$ is greater than $-U_{sw}$. In Fig. 13 this feature is present in the area enclosed by the abscissa and the dashed line (shaded area). For high swimming velocities the contour at which $h_{1max}$ is twice the actual $h_{1max}$ lies in this area. To avoid stagnation effects the caudal valves can be opened. Valve opening is particularly important for feeding with a high swimming velocity (as in the rainbow trout, see page 91), as otherwise the prey size would be limited by the necessarily smaller mouth aperture.

For the pike we found indeed a feeding behaviour in this direction (see Fig. 14). The valves tended to be opened at a smaller mouth gape when swimming faster. But also the maximal mouth aperture tended to be reduced. The experimental results obtained by Rand and Lauder (1981) for *Esox niger* are also in accordance with this theory.
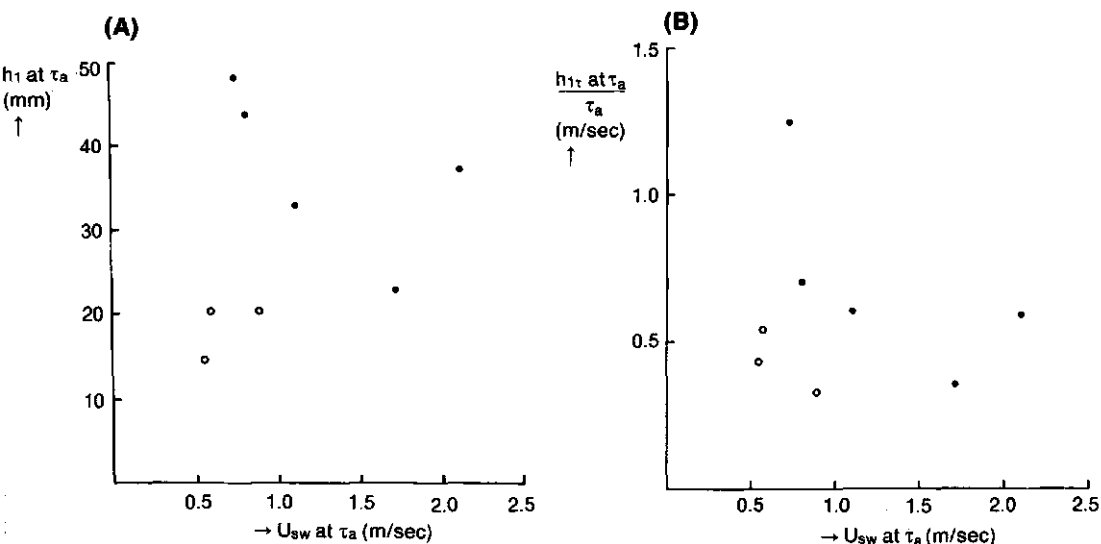
102

Fig. 14. A. mouth radius $h_1$ at $\tau_a$, the actual moment of the opening of the opercular and branchioste-gal valves, against $U_{sw}$ at $\tau_a$. $h_1$ is measured as half the height of the mouth aperture.
B. Mean expansion rate till $\tau_a$ against $U_{sw}$ at $\tau_a$.
The black dots in these graphs represent data of a pike of SL 485 mm, the circles are data of a pike of SL 195 mm. Each datum represents a separate feeding act. (A) indicates the tendency of a reduction of $h_1$ at $\tau_a$ with a higher $U_{sw}$. (B) indicates a tendency of a reduction of the mean expansion rate of the mouth opening before $\tau_a$ with a higher $U_{sw}$.

## 5.4. THE INFLUENCE OF THE PRESSURE ON THE MOUTH EXPANSION

The pressure inside the mouth cavity varies as a function of time and position inside the mouth. The pressure is influenced by the mouth expansion, but also by swimming movements (see e.g. Muller et al., 1982). Now, one may wonder how a fish should expand its mouth, so that with the delivered effort (not neces-sarily maximal) the chance of prey capture is maximized.

The pressure inside the mouth can be calculated for each combination of ros-tral and caudal expansion using the model of Muller et al. (1982, see their formu-la 43). For each initial prey distance in Fig. 7 the combination of $\alpha_2$ and $t_{half2}$ was determined for which the contribution of the caudal expansion to the magni-tude of the negative pressure was lowest. The obtained curve intersects the con-tours in Fig. 7. The magnitude of the pressure shows a strong, non-linear, in-crease with the initial prey distance and thus the mean velocity of the prey (see Fig. 15). A similar calculation was carried out for the relation between the mini-mal possible pressure and the prey velocity in the mouth aperture (see Fig. 8B and Fig. 15). Here a similar relation was found, but the pressure increase was a lot slower. *Again, the fish gains more if it tries to optimize the ultimate velocity than it would gain in optimizing the initial prey distance.* Fig. 8B shows that the optimal phase relationship, i.e. the situation with the highest ultimate velocity with a given pressure, overlaps the maxima of each contour.
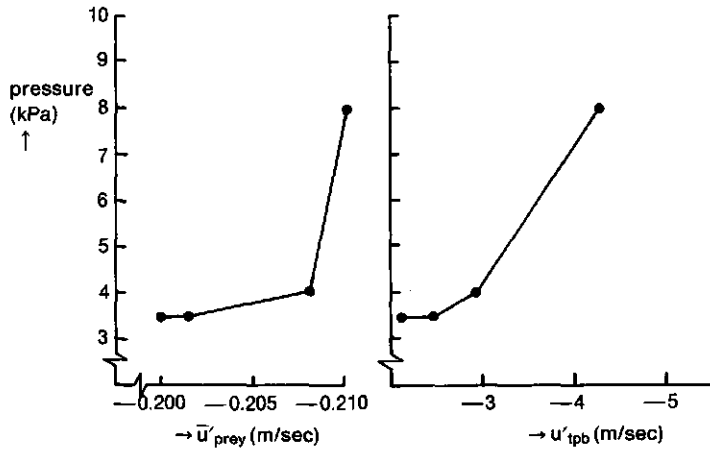
103

Fig. 15. Graph of the extra pressure halfway inside the mouth due to the caudal expansion against $u'_{tpb}$ and $\bar{u}'_{prey}$. Calculations were done using the model of Muller et al. (1982). The movement data of the pike, shown in Fig. 2 were used as input data for the simulation, with the exception that $\alpha_2$ was varied (and thus $t_{r2}$) to obtain the variation in $u'_{tpb}$. $t_{half2}$ was chosen such that each simulation was positioned on the heavy curves shown in Fig. 8, denoting the feeding acts with the minimal possible magnitude of the pressure.
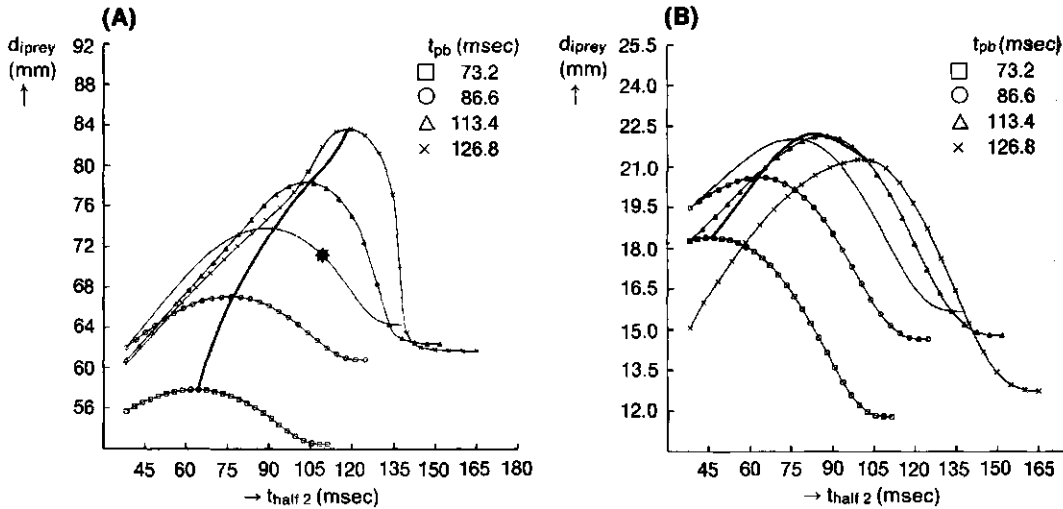


Fig. 16. Graphs of $d_{iprey}$ against $t_{half2}$, obtained by simulations, using the movements data of the pike shown in Fig. 2. The contours show values of $t_{pb}$. The contours without symbols represent $t_{pb} = t_{h1max}$. Note that each point on a contour represents a simulation of a single feeding event. Heavy curves connect maxima of contours.
A. $U_{sw} = 0.61$ m/sec, the actual mean swimming velocity. The maximal possible $d_{iprey}$ increases with a larger $t_{pb}$ (at least in the simulated range).
B. $U_{sw} = 0.0$ m/sec. Now $d_{iprey}$ is maximized if $t_{pb}$ is chosen slightly larger than $t_{h1max}$, with the proper $t_{half2}$.
Both (A) and (B) show that a change in $t_{pb}$ has only little influence on $d_{iprey}$ if $t_{half2}$ is chosen properly.

104

The optimal $t_{half2}$ as shown by the heavy curve in Fig. 8B is little influenced if the mouth opening curve changes, as is apparent from Fig. 12.

### 5.5. Prey uptake before and after peak mouth gape

The above considerations were made with the assumption that $t_{pb} = t_{h1max}$. Now, we will consider the effects on $d_{iprey}$ and $u'_{tpb}$ of other moments of prey passage through the mouth.

#### 5.5.1. Initial prey distance

The contours in Fig. 16A show again graphs of $d_{iprey}$ against $t_{half2}$. Now, each contour shows the situation for a particular $t_{pb}$. $U_{sw} = 0.61$ msec, the actual mean swimming speed. The $h_1$ and $h_2$ shown in Fig. 2 were again used as input functions, with the exception that $t_{half2}$ (and thus $t_{v2}$) were varied. *The maximum $d_{iprey}$ that can be achieved increases with a higher $t_{pb}$.* This may not be a suprise as $t_{pb}$ shows the time available for prey capture. *This is however not generally true for a very low swimming speed* (see Fig. 16B).
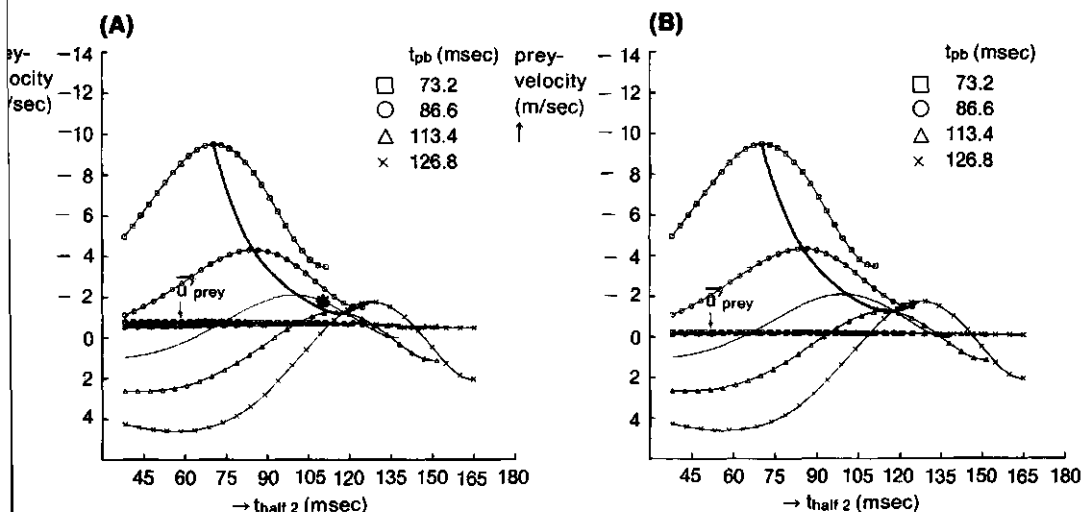
**(A)**                                     **(B)**



Fig. 17. Graphs of $u'_{tpb}$ and $\bar{u}'_{prey}$ against $t_{half2}$. Input data for simulations equal those used for Fig. 16. The contours show again values of $t_{pb}$. The contours without symbols represent $t_{pb} = t_{h1max}$. Each point on a contour represents a simulation of a particular feeding event.
A. $U_{sw} = 0.61$ m/sec, the actual mean swimming velocity. This plot corresponds to Fig. 16A. The bunch of curves plotted over each other represent data of $\bar{u}'_{prey}$, other curves, of which the maxima are connected via the heavy curve, represent $u'_{tpb}$. B. $U_{sw} = 0.0$ m/sec. Contours are similarly arranged as in (A).
(A) and (B) show that if $t_{pb}$ is changed the fish should shift $t_{half2}$ into the same direction, because than $u'_{tpb}$ can be kept maximal. If $t_{half2} < t_{h1max}$ both $h_1$ and $h_2$ are expanding and a high $u'_{tpb}$ can be acnieved if $t_{pb}$ is chosen likewise smaller than $t_{h1max}$. A $t_{pb}$ greater than $t_{h1max}$ seems to be unfortunate, as than $h_1$ is contracting, so that a large gain in $u'_{tpb}$ is impossible.

### 5.5.2. *Ultimate prey velocity*

Generally, the maximum $\bar{u}'_{prey}$ that can be achieved increases with a lower $t_{pb}$ (at least in the simulated range, Fig. 17A,B). *The magnitude of $u'_{tpb}$ increases with a lower $t_{pb}$, if $t_{pb} < t_{h1max}$.*

The $t_{pb}$ that can be used by the fish depends on the size of the prey and $d_{iprey}$. *If the prey can be approached closely, e.g. while feeding near substrates, it may be advantageous to use a $t_{pb}$ less than $t_{h1max}$.* If this is done the fish should preferably decrease its $t_{half2}$ too, to optimize $u'_{tpb}$. This simultaneous shift of $t_{pb}$ and $t_{half2}$ towards a value below $t_{h1max}$ was observed for *Pterois russelli* (see also pages 98 and 108).

## 6. General discussion

Several authors have discussed the prey capture mechanisms in bony fish. The first quantitative treatment was given by Alexander (1967), who estimated the distance from which a prey can be sucked into the mouth. As mentioned by Alexander, the estimates were quite rough, as no account was taken of forward motion, protrusion and the variation of the mouth radius, apart from other simplifications. Nyberg (1971) made estimates of the effect of protrusion on $d_{iprey}$, but took only account of the translation effect of protrusion. Weihs (1980, using steady flow assumptions) calculated particle trajectories in a flow field consisting of a sink and a uniform flow. In this approach the velocity is infinite at the mouth aperture ('the sink') and a reverse calculation of $d_{iprey}$ as carried out in the present paper is impossible. Webb (1976) discussed the predator-prey interaction, using the model of Howland (1973). He took account of the accelerations and possible turning radii of predator and prey. He omitted, however, the final suction act, a possible effect of protrusion and stagnation effects due to forward motion. Muller et al. (1982) presented the most useful quantitative model of suction feeding in fish to date. Attention has already been paid to this model in the methods. The present paper is an extension of this model.

The present paper provides calculations of the initial prey distance and the velocity of the prey as a function of time and position. It takes account of the unsteady nature of the flow and the variation of the mouth radius. The effects of movements of the expanding mouth, forward motion of the fish and protrusion on $u'_{prey}$ are quantitatively assessed.

The present approach is limited to an analysis along the $X'$-axis, away from the substrate, and a mouth cavity with closed opercular and branchiostegal valves before $t_{pb}$. Also, escape movements of the prey were omitted in the analysis. A treatment of the complete field of flow shows that the analysis along the $X'$-axis is a valid procedure (see Muller & Van Leeuwen, in prep.). An exact calculation of $u'_{prey}$ after valve opening could not be achieved for reasons mentioned in Muller & Osse (in press).

Escape movements of elusive preys are hard to predict for us. This may also

106

be difficult for a prey capturing fish. An elusive prey may elicit a more powerful prey capture act than a sluggish prey (see Elshoud-Oldenhave, 1979). A more powerful feeding act increases $\bar{u}'_{prey}$ and $u'_{tpb}$ and hence decreases the time of prey capture. This will decrease the effect of a possible escape response. It seems difficult for the fish to correct beforehand for the direction of an escape response. Most suction acts are so fast that an in between adjustment of the predator as a response to prey behaviour seems to be impossible (Osse & Muller, 1980). An escape along the $X'$-axis can be easily incorporated in the present approach.

The present paper discusses three different options to increase the relative velocity of the prey towards the fish's mouth: suction by mouth expansion, protrusion of the jaws and swimming. The contributions of these options to $u'_{prey}$ vary among different species of fish and among different feeding events of one species. In the open water full advantage can be taken of swimming. Suction remains important to compensate for stagnation effects due to swimming. Stagnation effects can also be avoided by opening of the caudal valves (see e.g. Van Leeuwen, in prep.).

Swimming will be necessarily unimportant in feeding from substrates. Here protrusion is an important means to obtain the prey. The acquisition of a large $d_{iprey}$ will be rather unimportant under these circumstances, as the prey can be more closely approached. It is probably more important to generate a high velocity of the prey, especially if the prey has a higher density than water. Therefore, a small mouth aperture at $t = t_{pb}$ is probably advantageous, as this increases $u'_{tpb}$. This may be obtained by a reduction of $h_{1max}$, as in *Esox* (see Rand & Lauder, 1981) or by a reduction of $t_{pb}$, so that the prey is captured before $t_{h1max}$, as in *Pterois* (see pages 98 and 106).

This paper is mainly concerned with the problem of how a fish should move (i.e. translation of the body, expansion of the head and protrusion of the jaws) if it seeks to maximize the chance of prey capture. An adequate morphological basis is required for an (close to) optimal performance. Consider e.g. the following example. The main power for the expansion of the mouth cavity is generated by the trunk and sternohyoid muscles. A substantial fraction of this power is mediated via the hyoids to lower the mandible and to abduct the suspensoria and gill covers. The position of the hyoids during mouth expansion changes so that first the depression of the mandible is effected most and thereafter the abduction of suspensorium and hyoid (see Osse, 1969). Barel (in prep.) found that the power of the trunk is most effectively transmitted for the abduction of the suspensorium and gill cover if the angle of the hyoids with the medial plane ($\beta$) is about 45 degrees. We suggest that shorter hyoids may allow an earlier achievement of this situation, so that $t_{half2}$ can be shortened. First, shorter hyoids can be positioned at a larger $\beta$ at the start of mouth expansion and second $\beta$ can be increased relatively faster. The consequence would be that the feeding act is shortened and the possible volume increase of the mouth reduced. On page 92 it was argued that protrusion allows less water to be sucked and the feeding act to be shortened. So, the presence of relatively short hyoids, with

107

a well developed protrusion apparatus and the use of a relatively small $t_{half2}$ seems to be a profitable combination, especially suitable when the prey can be approached closely. At present we have not enough data for a rigorous verification of this hypothesis, although the data of *Pterois* give already some support.

The consequence of a small $t_{half2}$ may be that the caudal valves have to open relatively early, as the expansion rate of the mouth aperture drops earlier under the critical rate (Van Leeuwen, in prep.). This may explain why protrusion and an early moment of valve opening are often found to combine (i.e. low-$\tau$-suction with protrusion, see Muller & Osse, in press).

This example shows that different structures within the fish's prey capture apparatus are functionally interrelated with each other. A change in one element requires also changes in other elements. Other examples, also based on a quantitative approach can be found in Muller & Osse (in press) and Van Leeuwen (in prep.).

## 7. Summary

The separate contributions of forward body motion, mouth expansion and jaw protrusion to prey capture in fish were derived quantitatively (see formula (8)). These contributions were shown for feeding events of *Salmo gairdneri*, *Platichthys flesus* and *Pterois russelli*. Protrusion appeared to be a very effective means to obtain a high speed of the prey relative to the fish.

Model simulations showed maximization of the initial prey distance by an exact adjustment of mouth expansion to be rather useless for a fish. Much more is gained by an optimization of the prey velocity while it enters the mouth (at $t_{pb}$). To achieve this, the fish should abduct its operculars at the maximal rate at $t_{pb}$.

A high swimming speed increases the danger of pushing the prey forward in an earth-bound frame. A larger mouth aperture increases this effect. Stagnation effects can, however, be avoided by decreasing the maximal mouth gape when swimming faster and by opening of the opercular and branchiostegal valves. This last possibility permits preys of a considerable size to be captured at a high swimming speed. The pike (*Esox*) seems to use both options.

For big preys, it seems favourable for the fish to let the prey pass through the mouth aperture when it is opened widest. A smaller mouth gape allows a higher velocity of the prey to be generated at the moment of prey seizure. If the prey can be approached closely, it can be advantageous to capture the prey before peak mouth gape, because then the speed of the prey can be increased.

108

## 8. References

Alexander, R.McN. (1967). The function and mechanisms of the protrusible upper jaws of some acanthopterygian fish. *J. Zool., Lond.* **151**: 43-64.

Barel, C.D.N. (in prep.). Title still unknown.

Elshoud-Oldenhave, M.J.W. (1979). Prey capture in the pike-perch, *Stizostedion lucioperca* (Teleostei, Percidae): A structural and functional analysis. *Zoomorphologie* **93**: 1-32.

Howland, H.C. (1973). Optimal strategies for predator avoidance. The relative importance of speed and manoeuvrability. *J. theor. Biol.* **47**: 333-350.

Kremers, J.J.M. & Leeuwen, J.L. van (in prep.). The influence of growth on the prey capture mechanism of the pike (*Esox lucius*).

Lauder, G.V. (1980). The suction feeding mechanism in sunfishes (*Lepomis*): an experimental analysis. *J. exp. Biol.* **88**, 49-72.

Leeuwen, J.L. van (in prep.). A quantitative study of flow in prey capture by rainbow trout, with general consideration of the actinopterygian system.

Leeuwen, J.L. van & Muller, M. (in prep.). The recording and interpretation of pressures in prey sucking fish.

Muller, M & Leeuwen, J.L. van (in prep.). Title still unknown.

Muller, M. & Osse, J.W.M. (in press). Hydrodynamics of suction feeding in fish. *Trans. Zool. Soc. Lond.*

Muller, M., Osse, J.W.M. & Verhagen, J.H.G. (1982). A quantitative hydrodynamical model of suction feeding in fish. *J. theor. Biol.* **95**: 49-79.

Nyberg, D.W. (1971). Prey capture in the largemouth bass. *Am. Midl. Nat.* **86**: 128-144.

Osse, J.W.M. (1969). Functional morphology of the head of the perch (*Perca fluviatilis* L.): an electromyographic study. *Neth. J. Zool.* **19** (3): 289-392.

Osse, J.W.M. & Muller, M. (1980). A model of suction feeding in teleostean fishes with some implications for ventilation. In: *Environmental physiology of fishes* (ed. M.A. Ali) NATO-ASI. Series A. Life Sciences. pp 335-352. Plenum Publishing Corporation, New York.

Rand, D.M. & Lauder, G.V. (1981). Prey capture in the chain pickerel, *Esox niger*: correlations between feeding and locomotor behavior. *Can. J. Zool.* **59** (6): 1072-1078.

Webb, P.W. (1976). The effect of size on the fast-start performance of rainbow trout *Salmo gairdneri*, and a consideration of piscivorous predator-prey interactions. *J. exp. Biol.* **65**: 157-177.

Weihs, D. (1980). Hydrodynamics of suction feeding of fish in motion. *J. Fish Biol.* **16**: 425-433.

## 9. Appendix: mathematical equations

The velocity in the mouth aperture due to suction at $x' = l$ for a, posteriorly closed, expanding cone is (from formula 18 of Muller et al., 1982):

$$u'_{mlc} + u'_{mprot} = \frac{-l}{3h_1^2}\left\{(2h_1 + h_2)\dot{h}_1 + (2h_2 + h_1)\dot{h}_2\right\} \tag{11}$$

where $l = l_0 + l_{prot}$. Note that $l_{prot}$ is a function of time.
The initial prey distance $d_{iprey}$ is obtained by solving:

$$d_{iprey} = \int_{t_{pb}}^{0} \frac{u'_m(l,t)\,h_1{}^3}{\sqrt{(d^2{}_{prey} + h_1{}^2)^3}}\,\mathrm{d}t + \int_{t_{pb}}^{0} \frac{U_f(h_1{}^3 - \sqrt{d^2{}_{prey} + h_1{}^2)^3})}{\sqrt{(d^2{}_{prey} + h_1{}^2)^3}}\,\mathrm{d}t \quad (12)$$

with $d_{prey} = 0$ at $t_{pb}$.

110

# The recording and interpretation of pressures in prey-sucking fish

# The recording and interpretation of pressures in prey-sucking fish

J. L. VAN LEEUWEN AND M. MULLER*

(Department of Experimental Animal Morphology and Cell Biology,
Agricultural University, Marijkeweg 40,
6709 PG Wageningen, The Netherlands)

## Summary

Possible pitfalls of techniques used to record pressures in prey-sucking fish have been analysed by applying control systems and hydrodynamic theory. Fourier analysis revealed a bandwidth of 1 kHz to be generally sufficient for an accurate recording of the overall pressure waveform. The exact bandwidth needed depends on the species, specimen size and intensity of the feeding act. A bandwidth greater than 1 kHz may be needed when secondary fluctuations (e.g., due to vortices) are also to be recorded accurately. Large errors (i.e. of the same order of magnitude as the real pressure) due to the dimensions of the transducer itself cannot be excluded on theoretical grounds. Most reliable pressure records were made with catheter tip pressure transducers, possessing small dimensions and a broad bandwidth (about 3 kHz).

Pressure records were made for *Amia calva, Salmo gairdneri, Esox lucius, Gadus morhua* and *Perca fluviatilis*. The largest negative pressure peak was measured in *Gadus* (-42 kPa). Accurate simulations of the pressure records were made using the hydrodynamic model of suction feeding of Muller, Osse and Verhagen (1982), to which new boundary conditions were added. This model takes into account the unsteady nature of the flow. The good correlation between measured and simulated pressures strongly suggests that:
1. the model is a very good description of the process of suction feeding.
2. the errors in the pressure records obtained with catheter tip pressure transducers are small.

The pressure inside the mouth of a prey-sucking fish has velocity and acceleration components due to head expansion and forward motion of the fish. Forward motion strongly influences the pressure profile in feeding events of the two fast-swimming fish studied, *Salmo gairdneri* and *Esox lucius*.

The literature on pressure measurements in prey-sucking fish is reviewed.

* Authors listed alphabetically. No priority of author is implied.

113

## Contents

# 1. Introduction

At least half of the more than 20.000 species of teleost fish capture their prey by suction feeding: a rapid expansion and compression of the buccal and opercular cavities causing water, containing the prey, to flow into the mouth. During this very unsteady process (with a duration time in the order of 50 msec) water velocities of about 10 m/s (Muller and Osse, in press) can occur, while the pressure inside the mouth cavity may vary from −65 to +10 kPa relative to the ambient pressure (Alexander, 1969 and 1970; Casinos, 1973 and 1974; Lauder, 1980a and b; Lauder and Lanyon, 1980; Muller et al., 1982; Osse and Muller, 1980 and Osse, 1976).

Knowledge of the pressures generated can give insight into the mechanical loading to which the head of the fish is subjected. Therefore predictions and measurements of the pressures inside the buccal and opercular cavities (together denoted as the mouth cavity) during the suction event are important in the study of the functional design and evolution of the fish head. The continuously working respiratory pumps (Hughes and Ballintijn, 1963) also create pressure fluctuations in the mouth cavity. These fluctuations, however, are generally less than 1 kPa, so the load on the fish's head caused by these pressures is negligible compared to the load generated during feeding.

The present paper deals with problems met in measuring and interpreting pressures inside the fish's mouth cavity during feeding. In addition it evaluates previous work, discusses a new technique with catheter tip pressure transducers and presents new data for perch (*Perca fluviatilis*), cod (*Gadus morhua*), rainbow trout (*Salmo gairdneri*), pike (*Esox lucius*) and bowfin (*Amia calva*).

The hydrodynamical model of fish feeding, as designed by Muller et al. (1982), provides an important tool for predicting the pressure from the fish's mouth cavity expansion and forward motion.

# 2. Materials and methods

### 2.1. THE ACQUISITION AND INTERPRETATION OF PRESSURE RECORDS: SOME PRINCIPLES

Several reviews about physiological pressure measurement can be found in the literature. These papers are mostly concerned with recordings in the cardiovascular system (e.g. Gabe, 1972). The pressure fluctuations in this system are of a low frequency ($< 5$ Hz) and amplitude ($< 15$ kPa). In the fish's sucking system, however, we are concerned with a completely different region of frequency, $f$, and amplitude, $p$ (10 Hz $< f < 4$ kHz and $+10$ kPa $> p > -70$ kPa). So recording techniques suitable for the cardiovascular system are not, a priori, applicable to the sucking system.

We will now discuss the prerequisites, from both a control systems and a hydrodynamical viewpoint, necessary for obtaining accurate records of the pres-

115

sures that occur in the mouth of a prey-sucking fish.

### 2.1.1. Damping coefficient and resonance frequency

The principles from control systems theory will be explained using the single degree of freedom system as an example (many transducer systems can be characterized adequately by such a system). For that system the following second order differential equation holds (see for symbols the Appendix):

$$\frac{d^2 y_o}{dt^2} + 2\zeta\omega_n\frac{dy_o}{dt} + \omega^2{}_n y_o = \omega^2{}_n x_i \tag{1}$$

(DiStefano et al., 1967)

where $t$ is time, $x_i$ is the input signal, $y_o$ is the output signal, $\zeta$ is the damping ratio and $\omega_n$ is the undamped natural angular frequency of the system. The relation between the frequency, $f$, (expressed in Hz) and the angular frequency, $\omega$, (expressed in rad/s) is: $\omega = 2\pi f$. The time constant of the system is given by:

$$t_c = \frac{1}{\zeta\omega_n} \tag{2}$$

Three important frequencies are associated with a system for which $0 < \zeta < 1$ (an underdamped system): the undamped natural frequency, the damped natural frequency and the resonance frequency (see e.g. Jones, 1961). The damped natural frequency occurs as a reaction to a step or impulse shaped input signal, and is given by:

$$\omega_d = \omega_n\sqrt{1 - \zeta^2} \tag{3}$$

For $\zeta > 1$ $\omega_d$ has no real value; the system is overdamped. An example of the step response of an underdamped system is given in Fig. 1A. The resonance frequency (that frequency at which a forced oscillation has maximal amplitude) is given by:

$$\omega_r = \omega_n\sqrt{1 - 2\zeta^2} \tag{4}$$

For systems with $\zeta > 1/\sqrt{2}$ a real value for $\omega_r$ does not exist and resonance is impossible. As is clear from (3) and (4): $\omega_r < \omega_d < \omega_n$.

Two important characteristics of the system (defined in the frequency domain) are its magnitude and its phase angle, $\phi$, as a function of angular frequency. These relationships are conveniently laid down in Bode plots, in which both the magnitude and $\omega$ are set at logarithmic scales and $\phi$ at a linear scale. Figs. 1B and 1D show these plots for various values of $\zeta$ for a single degree of freedom system. The frequency at which the asymptotes in the Bode magnitude plot intersect is the undamped natural frequency (Fig. 1B). The frequency at which the

116

magnitude plot reaches the maximum value is the resonance frequency, $\omega_r$, of underdamped systems.

### 2.1.2. *Distortions in pressure records due to inadequate bandwidth and phase relationship*

The Bode magnitude plot of a particular system shows its bandwith, often defined as that range of frequencies over which the magnitude ratio does not differ by more than -3 dB from its value at a specified frequency. The plot is a measure for the speed of response of a system (DiStefano et al., 1967). Generally the following rule is accepted in the literature to designate a signal as an accurate reproduction of an event: "The recording equipment should be able to reproduce frequencies up to the 10th harmonic of the fundamental frequency of the event, otherwise the records will be seriously distorted" (see e.g. Gabe, 1972). Therefore, knowledge of the expected frequency content of the event is a prerequisite for the choice of appropriate equipment. The fundamental frequency of the feeding event generally lies in the order of 10 to 100 Hz, as will be illustrated in the results (determined by Fourier analysis, see e.g. Fig. 6). Thus a bandwidth of 1 kHz will be suffient in most cases to record the overall pressure faithfully.

The complex formula of the pressure in a fish's mouth obtained by Muller et al. (1982) shows that the pressure depends upon the intensity of the suction act, the position in the mouth cavity, the acceleration of the fish's body and upon the species and size of the predator. These effects, computer simulations and experimental results (e.g. Fig. 16) show that high frequencies, up to at least 100 times the fundamental one, occur in the records. These may contribute importantly to the load exerted on the system. A bandwidth of greater than 1 kHz will generally be required for accurate measurement of minor fluctuations (freq. $> 100$ Hz).

Distortions in the pressure records might be due also to an inadequate phase relationship of the recording system. Ideally the phase angle should be zero in the required bandwidth, as no distortions or time shift will occur in this case. To avoid distortions the natural frequency of the transducer should be as high as possible (about 50 times the fundamental frequency to be analysed), and the damping ratio $1/\sqrt{2}$ or very low in higher order systems. Consider e.g. the following transducer. Let $\omega_n$ be $4*10^4.\pi$ rad/s and $\zeta$ be 0.1. The time shift, $\Delta t$, at a frequency $\omega$, equals $\phi/\omega$. The value of $\phi$ can be read from Fig. 1C or 1D. For example, when $\omega = 8*10^3\pi$ rad/s, $\phi$ equals $\pi/90$ rad. Hence $\Delta t = -1.4\,\mu$sec. Distortions can also be avoided when a linear relationship between $\phi$ and $\omega$ is present in the required frequency range. Adjustment of $\zeta$ to $1/\sqrt{2}$ is advisable for a transducer whose undamped natural frequency is less then about 50 times the fundamental frequency to be recorded. In this case a linear relationship between $\phi$ and $\omega$ exists up to $\omega_n$, and the bandwidth over which reliable recordings

117
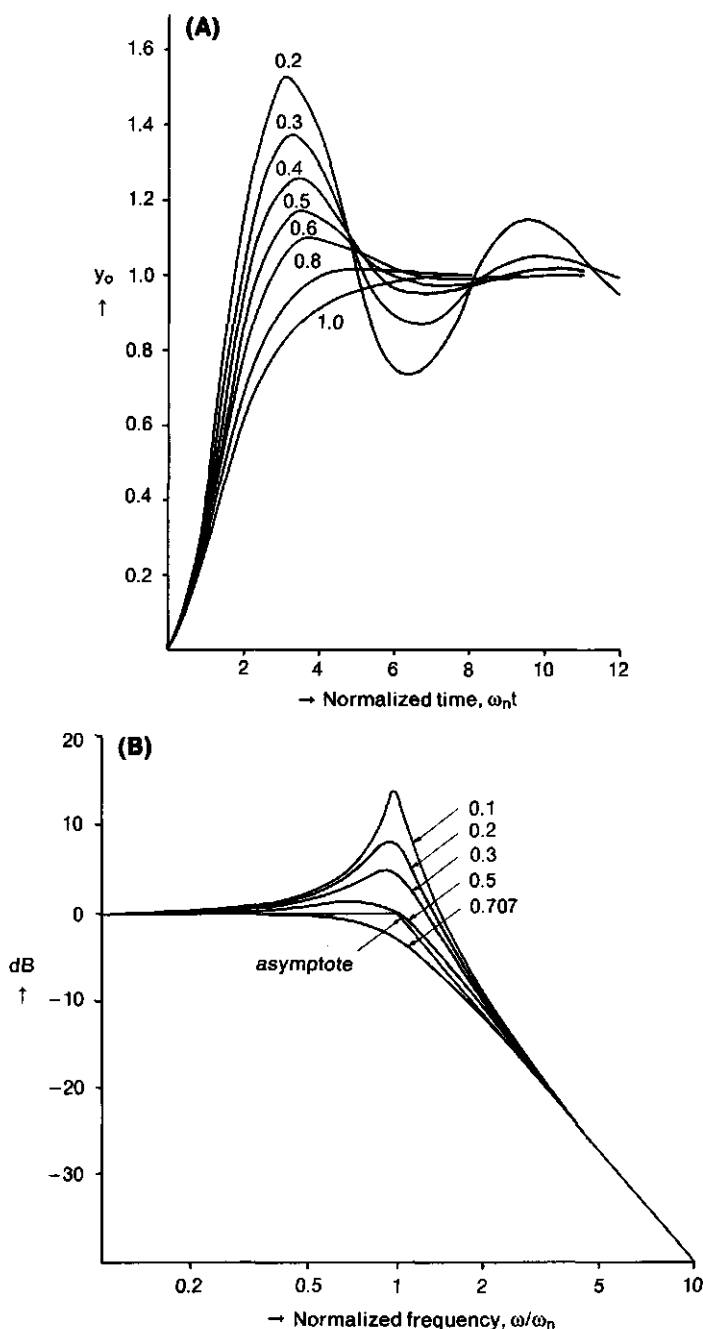
Fig. 1. A. Unit step response of a single degree of freedom system (equation 1), for different values of the damping ratio $\zeta$ (denoted near each curve). $y_o$ is the output signal and $\omega_n t$ the normalized time.

B. Bode magnitude plot of a single degree of freedom system. Note that $dB = 20\ ^{10}\log |P|$, where $|P|$ is the magnitude of the transfer function of the system. The normalized frequency, $\omega/\omega_n$, is set at logarithmic scales. Contours show values of $\zeta$.

118

**(C)**



**(D)**
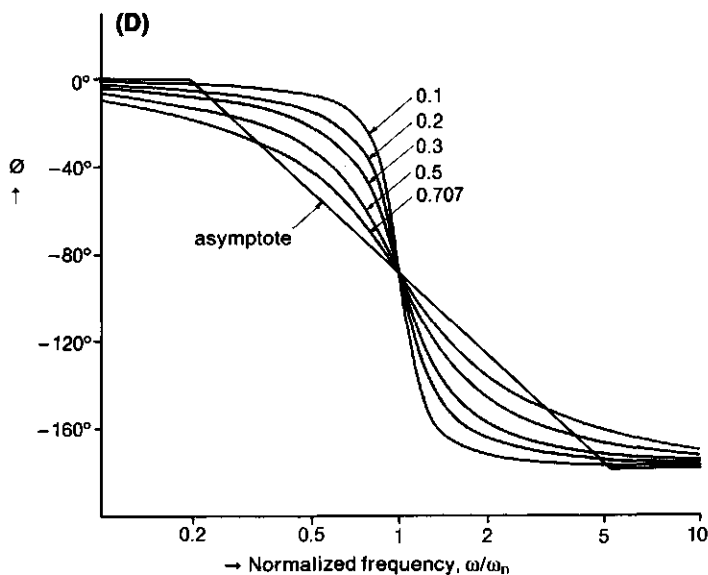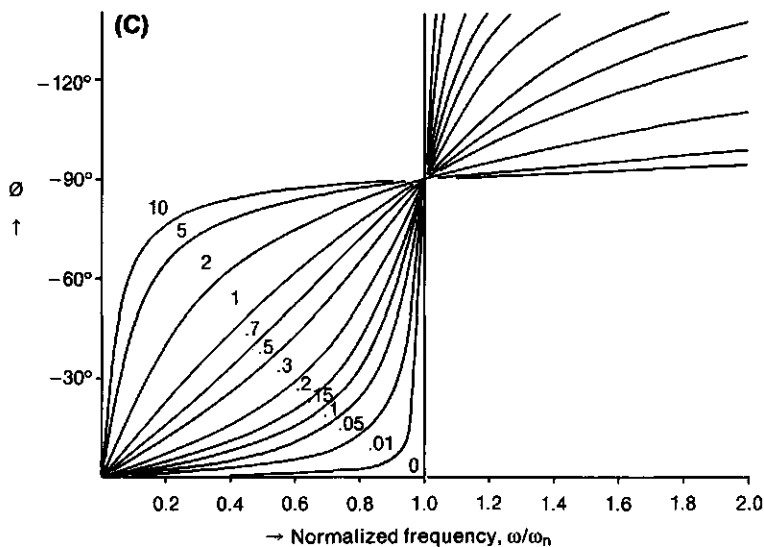
C. Plot of phase angle against normalized frequency, both set at linear scales. Contours show values of $\zeta$. Note that an almost linear relation between $\phi$ and $\omega$ exists up to the undamped natural frequency, $\omega_n$, for $\zeta$ is about 0.7. This means that the input signal is not distorted by the transducer system if it does not contain frequencies above $\omega_n$. A delay of $\phi/\omega$ however does occur in this case.

D. Bode phase angle plot of a single degree of freedom system. The phase angle, $\phi$, is set at a linear scale and the normalized frequency at a logarithmic scale. Contours show values of $\zeta$.

119

can be made is about doubled compared to a value of $\zeta$ of 0.1. However, so doing a time delay of $\phi/\omega$ must be accepted. As an example consider a system with a $\omega_n$ of $200\pi$ rad/s ($f = 100$ Hz). The time delay is, with a damping ratio of 0.7, about 2.5 msec. This is a time shift of about 10% in a fast feeding event. Adjustment of $\zeta$ is conveniently done by electronic filtering, and not by filling the transducer equipment with fluid mixtures.

Furthermore a transducer with a linear relationship between in- and output signals is evidently preferred, because a linearization procedure is avoided and the experimental results can be understood more directly.

### 2.1.3. *Effects of the dimensions of the transducer on pressure records*

Other distortions in the pressure records can be caused by an inappropriate form of the pressure tranducer. Ideally, the velocity of the flow near the sensitive part of the transducer is not affected by the presence of the transducer. In this case no distortions will occur in the records due to the presence of the transducer. As an example we will discuss the flow past our Millar transducers (see 2.2.1.). The sensitive part of the transducer is mounted in a ditch at the side of the tip of a dracon catheter (Fig. 2A). The flow past the transducer can be modelled as the flow past a sphere and a blunt nosed body (Fig. 2B). The stream function of this conformation in a uniform stream, $U$, is given in the Appendix. Evidently,
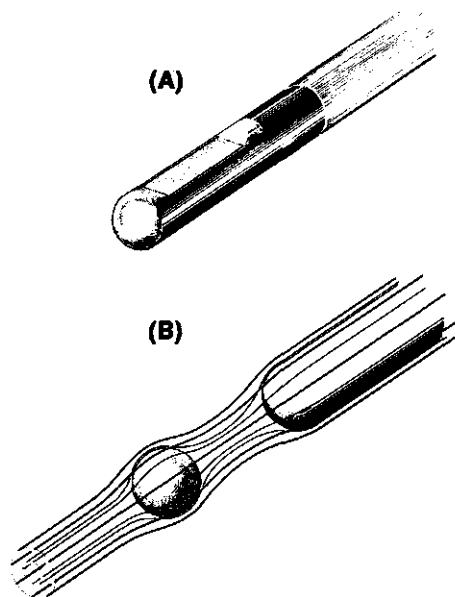


Fig. 2. A. Catheter tip pressure transducer, diameter of catheter is 1.67 mm.
B. The flow past the transducer is modelled as a flow past a sphere and a blunt nosed body. Further explanations are given in the text.

120

this stream function does not hold when $U$ makes an angle with the $X$-axis, i.e., when the flow is not parallel to the dracon catheter. In the fish's mouth the velocity around the transducer along its long axis is given by:

$$u_p = u_f c(x,\tilde{\omega}) \qquad (5)$$

where $u_f$ is the velocity of the water in the fish's mouth without a transducer and $c(x,\tilde{\omega})$ a function of the position and the dimensions of the transducer (see Appendix). To calculate the change in pressure due to the introduction of a pressure transducer one could proceed as follows. Muller et al. (1982) modelled the sucking fish as an expanding and compressing cone. They solved the equation of continuity and motion and obtained values for $u_f$, $U_f$ (the velocity of the cone) and $p$ (the pressure inside the cone). The error in the pressure measurement could be calculated by subtraction of the extra pressure component due to the presence of the transducer from the recorded pressure. However, this procedure would be very laborious, and the results would probably not be very accurate, as slightly different orientations of the transducer may give very different pressure values. Therefore we will try to give a good estimate of the maximal error that might occur. From Bernoulli's equation it follows that the deviation in the velocity component of the pressure equals $\frac{1}{2}\rho(1 - c^2)u^2_f$. At the sensitive part of the transducer, $(1 - c^2)$ has a fixed value which can be calculated from the dimensions of the transducer. $(1 - c^2)$ is about 0.025 for our Millar transducers. Hence, large deviations in the velocity component of the pressure do occur when $u_f$ is high. For instance, with $u_f = -1$ m/s the pressure deviation is only 13 Pa, while with $u_f = -5$ m/s and $u_f = -15$ m/s this value becomes respectively 0.3 kPa and 2.8 kPa. This last value represents an error of about 10%. Highest velocities generally occur at the mouth aperture (generally less than 10 m/s, see Muller and Osse, in press), so that largest errors are to be expected here (as far as the "steady part" of the pressure is concerned). The errors in the opercular region will be negligible.

In calculating the pressure, not only the velocity, but also the accelerations should be taken into account. Changes in the acceleration of the water near the transducer's membrane which are in the order of magnitude of the accelerations generated by the fish cannot be excluded. This means that errors in the order of 100% might be present in the pressure records. The errors might increase when the transducer's membrane is rotated from a parallel to a perpendicular position relative to the flow. An extensive model would be necessary for a good estimate of the errors that do occur in the acceleration part of the pressure, irrespective of which transducer type is used. This, however, has not been accomplished and was judged to be too farfetched. However, in our opinion pressure measurement is still worth doing, although the errors might be as large as 100%. In the first place the measurements are the best indications of the pressures that occur in the mouth of a sucking fish. Secondly, they can be compared with computer simulations using the model of Muller et al. (1982). A good agreement between the two methods would suggest that the errors are relatively small.

121

## 2.1.4. *Effects of a boundary layer around a pressure transducer*

Muller et al. (1982) derived a formula for the thickness $\delta$ of the boundary layer:

$$\delta = \sqrt{\upsilon T} \tag{6}$$

were $\upsilon$ is the kinematic viscosity and $T$ the duration time of the feeding act. Taking $10^{-5}$ m$^2$/s and $5 \times 10^{-2}$ s as characteristic values for $\upsilon$ and $T$ gives an estimate of 0.7 mm for the thickness of the boundary layer. The boundary layer might influence the frequency response of the transducer by the additional mass of water it represents. Consider e.g. the analogy of a spring hanging, on a rigid wall, with a mass $m_1$ attached to it. Let the spring constant be $K$. Then the undamped natural frequency of the system equals $\sqrt{K/m_1}$ (Jones, 1961). Addition of a second mass $m_2$ results in a decrease of the damped natural frequency by $\sqrt{m_1/m_1 + m_2}$. A similar phenomenon might alter the bandwidth of a catheter tip pressure transducer during the gradual formation of the boundary layer. In the worst case the additional mass is comparable to the mass of the sensitive membrane. Hence, a decrease of 0.7 times the original damped natural frequency would occur if the effect of the additional mass is similar as for the spring. This should not seriously influence our measurements as the damped natural frequency of our catheter tip pressure transducers is very high (about 25 kHz, see also paragraph 3.1.). Clearly, the frequency response of pressure transducers with fluid filled catheters will be hardly influenced by the presence of a boundary layer.

## 2.1.5. *Effects of hydrostatic components on the recording of pressures*

Generally, the difference in height between the sensitive part of the transducer and the water surface in the aquarium will add to the pressure record. This hydrostatic pressure has a constant value when transducers connected via a liquid filled tube to the measuring point are used. In this case the height between the transducer and the water surface is constant and can even be eliminated (through choice of position or by electronical means). In case of a catheter tip pressure transducer the hydrostatic component is determined by the depth of the transducer in the aquarium. During the feeding attempt this depth may vary a few centimeters due to the displacement of the fish. This will obviously result in a slight distortion of the pressure record (error in the order of a few percents). Care must be taken that the signal to be measured falls within the sensitive range of the transducer after addition of the hydrostatic pressure.

## 2.1.6. *Effects of accelerations of the transducer system on pressure records*

During feeding the pressure transducer or the fluid filled cannula will be accelerated. The effect of the acceleration will be quite small when catheter tip pressure transducers are used whose sensitive membranes are of low mass. As an example consider a membrane with mass $m$ and surface $A$ that is accelerated (perpendicular to its surface) with $a$ m/s . Then there will be a deviation of $(m.a)/A$ in the pressure record due to the acceleration of the transducer. Substituting

122

some characteristic values of the three parameters, e.g. $a = 100$ m/s$^2$, $m = 10^{-6}$ kg and $A = 2\text{x}10^{-6}$ m$^2$, a value of 50 Pa is obtained for the deviation, which represents an error of less than 1% in most cases.

Errors due to acceleration are more serious when fluid filled catheters are used. Consider e.g. a pressure transducer to which is connected a stretched water filled catheter of length $l_c$. Suppose that this system is accelerated with $a$ m/s along a line making an angle $\alpha$ with the long axis of the tube. The pressure measured due to this acceleration will be $(l_c.a.\cos\alpha)$ kPa. Taking $l_c = 0.1$ m, $a = 100$ m/s$^2$ and $\alpha = 0$ rad one obtains 10 kPa for the acceleration pressure, a value comparable to the pressure generated by the sucking fish. Thus, considerable errors are likely to be present in pressure records from moving fish made with liquid filled catheters connected to an external transducer.

### 2.1.7. *Temperature effects on the transducer output signal*
When transducers are used in combination with liquid filled catheters (e.g. Statham tansducers or related types) a temperature effect will be negligible, as no water flows along the sensitive membrane. However, in the case of catheter tip pressure transducers the fluid flow along the transducer might decrease the operating temperature of the strain gauges, and hence change their resistance. This cooling effect might strongly influence the transducer output when no effective temperature stabilizing system is present. When a pressure transducer with a fixed air filled volume behind the sensitive membrane is used, cooling might result in a positive deviation of the recorded pressure relative to the actual one (the law of Boyle-Gay-Lussac can be applied to the volume of air). As this deviation is large, catheter tip pressure transducers must have an open connection between the inner side and the atmosphere.

### 2.1.8. *Interpretation of pressure records; earth-bound and moving frame*
An important aspect to be considered in interpreting pressure records is the frame of reference in which pressures are measured. Pressure recordings in an earth-bound frame will give other results than those in a frame fixed to the sucking fish, the moving frame (see Muller et al., 1982 and Muller & Osse, in press). In the moving frame the pressure is measured with respect to the fish, i.e. the position of the pressure transducer remains constant relative to the fish, but its position in the aquarium changes with time. Analogously, when the pressure transducer is fixed in the aquarium the fish sucks itself (generally supported by swimming) over the pressure transducer (e.g. in the measurements of Alexander, 1969) and so the pressure is successively measured at different sites in the fish's mouth. It is clear that the two methods lead to completely different pressure-time curves.

### 2.2.1. *Experimental set up*

Feeding events by two specimens of *Salmo gairdneri* and *Amia calva* and one specimen each of *Gadus morhua, Perca fluviatilis* and *Esox lucius* were studied by pressure measurements inside their mouth cavities. Table 1 summarizes their dimensions and the conditions in which they were kept. During experimentation they were fed with live cyprinids (young *Cyprinus carpio, Barbus conchonius* or *Carassius auratus*).

Earliest experiments were done with two almost identical Statham P23 Db strain gauge type manometers, connected to the measuring position by polyethylene tubes (o.d. 1.63 mm, i.d. 1.14 mm) filled with boiled, air free water. Care was taken that the system was air bubble free. The output voltages of the transducers were amplified using Elema-Schonander EMT 311 amplifiers (bandwidth 0-700 Hz). The pressure curves were photographed from a storage oscilloscope screen (bandwidth 0-10 kHz). Alternatively, the information was stored on magnetic tape, using a Bell and Howell instrumentation recorder (bandwidth 0-2.5 kHz in FM-mode) and played back through a Siemens EMT 311 oscillomink (bandwidth 1 kHz) for analysis. The Statham transducers were the limiting factor in the frequency response of the recording equipment (see paragraph 3.1.).

In later experiments Millar PC 350 and PC 340 catheter tip pressure transducers (semi-conductor strain gauge types) attached to woven Dracon catheters (filled with air and having an open end outside the aquarium, o.d. 1.67 mm or 1.33 mm) were used. Here the output voltages were amplified with Grass P15 preamplifiers. The lower frequency limit was set at 0.1 or 0.3 Hz and the upper frequency limit was taken to be 50 kHz. The amplified signals were stored using the B&H recorder (speed 30 inch/s, bandwidth 0-10 kHz) and played back (at 7.5 inch/s) to be visualized on a storage oscilloscope (set at a frequency range of 0-10 kHz). In several cases the pressure records were filtered at 2 kHz (12 dB/oct.) to eliminate high frequency events, probably due to vortices (see paragraph 4.3.). An Entran EPA-125E-10SW miniature pressure transducer (strain

TABLE 1. Fish specimen used. SL is standard length, *l* is head length, Prot. is protrusion of upper jaws. T is temperature of water, LA, WA and HA are length, width and height of aquarium.

| species | SL (mm) | *l* (mm) | Prot. (mm) | T (°C) | LA (m) | WA (m) | HA (m) |
|---|---|---|---|---|---|---|---|
| Amia calva | 365 | 92 | 0 | 17 | .9 | .5 | .4 |
| Amia calva | 395 | 100 | 0 | 19 | .9 | .5 | .4 |
| Salmo gairdneri | 240 | 56 | 0 | 14 | .8 | .5 | .4 |
| Salmo gairdneri | 230 | 53 | 0 | 15 | .7 | .5 | .3 |
| Esox lucius | 253 | 73 | 0 | 15 | .8 | .5 | .3 |
| Gadus morhua | 225 | 58 | 1 | 13 | .9 | .5 | .4 |
| Perca fluviatilis | 160 | 48 | 5 | 15 | .8 | .5 | .3 |

gauge type) was initially tested, but found to be unsuitable for our experiments (see paragraph 3.1.). The fishes were filmed (200-400 frames/sec) and trained as described by Muller and Osse (in press). Measurements of the mouth opening, suspensorial abduction, hyoid depression and opercular dilatation were made as described by Muller and Osse (see their Fig. 11).

### 2.2.2. *Testing of the transducers*

Before experimentation several tests were carried out with the transducers:

A. All transducers were calibrated hydrostatically.

B. A "transient test" was carried out for both the Statham and Millar transducers, using a metal cylinder (height 1 m, wall thickness 7 mm, i.d. 82 mm). The pressure transducers were inserted into the cylinder at 0.7 m from the closed bottom. The cylinder was filled with water, up to about 0.99 m and closed with a cellophane membrane. The pressure was increased to about 40 kPa via a hole just underneath the membrane. The membrane was punctured with a knife to produce a sudden change in the pressure. In some cases the cylinder wall was hit with the knife after rupturing the membrane. The recordings of the transducers were displayed on a storage oscilloscope screen (bandwidth 1 MHz), or at first instant stored on magnetic tape (speed 60 inch/s, bandwidth 20 kHz). The length of the polyethylene tube attached to the Statham transducer was 1 m, 0.5 m and 0 m in these experiments. The frequency content of the response of the transducers was determined by Fourier analysis, using a Minc-11 computer. The damping ratios and the damped natural frequencies of the transducers were calculated from the test results using the method of Gabe (1972). The resonance and undamped natural frequencies were calculated from equations (3) and (4).

C. The effect of the position of the pressure cannula aperture relative to the flow direction was tested in the case of the Statham transducers in a flow tube. The aperture of one transducer was positioned parallel to the flow direction, whereas the other was orientated perpendicular (either facing the flow or in the opposite direction) and pressures were recorded simultaneously. The catheters used were of equal length. In vivo a similar experiment was performed in the buccal cavity of a specimen of *Salmo gairdneri*. The tube with the parallel aperture was mounted through the ethmoid region as described by Liem (1978). The other tube was fastened to the first one. Both apertures were kept perpendicular (see Fig. 8A). The latter tube entered the mouth cavity through the opercular slit. In contrast to the flow tube experiment the tubes were accelerated in this experiment. The acceleration of the tubes would have differed as they were not orientated in the same way.

D. Artefacts introduced by tube movement were studied further by tube shaking, keeping the tube aperture in a fixed position.

E. The effect of tube length was investigated in vivo by mounting two tubes on the head of a specimen of *Salmo gairdneri*, parallel to its longitudinal axis and connected to the Statham transducers (see Fig. 10A). Measurements were taken with equal tube length (890 mm) and a length difference of 50 mm (890 and 840 mm) and 100 mm (890 and 790 mm).

F. The Statham, Millar, and Entran transducers were put in a calibration tank to investigate the effect of cooling. Both the pressure and the velocity were varied (related to each other via Bernoulli's equation).

G. The frequency content of pressure records of *Amia calva* obtained with the Millar transducers was determined using Fourier analysis.

### 2.2.3. *Pressure measurements in prey-sucking fish*

Statham transducers were used in the pressure measurements during feeding in *Amia calva, Salmo gairdneri* and *Perca fluviatilis*. In *Salmo* (specimen of 240 mm SL.) and *Perca* (SL. 160 mm) pressures were recorded in the buccal cavity. The cannulas were mounted as described by Liem (1978). In *Amia* (SL. 395 mm) one cannula was placed in the opercular cavity and another in the buccal cavity, and the pressures were recorded simultaneously. Both cannulas entered the mouth cavity medially from the supra-cleithrum in the dorso-caudal corner of the opercular cavity. The aperture of the opercular cannula was more or less fixed to the shoulder girdle and parallel to the flow direction. The buccal cannula was bent distally to position the aperture parallel to the flow direction. The flared end of this cannula was not firmly fixed to one of the buccal walls. All measurements with Statham transducers in *Amia calva* were carried out in 1970 by Prof. Dr. Osse and used for comparison with the results obtained with catheter tip pressure transducers.

Millar transducers were used in measuring pressures in a specimen of *Amia calva* (SL. 365 mm), a specimen of *Salmo gairdneri* (SL. 230 mm), a specimen of *Esox lucius* (SL. 253 mm) and a specimen of *Gadus morhua* (SL. 225 mm). The specimen of *Amia calva* was trained to feed with a battery of filming lights (power input of 12 kW, effectively, however, almost equivalent to 24 kW due to focussing) and 400 fr/s films were made of about 30 feeding events, with or without pressure transducers. A transducer was mounted in the opercular cavity or in both the buccal and opercular cavities. The catheters were fastened to the outer side of the cleithrum, directly ventral to the supra-cleithrum, such that the opercular cavities could be closed completely. The buccal transducer was sewn to the roof of the mouth, directly lateral to the parasphenoid. In *Esox* pressure measurements and training were performed similar to those in *Amia*.

Fig. 3. "Transient test" for a Millar PC 350 catheter tip pressure transducer and a Statham P23 Db pressure transducer.
A. Response of Millar transducer. Oscillations in the record are due to oscillations of the metal testcylinder plus its water content (see text). So the "test" cannot be designated as "transient" for this transducer.
B. Response of Statham transducer, connected via a polyethylene tube of 0.5 m length to the metal test cylinder. Oscillations as in (A) are not present, owing to the very low frequency response (mainly a result of the fluid filled cannula).
C. As (A), but with a different time scale.
D. Response of the Statham transducer of (B) (to another transient test), but now connected via a needle to the test cylinder. This system is less damped than in (B). The cylinder has the same resonance properties as in (A) and (B); note the similarities in the oscillations between (A) and (D).

126

In *Salmo* and *Gadus* pressures were only recorded in the opercular cavity. In *Salmo* the transducer entered the opercular cavity directly anterior to the basis of the pectoral fin, whereas in *Gadus* a position dorsal to the pectoral fin was preferred. These positions were selected to allow complete closure of the opercular cavity by the opercular and branchiostegal valves.

To illustrate the effect of the acceleration of the fish on the pressure inside
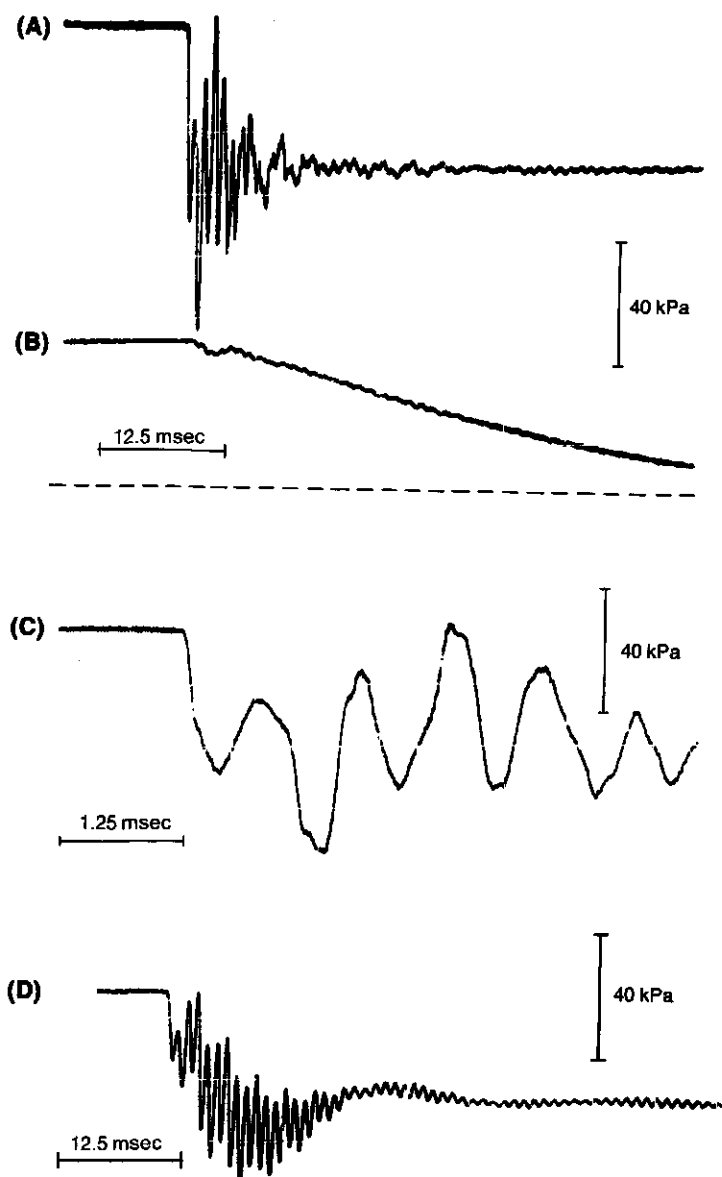
the mouth cavity a tube was mounted on the head (screwn to the parietals) of *Amia*, parallel to the longitudinal axis of the body. The tube was opened at its anterior end and closed at the posterior end. A pressure transducer was positioned posteriorly inside the tube at 4 cm from its rostral end. When the tube is accelerated along its axis a pressure of $l_p.a$ kPa will be recorded, where $l_p$ is the distance between the transducer and the rostral end of the tube and $a$ the acceleration. Another transducer was brought into the opercular cavity. Pressures were recorded simultaneously.

In all experiments care was taken that the tube apertures (in case of the Statham transducers) or the sensitive membranes were orientated parallel to the flow. In each case the fish could swim freely.

## 3. Results

### 3.1. TRANSDUCER CHARACTERISTICS

The results of the transducer tests will be presented in the sequence of their previous methodological description (see paragraph 2.2.2.).

A. All transducers tested showed a linear pressure-voltage relationship in the required range (−60 kPa to + 10 kPa), when hydrostatically tested.

B. The results of the transient tests for the Statham and Millar transducers are illustrated in Figs. 3, 4 and 5. From these tests the resonance, damped natural and undamped natural frequencies are calculated or estimated, as well as the damping ratios. These values are summarized in Table 2, together with the upper frequency limit for accurate recording. The Statham transducers have a very limited frequency response (about 8 to 15 Hz, dependent on the tube lenght) as is apparent from Figs. 3B and 4. They are largely damped when a catheter of length 0.5 m is connected to them ($\zeta > 1$). They are less than critically damped when this cannula is absent (see Figs. 3D and 4B, $\zeta$ is about 0.35). At first, the damped natural frequency of the Millar transducers seemed to be only about 1 kHz (Figs. 3A and 3C). However, the same oscillations were registered (although highly damped) by the Statham transducers when connected to the cylinder via a needle instead of a polyethylene tubing. Without the tubing a higher

TABLE 2. Dynamic properties of Statham P23 Db and Millar PC 350 pressure transducers. The PC 340 transducer has similar properties as the Millar PC 350 transducer.
$f_r$ = resonance frequency, $f_d$ = damped natural frequency, $f_n$ = natural frequency, $\zeta$ = damping ratio and $f_l$ = upper frequency limit for accurate recording.

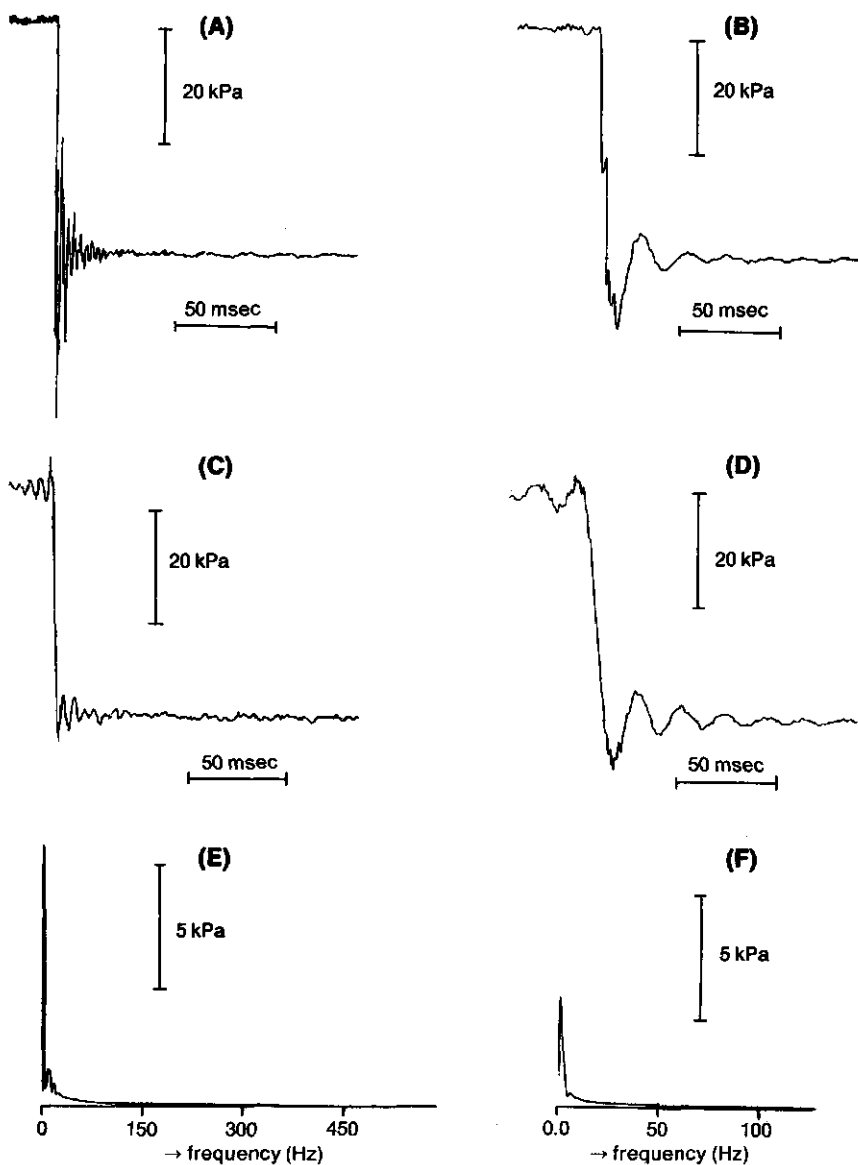| transducer type | $f_r$ | $f_d$ | $f_n$ | $\zeta$ | $f_l$ |
|---|---|---|---|---|---|
| Statham P23 Db + tube of 0.5 m | — | — | 46 Hz | >> 1 | 8 Hz |
| idem, without tube | 40 Hz | 43 Hz | 46 Hz | 0.35 | 15 Hz |
| Millar PC 350 | 27 kHz | 27 kHz | 27 kHz | 0.025 | 3 kHz |

Fig. 4. Transient test as in Fig. 3, with the Statham pressure transducer attached via a needle to the test cylinder. The resonance properties of the test cylinder were slightly different from those shown in Fig. 3. The main frequency was less than 300 Hz.

A. Response of Millar transducer, PC 350.

B. Response of Statham transducer. The oscillations present in the Millar record are also recorded, but highly damped.

C. The response of the Millar transducer, but with the amplitudes of all frequencies above 200 Hz removed. The curve starts to oscillate before the moment of the "transient". Thus, the high frequency components are needed to follow the transient. *(Continued pag. 130)*

frequency response is possible (Figs. 3D and 4B). This shows that the oscillation of about 1 kHz has to be ascribed to oscillations of the fluid and air in the metal test cylinder. Similar oscillations were recorded by Gabe (1972). He mentioned that their origin is not clear, but suggested that they could be the result of longitudinal wave transmission in the catheter wall. The recording of these oscillations with catheter tip pressure transducers, without a fluid filled catheter, shows this suggestion to be incorrect. Also, the frequency of these oscillations was easily reduced by putting some gravel at the bottom of the cylinder.

Fourier analysis was applied to the recordings of Figs. 4A and 4B (obtained with a test cylinder with different resonance properties than in Fig. 3). Figs. 4E and 4F show the amplitude spectra of the response of the Millar and the Statham transducers. The response of the Millar transducer contains more high frequency components than that of the Statham transducer. Figs. 4C and 4D show the transducer responses after removal of the high frequency components. The pressure drop induced by rupturing the membrane cannot be regarded as a transient test for the Millar transducer. The Statham transducer reacts much more slowly and starts to oscillate around the new mean pressure level. These oscillations are absent when a polyethylene tubing is connected to the transducer; then the system is highly damped (see Table 2).

In Figs. 5A,B an example is shown in which the cylinder wall is hit just after the rupturing of the membrane (see arrow). This impact event caused a secondary oscillation in the output of the Millar transducer. This oscillation of about 27 kHz must be regarded as the real damped natural frequency of the transducer system. (The amplitude of oscillation is diminished because of the primary storage on magnetic tape with a frequency response of 20 kHz). The damping ratio of the transducer was calculated from a similar (submerged) impact event, without a preceding pressure drop, displayed directly on a storage oscilloscope (see Fig. 5C). The calculated value was 0.025. It can be concluded (by using Fig. 1) that the Millar transducers are suitable for measuring pressures accurately up to at least 3 kHz.

The importance of an adequate bandwidth of the pressure recording equipment is illustrated in Fig. 6. Fourier analysis was applied to a buccal and an opercular pressure record obtained for *Amia calva* with Millar transducers. In Fig. 6A the two pressure records are low-pass filtered (12 dB/octave) at 2 kHz, 500 Hz, 100 Hz and 20 Hz. A considerable amplitude decrease and phase displacement occurs at low frequencies. The fundamental frequency of this feeding event lies in the order of 10 Hz. However, secondary oscillations up to 1 kHz are

D. The remains of the response of the Statham transducer after removal of the frequencies above 50 Hz. The main frequency of oscillation left approximates the damped natural frequency of the transducer system (about 45 Hz). From this figure the damping ratio can be determined (see Table 2).

E. Amplitude spectrum of the frequency content of the response of the Millar transducer. Above 350 Hz all amplitudes are virtually zero. The separate points of the amplitude spectrum are connected with a spline function.

F. Amplitude spectrum of the frequency content of the response of the Statham transducer.
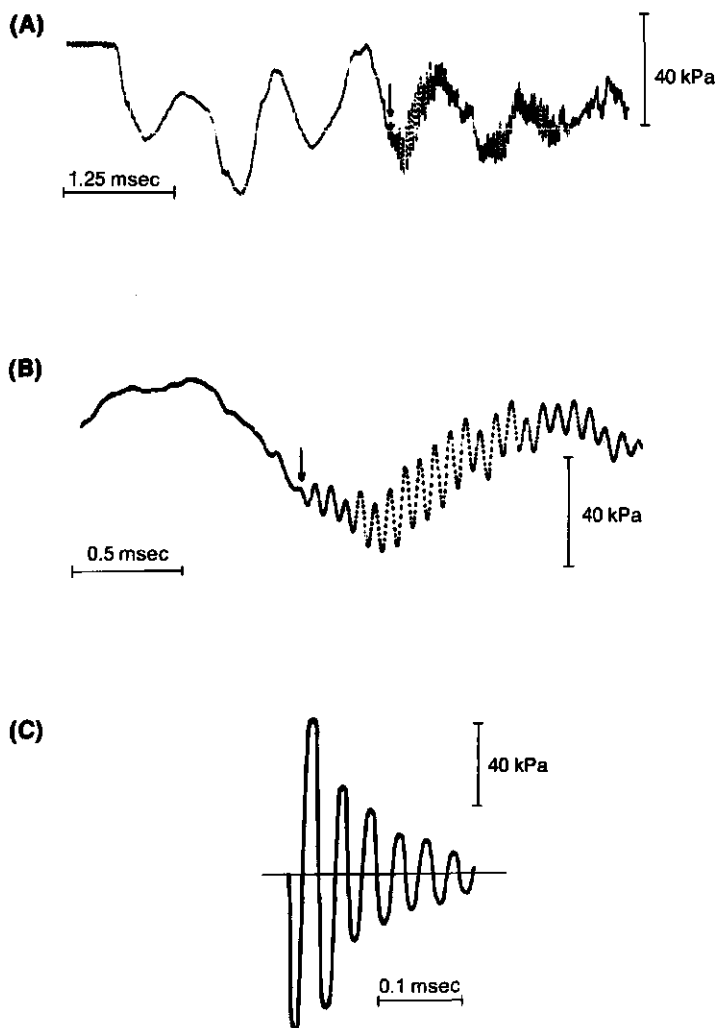
130

Fig. 5. Response of a Millar PC 350 transducer to rupture of a membrane enclosing a metal test cylinder. After the membrane was ruptured the cylinder wall was hit with a knife (see arrows in (A) and (B)), causing a secondary oscillation of about 27 kHz in the output of the transducer. The real amplitudes of these oscillations were not recorded, as the recording equipment had only a bandwidth of 20 kHz. (B) shows a part of (A) at a different time scale. (C) shows the impulse response of the Millar transducer when hit against a solid. This record was made using a storage oscilloscoop with a MHz bandwidth. The frequency of oscillation is the same as in (A) and (B). This test was used to calculate the damping ratio of the Millar transducers.
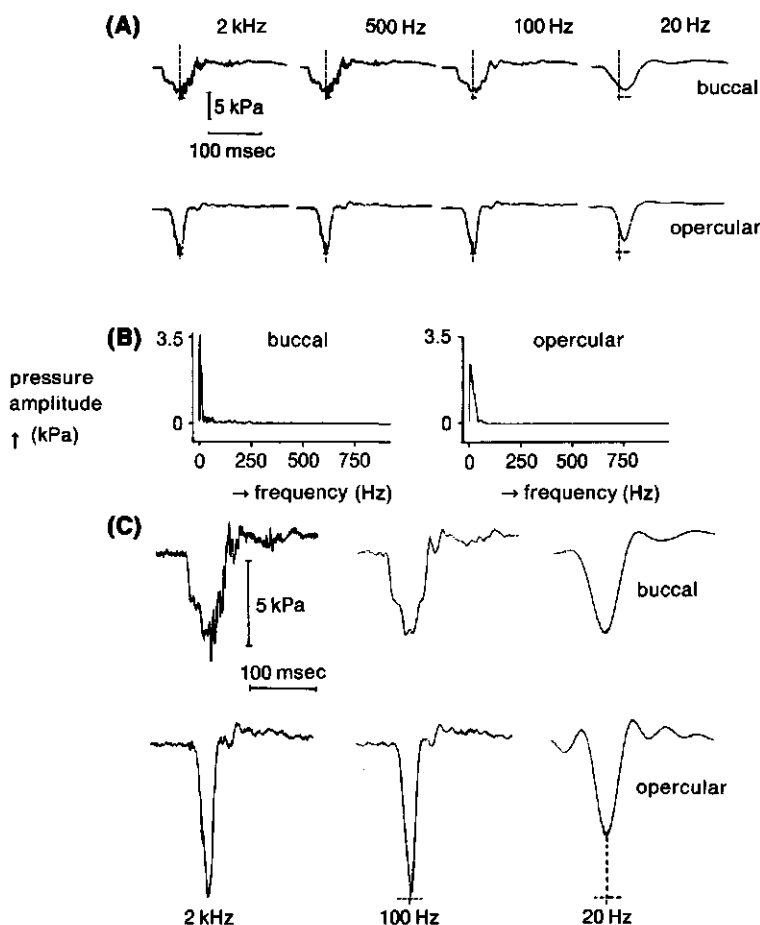
131

Fig. 6. A. Buccal (upper curves) and opercular pressure records of the bowfin (*Amia calva*, SL. 365 mm), low-pass filtered at 2 kHz, 500 Hz, 100 Hz and 20 Hz (12 dB/oct). Filtering at 500 Hz hardly affects the curves, contrary to the situation at 100 Hz and especially 20 Hz, where a decrease in amplitude and a phase shift occurs (denoted by the dashed lines).

B. Amplitude spectra of the curves shown in (A). The main frequency components are less than 100 Hz. Greater amplitudes are present in the buccal record at high frequencies compared to the opercular record.

C. The same records as in (A) but now filtered at 2 kHz, 100 Hz and 20 Hz. This means that after all frequency components in the amplitude spectra were set to zero above the mentioned levels, the curves were transformed from the frequency domain to real time. It is impossible to filter very sharply if electronic filtering is used as in (A). Filtering like in (C) has the drawback of a disturbed balance between the components of the Fourier series, so that the curves start to oscillate even before the "actual" pressure drop. A time shift of the moment of the largest amplitude is absent by this method (see dashed lines in opercular records). Low-pass filtering resembles the situation of a pressure transducer with a low frequency response better than filtering by removing components of the Fourier series.

132

present in the records. The amplitude spectra of the recorded pressures are shown in Fig. 6B. The buccal record contains more high frequency components than the opercular record. Frequency components up to 750 Hz are present, but above 250 Hz the amplitudes are hardly visible. A removal of all frequency components above 100 Hz and 20 Hz results in a decrease of the amplitude and oscillations even before the actual pressure drop, but no delay of the peak negative pressure.

The analysis of the frequency response of the transducers shows that the Statham transducers are unsuitable for the recording of pressures in prey-sucking fish, due to their limited frequency response (0-15 Hz). This is even true for a large specimen of *Amia calva* for which the suction act lasts relatively long.

C. Fig. 7 shows that different orientations of the tube apertures of the Statham transducers had no appreciable effect on the measurements in a flow tube. This result suggests that the distortions in the pressure records due to the dimensions of the transducer might be less serious than expected on theoretical considerations. The oscillations are, however, of a low frequency (about 2 to 18 Hz), so that conclusions for the situation of the fish's sucking system can not be drawn. Fig. 8 shows the results of an equivalent experiment in vivo with a specimen of *Salmo gairdneri*. Different orientations of the polyethylene tubings resulted in markedly different pressure records. Together with the result of the flow tube experiment this suggests that the records are very seriously distorted by accelerations of the tubes.

D. Fig. 9 shows the effect of tube shaking on the output of the Statham transducers. Pressure fluctuations of about 10 kPa can easily be evoked by shaking. This feature stresses the sensitivity of the Statham transducers to accelerations. The sucking fish also produces movements with high accelerations. Therefore, the use of this type of transducers for the study of suction feeding should be accompanied with great care and if possible avoided.
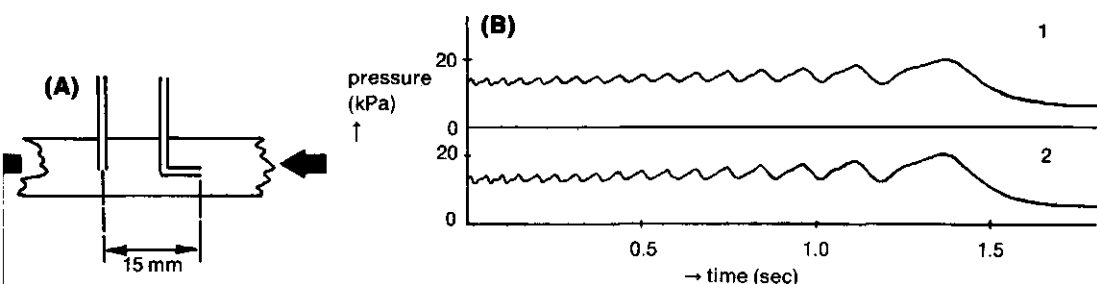


Fig. 7. Records of pressure fluctuations in a flow tube simultaneously made with two identical Statham transducers, connected via polyethylene tubings to the tube.
(A) shows the orientations of the apertures of the tubings in the flow. Heavy arrows denote the flow direction. The pressure in the tube was varied by a periodical opening and closing of a valve in the flow tube.
Curve 1 in (B) is the record with the aperture parallel to the flow.
Curve 2 shows the record with the aperture perpendicular to the flow.
Curves 1 and 2 are very similar. See text for further explanations.
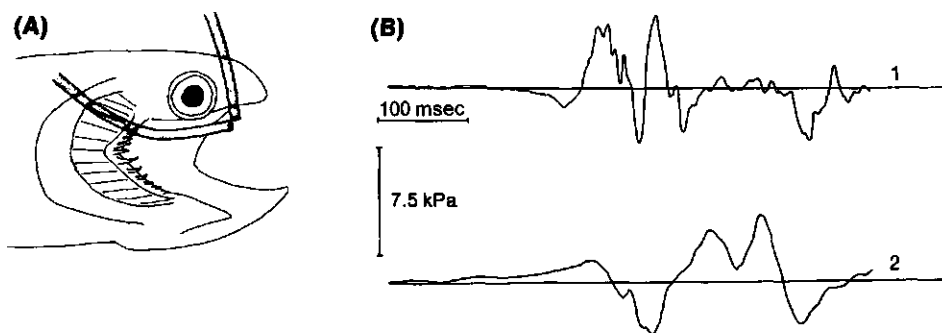
133

Fig. 8. Pressure recordings during feeding in the buccal cavity of a rainbow trout (*Salmo gairdneri*, (SL. 240mm), using Statham transducers and tube orientations as shown in (A). Record 1 in (B) is obtained with the tube through the ethmoidial region, whereas 2 is obtained with a tube through the opercular slit. The records differ a great deal. Tube orientation and mounting have a strong influence on the measurements.
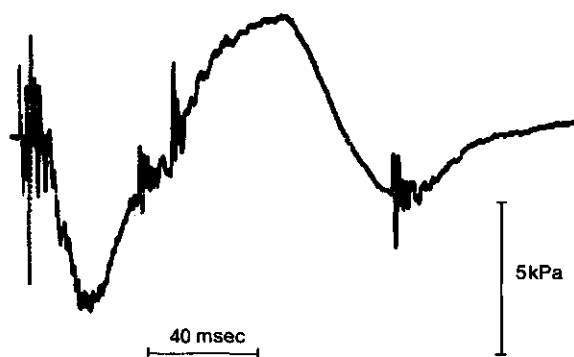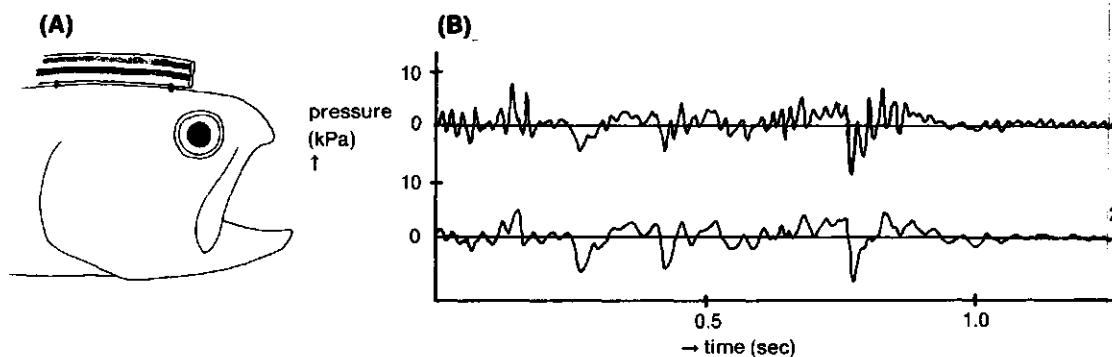


Fig. 9. Effect of shaking of the polyethylene tube connected to a Statham transducer on the output signal. The end of the polyethylene tube was fixed. This record shows that pressure fluctuations of a magnitude comparable to the maximal amplitude of the pressure generated inside the mouth during feeding may occur if the tube is accelerated, e.g. by swimming.
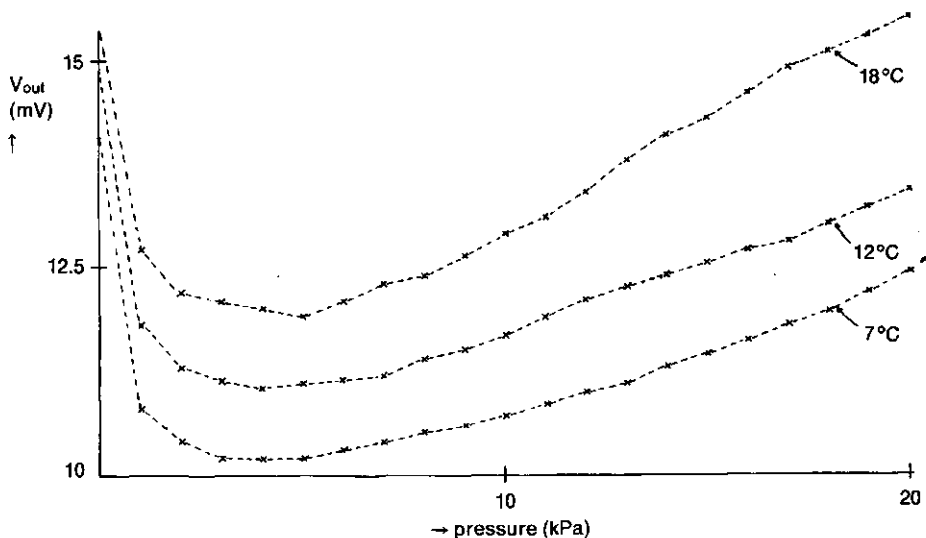


134

Fig. 11. Results of a calibration of an Entran pressure transducer in a flow tube for three different water temperatures. A pressure increase is accompanied by an increase in the velocity of the flow along the transducer (a steady flow regime was used). $V_{out}$ is the output voltage of the transducer. A lower temperature of the water decreases the output of the transducer. The non-linear behaviour at low pressure levels is due to cooling effects by the flow.

E. Fig. 10 illustrates the effect of tube length on the output of the Statham transducers. Equal tube lengths resulted in identical recordings, whereas a length difference of 100 mm gave very different results. Even a doubling of the input frequency may occur with particular tube lenghts.

F. The Statham and Millar transducers appeared to be stabilized for temperature effects. The Entran pressure transucers, however, showed a strong temperature effect. A calibration whereby a laminar stream of increasing strength was applied to the transducer did not give a linear relationship between pressure and output voltage (Fig. 11). The initial decrease of the output voltage might be due to a cooling effect of the fluid flow on the strain gauges. This effect could be minimized using a lower input voltage, accompanied of course by a loss in the sensitivity of the transducer. So a distinction has to be made between the dynamical properties of a pressure transducer responding to variations in the hydrostatic pressure and such properties when a dynamically varying flow is applied.

Fig. 10. Pressure records made simultaneously with two Statham transducers. The polyethylene tubings were mounted on the head of a rainbow trout, as shown in (A). The tubings were glued together, to ensure equal movements. Curve 1 in (B) represents a record made with a tube length of 0.89 m, whereas curve 2 is obtained with a tube length of 0.79 m. The records are very different. They were, however, identical if the lengths of the tubes were taken equal (not shown in this illustration).
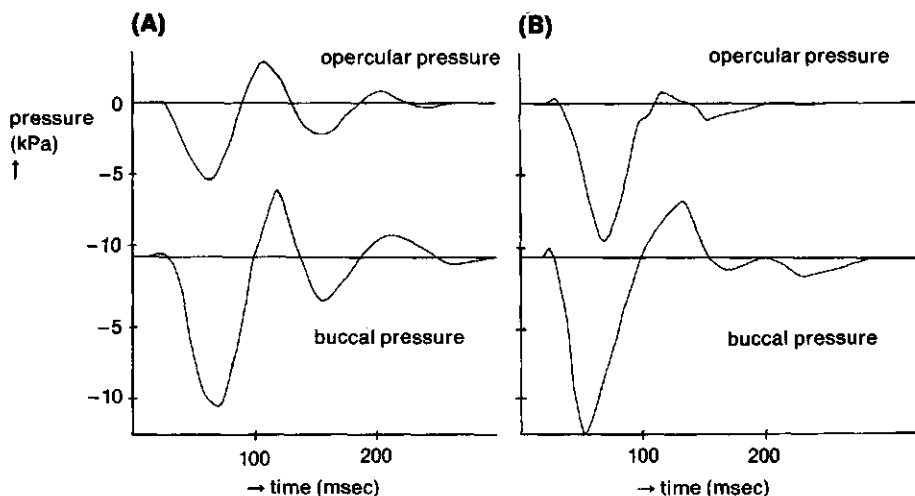
Fig. 12. Records of the pressure in buccal and opercular cavity of a bowfin (*Amia calva*, SL. 395 mm, head length 100 mm) during prey capture. The records were made with a Statham pressure transducer, connected via polyethylene tubings to the fish's mouth. Large errors may be present in these records as these transducers have a very low frequency response, besides their extreme sensitivity for accelerations of the tubes. The scale of the pressure in (B) equals that of (A).

## 3.2. PRESSURE AND MOVEMENT RECORDS

An adequate interpretation of pressure records requires knowledge of the positions of the pressure transducers inside the mouth cavity. They will be given as a percentage of head length (opercular valve = 0% and mouth aperture = 100%). Fig. 12 shows pressure records obtained for a specimen of *Amia calva* (SL. 395 mm), using Statham P23 Db transducers. Pressures were recorded simultaneously in the buccal and opercular cavity (head length is 100 mm, transducers at 10 and 60%). Peak negative pressures are slightly larger in the buccal cavity than in the opercular cavity. The buccal negative peak lasts about 70 msec, in the opercular cavity this is 65 msec. In the records of both cavities a positive phase is present after the main negative one. An initial positive phase is present before the main negative one in all records. Note the similarity between these records and those of Fig. 6A which were low-pass filtered at 20 Hz (original records obtained with Millar transducers with a high frequency response).

Another specimen of *Amia* (SL. 365 mm) was used for pressure measurements with Millar transducers. Fig. 13 shows three opercular pressure records (head length 93 mm, transducer at 14%). The first record shows the most negative pressure peak obtained (−13.6 kPa). Note the initial rapid fluctuations in the two other records. Also, at the end of the records, rapid fluctuations often occur.

Figs. 14 and 15 show similar records correlated with movement graphs of the mouth opening and opercular abduction. Fig. 14 shows a record of two

136
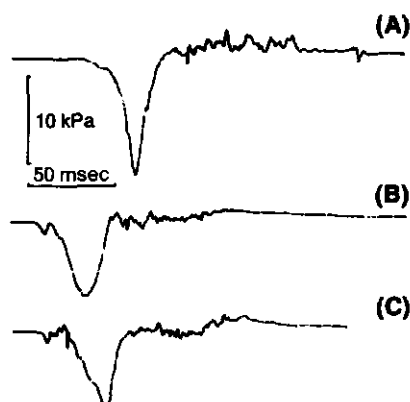
Fig. 13. Three records of the pressure in the opercular cavity of a bowfin (*Amia calva*, SL. 365 mm, head length 93 mm) during prey suction. These records are obtained with Millar PC 350 transducers. (A) shows the record with the largest obtained amplitude (13.9 kPa). Note the initial fluctuations in the pressure in (B) and (C).
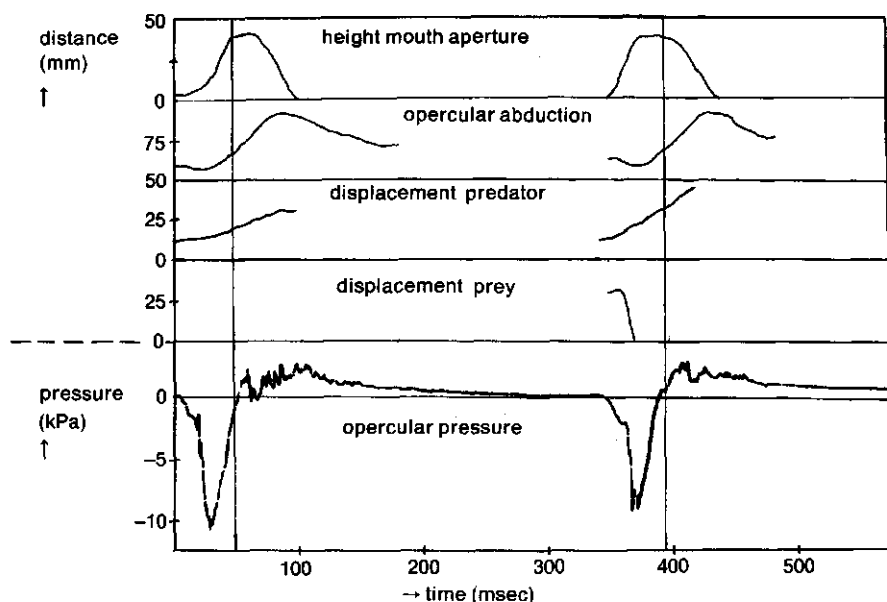


Fig. 14. Records of the height of the mouth aperture, the distance between the caudal edges of the operculars, the displacement of the predator, the displacement of the prey (earth-bound frame) and the pressure inside the opercular cavity, during feeding in the bowfin (*Amia calva*, SL. 365 mm). The first suction act is a failure. In the second attempt the prey was caught. The movements and the pressure fluctuations are very similar to those of the first suction event. The vertical lines denote the moments of the opening of the opercular valves.

137

Fig. 15. Records of head movements and of pressure fluctuations in the opercular cavity of a bowfin (*Amia calva*, SL. 365 mm), as in Fig. 14. The suction acts of Fig. 14 are faster and the valves open earlier (moment denoted by the vertical line).

attempts to capture the prey of which the first is a failure. Note the striking similarity between the movements and pressure fluctuations of both suction events. In several cases the pressure drops already slightly (in the order of 0.5 kPa) before any movement of the mouth or opercu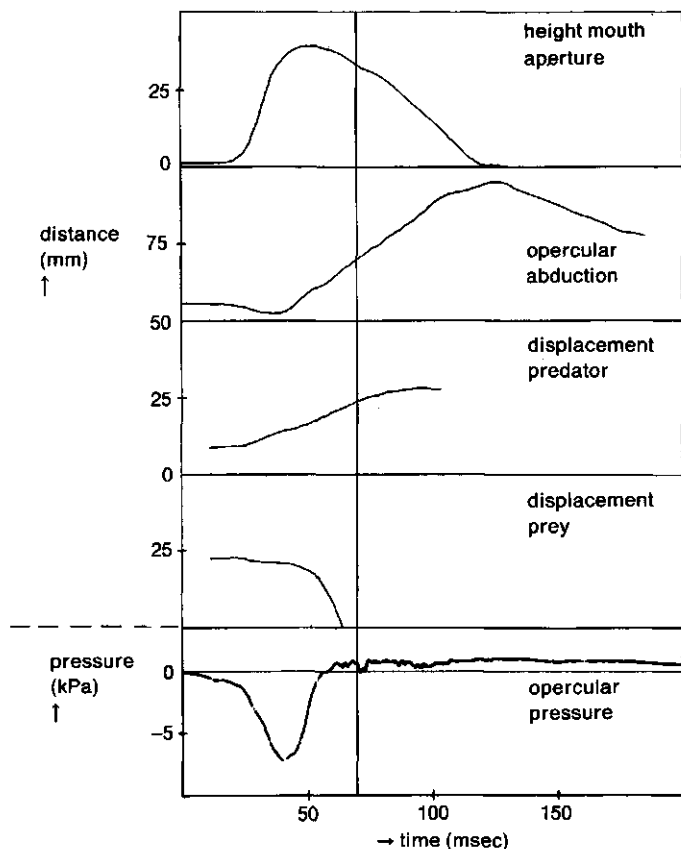la can be detected. Suction starts when the mouth opens. At the same time the pressure drops very rapidly. Initially, the opercula move slightly inwards, thereby decreasing the volume of the opercular cavity. After this initial phase the gill covers move outwards and the opercular cavity is very much enlarged. During prey capture the fish moves forward due to the impulse given to its body by the expanding mouth and additional swimming. At a certain moment ($t = \tau$) the opercular and branchiostegal valves (caudal valves) open. The relative time of opening depends on the intensity of the suction act. In rapid suction events the valves open relatively early and the measured pressure is still slightly negative at $\tau$ (see e.g. Fig. 14, the first

138
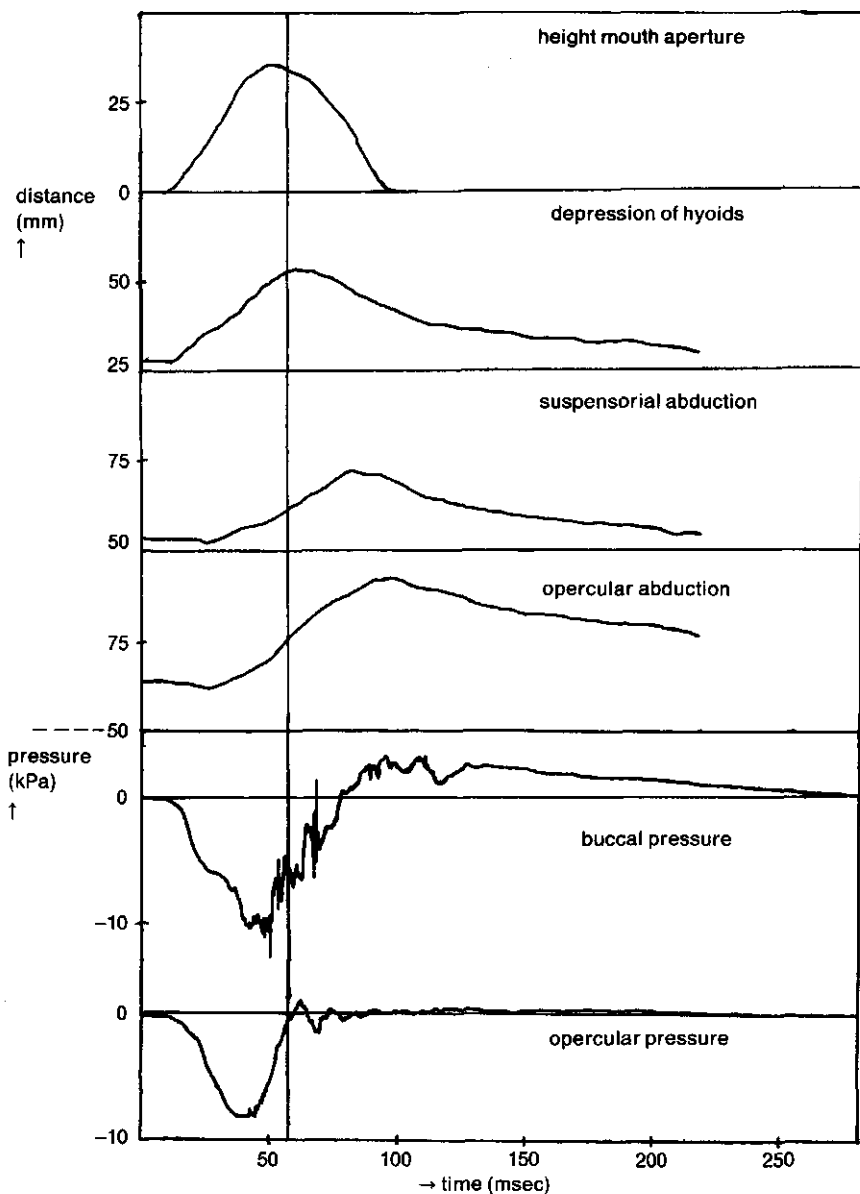
Fig. 16. Graphs of the height of the mouth aperture, the depression of the hyoids, the abduction of the suspensoria and the abduction of the opercula, together with records of the pressure in the buccal and opercular cavity during a feeding event of a bowfin (*Amia calva*, SL. 365 mm). The movement records were obtained as described in Muller & Osse (in press). The pressures were recorded with Millar pressure transducers. The rapid fluctuations in het buccal pressure record may be due to vortices passing along the transducer. Note that the negative phase in the buccal record lasts longer than in the opercular record. The opercular and branchiostegal valves start to open when the opercular pressure crosses the zero-level, denoted by the vertical line. The movement data of this feeding act were used for a simulation of the pressures and velocities in the fish's mouth, see Fig. 24D.

139

attempt). In slow suction acts (e.g. Fig. 15) $\tau$ falls relatively late and the pressure is already positive. A negative pressure at the time of valve opening in the opercular cavity does not need to imply that an inward flow of water through the opercular slits occurs, as the suction event is a highly unsteady process.

Fig. 16 shows synchroneous records of the pressure at positions in the buccal and opercular cavity (transducers at 80% and 9% of head length) correlated with kinematic data (mouth opening, hyoid depression, suspensorial abduction and opercular abduction). Hyoid depression, suspensorial abduction and opercular abduction are delayed relative to mouth opening and start in the mentioned sequence. Opening of the valves occurs when the opercular pressure (at 9% of the head length) is almost equal to the ambient pressure. The negative phase lasts longer in the buccal pressure record than in the opercular one. After this phase a positive phase can be observed in all records, reaching higher values in buccal records than in those of the opercular cavity.

Fig. 17 shows simultaneous records for *Amia* of an opercular cavity pressure (at 5% of the head length) and the pressure at 40 mm from the rostral end of the tube mounted on its head (see paragraph 2.2.3.). Before suction started swimming occurred (unfortunately, no film was made), reflected by the positive acceleration pressure in the tube. It was calculated that the maximal value of the forward acceleration was 5.5 m/s² (using the formula on page 126). When suction starts this acceleration pressure is even increased, probably due to an extra impulse caused by mouth expansion. Thereafter the pressure curve becomes more difficult to explain. The rotation of the neurocranium makes the movements of the tube very complicated. The high frequency events later on in the record may be caused by a bouncing effect within the tube. This experiment shows
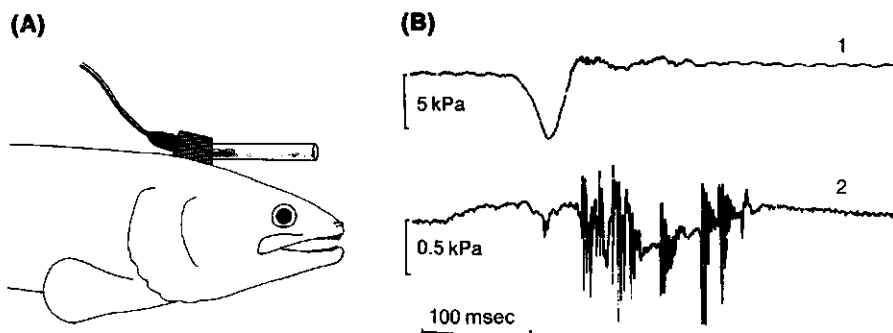


Fig. 17. Synchroneous records of the pressure in the opercular cavity of a bowfin (*Amia calva*, SL. 365 mm) and in a tube mounted on its head. The records are made with Millar transducers. In (A) the way of mounting is shown. Curve 1 in (B) is the opercular record; curve 2 represents the pressure in the tube. Note the different pressure scales. The fish accelerated towards the prey by swimming movements. This results in a positive pressure in the tube on the fish's head. From this pressure the forward acceleration of the fish can be calculated (see text). The maximal value was 5.5 m/s². Thereafter the neurocranium is rotated upwards, resulting in quite unpredictable pressure fluctuations.

140

Fig. 18. A. Record obtained with Statham transducers of the pressure in the buccal cavity of a rainbow trout (*Salmo gairdneri*, SL. 240 mm). The rainbow trout uses considerable swimming during feeding. This causes accelerations of the fluid in the polyethylene catheter. These records do not give a realistic picture of the pressure inside the mouth cavity of the fish. Actually, a positive initial pressure peak is generally absent in valid records of the pressure close to the mouth aperture.
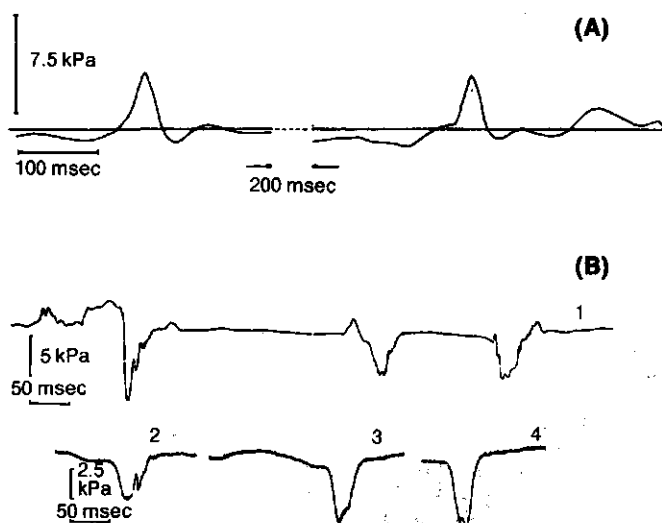B. Records of the pressure in the opercular cavity of another specimen of *Salmo gairdneri* (SL. 230 mm), obtained with a Millar PC 350 transducer. Curves 2 to 4 have the same scales. No films were taken during the feeding acts. Another feeding act was used to make a simulation of the pressure fluctuations in the mouth. A striking similarity was obtained with curve 2. The first negative peak in curve 1 represents the pressure fluctuation during prey capture. The two other peaks were generated during prey handling.

that the acceleration of the fish has a significant influence on the value of the pressure in the mouth cavity.

Fig. 18A shows buccal pressure records of a specimen of *Salmo gairdneri* (head length 56 mm, transducer at 80%), obtained with a Statham transducer. The tube aperture was positioned perpendicular to the flow direction. Quite large positive pressure peaks in the records are present, probably mainly due to swimming movements, causing the fluid in the catheters to be accelerated.

Fig. 18B shows opercular pressure records for another specimen of *Salmo gairdneri* (head length 53 mm, transducer at 25%). Quite often considerable positive pressures occur at the start of the pressure waveforms, probably mainly caused by swimming. (No films were made synchroneously with the pressure records, but swimming plays an important role in the prey capture mechanism of the rainbow trout as pointed out by Van Leeuwen, in prep.). During the negative phase secondary fluctuations might be present. Peak negative pressure equals –8.8 kPa (curve 1). It must be stressed that the pressure records obtained
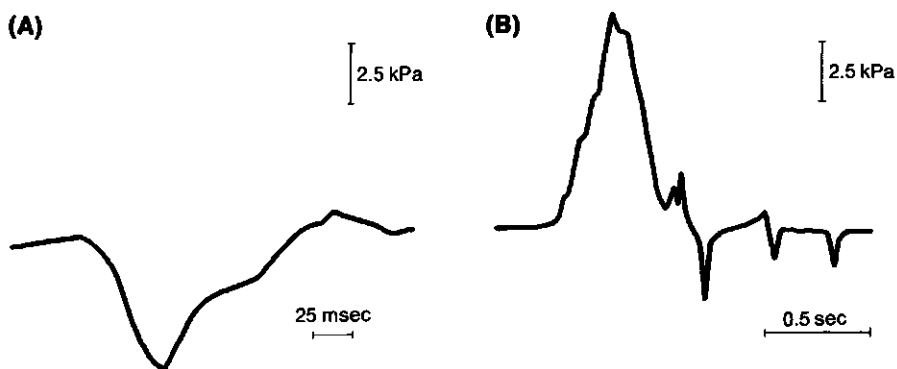
141

Fig. 19. Buccal (A) and opercular (B) pressure records of the pike (*Esox lucius*, SL. 253 mm), obtained with a Millar PC 340 transducer. The forward acceleration of the fish is reflected by the strong positive peak in the opercular record. The peak acceleration of the fish would have been 120 m/s² if this positive pressure peak is only to be attributed to forward motion. A film was taken during measurement of the buccal pressure. The movements of the fish were measured and used to simulate the pressure in the mouth cavity. The results are shown in Fig. 24B.
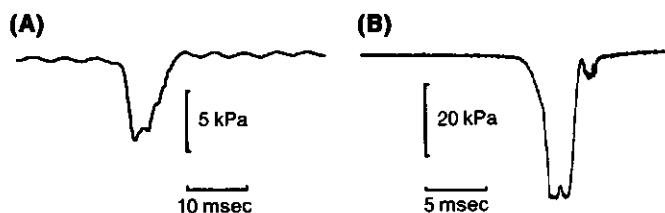


Fig. 20. Opercular pressure records for a cod (*Gadus morhua*, SL. 225 mm), obtained with a Millar PC 350 transducer. Note the different time scales in (A) and (B). In (A) the prey was not caught. Prey capture event (B), however, was succesful. No films were taken during these feeding acts. The movements during feeding of another cod were used to simulate the pressure inside the fish's mouth (see Fig. 24C).

for *Salmo* are not directly comparable to those of *Amia* as both the head lengths and the relative positions of the transducers are different.

Fig. 19 shows a buccal and an opercular pressure record of the pike, *Esox lucius* (head length 73 mm, transducer at 80% and 10% respectively). This fish generally accelerates towards the prey by powerful swimming movements (Webb and Skadsen, 1980). This is reflected by the high positive pressure in the opercular record (8.5 kPa) during the first part of the feeding act. This record strongly supports the suggestion that movements of the predator as a whole influence significantly the pressure inside the mouth cavity. The peak acceleration of the fish must have been about 120 m/s² if the positive pressure peak was only caused by forward motion.

142

Fig. 20 shows two opercular pressure records for *Gadus morhua* (head length 58 mm, Millar transducer at 5%). The first record represents a relatively slow suction act, whereas the second represents an extremely fast one. The duration time of the negative phase of the second attempt is only 5 msec and the peak negative pressure is –42 kPa. Obviously, such pressure fluctuations cannot be recorded accurately with Statham transducers or related types.

Fig. 21 shows two buccal pressure records obtained for a specimen of *Perca fluviatilis* with Statham transducers (SL. 160 mm, head length 48 mm, transducer at 80%). No initial positive phase is present. The peak negative pressure is –7.5 kPa. The negative phase lasts about 90 msec. Probably, these feeding attempts should be regarded as relatively slow for a perch of this size. Large errors may be present in these records due to the unreliable properties of the measurement system (see above).
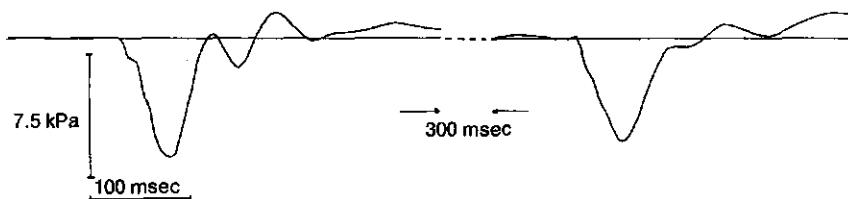


Fig. 21. Buccal pressure records for the perch (*Perca fluviatilis*, SL. 160 mm), obtained with a Statham P23 Db transducer (connected via a polyethylene catheter to the mouth cavity. Large errors may be present in the records due to accelerations of the catheter and the limited frequency response.

### 3.3.1. *The model of Muller, Osse and Verhagen (1982)*

Muller et al. (1982) discussed a mathematical model of suction feeding in teleost fish. Their model consists of a conical profile along the $X$-axis with dictated radial movements. Fig. 1 of chapter 2 of this thesis illustrates the model approach. At one end of the profile $(x = 0)$ a valve ("the opercular and branchiostegal valves") was defined, opening at $t = \tau$. The equations of continuity and motion for the expanding and compressing profile were solved to obtain the velocities and pressures inside the mouth. The formulae of the velocities and pressures are given in the Appendix.

Before $t = \tau$ the velocity at $x = 0$ is zero, which is a valid boundary condition for calculating the velocities and pressures inside the profile. To obtain the velocities and pressures for $t > \tau$ the velocity or the pressure at a particular point for which $0 < x < l$ has to be prescribed. Muller et al. (1982) did not expect a considerable suction force to be present after the opening of the caudal valves. Therefore they obtained the necessary boundary condition for $t > \tau$ by the assumption of a constant velocity in the mouth aperture. Valve opening was chosen to occur at an extreme value of the velocity in the mouth aperture, to avoid a discontinuity in the pressure. Generally, the velocity in the mouth aperture is double peaked due to the delay between the rostral and caudal expansion. Thus only two minima are present. In some cases the second minimum is even absent (see Muller et al., 1982 and Muller and Osse, in press). Thus the possibility of valve opening is restricted to one or two moments in this approach. At these moments quite large negative pressures might be present in the mouth cavity, an unfavourable condition for the fish to open its valve, as much muscular effort would probably be needed. As mentioned above a negative pressure in the opercular cavity does not necessarily correlate with an inward flow of water through the opercular slit, as the flow is unsteady.

The disadvantages of obtaining the boundary condition from the pressure have already been put forward by Muller et al. (1982). Experimental evidence given in the present paper and the paper by Van Leeuwen (in prep.) suggested a new approach for tackling the choice of $t = \tau$ and the formulation of a new boundary condition.

### 3.3.2. *The choice of the moment of valve opening*

The ideal moment of valve opening depends on the forward velocity of the profile (the "fish's velocity") $U_f$ and the expansion of the head as pointed out by Van Leeuwen (in prep.). Once the mouth expansion rate is less than a certain critical value the valves should be open, otherwise the fish would push water forward in the mouth aperture in the earth-bound frame.

The present results of the experiments with *Amia calva* (Figs. 15 to 17) suggest that two other conditions should be fulfilled before valve opening is likely to occur:
1. The pressure at $x = 0$ inside the profile ("the most caudal opercular pressure")

144

should be close to the ambient pressure. In *Amia* the deviation from the ambient pressure is less than 10% of the amplitude of the peak negative pressure.

2. The profile has to expand to a certain amount before the valve is able to open. Experimental evidence for this aspect is also given by several other papers such as Muller and Osse (in press).

A third condition was formulated on the basis of simulations with the model of Muller et al. (1982) and the analysis given by Van Leeuwen (in prep.), and from the need of the formulation of an adequate boundary condition for $t > \tau$ (see paragraph 3.3.3.):

3. The acceleration of the water in the mouth aperture should be equal to or greater than zero ($u'_v(l,\tau) \geqslant 0$). When $u'_v(l,\tau) < 0$ the water in the mouth aperture is sucked caudally with an increasing rate. Hence any pushing problems are still absent and there is no need to open the valves (see Van Leeuwen, in prep.).

We will illustrate the feasibility of condition 3 further with the aid of the simulation of a profile with an apparent cone-like movement (see Fig. 22). The velocity at the mouth aperture is double peaked and divided for convenience into 4 phases. In phase 3 the pressure becomes more negative while water is accelerated backwards (This is not generally true during phase 1 as the acceleration component due to forward motion of the fish in the pressure is very important at that time). The same feature was found for 20 other simulations, indicating that condition 3 ascertains that the pressure is not significantly decreasing after valve opening. This depends also on the boundary condition for $t > \tau$, to be discussed in the next paragraph.

Effectively, conditions 1 to 3 allow the valve to open during phases 2 and 4 of Fig. 22. In case of a single peaked velocity curve at the mouth aperture phases 3 and 4 are absent and valve opening is possible in phase 2. In actual simulations of feeding events the movement curves of the mouth opening and opercular abduction, found by cinematographic analysis, were fitted with e-power functions (see Muller et al., 1982 and Muller and Osse, in press). These
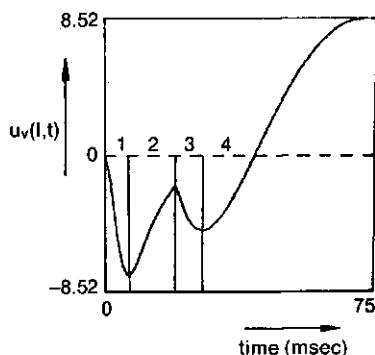


Fig. 22. Velocity fluctuation in the mouth aperture for a profile with a cone-like expansion equal to that of Fig. 23 (i.e. there is a clear delay time between the expansion at $x = l$ and the expansion at $x = 0$). The velocity in the mouth aperture is given relative to the profile. The phases numbered 1 to 4 are discussed in the text. The caudal valve is assumed to be continuously closed, so that water leaves the profile anteriorly when its volume is again decreasing.

145

functions were used in the calculation of the velocity and pressure inside the conical profile. From the film the amount of opercular abduction $h_2$ was determined at $t = \tau$. In simulations valve opening was often chosen to occur at the instant that $h_2 > h_2(\tau)$. This only leads to slight differences between experimentally determined $\tau$ and $\tau$ used in the simulations. Following this approach no cases were found where $\tau$ fell in phase 3.

### 3.3.3. Formulation of a new boundary condition

Van Leeuwen (in prep.) was able to calculate the boundary value for $t > \tau$ for a cylinder model when the motion of the fish is also prescribed. He pointed out that the mean velocity with open valve in $X$-direction in an earth-bound frame is zero halfway inside the cylinder (at $x = 0.5*l$) if no inertial effect is present due to the previous closed situation. From conservation of mass it follows that after valve opening:

$$u_n(0,t) = \frac{l}{h} \cdot h' - U_f \tag{7}$$

where $h$ is the radius of the cylinder, and $h'$ its expansion rate which can be substituted in (14):

$$u_n(x,t) = u_v - U_f + \frac{l}{h} \cdot h' \tag{8}$$

Hence, the velocity after valve opening can be completely deduced from the continuously closed phase in combination with the velocity of the fish.

The position of a point of zero flow inside a conical profile with independent anterior and posterior expansions and an open valve cannot be easily derived due to unsteady effects (Van Leeuwen, in prep.). Although some important features of the suction feeding mechanism can be explained with the cylinder model it is a less accurate representation of the sucking system than the cone, especially during mouth closure. Therefore we tried to develop also a reasonable boundary condition for the cone although an exact calculation is not yet possible.

Obviously, the velocity at the mouth aperture is zero after mouth closure at $t = t_d$. Thus a valid boundary condition for $t > t_d$ is: $u_n(l,t) = 0$. Generally $t_d > \tau$, thus a boundary condition for $\tau < t < t_d$ has also to be formulated. As we could not formulate solid arguments for a boundary condition during this phase, we decided to keep the boundary condition as simple as possible. Condition 3 of paragraph 3.3.2. made sure that we did not have to define a function starting with a negative value, a negative first time derivative and ending with zero values for both functions (Besides, when $u'_v < 0$ we had no arguments for the formulation of a minimum). In fact, computer simulations showed that $u'_v(l,\tau) > 0$ in every case.

For $u'_n(l,\tau) = 0$ we formulated the following boundary condition:

$$\left. \begin{array}{ll} u_n(l,t) = u_v(l,t)\left[{}^1\!/_2 + {}^1\!/_2 \cos\left\{\dfrac{\pi(t-\tau)}{t_d-\tau}\right\}\right], & \text{for } \tau \leqslant t \leqslant t_d \\ \text{and } u_n(l,t) = 0 & \text{,for } t \geqslant t_d \end{array} \right\} \tag{9}$$

146

giving the required values for $u_n(l,t)$ and $u'_n(l,t)$ at $\tau$ and $t_d$. Unfortunately, a simple trigonometric function with a positive first time derivative during $\tau < t < t_d$ cannot be easily found when $u'_v(l,\tau) > 0$. A polynome could be a solution to the problem. However, uncontrolled amplitudes cannot be excluded in this case. There is no physical support for such oscillations to take place. Finally, we have chosen for an e-power function:

$$u_n(l,t) = u_v(l,\tau)\left\{e^{\dfrac{u'_v(l,\tau)\ (t-\tau)}{u_v(l,\tau)}}\right\} \quad , u'_v(l,\tau) > 0, \quad t \geqslant \tau \tag{10}$$
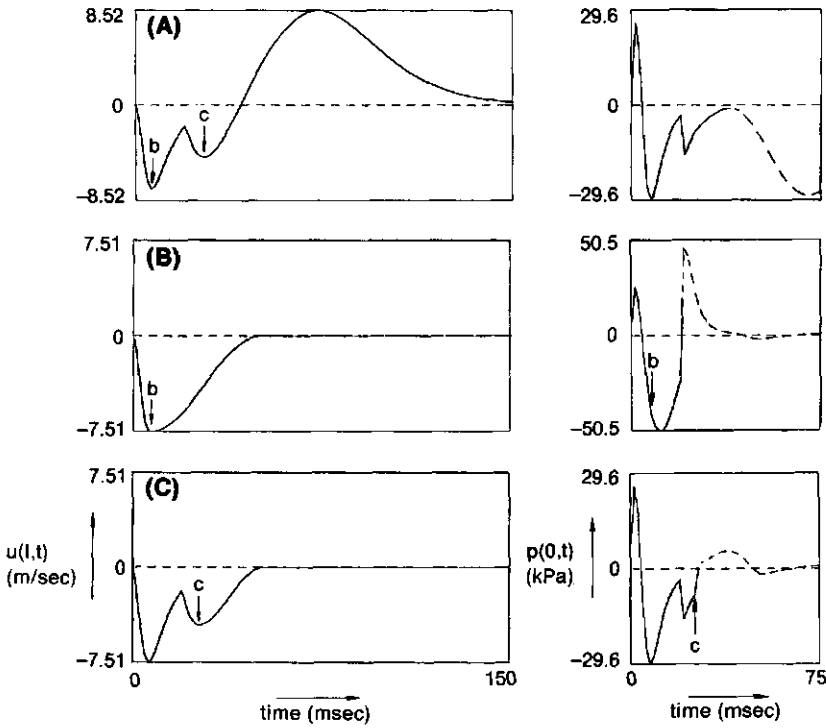


Fig. 23. Velocity (in the moving frame) in the mouth aperture ($x = l$) and the pressure near the valve ($x = 0$) for the profile chosen by Muller et al. (1982, see their Fig. 11). The movements were kept the same, but different values for $\tau$ and the boundary condition for $t > \tau$ are used.
A. Situation with continuously closed valves. The velocity is double peaked. The initial positive value of the pressure is caused by a forward acceleration of the profile. Water is blown out through the mouth aperture at the end of the suction act. Arrows denoted with (b) and (c) depict moments of valve opening in (B) and (C).
B. Situation with moment of valve opening at the first minimum of the velocity ($\tau = 6.3$ msec). The cosine function is used as a boundary condition.
C. As (B) but now the valves open at the second minimum ($\tau = 25.6$ msec).
The dashed parts of the pressure curves denote the non-valid range of the calculations. Further explanations are given in the text.

147

This function has the required values for $u_n(l,t)$ and $u'_n(l,t)$ at $\tau$ but not at $t_d$. However, it was concluded from an analysis of 20 simulated feeding events that:

1. The velocity at $t=\tau$ is always less than 20% of the minimum velocity for velocity curves with one minimum, resulting in only small deviations from zero (a few cm/sec) for $t > t_d$.

2. The valves open very shortly after the second minimum has been reached for the velocity curves with two minima. Hence, the first boundary condition can be used in this case, with $\tau$ chosen to fall at the second minimum. It must be stressed that simulated pressures will depend on the choice of these functions, as in the calculations they are compared with the chosen movement functions of the mouth. A careful choice, based on the observation of many suction events is therefore required to avoid unrealistic results.

Examples of simulated feeding events will be discussed in the next paragraph.

### 3.3.4. *Simulation of pressure curves*

Fig. 23B shows a simulation with the new boundary condition (the cosine function was used) for the profile chosen by Muller et al. (1982), leaving all movements and parameter $a$ the same. The valve was chosen to open at the first extreme of $u_v(l,t)$ at $t=6.3$ msec. Mouth closure was chosen to fall at $8*\tau$, thus $t_d=50.4$ msec. The pressure in the profile becomes less negative, compared to the value obtained by Muller et al. ($-50.5$ kPa versus $-58.5$ kPa at $x=0$). The main advantage is the better form of the velocity curve (including mouth closure). However, several disadvantages still exist. The valve opens when the pressure in the opercular cavity is still largely negative ($p(0,\tau)=-25$ kPa) and decreases even more after $t=\tau$. Also, valve opening occurs even before the expansion at $x=0$ has been started. These unrealistic features result from an unappropriate choice of $\tau$.

Fig. 23C shows a simulation with the same profile and movements, but valve opening was chosen to coincide with the second minimum of $u_v(l,t)$, and $t_d = 2\tau = 51.3$ msec. The new choice of $\tau$ results in pressure curves with two minima, corresponding to the two minima in the velocity curve at the mouth aperture ($u_v(l,t)$). The pressure near the valve at $t=\tau$ is less negative than in the first example ($p(0,\tau) = -7$ kPa). After $t=\tau$ the pressure at $x=0$ becomes positive within 1.5 msec.

Starting with movement data obtained from films, simulations of velocities and pressures in the mouth cavity were made of four different fish species. For *Amia* and *Esox* synchroneous records of movements and pressures were available, so that measured and simulated pressures could be compared for the same feeding event. For *Salmo* and *Gadus* such data were lacking. We used movement data of feeding acts of different specimens to simulate the measured pressures. The movements were fitted with e-power functions shown in chapter 2 of this thesis. The values of the parameters used in the simulations are given in Table 3. In all cases the e-power function was chosen for the boundary conditions for $t > \tau$.

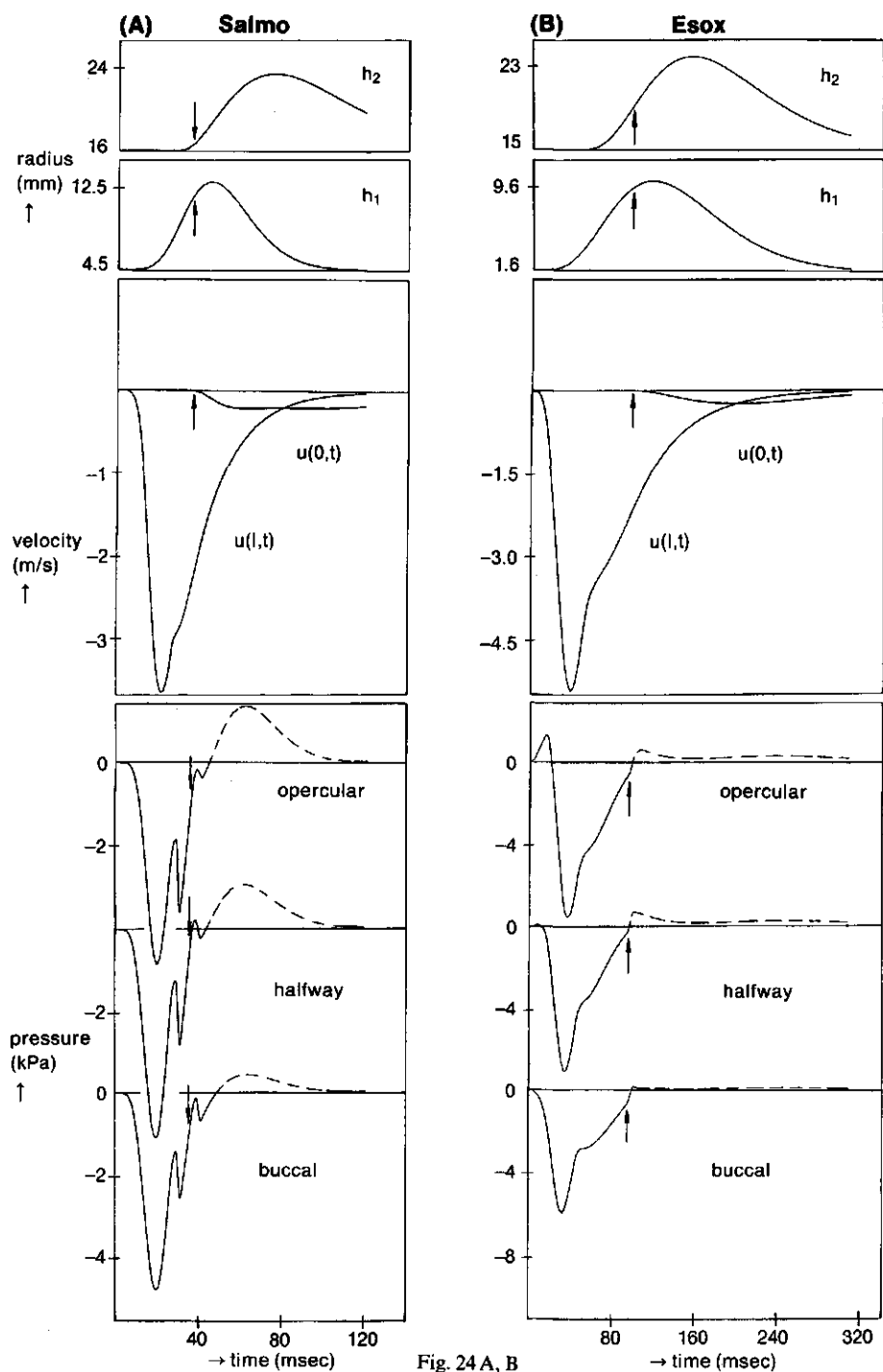Fig. 24A shows a simulation for a rainbow trout (*Salmo gairdneri*). The obtai-
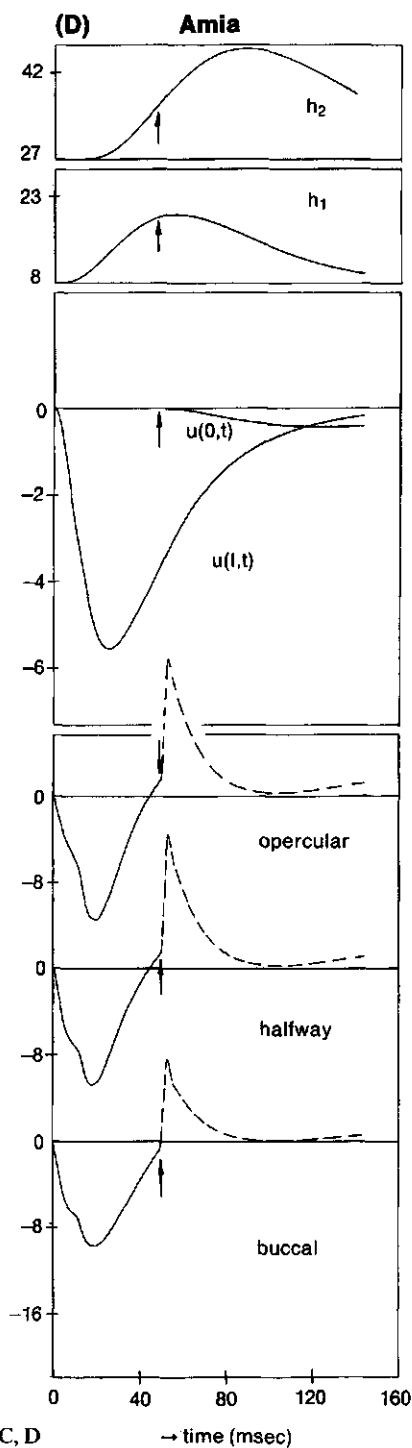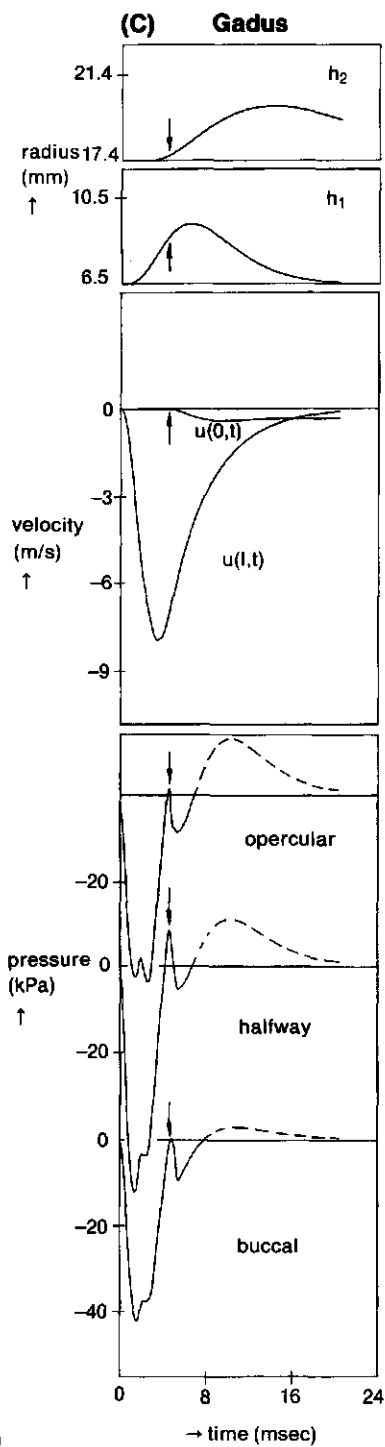
148

Fig. 24 A, B

(C) Gadus  (D) Amia

Fig. 24 C, D

150

→ time (msec)

ned double peaked pressure at $x = 0.2\ l$ is very similar to the pressure curve 2 of Fig. 18. The second negative peak is caused by the caudal expansion. The velocity in the mouth aperture and the velocity at the valve resemble the velocity records obtained by Muller and Osse (in press), using hot-film anemometry. The valves generally open very early in *Salmo* (see Van Leeuwen, in prep.). In the simulation valve opening was chosen to occur slightly before the actual moment of opening. The lowest simulated pressure in the entire mouth is found at $x = 0.5\ l$ and equals about $-5$ kPa.

Fig. 24B shows a simulation for a pike (*Esox lucius*). Synchroneous movement data belonging to pressure curve (A) in Fig. 19 were used for the simulation. A positive initial pressure peak is present in the opercular pressure curve due to a forward acceleration of the profile (parameter *a* was chosen to be 3). The measured and simulated buccal pressure are very similar, although a larger pressure drop was simulated than measured. Mouth expansion at $x = 0$ does result in a plateau phase, but not in a second negative pressure peak.

Fig. 24. Simulations of feeding acts of four different fish species. These simulations were obtained by assigning values measured from movie pictures to the parameters of the model. Starting from these values the pressures generated by the model were compared to pressures measured in the same or another individual. The model parameters then were adjusted within the range of experimental error untill the simulated pressure waveform and magnitude resembled the measured values. The dashed lines indicate pressure values which are strongly influenced by the chosen boundary conditions and thus are not realistic. A survey of the model-parameters used can be found in Table 3. Valve opening is denoted by arrows.
A. *Salmo gairdneri*. The measured movement and pressure data were obtained from different snaps of the same animal. In the simulation the opercular valve opens up rather early, viz. 35 msec (actual time 45 msec). The calculated and measured pressures are very similar. The velocity curve is likewise in good agreement with the actual velocity curve. Muller & Osse (1982) have published velocity data showing that the actual velocities can be of the same form and magnitude. To compensate for an overestimate of the mouth volume by the model the length of the simulated mouth was taken less than the actual mouth length. Note the similarity between the simulated pressure curve in the opercular region and curve 2 in Fig. 18B.
B. *Esox lucius*. This simulation is based on a feeding event of which both movement and pressure data were obtained. The recorded pressure waveform in the buccal cavity is shown in Fig. 19A. Again a good similarity between measured and simulated pressure waveform exists. The amplitude of the simulated pressure is greater than the amplitude of the measured pressure. This presumably is due to an overestimate of the volume sucked and slight differences in the area of the mouth aperture just after the start of mouth expansion. Again the mouth length was taken smaller in the simulations. The actual moment of valve opening fell 3 msec later than the simulated moment.
C. *Gadus morhua*. The pressure record shown in Fig. 20B should be compared with the simulated pressure in the opercular region. The movement data of another (larger) specimen were used for this simulation, after having reduced the amplitudes of the movements, the mouth length and the duration time to the required scale. A very good resemblance was found between simulated and measured pressures, both in amplitude and waveform.
D. *Amia calva*. The movement data shown in Fig. 16 were used for this simulation. In this case two synchroneously recorded pressure waveforms were available (opercular and buccal cavity). The mouth length was taken smaller than the actual one, to compensate for an overestimate of the volume of the mouth by the cone. Experimentally a lower pressure was found in the buccal cavity than in the opercular cavity. The reverse effect was found in the simulation. The simulated pressure waveforms resemble the experimentally obtained waveforms quite closely. The chosen boundary condition has quite a big influence on the calculated pressure after valve opening.

151

TABLE 3. Values of parameters used in the simulations shown in Fig. 24. Symbols are explained in the Appendix. The actual values for $l$ are given between brackets.

| species | Esox | Amia | Salmo | Gadus |
|---|---|---|---|---|
| code | 100190 | 100189 | 100187 | 100188 |
| $h_{1nul}$ (mm) | 1.6 | 8 | 4.5 | 6.5 |
| $h_{1max}$ (mm) | 10.3 | 20 | 13 | 9.3 |
| $\alpha_1$ | 5 | 3.2 | 8.3 | 3.9 |
| $t_{h1max}$ (msec) | 11.5 | 5.65 | 4.5 | 0.65 |
| $t_{v1}$ (msec) | 0 | 0 | 0 | 0 |
| $h_{2nul}$ (mm) | 15 | 27 | 16 | 17.4 |
| $h_{2max}$ (mm) | 24 | 46.5 | 23.5 | 20 |
| $\alpha_2$ | 3.5 | 3.35 | 2.5 | 2.5 |
| $t_{h2max}$ (msec) | 15.5 | 8.8 | 7.5 | 1.4 |
| $t_{v2}$ (msec) | 4.75 | 1.03 | 2.85 | 0.235 |
| $h_{klep}$ (mm) | 1.94 | 3.8 | 1.70 | 1.772 |
| $\tau$ (msec) | 100.4 | 51.15 | 37.9 | 4.63 |
| $l$ (mm) | 62 (73) | 85 (92) | 47 (53) | 48 (58) |
| a | 3 | 5 | 5 | 5 |
| pressure shown at: ($*.l$) | 0.1/0.5/0.8 | 0.1/0.5/0.8 | 0.2/0.5/0.8 | 0.1/0.5/0.9 |

Fig. 24C shows a simulation of a feeding event of a cod (*Gadus morhua*). The simulated pressure should be compared to the second pressure curve of Fig. 20. The movement data were obtained from a different specimen. The lowest pressure drop is found halfway along the length of the mouth. Experiment and simulation show a striking similarity, both in form and amplitude. Even a plateau phase as in the record was simulated, although at a different position.

Fig. 24D shows a simulation of the feeding event of *Amia calva* shown in Fig. 16. The form of the pressure curves closely resembles the measured pressures. The measured peak buccal pressure is more negative than the peak opercular pressure. A reverse effect was obtained in the simulation. Some time after valve opening the pressure calculations are not realistic anymore, because of the large influence of the chosen boundary condition.

We may conclude that the model gives a good description of the hydrodynamic events during feeding. The shown similarities between measured and simulated pressures are generally not present in the first simulation of a feeding event, as it is impossible to obtain the accelerations of the movements accurately enough from the 16 mm films. Adjustment of the parameters within the range of experimental error gives, however, very satisfying results. The volume increase of the fish's mouth is generally overestimated with the cone model. We compensated for this effect by decreasing the value of $l$ (the length of the mouth).

### 3.3.5. *The components of the pressure*

Several features of the pressure fluctuation can be understood when the separate components of formula (15) are looked at (see e.g. Muller and Osse, in

152

press). In the opercular pressure records in *Amia* (Figs. 13 and 14) fluctuations are often visible at the start of the suction act. Terms (b) and (c) of equation (15) are very important in the opercular cavity as $x$ is small in this region. Term (b) is always positive and particularly important when the fish has a high acceleration. The other terms of equation (15) are all negative in the initial phase. The sum of all terms might easily fluctuate like the pressure records actually do. Such fluctuations were also obtained in simulations of pressure waveforms.

In several of the opercular pressure records of *Salmo gairdneri* positive peaks are present in the pressure curves. The trout is a rapid swimmer and much of the positive peaks may be caused by swimming movements. Slow pressure changes may be caused by swimming in a vertical direction. In the cod a clearly definable positive acceleration peak could not be demonstrated.

Near the mouth aperture terms (a), (b) and (c) of equation (15) are very much reduced and positive acceleration pressures due to the movements of the fish were indeed not measured. The results of the pressure measurements in the tube on the head of *Amia calva* show the influence of forward movement of the fish on the pressure inside the mouth.

More attention will be paid to the pressure components in our version of this paper that will be submitted to the Neth. J. Zool.


## 4. Discussion

### 4.1. PRESSURE TRANSDUCERS

The present results show that pressure measurement systems consisting of fluid filled catheters in combination with strain gauge type manometers are unsuitable for recordings in the teleost feeding apparatus. The limited frequency response of these systems is clearly shown by the results of the transient tests (see paragraph 3.1.). Another disadvantage is the distortions in the pressure records due to accelerations of the catheters. Catheter tip pressure transducers lack these disadvantages.

We do not know exactly the influence of the dimensions of the transducer itself on the measured pressure. The striking similarity between measurements and simulations suggests, but does not prove, that it is small.

The acceleration of the sucking and swimming fish contributes significantly to the pressure in the mouth cavity. Hence, it is important to fix the transducer rigidly to the fish.

### 4.2. A REVIEW OF PRESSURE MEASUREMENTS

Before discussing the present pressure data we will review the literature on pressure measurents in suction feeding. Remarkably, data about the head length, standard length and body mass of the experimental animals are often lacking in the literature. Also, details about the exact positions of the transducers inside

153

the mouth are generally absent. Therefore no reliable simulations with our model could be made from these literature data.

The first pressure measurements in prey sucking fish were performed by Alexander (1969, 1970), using a SE 4-81 pressure transducer. The fishes were trained to suck food from a nylon tubing connected via a thicker copper tubing to the transducer. Alexander measured a damped natural frequency of 100 Hz, when the system was filled with water. Before experimentation he damped the system critically ($\zeta = 1$, a damping ratio of $1/\sqrt{2}$ would have been better, see paragraph 2.1.2.) by replacing a certain amount of water by glycerol. Alexander (1969) stated that the transducer was designed to respond to pressures fluctuating up to 100 Hz. However, at 100 Hz there is already a drop in the amplitude response of about 50% (see Fig. 1A), assuming that his transducer functioned as a single degree of freedom system. A more accurate estimate of the bandwidth of Alexander's system is 0-30 Hz. In this range the amplitude response is flat and the phase relationship is almost linear (see Fig. 1).

Another disadvantage of Alexander's system is that it may evoke unnatural feeding movements. Muller et al. (1982) pointed out that the pressure waveform is highly sensitive to only small alterations in the movements of the structural elements of the head of the fish. Furthermore, the prey and tubing might seal the mouth aperture during much of the suction event, resulting in the production of abnormal high negative pressures. Also the initial pressure waveform is lacking as the pressure in the mouth cavity is only recorded after the mouth has opened to a certain degree. Alexander measured the pressure in the earth-bound frame (see paragraph 2.1.8.).

Although the measurements of Alexander only gave a rough indication of the pressures that act in reality during the suction event, they were valuable at the time they were made as they showed that pressure calculations based on steady flow assumptions (Osse, 1969) are invalid.

The peak negative pressures measured by Alexander ranged from –7.5 kPa in *Ictalurus* to –40 kPa in *Pterophyllum*.

Casinos (1973, 1974) used the technique of Alexander (1969). Some of his peak negative values are: *Gadus*: –15 kPa; *Pollachius*: –6 kPa and *Mottella*: –7 kPa.

Several authors used Statham transducers in combination with fluid filled polyethyelene tubings to measure pressures in prey sucking fish. The disadvantages of this system are detailedly discussed in the present paper.

Osse (1976) measured synchroneously pressures inside the buccal and opercular cavities in prey sucking *Amia calva*. Fig. 12 in the present paper shows examples of the pressure waveforms obtained. The recorded maximal peak negative values by Osse were: buccally: –17 kPa and opercularly: –9.5 kPa. In the buccal records a small positive pressure peak at the start of the suction event is visible. Such a positive phase has not been recorded with the Millar transducers and might be caused by the acceleration of the fluid in the catheter, due to swimming and head movements.

Liem (1978) recorded pressures inside the buccal cavity of *Serranochromis*

*robustus* and *Haplochromis compressiceps*, using the Statham P23 Db pressure transducer. He implanted the tubing (diam. 2 mm) through the ethmoid bone and orientated the tube aperture parallel to the flow direction. Liem gave no information about a calibration procedure, nor about the bandwidth of his recording equipment. The properties, however, will be similar to those given for our Statham transducers (see paragraph 3.1.). Liem presented a few graphs of his measurements, showing curves with an amplitude of –6 m water (or about –60 kPa) or more in amplitude. The duration time of the negative peak given was in the order of 300 to 500 msec. Probably the real duration times should be in the order of 30 to 50 msec, as no fish of the sizes used by Liem (about 20 cm of standard length) is able to create such low pressures during such a long time.

Elshoud-Oldenhave (1979) reported pressure measurements in *Stizostedion lucioperca* with Statham P23 Db pressure transducers (the same transducers as used by Osse; test report in paragraph 3.1. of the present paper). Polyethylene tubings (d = 1–1.2 mm) were implanted in both the buccal and opercular cavity and pressures were recorded synchronously. Peak negative pressures varied from –5 to –11.5 kPa in the buccal cavity, whereas 10 to 15% lower values were found in the opercular cavity.

Lauder and Lanyon (1980) measured pressures in the opercular cavity of *Lepomis macrochirus*, synchronously with strain gauge measurements on the operculum. Again Statham P23 Db transducers were used in combination with polyethylene tubings. Calibration was performed using the method of Gabe (1972). A damped natural frequency of 70 Hz was found, in combination with a damping ratio, $\zeta$, of 0.138. In certain experiments the viscosity of the fluid in the tubing was increased by exchange of water by glycerine (method of Alexander, 1969) which resulted in $\zeta = 0.524$. The authors did not pay attention to resonance properties of their test cylinder. The catheter was mounted through a hole in the cleithrum (after Liem, 1978). From Fig. 1 it appears that with $\zeta = 0.138$ accurated recording is only possible up to about 30 Hz. With $\zeta = 0.524$ this limit is only slightly higher. The inadequate frequency response is illustrated by the time delay of 15 to 20 msec (see their Fig. 5) between the strain gauge records and the pressure records.

Lauder (1980a) shows pressure fluctuations in *Lepomis*, recorded synchronously in the buccal and opercular cavity. Statham P23 Gb transducers were used in combination with plastic cannulae (out. diam. 1.52 mm, inner diam. 0.86 mm), filled with a mixture of 53% boiled glycerine and 47% boiled water to adjust $\zeta$ to 0.65. According to Lauder the frequency response of the system was 75 Hz. The maximal negative pressures recorded in the buccal and opercular cavity were about -65 kPa and -13 kPa respectively.

Lauder (1980b) used the same equipment as Lauder (1980a). This time a mixture of 55% glycerine and 45% water was used to obtain a damping ratio of 0.65. The damping ratio is obviously not only dependent on the mixture of glycerine and water, but also, importantly, on the length of the catheters as shown in paragraph 3.1. With $\zeta = 0.054$ a damped natural frequency was obtained of

155

250 Hz. Lauder paid no attention to the influence of the resonance of the testing cylinder on his calibrations. From Fig. 1 it is apparent that measurements up to 100 Hz (with $\zeta = 0.65$) have to be regarded as faithful if no troubles existed with resonance of the testing cylinder. Large errors are caused by accelerations of the catheters (see the present paper).

Lauder's measurements give an impression of the overall pressure waveform. However, the bandwidth of his equipment was insufficient to record pressure fluctuations occuring within 10 msec accurately.

Osse and Muller (1980) published simultaneous records of the pressure in the buccal and opercular cavity in *Amia calva*, obtained with Statham P23 Db transducers. Details of their technique are given in the present paper. The authors stated that the response time of their system was 10 msec. As shown the actual response time is about 50 msec. Thus the curves obtained by Osse and Muller also give only an indication of the overall pressure waveform (the duration time of the negative phase in the pressure curves is only about 50 msec).

### 4.3: INTERPRETATION OF PRESSURE RECORDS

The Statham pressure records resemble the filtered Millar records (20 Hz, 12Db/oct, see Fig. 6A). Pressure curves obtained by Statham transducers are always smooth whereas the Millar records often show rapid secondary fluctuations (duration in the order of 1 msec). This is particularly true for the buccal records of *Amia calva*. A possible explanation for this phenomenon is the passage of small vortices along the transducer.

At the start of the suction process water flows more rapidly in the anterior part of the mouth cavity than in the posterior part. Thus, pressure fluctuations due to passing vortices will occur first in the buccal cavity and only later on in the opercular cavity. This indeed is observed in most of our *Amia* records. An estimate can be made of the dimension of the vortex. For instance, in the mouth aperture one pressure oscillation lasts about 0.5 msec. Taking for the velocity a characteristic value of 1 m/s one obtains 0.5 mm for the diameter of the vortex.

Other causes of the rapid pressure fluctuations can be thought of, e.g. influences of the prey on the water flow and impact events on the catheters by the prey (in the buccal cavity).

Lauder's explanation (1980a,b) of his pressure records is based on steady flow assumptions, although the author claimed that inertial effects are important (Muller et al., 1982 and Muller and Osse, in press). He tried to explain the big difference between buccal and opercular pressure in *Lepomis* by assuming a high resistance of the gills. The second negative peak in the buccal pressure records of *Lepomis* is considered to be caused by mouth closing (Lauder, 1980a,b: "waterhammer effect").

Several objectives can be formulated against Lauder's ideas about suction feeding (Muller and Osse, in press). First it is impossible to derive the flow direction from the pressure regime in an essentially unsteady flow (Muller et al., 1982).

Second, without the assumption of any gill resistance our simulated pressures are very similar to the measured pressures as demonstrated for *Amia calva*, *Salmo gairdneri*, *Esox lucius* and *Gadus morhua*. Thus gill resistance plays only a minor role in the suction process. Third, the initial positive opercular pressure peak is mainly caused by forward motion of the fish and not by an active opercular adduction. When the fish's forward velocity is below a certain critical value a caudal inflow into the opercular cavities would occur in case of open opercular and branchiostegal valves as pointed out by Van Leeuwen (in prep.). The gill covers are an important tool to prevent such an inflow. The generally found slight initial activity of the M. adductor operculi (as measured for the first time by Osse, 1969) is necessary to seal the valves as both the threshold swimming speed and the pressure near the valves may initially (the first 10 msec) fluctuate rapidly (see Van Leeuwen, in prep. and Muller and Osse, in press). It is likely that this slight initial activity does not contribute significantly to the initial positive pressure peak nor to the initial adduction of the operculars, found in e.g. *Lepomis* and *Amia*. The initial adduction will be mainly caused by the more powerful buccal expansion in combination with the small mouth aperture at this instant, forcing the gill covers to move inwards. Van Leeuwen and Muller (in prep.) pointed out that the initial opercular adduction reduces the negative pressure peak and hence allows a faster opening of the mouth.

An initial internal reverse flow in the opercular cavity will definitely occur, as the opercula move inwards. It has, however, to be considered as being of minor importance in the suction process.

Volume enlargement of the opercular cavity is coupled with suspensorial abduction and thus with hyoid abduction, in addition to the enlargement created by the activity of the M. dilatator operculi (abducting the opercula) and the M. hyohyoideus inferior (fanning out the branchiostegal rays). The relative importance of the opercular cavities in suction feeding varies throughout the teleosts. In two extreme types of prey suction, viz. *low-τ-suction with protrusion* and *low-τ-suction with swimming* (see Muller and Osse, in press), the opercular cavities are only slightly enlarged before the moment of caudal valve opening. Before that moment the main function of the gill covers is the sealing of the opercular cavity, so that a caudal inflow is prevented. A significant caudal inflow could ruin the gill filaments. After valve opening, however, suction by gill cover abduction can still be continued effectively when the threshold swimming speed is attained (see Van Leeuwen, in prep.).

In *high-τ-suction* (see Muller and Osse, in press), another extreme type of suction, the valves open relatively late and at a large abduction of the opercula. Hence, the suction function before valve opening is increased relative to low-τ-suction.

The term "waterhammer effect" used by Lauder is invalid (see also Muller & Osse, in prep.). This term is used for the events occuring in a flow tube when the flow is suddenly stopped by a closing valve. In a fish the walls of the mouth cavity move towards each other after mouth closure. Mouth closing does not occur instantaneously. Quite complicated flow patterns may occur during this

157

phase (see Van Leeuwen, in prep.).

The present survey of pressure recording techniques and the interpretation of the experimental results demonstrates the need of a physical approach in studying hydrodynamic events in prey-sucking fish. It shows that pressures should be calculated from the movements of the fish, and not vice versa. In this way accurate simulations of pressures generated by fishes during suction feeding can be made. The effect of changes in movements or dimensions of the fish on the pressures and velocities can be studied in general, providing quantitative requirements for optimized prey capture mechanisms (see also Van Leeuwen & Muller, in press).

## 5. Conclusions

1. Pressure transducers, connected via fluid filled tubes to the mouth cavity of the fish, are unsuitable for measurements during prey uptake because of their limited frequency response and distortions owing to accelerations of the fluid in the tubes.

2. At present, catheter tip pressure transducers offer the most useful measuring devices, owing to their large bandwidth and small dimensions.

3. The pressure inside the fish's mouth is built up of velocity and acceleration components due to mouth expansion and forward motion (caused by suction forward and swimming). Therefore, the velocity of the water cannot be derived from the pressure.

4. Positive pressure peaks caused by forward acceleration of the fish do often occur during feeding by *Salmo gairdneri* and *Esox lucius*.

5. The striking similarity between simulated and measured pressures strongly suggests that the model of Muller et al. (1982) provides a valid description of hydrodynamic events during suction feeding in fish.

## 6. References

Alexander, R.McN. (1969). Mechanics of the feeding action of a cyprinid fish. *J. Zool.*, Lond. 159, 1-15.

Alexander, R.McN. (1970). Mechanics of the feeding action of various teleost fishes. *J. Zool.*, Lond. 162, 145-156.

Casinos, A. (1973). El mechanisme de deglucio de l'aliment a *Gadus callarias*, Linnaeus 1758 (Dades preliminars). *Bull. de la Soc. Catalana de Biologia*, (1), 43-52.

Casinos, A. (1974). Registres de la chute de pression de la cavite buccale chez quelques gadiformes de nos cotes. XXIV-*e Congr. Ass. Plen. de Monaco.* pp. 1-4.

DiStefano, J.J., Stubberud, A.R. & Williams, I.J. (1967). *Theory and problems of feedback and control systems*, Schaums outline series. New York. McGraw-Hill.

Elshoud-Oldenhave, M.J.W. (1979). Prey capture in the pike-perch, *Stizostedion lucioperca (Teleostei, Percidae)*: A structural and functional analysis. *Zoomorphology*. 93, 1-32.

Gabe, I.T. (1972). Pressure measurement in experimental physiology. In: *Cardiovascular Fluid Dynamics* (ed. D.H. Bergel), pp. 11-50. London. Academic Press.

Hughes, G.M. & Shelton, G. (1958). The mechanism of gill ventilation in three freshwater teleosts. *J. exp. Biol.* 35(4), 807-823.

Jones, D.S. (1961). *Electrical and mechanical oscillations*. Plymouth. Latimer Trend Co. Ltd.

Lauder, G.V. (1980a). Hydrodynamics of prey capture by teleost fishes. *Proceedings of the second Conference on Bio-Fluid Mech.* 2, 161-181. New York. Plenum Press.

Lauder, G.V. (1980b). The suction feeding mechanism in sunfishes (*Lepomis*): an experimental analysis. *J. exp. Biol.* 88, 49-72.

Lauder, G.V. & Lanyon, L.E. (1980). Functional anatomy of feeding in the bluegill sunfish, *Lepomis macrochirus*: in vivo measurement of bone strain. *J. exp. Biol.* 84, 33-55.

Leeuwen, J.L. van (in prep.). A quantitative flow study of prey capture in the rainbow trout with general considerations of the actinopterygian mechanism.

Leeuwen, J.L. van & Muller, M. (in press) Optimum sucking technigues for predatory fish. *Trans. Zool. Soc. Lond.*

Liem, K.F. (1978). Modulatory multiplicity in the functional repertoire of the feeding mechanism in cichlid fishes. *J. Morph.* 158, 323-360.

Milne-Thomson, L.M. (1968). *Theoretical hydrodynamics*, 5th edition. London. MacMillan Ltd.

Muller, M. & Osse, J.W.M. (in press). Hydrodynamics of suction feeding in fish. *Trans. Zool. Soc. Lond.*

Muller, M., Osse, J.W.M. & Verhagen, J.H.G. (1982). A quantitative hydrodynamical model of suction feeding in fish. *J. theor. Biol.* 95, 49-79.

Osse, J.W.M. (1969). Functional morphology of the head of the perch (*Perca fluviatilis* L.): an electromyographic study. *Neth. J. Zool.* 19 (3), 289-392.

Osse, J.W.M. (1976). Mecanismes de la respiration et la prise des proies chez *Amia calva* Linnaeus. *Rev. Trav. Inst. Peches Marit.* 40, 701-702.

Osse, J.W.M. & Muller, M. (1980). A model of suction feeding in teleostean fishes with some implications for ventilation. In: *Environmental physiology of fishes* (ed. M.A. Ali) NATO-AS Series A. Life Sciences. *Trans. Zool. Soc. Lond.*

Webb, P.W. & Skadsen, J.M. (1980). Strike tactics of *Esox*. Can. J. Zool. 58, 1462-1469.

# 7. Appendix

### 7.1. NOMENCLATURE

| | |
|---|---|
| $a$ | acceleration, or parameter in model of Muller et al. (1982) |
| $A$ | surface area |
| $c(x,\tilde{\omega})$ | function relating velocity around pressure transducer to velocity without pressure transducer |
| $d$ | distance between source and sphere (see page 120) |
| $f$ | frequency |
| $h_1$ | profile radius at 'mouth aperture' ($x' = l$) |
| $h_2$ | profile radius at 'opercular region' ($x' = 0$) |
| $h*_{max}$ | maximal value of profile radius, $* = 1$ or 2 |
| $h*_{min}$ | minimal value of profile radius, $* = 1$ or 2 |
| $k$ | spring constant |
| $l$ | length of profile (or fish's mouth cavity) |
| $l_c$ | length of catheter |

| $l_p$ | position of transducer in tube mounted on the head of Amia |
|---|---|
| $m$ | mass |
| $p$ | pressure |
| $t$ | time |
| $t_c$ | time constant |
| $t_d$ | time at which mouth aperture closes |
| $t_{h\cdot max}$ | time at $h\cdot max$, $\ast = 1$ or $2$ |
| $t_{v\cdot}$ | delay time, $\ast = 1$ or $2$ |
| $T$ | characteristic duration of feeding event |
| $u_f$ | velocity of water in the fish's mouth used for calculating $u_p$ |
| $u_p$ | velocity around a pressure transducer |
| $u_n(x,t)$ | velocity in the mouth cavity in fish-bound frame after valve opening |
| $u_v(x,t)$ | idem, but before valve opening |
| $u_1$ | $= u_v(l,t)$ |
| $U$ | velocity in uniform flow |
| $U_f$ | velocity of fish's body |
| $x$ | coordinate of long axis in fish-bound frame |
| $X,Y,Z$ | axes of fish-bound frame |
| $x_i$ | input signal |
| $y_0$ | output signal |
| $x$ | angle between long axis of tube and the direction of acceleration of the tube |
| $\alpha_\ast$ | shape coefficient of profile movement, $\ast = 1$ or $2$ |
| $\delta$ | thickness of boundary layer |
| $\Delta h\cdot max$ | $= h\cdot max - h\cdot nul$, $\ast = 1$ or $2$; amplitude of movement |
| $\zeta$ | damping ratio |
| $\rho$ | density of water |
| $\phi$ | phase angle |
| $\tau$ | moment of opening of opercular valve |
| $\upsilon$ | kinematic viscosity |
| $\Psi$ | stream function |
| $\omega$ | $= 2\pi f$, angular frequency |
| $\omega_d$ | damped natural frequency |
| $\omega_n$ | undamped natural frequency |
| $\omega_r$ | resonance frequency |
| $x, \tilde{\omega}$ | cylindrical coordinates |

## 7.2. FORMULAE

The stream function of a uniform flow $-U$ past a sphere (radius, r) and a blunt nosed body, max. diam: $4b$, (see Fig. 2B) is given by:

$$\Psi = \tfrac{1}{2}U\tilde{\omega}^2 \left(1 - \frac{r^3}{(x^2+\tilde{\omega}^2)^{3/2}}\right) + \frac{(x+d)b^2U}{((x+d)^2+\tilde{\omega}^2)^{1/2}} , \qquad (11)$$

a combination of the formulae of Milne-Thomson (1968) for a sphere and a source in a uniform stream, $U$, written in cylindrical coordinates. The centre of the sphere is positioned at $x=0$ and the source at $x=-d$. The velocity in the $X$-direction in this field of flow is given by:

$$u_p = -\frac{1}{\tilde{\omega}}\frac{\partial\Psi}{\partial\tilde{\omega}} = -U\{1 - r^3(x^2+\tilde{\omega}^2)^{-3/2} + {}^3/_2 r^3\tilde{\omega}^2(x^3+\tilde{\omega}^2)^{-5/2} + \qquad (12)$$

$$-b^2(x+d)((x+d)^2+\tilde{\omega}^2)^{-3/2}\}$$

The part between braces in (12) is equal to $c(x,\tilde{\omega})$ in formula (5).

Muller et al. (1982) derived the velocity in the $X$-direction inside an expanding rotationally symmetric profile of length $l$:

160

$$u_v(x,t) = -\frac{1}{A} \int_0^x \frac{\partial A}{\partial t}\, dx \qquad ,(t \leqslant \tau) \tag{13}$$

and

$$u_n(x,t) = u_v(x,t) + \frac{u_n(0,t) \cdot A(0,t)}{A(x,t)} \qquad ,(t \geqslant \tau) \tag{14}$$

These velocities were used by these authors to calculate the pressure (derived from the equation of motion):

$$\frac{\Delta p_v(x,t)}{\rho} = \int_x^l \underbrace{\left[\frac{\partial u_v}{\partial t} + u_v \frac{\partial u_v}{\partial x}\right] dx}_{(a)} + \underbrace{\frac{u'_1}{(a+1)}(x-l)}_{(b)} + \underbrace{\frac{u_1}{(a+1)}(u_v - u_1)}_{(c)} +$$

$$+ \underbrace{{}^1\!/_2 \left[\frac{1}{(a+1)^2} - 1\right] u_1{}^2}_{(d)} + \underbrace{\frac{a}{a+1}(u_1 h_1)'}_{(e)} \tag{15}$$

The symbols are explained in paragraph 7.1.

# Curriculum vitae

Ik ben geboren te Delft op 13 januari 1956. Van je jeugd moet je genieten, vandaar dat ik ben begonnen om de kleuterschool over te slaan. September 1963 ben ik, na enig protest, dan toch begonnen op de lagere school. Daar moet "rekenen" mijn sterkste kant zijn geweest, althans dat suggereren de zorgvuldig bewaarde rapportboekjes.

Augustus 1968 ben ik overgestapt naar het Christelijk Lyceum voor Delft en Rijswijk. De sport (basketbal, volleybal en vooral atletiek) heeft gedurende mijn middelbare school periode een minstens even belangrijke rol gespeeld als het leren. Al vroeg interesseerde ik mij voor het functioneren van het bewegingsapparaat, een belangstelling die gevoed werd vanuit mijn sportieve aktiviteiten. Deze belangstelling breidde zich al snel uit tot een bredere biologische interesse. Na het behalen van mijn atheneum-b diploma in mei 1974, ben ik dan ook biologie gaan studeren aan de Landbouwhogeschool te Wageningen.

Na een min of meer afsluitende daad gesteld te hebben in het sportgebeuren door universitair kampioen te worden op de 800 m hardlopen, heb ik januari 1978 mijn kandidaats-diploma behaald "met lof". In mijn doctoraal heb ik een drietal onderwerpen bewerkt:
1. De functie van het branchiostegaal-apparaat in de zuigende voedselopname door vissen o.l.v. Prof. dr. J. W. M. Osse en Drs. M. Muller.
2. De ontwikkeling van de m. adductor mandibulae van Barbus conchonius o.l.v. Prof. dr. L. P. M. Timmermans en Drs. P. M. G. Barends.
3. De rol van de pootspieren in de locomotie van Testudo o.l.v. Prof. dr. R. McN. Alexander en Mr. A. Jayes (University of Leeds, U.K.).
Het ingenieursdiploma in de biologie heb ik op 23 januari 1980 "met lof" behaald. 1 december 1979 ben ik gestart met een 3-jarig promotie-onderzoek, waarvan dit proefschrift een resultaat is. Nog deze zomer hoop ik te beginnen met een nieuw onderzoeksproject aan het Zoölogisch laboratorium van de Rijksuniversiteit te Leiden.